Supercomplexes of Prokaryotic Aerobic Respiratory Chains

Escherichia coli and *Bacillus subtilis*
supramolecular assemblies

Pedro M.F. Sousa

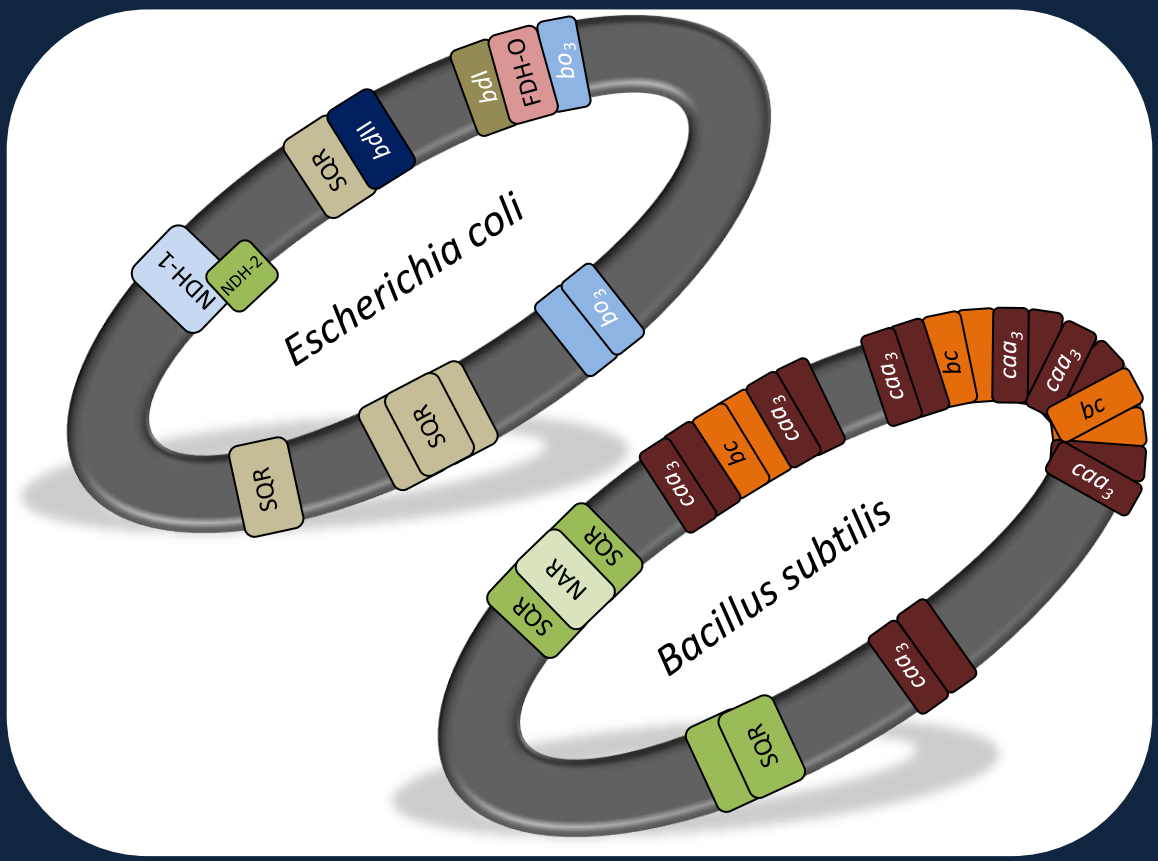

Dissertation presented to obtain the Ph.D degree in Biochemistry

Instituto de Tecnologia Química e Biológica | Universidade Nova de Lisboa
Instituto de Investigação Científica Tropical

Oeiras,
December, 2013

IICT Instituto de Investigação Científica Tropical

INSTITUTO DE TECNOLOGIA QUÍMICA E BIOLÓGICA /UNL
Knowledge Creation

Supercomplexes of Prokaryotic Aerobic Respiratory Chains

Escherichia coli and *Bacillus subtilis*
supramolecular assemblies

Pedro M.F. Sousa

Dissertation presented to obtain the Ph.D degree in Biochemistry

Instituto de Tecnologia Química e Biológica | Universidade Nova de Lisboa
Instituto de Investigação Científica Tropical

Supervisor: Ana M.P. Melo
Co-supervisor: Miguel Teixeira

Oeiras, December, 2013

IICT Instituto de Investigação Científica Tropical
INSTITUTO DE TECNOLOGIA QUÍMICA E BIOLÓGICA /UNL
Knowledge Creation

From left to right: Prof. Miguel Teixeira, Dr. Lígia Saraiva, Prof. Carlos Romão, Prof. Thorsten Friedrich, Pedro Sousa, Dr. Margarida Duarte, Prof. João Arrabaça, Dr. Ana Melo.

Instituto de Investigação Científica Tropical (IICT)
Rua da Junqueira Nº86, 1º
1300-344 Lisboa
Portugal
Tel. (+351) 213 616 340

Instituto de Tecnologia Química e Biológica (ITQB)
Av. da República
Estação Agronómica Nacional
2780-157 Oeiras
Portugal
Tel. (+351) 214 469 323

The molecular cup is now empty. The time has come to replace the purely reductionist "eyes-down" molecular perspective with a new and genuinely holistic "eyes-up" view of the living world, one whose primary focus is on evolution, emergence, and biology's innate complexity.

Carl R.Woese (1928 – 2012)

in "A new biology for a new century" Microbiology and Molecular Biology Reviews 68(2), 173 – 186 (2004)

Acknowledgements

The work summarized in this thesis is the product of several collaborations established during my research grant. It is with great appreciation that I would like to acknowledge the following groups and people:

Ana Melo, my supervisor, for her endless support on my work. I'm truly honored of being her first PhD student and I have learned with Ana how to be constantly motivated, focused, and above all, how to critically analyze scientific results. I appreciate her confidence in my work, friendship and her ability to promote useful discussions.

Miguel Teixeira, my co-supervisor, for his support on my work, useful discussions, and for the opportunity conceded.

Lígia Saraiva and Célia Romão, for following the work developed these years and promoting fruitful discussions.

Marco Videira, Filipe Santos, Sara Silva and Levi Bolacha, for the outstanding contribution they have provided to the work reported in this thesis. Furthermore, I would like to acknowledge Sara for supporting me all the times I needed, with unconditional love and friendship.

For providing a friendly environment and a stimulating workplace, I would like to thank all my colleagues from IICT, namely, José Ramalho, Ana Ribeiro, António Leitão, Luís Goulão, Ana Fortunato, Paula Batista-Santos, Inês Graça, Elisabete Lopes, Paula Alves, Isabel Palos, Micaela Sousa and Tiago David.

Brian Hood and Thomas Conrads from the Gynecologic Cancer Center of Excellence, Women's Health Integrated Research Center at Inova Health System, USA and Nuno Charro, Fátima Vaz and Deborah Penque from the Proteomics Laboratory at Instituto Nacional de Saúde Dr Ricardo Jorge, for their contribution with the mass spectrometry sequencing of the supercomplexes described herein.

Andreas Bohn and Luís Goulão from ITQB and IICT, respectively, for the valuable insights on the statistical analysis performed in this work.

João Carita from ITQB is acknowledged for the large scale growth of *Escherichia coli* wild-type and mutant strains.

Natalya Dudkina and Egbert Boekema from Groningen University, Netherlands, for valuable insights on the methodology used in this work regarding the electrophoretic analysis of supercomplexes.

Julia Steuber and Thomas Vorburger from Stuttgart University, for allowing me to work on their laboratory and for their useful discussions.

My family and friends, for providing me the knowledge and environment I needed to become a better person. I thank Luís Sousa, Maria Sousa, Ana Sousa, Sara Silva, Ricardo Alves, Mário Coelho and Bruno Pais.

Fundação para a Ciência e Tecnologia (FCT) for my fellowship SFRH/BD/46553/2008.

Thesis publications

Pedro M.F. Sousa, Sara T.N. Silva, Brian L. Hood, Nuno Charro, João N. Carita, Fátima Vaz, Deborah Penque, Thomas P. Conrads, Ana M.P. Melo (2011), "Supramolecular organizations in the aerobic respiratory chain of *Escherichia coli*", *Biochimie* 93, 418-425.

Pedro M.F. Sousa, Marco A.M. Videira, Andreas Bohn, Brian L. Hood, Thomas P. Conrads, Luis F. Goulao, Ana M.P. Melo (2012), "The aerobic respiratory chain of *Escherichia coli*: from genes to supercomplexes", *Microbiology* 158, 2408-2418.

Pedro M.F. Sousa, Marco A.M. Videira, Ana M.P. Melo (2013), "The formate:oxygen oxidoreductase supercomplex of *Escherichia coli* aerobic respiratory chain", *FEBS Lett.* 587, 2559-2564.

Pedro M.F. Sousa, Marco A.M. Videira, Filipe A.S. Santos, Brian L. Hood, Thomas P. Conrads, Ana M.P. Melo (2013), "The *bc*:*caa*$_3$ supercomplexes from the gram positive bacterium *Bacillus subtilis* respiratory chain: a megacomplex organization?", *Arch. Biochem. Biophys.* 537, 153-160.

Other publications not included in this thesis

Pedro M.F. Sousa, Marco A.M. Videira, Thomas Vorburger, Sara T.N. Silva, James W. Moir, Julia Steuber, Ana M.P. Melo (2012), "The novel NhaE-type Na^+/H^+ antiporter of the pathogenic bacterium *Neisseria meningitidis*" *Arch. Microbiol.* 195, 211-217.

Dissertation Abstract

Aerobic respiratory chains are composed of a series of membrane complexes that catalyze the electron transfer from reducing substrates to oxygen. The energy released through this process is used to translocate protons across the membranes, thus generating a proton motive force that activates F_1F_O-ATP synthase to synthesize ATP. The arrangement of these enzymes in the inner mitochondrial membrane is well characterized in mammalian mitochondria, where different sets of supramolecular assemblies, or supercomplexes, involving the majority of the respiratory complexes were described, reinforcing the idea of an operational solid state model wherein the oxidative phosphorylation processes are optimized.

A broader perspective of the ubiquity of such assemblies is obtained when analyzing the prokaryotic components that lead to oxygen utilization. The aerobic respiratory chain of these organisms is more flexible than the mitochondrial one, bearing alternative pathways in response to the metabolic needs of the cell, which reflect the ability of these organisms to cope with extreme environmental conditions.

The PhD thesis here presented focuses on the identification and characterization of *Escherichia coli* and *Bacillus subtilis* aerobic respiratory chains supercomplexes, taking advantage of the milder solubilization properties of non-ionic detergents such as digitonin, which has allowed the isolation of such supramolecular assemblies in the respiratory chains of other organisms. Solubilized membrane components from wild type and respiratory chain mutant strains were analyzed by Blue Native Polyacrylamide Gel Electrophoresis (BN-PAGE) where heme staining and *in gel* enzymatic activities detection allowed the identification of protein complexes with higher molecular masses than those deduced for the individual complexes of both organisms respiratory chains.

The *Escherichia coli* aerobic respiratory chain is composed of at least six enzymes, namely type I (NDH-1) and II (NDH-2) NADH:quinone oxidoreductases, succinate:quinone oxidoreductase (SQR), cytochrome bo_3 oxygen reductase and type I and II cytochromes *bd* oxygen reductases, that accomplish the transfer of electrons from the reducing substrates NADH and succinate to O_2, with proton translocation through NDH-1 and cytochrome bo_3 oxygen reductase. Other enzymes such as lactate, formate (FDH-O) and glycerol-1-phosphate dehydrogenases may also participate in this process.

In this thesis, the supercomplexes of *E. coli* aerobic respiratory chain were reported for the first time. Prior to supercomplex detection, a thorough spectroscopic and kinetic characterization was performed in *E. coli* membranes, allowing the detection of the respiratory chain components operating in this Gram negative bacterium.

The analysis of supercomplex composition in this bacterium revealed at least three distinct supercomplexes, one resulting from the association of NADH:quinone oxidoreductases NDH-1 and NDH-2, one composed of FDH-O and cytochromes bo_3 and *bdI* oxygen reductases, and another comprising SQR and cytochrome *bdII* oxygen reductase. In addition, two homo-oligomers were described in this respiratory chain, namely the trimeric assembly of SQR and the dimeric form of cytochrome bo_3 oxygen reductase.

To establish the composition of NADH:ubiquinone oxidoreductase supercomplex three fundamental requirements were obtained, *i*) the detected BN-PAGE NADH:NBT oxidoreductase active band apparent mass of 606 ± 5 kDa is in agreement with the sum of NDH-1 and NDH-2 individual masses; *ii*) several peptides of NDH-1 subunits were identified by MALDI-TOF/TOF and LC-MS/MS analysis; and *iii*) the same band was undetected in solubilized membranes of *E. coli* strains devoid of NDH-1 or NDH-2 enzymes. Interestingly, NDH-1 stability seems to be influenced by the presence of NDH-2, since no free NDH-1 complexes were detected in the BN-PAGE analysis.

Concerning the formate:oxygen oxidoreductase supercomplex (FdOx), the same requirements were obtained. Its corresponding BN-PAGE band, detected by NADH: and formate:NBT oxidoreductase activities in *E. coli* wild type digitonin solubilized membranes, was nearly absent in mutant strains devoid of FDH-O or cytochromes bo_3 or *bdI* oxygen reductases, although maintaining the same intensity in other respiratory chain mutants. Its composition was further confirmed by the mass spectrometry identification of several peptides belonging to subunits of these complexes. Moreover, a molecular mass of 432 ± 7 kDa is in agreement with the sum of the individual complexes present in FdOx, which was shown to dissociate in a smaller subcomplex when harsher solubilization conditions were applied. FdOx was capable of cyanide sensitive quinol: and formate:oxygen oxidoreductase activities. The kinetic parameters of the latter activity were established, the K_M for formate oxidation being 169 ± 21 μM and the corresponding V_{MAX} 117 ± 15 nmol $O_2.min^{-1}.mg^{-1}$. As expected, this activity was severely impaired in the above mentioned mutant strains, in agreement with the composition of FdOx.

In the scope of these results, an investigation of the prevalence of these assemblies during the bacterial growth was performed, complemented by a gene transcription analysis and enzyme activities of the respiratory chain components. The obtained results were globally analyzed and correlations between gene transcription, enzyme activities and bacterial growth were established, providing a multi-level perspective of the *E. coli* respiratory chain. Interestingly, both supercomplexes were detected throughout growth, namely from the mid-logarithmic to the late-stationary phase. The positive correlations observed between the transcription of NDH-1 and NDH-2 encoding genes were in agreement with the identified NADH:ubiquinone oxidoreductase supercomplex. A similar correlation was established between the transcription of cytochromes bo_3 and *bdI* oxygen reductases encoding genes and the formate:oxygen oxidoreductase activity measured along growth, further confirming the identity of FDH-O partners in the FdOx supercomplex. A third important positive correlation

was observed between SQR and *bdII* oxygen reductase encoding genes, whose transcription profiles were identical, suggesting the association of these complexes in a supramolecular assembly. In fact, a polarographic analysis of wild type *E. coli* digitonin solubilized membranes resolved by sucrose gradient ultracentrifugation also suggested the presence of supercomplexes with cyanide sensitive succinate:oxygen oxidoreductase activities. The same activity was observed in a similar sucrose gradient analysis, although using *E. coli* solubilized membranes where cytochrome *bdII* was the sole oxygen reductase expressed, confirming the identification of a third supercomplex in the *E. coli* aerobic respiratory chain, composed of SQR and cytochrome *bdII* oxygen reductase.

The *B. subtilis* aerobic respiratory chain comprises at least seven enzymes. NDH-2 and SQR respectively promote the electron transfer from the reducing substrates NADH and succinate to O_2 via four different pathways. One involves a cytochrome *c* pathway where *bc* complex and *caa*$_3$ oxygen reductase operate, while the other pathways consist on *bd*, *aa*$_3$, or *bb*' menaquinol:oxygen oxidoreductases.

Similarly to what was described for the *E. coli* aerobic respiratory chain studies, a full kinetic and spectroscopic characterization was performed in *B. subtilis* membranes, prior to supercomplex detection, allowing the identification of the respiratory chain components operating in this Gram positive bacterium.

The *B. subtilis* respiratory chain was shown to contain at least four different supramolecular organizations, in addition to the dimeric assemblies of SQR and *caa*$_3$ oxygen reductase. The *bc* complex and *caa*$_3$ oxygen reductase were shown to be the only components of three identified supercomplexes with different stoichiometries, namely (*bc*)$_4$:(*caa*$_3$)$_2$, (*bc*)$_2$:(*caa*$_3$)$_4$ and 2[(*bc*)$_2$(*caa*$_3$)$_4$]. The fourth supercomplex was shown to comprise a dimeric SQR and nitrate reductase (NAR).

In detail, (SQR)$_2$:NAR supramolecular assembly was detected by the succinate:NBT and methyl viologen:nitrate oxidoreductase BN-PAGE activities, upon digitonin solubilization of wild type *B. subtilis* membranes. The detected

bands, with molecular masses between 301-337 kDa were shown to contain several peptides from SQR and NAR subunits, and were completely absent from *B. subtilis* membranes devoid of SQR. Moreover, the dimeric form of SQR dissociated from the supercomplex upon solubilization with different detergents in a 2D-BN-PAGE analysis.

The same techniques were applied for the identification of the *B. subtilis* respiratory chain *bc*:*caa*$_3$ supercomplexes. Cytochrome *c* oxidoreductase *in gel* activity and heme staining produced three high molecular mass bands in wild type *B. subtilis* digitonin solubilized membranes resolved by BN-PAGE, which were absent from *B. subtilis* membranes devoid of *bc* complex or *caa*$_3$ oxygen reductase. In addition, the dissociation of these supercomplex-containing bands with harsher solubilization conditions allowed the resolution of several spots with similar or smaller molecular masses in a 2D-BN-PAGE analysis, which were assigned to *bc*:*caa*$_3$ subcomplexes after identification by mass spectrometry analysis. Guided by this and the molecular masses of *bc* and *caa*$_3$ complexes, each band was assigned to $(bc)_4$:$(caa_3)_2$, $(bc)_2$:$(caa_3)_4$ and $2[(bc)_2(caa_3)_4]$ supercomplexes. In agreement, *bc*:*caa*$_3$ supercomplex bands were capable of cyanide sensitive TMPD/ascorbate:oxygen oxidoreductase activity. The identification of *bc*:*caa*$_3$ supercomplexes different stoichiometries allowed us to suggest a megacomplex organization of the *B. subtilis* respiratory chain. This was the first time such organization was proposed in a prokaryotic respiratory chain.

In summary, the work presented in this thesis allowed the identification of several supercomplexes in the aerobic respiratory chains of *E. coli* and *B. subtilis*, most of which had not previously been observed, giving strong support to the idea that the oxidative phosphorylation processes occurring in prokaryotic respiratory chains may be also dependent on the establishment of such supramolecular assemblies, similarly to what is observed in the eukaryotic respiratory chains.

Resumo da Dissertação

As cadeias respiratórias aeróbias são compostas por diferentes complexos membranares que catalisam a transferência de electrões da oxidação de substratos à redução do oxigénio. A energia transferida neste processo é aproveitada para promover a translocação de protões através das membranas, gerando uma força protomotriz que é utilizada pelo complexo F_1F_O-ATP sintase na síntese de ATP. Embora o estudo das cadeias respiratórias esteja bem documentado, a organização nativa dos complexos enzimáticos que as constituem é ainda discutida. Diferentes estruturas supramoleculares, ou supercomplexos, envolvendo a maioria dos complexos respiratórios foram descritas em mitocôndrias de mamíferos, reforçando a ideia de que esta organização, suportada pelo modelo do "estado sólido" das cadeias respiratórias, seja fisiologicamente relevante e contribua para a optimização dos processos de fosforilação oxidativa.

A cadeia respiratória aeróbia de procariotas distingue-se da mitocondrial pela sua maior flexibilidade, albergando múltiplas vias alternativas compostas por diferentes complexos enzimáticos cuja expressão está dependente das necessidades metabólicas da célula, assegurando a proliferação destes organismos em condições ambientais extremas. Não obstante, diversos supercomplexos foram descritos nas cadeias respiratórias aeróbias de procariotas, evidenciando a ubiquidade deste tipo de organizações.

A tese de doutoramento aqui apresentada incide na identificação e caracterização dos supercomplexos presentes nas cadeias respiratórias aeróbias de *Escherichia coli* e *Bacillus subtilis*, tirando partido das propriedades de solubilização conferidas pelos detergentes não-iónicos, como a digitonina, que demonstraram ser fundamentais no isolamento de supercomplexos das cadeias respiratórias de outros organismos. Neste trabalho, membranas das estirpes selvagens de *E. coli* e *B. subtilis*, bem como de mutantes dos complexos das

cadeias respiratórias aeróbias, foram solubilizadas e resolvidas em géis de electroforese nativos (BN-PAGE), permitindo a identificação de complexos de massas moleculares superiores às dos componentes individuais da cadeia respiratória de cada organismo.

A cadeia respiratória de *E. coli* é composta por seis enzimas, nomeadamente NADH:quinona oxidoreductases do tipo I (NDH-1) e II (NDH-2), succinato:quinona oxidoreductase (SQR), citocromo bo_3 reductase de oxigénio e citocromo *bd* reductase de oxigénio do tipo I e II, que catalisam a transferência de electrões da oxidação dos substratos NADH e succinato à redução do oxigénio, com concomitante translocação protónica através dos complexos NDH-1 e citocromo bo_3 reductase de oxigénio. Outros enzimas como as desidrogenases do lactato, formato (FDH-O) e glicerol-1-fosfato participam igualmente neste processo.

Nesta tese é descrita, pela primeira vez, a organização supramolecular da cadeia respiratória aeróbia de *E. coli*. Uma completa caracterização espectroscópica e cinética foi efectuada à cadeia respiratória deste organismo, em membranas obtidas no início da fase estacionária do crescimento, antes de se proceder à sua caracterização supramolecular permitindo a identificação dos complexos enzimáticos presentes na cadeia respiratória aeróbia deste organismo.

A cadeia respiratória aeróbia desta bactéria Gram negativa revelou conter, pelo menos, três supercomplexos diferentes, um resultante da associação das NADH:quinona oxidoreductases NDH-1 e NDH-2, outro composto pelos complexos FDH-O e citocromos bo_3 e *bd*I reductases de oxigénio e um terceiro contendo os complexos SQR e citocromo *bd*II reductase de oxigénio. Foram também identificados dois homo-oligómeros nesta cadeia respiratória, o trímero do complexo SQR e o dímero do citocromo bo_3 reductase de oxigénio.

A identificação da composição do supercomplexo NADH:ubiquinona oxidoreductase foi baseada em três requisitos fundamentais, *i*) a massa molecular aparente da banda detectada na actividade NADH:NBT oxidoreductase em BN-PAGE (606 ± 5 kDa) está de acordo com a soma das massas moleculares individuais de NDH-1 e NDH-2; *ii*) a mesma banda não foi detectada após

solubilização das membranas de *E. coli* cuja expressão dos enzimas NDH-1 ou NDH-2 foi abolida; e *iii*) foram identificados diversos péptidos das subunidades de NDH-1 através de análises de MALDI-TOF/TOF e LC-MS/MS. Curiosamente, a estabilidade de NDH-1 parece ser influenciada pela presença da proteína NDH-2, uma vez que não foram detectados quaisquer complexos NDH-1 no seu estado monomérico, nas análises electroforéticas efectuadas.

No que diz respeito à composição do supercomplexo formato:oxigénio oxidoreductase (FdOx) os mesmos requisitos foram verificados. A banda de BN-PAGE contendo este supercomplexo foi detectada através das actividades NADH: e formato:NBT oxidoreductase em membranas da estirpe selvagem de *E. coli* solubilizadas com digitonina, tendo desaparecido quase totalmente nas estirpes mutantes deste organismo em que a expressão dos complexos FDH-O e citocromos bo_3 e *bd*I reductases de oxigénio foi abolida, ao contrário do que foi verificado na análise de outros mutantes da cadeia respiratória. A composição deste supercomplexo foi confirmada pela identificação de vários péptidos das subunidades dos complexos FDH-O e citocromos bo_3 e *bd*I reductases de oxigénio através de espectrometria de massa. A massa molecular de 432 ± 7 kDa está de acordo com a soma das massas dos complexos individuais presentes em FdOx, sendo que a dissociação deste supercomplexo em subcomplexos de menor massa molecular foi obtida após solubilização com outros detergentes. A caracterização cinética deste supercomplexo revelou que o mesmo possui actividades quinol: e formato:oxigénio oxidoreductase inibidas por KCN. Os parâmetros cinéticos da actividade formato:oxigénio oxidoreductase foram calculados, tendo sido obtido um K_M de 169 ± 21 µM para a oxidação do formato e a correspondente V_{MAX} de 117 ± 15 nmol O_2.min^{-1}.mg^{-1}. Como esperado, de acordo com a composição do supercomplexo, esta actividade foi severamente reduzida nas estirpes mutantes acima referidas.

Com base nestes resultados, procedeu-se à investigação da prevalência destas organizações supramoleculares ao longo do crescimento bacteriano, complementando este estudo com a análise de transcrição génica e das

actividades enzimáticas dos componentes da cadeia respiratória deste organismo. Ambos os supercomplexos foram detectados ao longo do crescimento, desde a fase de crescimento “mid-logarithmic” até à fase “late-stationary”. As correlações positivas observadas entre o perfil de transcrição dos genes codificantes de NDH-1 e NDH-2 estão de acordo com a composição do supercomplexo NADH:ubiquinona oxidoreductase identificado. Uma correlação semelhante foi verificada entre a transcrição dos genes codificantes dos citocromos bo_3 e *bd*I reductases de oxigénio e a actividade formato:oxigénio oxidoreductase ao longo do crescimento, confirmando a identificação dos complexos na interacção com o FDH-O no supercomplexo FdOx. Uma terceira correlação positiva foi registada entre o perfil de transcrição dos genes codificantes de SQR e citocromo *bd*II reductase de oxigénio, sugerindo a associação destes complexos numa organização supramolecular. De facto, análises polarográficas a fracções de um gradiente de sacarose contendo membranas da estirpe selvagem de *E. coli* solubilizadas com digitonina sugeriram a presença de supercomplexos com actividade succinato:oxigénio oxidoreductase inibida por KCN. Esta actividade foi igualmente observada num gradiente de sacarose contendo membranas solubilizadas de uma estirpe de *E. coli* expressando apenas o citocromo *bd*II como único reductase de oxigénio.

A cadeia respiratória de *B. subtilis* é composta por sete enzimas. A proteína NDH-2 e o complexo SQR catalisam a transferência de electrões da oxidação dos substratos NADH e succinato, respectivamente, à redução de oxigénio através de quatro vias distintas. Uma consiste na via do citocromo *c*, da qual fazem parte os complexos *bc* e citocromo caa_3 reductase de oxigénio, ao passo que as outras vias consistem nos citocromos *bd*, aa_3, ou *bb*’ menaquinol:oxigénio oxidoreductases.

À semelhança do que foi descrito no estudo da cadeia respiratória de *E. coli*, foi efectuada uma completa análise cinética e espectroscópica às membranas de *B. subtilis*, antes de se proceder à sua caracterização supramolecular, permitindo

identificar os componentes da cadeia respiratória aeróbia desta bactéria Gram positiva.

A cadeia respiratória aeróbia de *B. subtilis* revelou conter, pelo menos, quatro supercomplexos, para além das organizações diméricas dos complexos SQR e citocromo caa_3 reductase de oxigénio. Três dos supercomplexos são constituídos pelos complexos *bc* e citocromo caa_3 reductase de oxigénio com diferentes estequeometrias, nomeadamente $(bc)_4$:$(caa_3)_2$, $(bc)_2$:$(caa_3)_4$ and $2[(bc)_2(caa_3)_4]$. O quarto supercomplexo é constituído pelos complexos SQR dimérico e nitrato reductase (NAR).

Em detalhe, a organização supramolecular $(SQR)_2$:NAR foi detectada em BN-PAGE através das actividades succinato:NBT e metil viologénio:nitrato oxidoreductase em membranas da estirpe selvagem de *B. subtilis* solubilizadas com digitonina. As bandas produzidas, com massa molecular de 301-337 kDa, não foram detectadas após solubilização de membranas de *B. subtilis* em que a expressão de SQR foi abolida. A composição deste supercomplexo foi confirmada pela identificação de vários péptidos das subunidades dos complexos SQR e NAR, sendo que a dissociação deste supercomplexo foi promovida após solubilização com diferentes detergentes e confirmada por 2D-BN-PAGE.

As mesmas técnicas foram aplicadas na identificação dos supercomplexos *bc*:caa_3. Três bandas de BN-PAGE contendo supercomplexos de elevada massa molecular foram detectadas através da actividade citocromo *c* oxidoreductase e coloração de hemos em membranas da estirpe selvagem de *B. subtilis* solubilizadas com digitonina, tendo desaparecido nas estirpes mutantes deste organismo em que a expressão dos complexos *bc* e citocromo caa_3 reductase de oxigénio foi abolida. A dissociação destes supercomplexos analisada por 2D-BN-PAGE após solubilização com diferentes detergentes e subsequente análise por espectrometria de massa permitiu identificar subcomplexos *bc*:caa_3 de igual ou menor massa molecular. De acordo com esta informação e com as massas moleculares dos complexos *bc* e citocromo caa_3 reductase de oxigénio, as três bandas de BN-PAGE foram atribuídas aos supercomplexos $(bc)_4$:$(caa_3)_2$,

(bc)$_2$:(caa_3)$_4$ and 2[(bc)$_2$(caa_3)$_4$]. A caracterização cinética destes supercomplexos revelou ainda que os mesmos possuem actividade TMPD/ascorbato:oxigénio oxidoreductase inibida por KCN. A identificação de diferentes composições estequiométricas destes supercomplexos permitiu-nos sugerir a organização de um megacomplexo na cadeia respiratória aeróbia de *B. subtilis*. Esta foi a primeira vez que este tipo de organização supramolecular foi proposta nas cadeias respiratórias de procariotas.

Em resumo, o trabalho apresentado nesta tese permitiu a identificação de diversos supercomplexos nas cadeias respiratórias aeróbias de *E. coli* e *B. subtilis*, a maioria dos quais nunca antes observado, dando ênfase à ideia de que os processos de fosforilação oxidativa ocorridos nas cadeias respiratórias de procariotas estejam também dependentes deste tipo de organização supramolecular, à semelhança das cadeias respiratórias eucariotas.

Abbreviations

Å	Angstrom
ADP	Adenosine diphosphate nucleotide
AOX	Alternative oxygen reductase
ATP	Adenosine triphosphate nucleotide
AU	Arbitrary units
BCA	Bicinchoninic acid
BN-PAGE	Blue native polyacrylamide gel electrophoresis
CO	Carbon monoxide
Complex III	Ubiquinol:cytochrome *c* oxidoreductase
Complex IV	Cytochrome *c*:oxygen oxidoreductase
Cyt *c*	Cytochrome *c*
DCPIP	Dichlorophenol indophenol
DDM	Dodecyl-β-d-maltoside
deNADH	Deamino-NADH
DNP-19	2-[1-(*p*-Chlorophenyl)ethyl]4,6-dinitrophenol
DSC	Differential scanning calorimetry
eV	Electron volts
EDTA	Ethylenediamine tetraacetic acid
ES	Early-stationary phase
FAD	Flavine adenine dinucleotide
FAO	Fatty acid β-oxidation complex
FDH-O	Aerobic formate dehydrogenase
FdOx	Formate:oxygen oxidoreductase supercomplex
FMN	Flavine mononucleotide
FRAP	Fluorescence recovery after photobleaching
HQNO	(2-heptyl-4-hydroxyquinoline *N*-oxide)
HS	Heme staining
$K_3[Fe(CN)_6]$	Potassium hexacyanoferrate(III)
KCN	Potassium cyanide
K_M	Michaelis Menten constant
LB	Lysogeny broth
LC-MS/MS	Liquid chromatography coupled to tandem mass spectrometry
LS	Late-stationary phase
MALDI-TOF/TOF	Matrix-assisted laser desorption/ ionization tandem time-of-flight
MES	2-(*N*-morpholino) ethanesulfonic acid
ML	Mid-logarithmic phase
MOPS	3-(*N*-morpholino) propanesulfonic acid
MS	Mid-stationary phase
NADH	Reduced nicotinamide adenine dinucleotide
NADPH	Reduced nicotinamide adenine dinucleotide phosphate
NAR	Nitrate reductase
NBT	Nitroblue tetrazolium
NDH-1	Type I NADH:quinone oxidoreductase or complex I
NDH-2	Type II or alternative NADH:quinone oxidoreductase
Na^+-NQR	Na^+-translocating NADH:quinone oxidoreductase
NO	Nitric oxide
OR	Oxidoreductase
OXPHOS	Oxidative phosphorylation
PCA	Principal component analysis
P_i	Inorganic phosphate
PMS	Phenazine methosulfate
PMSF	Phenylmethylsulfonyl fluoride
PVDF	Polyvinylidene fluoride
QFR	Quinol:fumarate oxidoreductase
qRT-PCR	Quantitative real-time PCR
ROS	Reactive oxygen species
SDS	Sodium dodecyl sulfate
SQR	Succinate:menaquinone oxidoreductase or complex II
TCA	Tricarboxylic acid
TMPD	Tetramethylphenylenediamine
Tris	Tris(hydroxymethyl)-aminomethane
UQ_1	Coenzyme Q1, analogue to ubiquinone
UQ^{*-}	Semiquinone
UQH_2	Ubiquinol
UV	Ultraviolet
V_{MAX}	Maximal velocity

Table of Contents

Part I – Introduction to aerobic respiratory chains

CHAPTER 1

Part II – Supramolecular organizations in the aerobic respiratory chain of *Escherichia coli*

Part IV – General Discussion and Conclusion

CHAPTER 8

Part I – Introduction to aerobic respiratory chains

Chapter 1

Chapter 1

1.1 Aerobic respiratory chains: an overview

ATP is recognized as being the energy currency of the biological world [1,2]. In eukaryotes, its synthesis is mainly coupled with the dissipation of a transmembrane electrochemical potential promoted by the mitochondrial oxidative phosphorylation (OXPHOS) system localized in this organelles' inner membrane. The four major protein complexes that constitute this system, *i.e.*, NADH:ubiquinone oxidoreductase (complex I), succinate:ubiquinone oxidoreductase (complex II), ubiquinol:cytochrome *c* oxidoreductase (complex III) and cytochrome *c*:oxygen oxidoreductase (complex IV) promote the electron transfer from reducing compounds such as NADH or succinate to molecular oxygen. This electron transfer is achieved by the two mobile redox components, ubiquinone (coenzyme Q), which mediates energy transfer from the reducing substrates via complexes I or II to complex III, and cytochrome *c*, a soluble protein that accomplishes the transfer of electrons from complex III to the terminal oxygen reductase, complex IV. Concomitantly with the electron transfer, in complexes I, III and IV, occurs a vectorial proton translocation across the inner membrane, from the mitochondrial matrix (N-side) to the intermembrane space (P-side), creating a proton motive force that empowers F_1F_O-ATP synthase (complex V) to generate ATP from ADP and inorganic phosphate (Figure 1) [3].

From a thermodynamic and electrochemical perspective, the electron transport chain is represented by a series of coordinated steps, or redox couples, that reflect a sequential free energy change of the system [4]. This free energy is related with the standard reduction potential of each couple, being the most drastic changes in potential the ones associated with the oxidation of NADH by ubiquinone and the reduction of oxygen to water, in eukaryotes. Overall, at neutral pH and atmospheric pressure, the transfer of one electron from the NAD^+/(NADH + H^+) or succinate/fumarate couples to the O_2/H_2O couple accounts to 1.1 and 0.8 electron volts (eV), respectively [5].

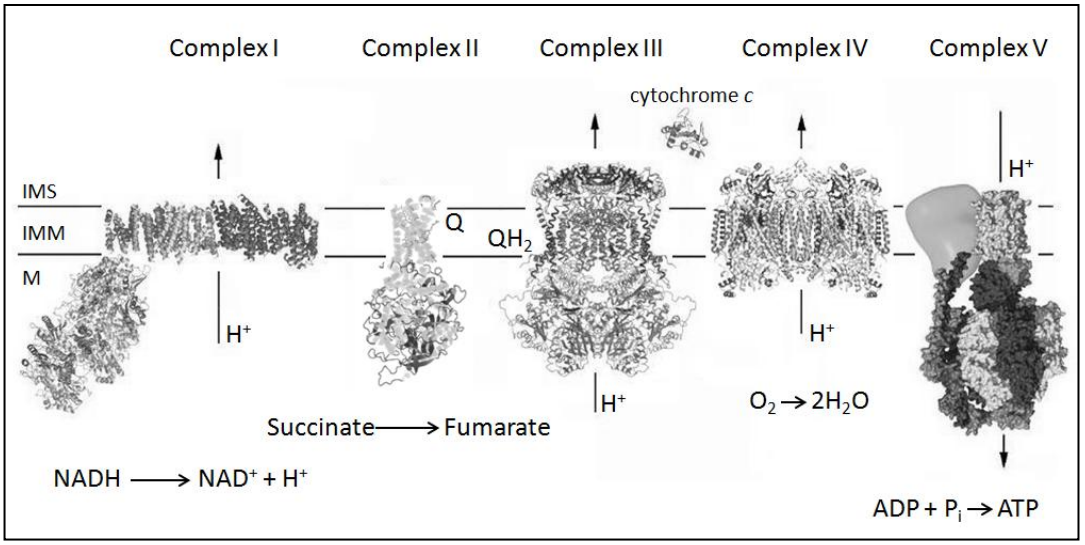

Fig. 1. The mammalian mitochondrial respiratory chain. Electrons from the oxidation of reducing substrates NADH and succinate by complexes I and II, respectively, are transferred via electron carriers through complexes III and IV, where O_2 is reduced to water. Concomitantly, proton translocation from the matrix (M) to the intermembrane space (IMS) allows the generation of a proton motive that promotes ATP production by complex V. IMM stands for inner mitochondrial membrane. Structures are of mitochondrial enzymes or bacterial analogs (complex I from *Thermus thermophilus*) and are not displayed according to the relative sizes. Adapted from [3, 36].

A broader perspective of the aerobic respiratory chain is obtained when analyzing the prokaryotic components that lead to oxygen utilization. The aerobic respiratory chain of these organisms is more flexible than the mitochondrial, bearing branched or alternative pathways that are essentially regulated by the growth conditions, specifically, the oxygen tension or the availability of reduced respiratory substrates such as NAD(P)H, succinate, $F_{420}H_2$ or glycerol-3-phosphate [6]. Bacterial aerobic respiratory chains are assembled in the cytoplasmic membrane, through which proton translocation occurs from the cytoplasm to the periplasmic space. Unlike mitochondria, bacteria may have type I, II and III NADH:quinone oxidoreductases [7], together with different types of oxygen reductases, such as cytochromes *bd*-like oxygen reductases and heme-copper oxygen reductases, the latter being either cytochrome *c*/high potential iron-

sulfur protein (HiPIP)/blue copper proteins or quinol oxygen reductases [6]. A good example of this flexibility can be found in *Paracoccus denitrificans*, whose aerobic electron transport system is similar to the mitochondrial counterpart [8]. The respiratory chain of this α-protobacterium contains three branches for oxygen utilization. In addition to a cytochrome aa_3 oxygen reductase similar to complex IV, a cbb_3 oxygen reductase can accept electrons from c_{552} or c_{550} *c*-type cytochromes, whereas oxygen may be directly reduced by a cytochrome ba_3 oxygen reductase that promotes electron transfer directly from the quinol pool [9].

Representatives of the mitochondrial electron transfer complexes are identified in many prokaryotes, although with a simpler subunit composition, the so-called minimal functional units. This feature has enhanced our knowledge regarding the mechanisms that are intrinsic to both eukaryotic and prokaryotic respiratory chain complexes.

The following sections will focus on the enzymes of the mammalian mitochondrial respiratory chain, the paradigm of aerobic respiratory chains. The minimal functional units of these enzymes, which are represented in the prokaryotic aerobic respiratory chains, will be taken into consideration in the description of each enzyme. In addition, other enzymes that are exclusively present on the aerobic respiratory chains of prokaryotes, fungi and plants will be described, in an attempt to give a broader comprehension of the diverse machinery that operates in oxygen respiring organisms. Although some of the *Escherichia coli* and *Bacillus subtilis* aerobic respiratory chain complexes are mentioned in this chapter, the organization of their electron transfer systems will be thoroughly discussed in the following chapters.

1.1.1 NADH:quinone oxidoreductases

At least three membrane-bound enzymes are able to perform NADH:quinone oxidoreductase activity. The classification of NADH:ubiquinone oxidoreductases

comprises: *i*) type I, or rotenone-sensitive NADH dehydrogenase, complex I (NDH-1); *ii*) type II, or alternative NAD(P)H dehydrogenases (see [7,10] for a review) and *iii*) type III, or Na^+-translocating NADH:quinone oxidoreductases (Na^+-NQR) (see [11] for a review).

i. Type I NADH:ubiquinone oxidoreductase (Complex I)

The mammalian NADH:ubiquinone oxidoreductase (complex I), also known as NADH dehydrogenase, catalyzes the electron transfer from NADH to ubiquinone coupled with the translocation of protons from the mitochondrial matrix to the intermembrane space, with a proton-pumping stoichiometry of $4H^+/2e^-$ [12,13]. Human and bovine complex I are a large L-shaped complex [14] comprising 45 different subunits with a total molecular mass of ~980 kDa [13,15]. Due to its complexity, this is the only enzyme of the mammalian respiratory chain for which a high resolution crystal structure is not available. Nevertheless, progress has been made in determining a structure for a mitochondrial complex I using the proteins from the fungi *Neurospora crassa* [16,17] and *Yarrowia lipolytica* [18]. Complex I L-shaped structure was shown to comprise two perpendicular sections, one hydrophilic peripheral arm that protrudes into the mitochondrial matrix and one hydrophobic membrane embedded arm suggested to mediate proton translocation [19,20].

As for other mitochondrial respiratory chain complexes, prokaryotic complex I (NDH-1) represents the minimal functional unit of the enzyme, bearing 13 to 14 core subunits that are highly conserved among eukaryotes and prokaryotes [21] and are essential for complex I catalytic function [21,22]. A notable feature of the mitochondrial enzyme is that the seven core subunits of the hydrophobic arm (ND1-6 and ND4L)[1] are all encoded for by mitochondrial DNA [23], whereas the seven core subunits of the hydrophilic arm (NDUFV1-2, NDUFS1-3 and NDUFS7-

[1] The nomenclature of NDH-1 subunits used in the text is from the *Homo sapiens* complex. Nomenclature from other organisms is displayed in Table 1.

8) and the remaining accessory subunits are nuclear-encoded [24]. Mammalian complex I 31 accessory subunits are essential for providing a protective shell around the core, although a specialized function has been attributed to some subunits [25]. For example, NDUFA1 subunit has been proposed to be required for the synthesis and assembly of the core mitochondria-encoded subunits of the hydrophobic domain [26], while GRIM19 subunit has been implicated in apoptosis [24] and NDUFA11 subunit is highly similar to inner membrane protein import components [14].

Complex I is proposed to have evolved through the addition of pre-existing protein assembly modules for coupled electron transfer and proton translocation [27-29]. This proposal arose from the observation that several complex I subunits display high similarity with other known proteins. In detail, the hydrophilic arm subunits NDUFS2 and NDUFS7 are similar to the large and small subunits of soluble Ni-Fe hydrogenases, respectively [30]. These, together with homologues of subunits NDUFVS3, NDUFS8 and ND1 are found in the multisubunit membranar Ni-Fe hydrogenases family. Furthermore, hydrophobic arm subunits ND2, ND4, ND4L and ND5 were suggested, through sequence similarity, to have evolved from a family of Na^+/H^+ antiporters called Mrp [29,31]. Taken together, Mathiesen and Hagerhall proposed that complex I and membranar Ni-Fe hydrogenases would share the same common ancestor, an integral membrane complex that originated from the assembly of Mrp-type antiporters and soluble Ni-Fe hydrogenases [29].

A better understanding of complex I structural and functional features is provided by the recent solved X-ray crystal structure of the prokaryotic NDH-1 from *Thermus thermophilus*, which contains the 14 conserved core subunits that display high similarity with the mitochondrial ones, representing the minimal functional unit of the mitochondrial complex I [32,33] (Figure 2).

The prokaryotic NDH-1 hydrophilic domain, composed of Nqo1-6 and Nqo9 subunits (for different nomenclatures, see Table 1) can be further separated, from

an evolutionary and functional perspective, in a quinone-reducing (Nqo4-6,9) and NADH-oxidizing (Nqo1-3) modules, Q and N modules, respectively [34]. The N module contains the NADH oxidation site, with one non-covalently bound flavin mononucleotide (FMN) molecule as the primary electron acceptor, whereas the Q module contains the ubiquinone reduction site.

Table 1
14 core subunits' nomenclatures that compose the hydrophilic and hydrophobic arms of complex I from different species. The conserved co-factors and the predicted transmembrane helices (TMHs) of *Bos taurus* complex are displayed. Adapted from [267].

Enzyme domain	*B. taurus*	*Homo sapiens*	*Y. lipolytica*	*E. coli*	*T. thermophilus*	Co-factors and TMHs
Hydrophilic arm	75 kDa	NDUFS1	NUAM	NuoG	Nqo3	$[2Fe\text{-}2S]^{2+/1+}$, $2x[4Fe\text{-}4S]^{2+/1+}$
	51 kDa	NDUFV1	NUBM	NuoF	Nqo1	FMN, $[4Fe\text{-}4S]^{2+/1+}$
	49 kDa	NDUFS2	NUCM	NuoCD	Nqo4	-
	30 kDa	NDUFVS3	NUGM		Nqo5	-
	24 kDa	NDUFV2	NUHN	NuoE	Nqo2	$[2Fe\text{-}2S]^{2+/1+}$
	PSST	NDUFS7	NUIM	NuoB	Nqo6	$[4Fe\text{-}4S]^{2+/1+}$
	TYKY	NDUFS8	NUKM	NuoI	Nqo9	$2x[4Fe\text{-}4S]^{2+/1+}$
Hydrophobic arm	ND1	ND1	NU1M	NuoH	Nqo8	8 TMHs
	ND2	ND2	NU2M	NuoN	Nqo14	8 TMHs
	ND3	ND3	NU3M	NuoA	Nqo7	3 TMHs
	ND4	ND4	NU4M	NuoM	Nqo13	13 TMHs
	ND5	ND5	NU5M	NuoL	Nqo12	16 TMHs
	ND6	ND6	NU6M	NuoK	Nqo10	5 TMHs
	ND4L	ND4L	NULM	NuoJ	Nqo11	3 TMHs

The two electrons that result from NADH oxidation are sequentially transferred between the two catalytic sites, through a chain of seven binuclear or tetranuclear [Fe-S] clusters [32]. An additional [Fe-S] cluster localizes near the FMN molecule and is suggested to play a protective role against reactive oxygen species (ROS) formation [35]. The terminal [Fe-S] cluster of the chain, N2, is suggested to transfer one electron to a ubiquinone molecule (UQ) [36,37], whose binding site is long and narrow and can be regarded as a chamber provided by Nqo4 and Nqo6 subunits, converting it to a semiquinone (UQ^{*-}). Ubiquinol (UQH_2) is then produced once the re-reduction of N2 by the second electron takes place, in a reaction that is dependent on the uptake of two protons from the mitochondrial matrix or prokaryotic cytoplasm [33].

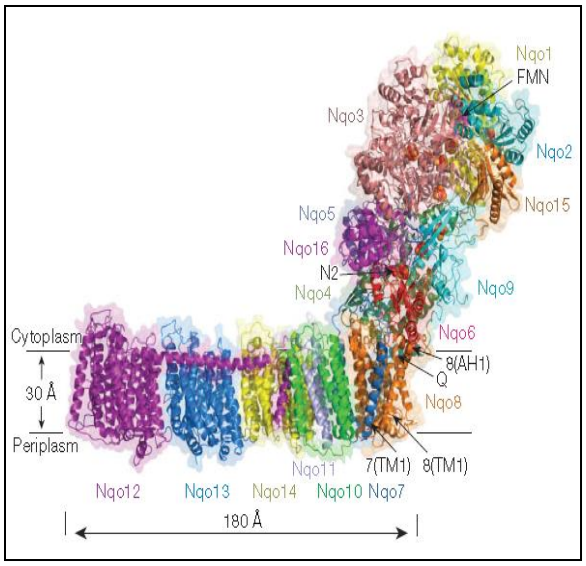

Fig. 2. X-ray crystal structure of the entire *T. thermophilus* complex I. The characteristic L-shaped complex comprises two domains. The hydrophilic arm contains subunits Nqo1-6,9, contacts the cytoplasm and bears an FMN molecule and all the [Fe-S] clusters (shown as magenta and red-orange spheres) that promote a sequential electron transfer from NADH to a quinone binding site, framed by Nqo8 helices TM1, TM6 and AH1. The hydrophobic arm is composed of subunits Nqo7-8,10-14 and contributes to the generation of a proton motive force. Adapted from [36].

The hydrophobic domain, composed of Nqo7-8 and Nqo10-14 subunits, has no redox groups and it is therefore expected that the translocation of four protons occurs by the induction of conformational changes, through an indirect mechanism, as a consequence of the hydrophilic domain redox reactions. Interestingly, Nqo12-14 subunits are connected by a long transmembrane α helix (HL) with ~110Å and by a β-hairpin-helix connecting element (βH) [38], on opposite sides of the membrane domain. Noteworthy, as previously mentioned, Nqo12-14 subunits display high similarity with proteins known to have Na^+/H^+ antiporter function [31]. This similarity suggests that three protons could be translocated in parallel, one proton per subunit. The fourth proton route could be provided by Nqo8 and Nqo10-11 subunits, since their structural organization allows the assembly of an antiporter-like channel (E-channel) [33]. Whether HL or βH helices are important for the coupling mechanism of complex I associated with a piston-like motion [36] or solely to maintain the antiporter-like subunits connected [39], it is still unknown.

It is worth mentioning that complex I from *E. coli* [40,41], *Rhodothermus marinus* [42] and *Klebsiella pneumoniae* [43] were suggested to translocate Na^+ ions, presumably through the antiporter-like subunits. A possible mechanism was

proposed in which two Na^+ ions could be translocated to the cytoplasm through each antiporter-like subunit, in opposite direction of one translocated proton, allowing the maintenance of the transmembrane charge separation. Furthermore, since antiporters are able of changing transport directionality, the authors suggested that these subunits could alternatively translocate Na^+ to the periplasm, depending on the environmental conditions [44].

Complex I inhibitors are classified in three groups, based on their resemblance with quinone or quinone-derived products such as semiquinone or quinol [45]. Piericidin A (type A, quinone antagonists), the classical rotenone (type B, semiquinone antagonists), or myxothiazol (type C, quinol antagonists) are among the wide variety of natural and commercial compounds that inhibit NADH:ubiquinone oxidoreductase activity.

ii. Type II NADH:ubiquinone oxidoreductase

Type II NAD(P)H dehydrogenases, also termed NDH-2, are rotenone-insensitive single polypeptides with a molecular mass around 50 kDa that catalyze the transfer of two electrons from NADH or NADPH to quinones [7]. These are non-proton pumping flavoproteins that are absent from the mammalian mitochondria but may represent a key player in the generation of alternative electron transfer pathways in plants [46], fungi [47,48], protist mitochondria [49] and several prokaryotes [50,51]. The number and specificity of type II NAD(P)H dehydrogenases varies significantly between organisms, but their primary structure generally contains one or two sequence motifs for binding NAD(P)H and flavin adenine dinucleotide (FAD) or FMN [7,52]. Some of these proteins oxidize NADPH instead of NADH, whereas the enzymatic activity of others is calcium-dependent [53].

In plant mitochondria at least four type II NAD(P)H dehydrogenases were described, two of which face the mitochondrial intermembrane space (external NAD(P)H dehydrogenases) and oxidize cytosolic NADH or NADPH that cannot

readily penetrate the inner mitochondrial membrane, whereas the remaining two proteins are matrix-facing enzymes (internal NAD(P)H dehydrogenases) [10]. Similarly, the fungus *N. crassa* also contains four NDH-2 enzymes, of which one is internal [54] and three are externally located [55-57]. Type II NAD(P)H dehydrogenases are expressed together with complex I in these organisms, their role being likely attributed, in this case, to the maintenance of [NADH]/[NAD^+] balance in the cell [7]. However, NDH-2 may also be the only membrane associated enzymes present, as in the yeast *Saccharomyces cerevisiae* [58], whose respiratory chain is devoid of complex I but contains three NDH-2 enzymes, of which one faces the matrix (NDI1) [59,60] and two are externally located (NDE1 and NDE2) [61]. Since complex I is absent, the physiological role of these NDH-2 enzymes may be attributed to respiratory chain-linked NADH turnover, with concomitant ATP production [7].

The prokaryotic respiratory chains may contain both NDH-2 and NDH-1, as in the case of *E. coli* [62] or express only one of these enzymes. For example, *P. denitrificans* contains only NDH-1 [63] whereas *B. subtilis* aerobic respiratory chain expresses solely NDH-2 [64]. Sequences encoding putative type II NADH dehydrogenases were identified in the genomes of hyperthermophilic bacteria [65,66] and archaea [67,68] and have been isolated from *Methylococcus capsulatus* [69].

iii. Na^+-translocating NADH:quinone oxidoreductases (Na^+-NQR)

Na^+-NQR, widely distributed in marine and pathogenic bacteria, oxidizes NADH and transfers two electrons to ubiquinone. This redox reaction is coupled to a vectorial translocation of two sodium ions across the membrane. Na^+-NQR (~200 kDa) is composed of six subunits [70] that harbor several prosthetic groups, including one $[2Fe\text{-}2S]^{2+/1+}$ cluster, one non-covalently bound FAD, two covalently bound FMN and one non-covalently bound riboflavin [11]. Although the efficiency of energy conservation by Na^+-NQR is approximately twofold lower than that of

complex I, in some bacteria it could entirely replace complex I function of oxidizing NADH and reducing ubiquinone. Possible metabolic roles of Na^+-NQR may include the maintenance of low Na^+ intracellular concentration levels in organisms prone to inhabit environments where this ion is abundant [71], and/or the generation of a membrane potential that would preserve the oxidative phosphorylation processes at high pH values [72].

1.1.2 Succinate:quinone oxidoreductases

Succinate:quinone oxidoreductase (SQR), also termed complex II, is a transmembrane enzyme that catalyzes the transfer of two electrons from succinate (via $FADH_2$), while concomitantly reducing quinone molecules to quinol (see [73,74] for a review). In contrast with complex I, SQR does not translocate protons and bears dual functionality, interconnecting the tricarboxylic acid (TCA) cycle and the respiratory chain [4,75].

The mammalian SQR, with a total molecular mass of 124 kDa [76], contains four subunits, of which two are hydrophilic and highly conserved among different species, A (Fp subunit) and B (Ip subunit). These subunits protrude into the mitochondrial matrix and promote succinate oxidation. Subunit A contains a covalently bound FAD to which the electrons are transferred from the oxidation of succinate, while subunit B assembles three sequentially positioned [Fe-S] clusters, $[2Fe\text{-}2S]^{2+/1+}$, $[4Fe\text{-}4S]^{2+/1+}$ and $[3Fe\text{-}4S]^{1+/0}$, that allow a vectorial electron transfer from FAD to the hydrophobic domain, where the quinone reduction takes place. It is generally accepted that the eukaryotic SQR contains, at least, two ubiquinone binding sites in the hydrophobic domain. One site (Q_P) is near the matrix side of the membrane, while the second (Q_D) localizes near the intermembrane space [76,77]. The hydrophobic domain is composed of two small membrane-anchored subunits, C (CybL subunit) and D (CybS subunit), that were suggested to form a tail-like structure that protrudes and is exposed into the intermembrane space [76].

This domain coordinates one low spin *b*-type heme [76,77]. Whether this heme participates in the electron transfer to the Q_D binding site or is solely important for the assembly of the single heme containing SQRs' hydrophobic domains, remains unknown [78]. Bovine SQR cytochrome b_{560} is not reducible by succinate [79], while *S. cerevisiae b*-type heme is not essential for catalysis [80]. In fact, the close proximity between the $[3Fe\text{-}4S]^{1+/0}$ cluster and the Q_P binding site potentially allows the occurrence of electron transfer [76].

In prokaryotic respiratory chains SQR is also expressed and can be replaced by a similar complex under anaerobic conditions, the quinol:fumarate oxidoreductase (QFR). This protein catalyzes the reverse reaction, *i.e.*, the coupling of quinol oxidation to the reduction of fumarate, termed fumarate respiration [81]. SQR and QFR complexes can be classified in five types, from A to E, based on their hydrophobic domain and heme content [82,83] (Figure 3).

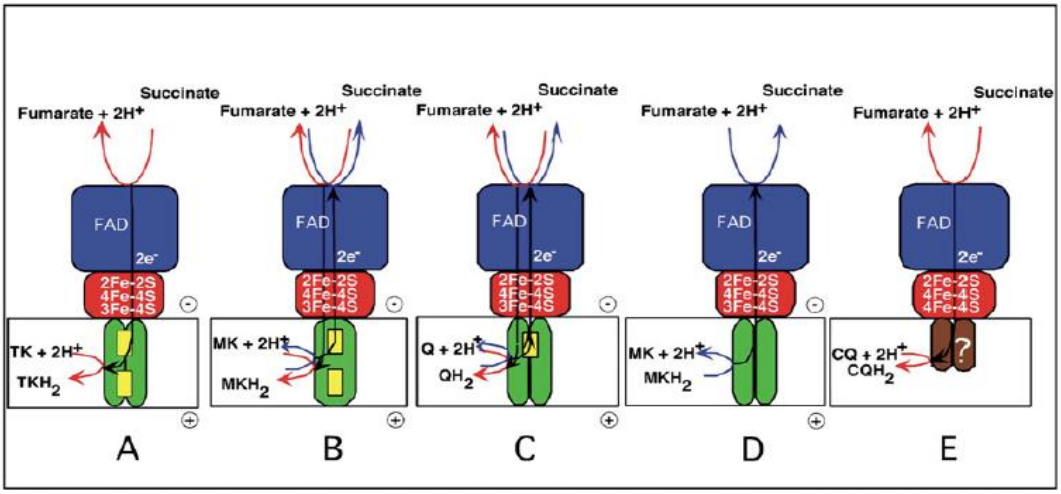

Fig. 3. Distribution of SQR/QFR types in prokaryotic and eukaryotic organisms (from A to E). In common, all enzymes' hydrophilic domain, which contacts the mitochondrial matrix or the prokaryotic cytoplasm, contain an FAD molecule and three [Fe-S] clusters to where electrons are sequentially transferred from the oxidation of succinate or for the reduction of fumarate to/from a quinone molecule located in the hydrophobic domain. These domains often contain *b*-type heme groups that are thought to deliver the electrons to quinone molecules of variable composition. Adapted from [74].

The mammalian complex II and *E. coli* SQR assemble a type-C hydrophobic domain, bearing only one *b*-type heme sandwiched between transmembrane helices of the two integral membrane subunits, SqrC and SqrD [84]. These subunits are also present in type-A domain, being distinguished from the former by the presence of an additional *b*-type heme group classified as b_D-type heme given its distal location from the hydrophilic domain in comparison with the proximal location of the b_P-type heme. SQR type-A domain is present in the archaea *Thermoplasma acidophilum* and the bacterium *T. thermophilus* [85,86]. Two *b*-type hemes are also present in the type-B domain of *B. subtilis* SQR and *Wolinella succinogenes* QFR [87,88]. What better distinguishes this domain is the exclusive presence of a single large hydrophobic subunit (C), which probably evolved from the fusion of the genes coding for the smaller subunits C and D [77]. Type-D domain is present in *E. coli* QFR [89] and contains the two integral membrane subunits but the *b*-type hemes are absent. In contrast, type-E SQRs lack the typical membrane anchoring subunits as found in the other four types of membrane domains. The proposed type-E domain consists of two polypeptides which lack transmembrane spanning helices and are not sequence-related to SqrC and SqrD, being renamed SqrE and SqrF subunits, respectively, for that reason [90]. Type-E subunits do not contain *b*-type hemes and SqrE was proposed to function as a monotopic membrane anchor of the enzyme, harboring the quinone binding site (caldariella quinone) and potentially assembling one [4Fe-4S]$^{3+/2+}$ cluster [91,92].

Besides complex II, three other membrane-bound enzymes are able to deliver electrons to ubiquinone without proton translocation in mammalian mitochondria: *i*) ETF:ubiquinone oxidoreductase; *ii*) dihydroorotate and *iii*) *s*,*n*-glycerophosphate dehydrogenases.

ETF:ubiquinone oxidoreductase, or electron transferring flavoprotein:ubiquinone oxidoreductase, is a globular protein that contains one FAD molecule, one [4Fe-4S]$^{2+/1+}$ cluster and one ubiquinone binding site. It catalyzes the oxidation of

electron transferring flavoproteins, which in turn accept electrons from FAD-containing dehydrogenases involved in mitochondrial fatty acid β-oxidation and amino acid catabolism, to ubiquinone [93].

Dihydroorotate and *s*,*n*-glycerophosphate dehydrogenases bind their substrates from the outer side of the membrane. The former contains a tightly bound FMN and is involved in pyrimidine biosynthesis, catalyzing the oxidation of dihydroorotate to orotate [94], while the latter contains one FAD, at least one [Fe-S] cluster and oxidizes *s*,*n*-glycerophosphate.

1.1.3 Quinol:cytochrome *c* oxidoreductase

The electron transfer from quinol to cytochrome *c*, with concomitant proton translocation, is catalyzed by quinol:cytochrome *c* oxidoreductase, also known as bc_1 complex or complex III in mammalian mitochondria. This membrane complex is also found in many species of bacteria and is similar in many aspects to the cytochrome b_6f complex of plant thylakoids (see [95] for a review). The mitochondrial complex III has been extensively characterized and X-ray crystal structures from bovine and chicken mitochondria, among others, are available [96,97]. It is a homodimeric complex, with each monomer consisting of 11 subunits with ~240 kDa, of which three assemble the redox groups and represent the catalytic core subunits [97].

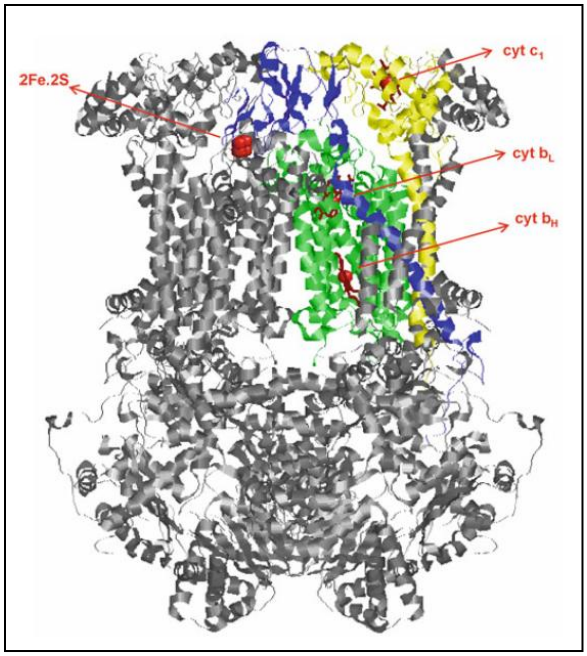

Fig. 4. X-ray crystal structure of complex III homodimeric assembly from mammalian mitochondria. Each monomer comprises eleven subunits, three of which represent the core catalytic subunits, *i*) a cytochrome *b* subunit (green) bearing two *b*-type hemes of different reduction potentials and the quinone binding centres Q_o and Q_i, *ii*) a Rieske Fe-S protein subunit (blue) containing a binuclear [Fe-S] cluster and *iii*) a cytochrome c_1 subunit (yellow) carrying one *c*-type heme. Adapted from [97].

In detail (Figure 4), one subunit (cytochrome *b* subunit) contains two low spin *b*-type hemes of lower and higher reduction potentials, b_L and b_H, respectively. b_L is located towards the P-side while b_H faces the N-side of the membrane, where the binding centres for ubiquinol oxidation and ubiquinone reduction, Q_o and Q_i, are respectively located. Another transmembrane subunit (Rieske Fe-S protein) is folded as a globular structure near the P-side of the membrane to which an [2Fe-2S]$^{2+/1+}$ cluster is attached. The third core catalytic subunit (cytochrome c_1 subunit) bears a globular domain that carries one *c*-type heme, to where one electron at a time is transferred in each monomer [98].

The bacterial bc_1 complex generally comprises only the three core subunits [99], of which Rieske Fe-S protein and cytochrome *b* subunits are conserved between different species. In contrast, the third core catalytic subunit strongly varies between phyla, cytochrome c_1-like subunit being only present in α-, β- and γ-proteobacteria, whilst ε-proteobacteria contain a diheme cytochrome *c* that belongs to the cytochrome c_4 family [100], which is replaced by a tetrahemic

cytochrome c_3, structurally unrelated with cytochrome c_1, in the δ-proteobacteria branch. Moreover, the cytochrome c_1-like subunit is replaced by an *f*-type cytochrome subunit in cyanobacteria respiratory chains (cytochrome b_6f complex) [101].

Some prokaryotes do not contain the typical bc_1 complex, as in the case of the thermohalophilic bacterium *R. marinus*, where a multihemic cytochrome *bc* complex lacking the Rieske center catalyzes the quinol:cytochrome *c* (HiPIP) oxidoreductase activity [102], hence termed alternative complex III (ACIII). In addition, some archaeal aerobic respiratory chains do not contain the canonical bc_1 complex. For instance, in *Sulfolobus acidocaldarius* aerobic respiratory chain, bc_1 complex analogs are found within two different supercomplexes, SoxEFGHIM (SoxM) and SoxABCD, which will be later analyzed in the context of the archaeal aerobic respiratory chain supramolecular assemblies. In common, SoxG and SoxC subunits of both supercomplexes are similar to the cytochrome *b* subunit from bc_1 complex, but the di-heme redox component is exclusively composed of two *a*-type hemes (A_S) [103,104].

Complex III concomitant electron transfer and proton translocation is explained by the protonmotive Q-cycle, first proposed by Peter Mitchell [105] and later refined by Crofts and colleagues (see [106] for a review). The Q-cycle is divided in two steps, each being initiated with the oxidation of a quinol molecule at the Q_o site. In both steps, this reaction releases two electrons that are separated in a bifurcated pathway [107]. One electron is transferred to the [Fe-S] cluster of the Rieske subunit, where it triggers a conformational change of the subunit globular domain that allows the electron to be transferred to cytochrome c_1, which in turn reduces the soluble cytochrome *c*. At the same time, two protons are released in the mitochondrial intermembrane space or in the prokaryotic periplasm. The second electron is provided by the oxidation of the semiquinone molecule that resulted from the quinol oxidation, producing a quinone molecule. This oxidation is performed by heme b_L and the resulting electron is transferred to the heme with

higher reduction potential (heme b_H). The quinone molecule produced in the reaction is, in theory, able to freely migrate to the Q_i site. There, heme b_H reduces the quinone molecule to a stabilized semiquinone [108]. In the second step, the bifurcated pathway is repeated with the concomitant translocation of two protons. At the Q_i site the stabilized semiquinone produced in the first step is reduced by heme b_H, yielding, together with the sequestration of two protons from the N-side of the membrane, a quinol molecule, which returns to the bulk pool, completing the cycle. The overall reaction catalyzed by complex III involves the oxidation of two quinol molecules in the Q_o site, the reduction of one quinone at the Q_i site, the reduction of two cytochromes c_1 and consequent transfer of two electrons to the soluble cytochrome *c*, the release of four protons at the P-side of the membrane and the uptake of two protons from the N-side of the membrane.

Antimycin A, stigmatellin and myxothiazol are typical inhibitors of complex III and have been essential for the elaboration of the Q-cycle mechanism. Antimycin A acts at the Q_i site, preventing the formation of semiquinone. Stigmatellin inhibits the electron flow from the quinol molecule to the Rieske Fe-S protein and myxothiazol acts at the Q_i site [109,110]. Interestingly, the use of antimycin A and myxothiazol results in the production of superoxide at the Q_o site.

It is worth mentioning that complex III monomers do not function independently. The two monomeric units interact with each other through the globular domain of the Rieske Fe-S protein of one monomer with the Q_o site and the cytochrome c_1 subunit of the other. Moreover, electrons can be transferred between both monomers' *b*-type hemes, creating an "H-shaped" electron transfer system that could be of great advantage in regulating the production of ROS [111]. The aerobic respiratory chains ROS production will be addressed with more detail later in this chapter, within the context of the respiratory chain supercomplex organization.

1.1.4 Oxygen reductases

The final step of the electron transfer chain in mitochondria and oxygen respiring prokaryotes is accomplished by oxygen reductases. These complexes couple the oxidation of electron carriers, such as cytochrome *c* or quinol molecules, to the reduction of dioxygen to water. There are three types of oxygen reductases, *i*) heme-copper oxygen reductases; *ii*) cytochrome *bd* oxygen reductases and *iii*) alternative oxygen reductases (AOX). X-ray crystal structures are not yet available for the cytochrome *bd* oxygen reductases, whereas the structure of AOX from the trypanosome respiratory chain was recently solved and many have been described for the heme-copper oxygen reductases superfamily, which will be the main focus of this section.

i. Heme-copper oxygen reductases

Heme-copper oxygen reductases superfamily is further classified in three families: A, B and C [112]. The mitochondrial cytochrome *c* oxygen reductase, or complex IV, belongs to the A-family, which includes also cytochrome *c* or quinol oxygen reductases from some prokaryotes. The B-family includes oxygen reductases from prokaryotes, such as the ba_3-type oxygen reductase from *T. thermophilus* [113], while the C-family is represented by cbb_3-type oxygen reductases [114]. X-ray structures from the three families have been elucidating the mechanism by which these complexes operate, which is far from being completely understood [113-117].

Mitochondrial complex IV catalyzes the sequential transfer of four electrons from the soluble cytochrome *c* to O_2, yielding two water molecules. Concomitantly, four protons are translocated to the mitochondrial intermembrane space (see [118] for a review). As in complex III, mitochondrial complex IV crystallizes as a dimer, which is essential for the stabilization of the entire quaternary structure of the

enzyme [119]. Each monomer contains 13 subunits (~205 kDa), in the case of mitochondria, from which only three constitute the catalytic core [120]. Subunits I and II represent the minimal functional unit [121] (Figure 5A), while subunit III is important for the structural integrity of the redox sites and was suggested to participate in the delivery of O_2 [122].

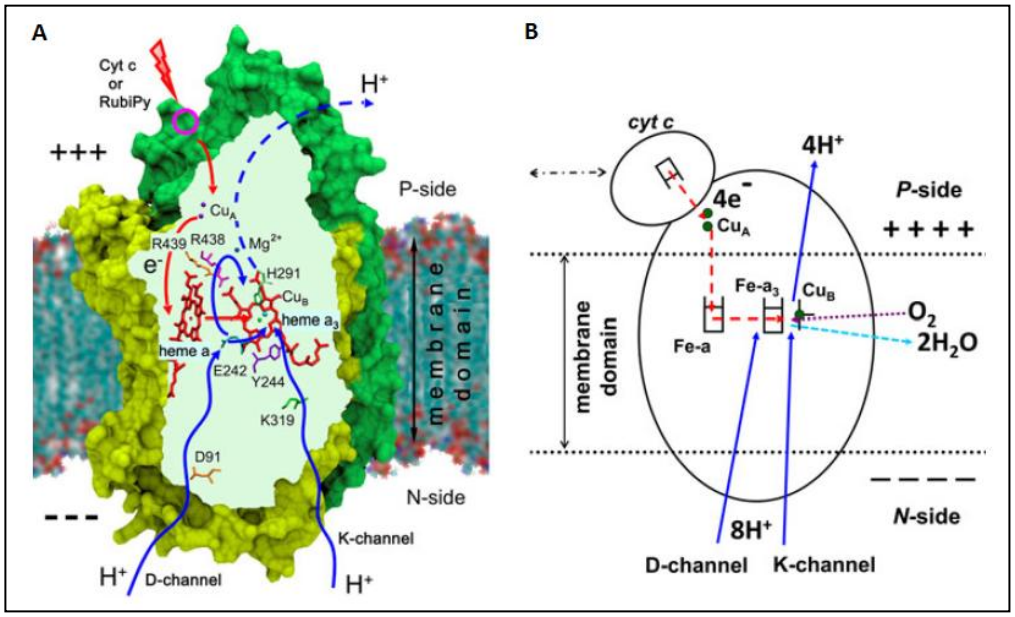

Fig. 5. Mammalian mitochondrial complex IV architecture and proposed mechanism. A) Structure of complex IV core subunits I and II are displayed in yellow and green, respectively, with the associated metal centers and the key amino acid residues. Electron transfer and proton translocation paths are shown as red and blue arrows, respectively B) Location of the redox sites and possible pathways for protons, oxygen, water and electrons. Adapted from [123].

In detail, complex IV contains four redox groups, distributed between subunits I and II (Figure 5). Subunit II has two transmembrane helices and a globular domain projected into the P-side of the membrane where a binuclear Cu_A centre, which is absent in quinol oxygen reductases, accepts one electron at a time from the soluble cytochrome *c*. The adjacent subunit I is composed of 12 transmembrane helices and contains one *a*-type heme and a binuclear complex consisting of a

second *a*-type heme (designated as a_3) together with Cu_B, to where the electron transfer sequentially proceeds and the reduction of oxygen takes place [123]. In some prokaryotes, the *a*-type heme (a_3) from the binuclear complex is replaced by *b*- or *o*-type hemes, hence designated as b_3 [114] and o_3 [124], respectively.

In this region, two hydrogen-bond networks ensure a connection from the reduction of oxygen to the N-side of the membrane, known as D- and K-pathways, where the uptake of four protons from the N-side of the membrane, necessary to produce two water molecules, is achieved (Figure 5B). The translocation of the remaining four protons to the mitochondrial intermembrane space or bacterial periplasm is still debated, although mutations of amino acid residues involved in K- and D- pathways has shown that both pathways contribute for this process [125,126].

A third pathway was also proposed exclusively for the proton translocation mechanism, the H-pathway [122]. It was suggested to run along the heme *a* surrounding helices and is composed of a hydrogen-bond network connected to the P-side of the membrane and a water channel opening to the N-side. However, the bacterial enzyme analogous H-pathway has shown that it is not required for proton translocation [127], thus its role in this mechanism remains elusive. Although enzymes from heme-copper oxygen reductases A-family utilize at least two proton pathways, either to the active site or for proton translocation, only one proton pathway is observed in the representatives of B and C families [113,114].

Among complex IV inhibitors, cyanide is the better characterized and it binds to the binuclear catalytic site in both oxidized and reduced states, blocking irreversibly the final step of the aerobic metabolism [128]. Nitric oxide (NO) and carbon monoxide (CO) are also capable of inhibiting complex IV activity at the binuclear centre (see [129] for a review). While the latter directly competes with oxygen in binding to the fully reduced centre, NO inhibition occurs in both fully oxidized and reduced forms of the enzyme.

ii. Cytochrome *bd* oxygen reductases

Cytochrome *bd* oxygen reductases are quinol oxygen reductases found in many prokaryotes and generally use ubiquinol or menaquinol as substrates (see [130] for a review). These membrane complexes are composed of two transmembrane subunits (I and II) which harbor three prosthetic groups: *i*) a low spin heme b_{558} located in subunit I and *ii*) a catalytic centre in subunit II, formed by two high spin hemes, b_{595} and *d*, suggested to form a binuclear centre similar to the one described for heme-copper oxygen reductases [131]. Cytochrome *bd* oxygen reductases do not translocate protons to the periplasm. Their function requires the uptake of four protons from the cytoplasmic side of the membrane for O_2 reduction and the release of two protons in the periplasmic side of the membrane for quinol oxidation with a concomitant transfer of four electrons through heme b_{558} to the O_2-reducing site. The quinol oxidation is performed, at least partially, in the hydrophilic region of subunit I, termed “Q-loop”, which distinguishes two groups of cytochrome *bd* oxygen reductases, the ones that harbor a long Q-loop, such as in the *E. coli* enzymes [132], and those in which an insert in the C-terminal portion is absent, bearing a short Q-loop [133]. The latter feature is observed in cyanide insensitive oxygen reductases, that include also enzymes in which the high spin heme *d* is replaced by a *b*-type heme, as in the case of *B. subtilis* cytochrome *bb*’-type quinol oxygen reductase [134].

iii. Alternative oxygen reductases (AOXs)

The AOXs were mainly described in the mitochondria of higher plants, fungi and protists but are also present in some prokaryotes and animal species (see [135,136] for a review). These are homodimeric enzymes insensitive to cyanide that, similarly to cytochrome *bd* oxygen reductase, do not translocate protons. They contain a non-heme di-iron carboxylate active site for O_2 reduction buried in a four-helix bundle [137], similar to other members of the di-iron protein family. It is

proposed that the protons required for O_2 reduction are the ones derived from quinol oxidation, yet the site where the latter process occurs remains elusive [136].

Nevertheless, since no proton translocation is registered, AOXs allow the presence of partially or completely "uncoupled" pathways. The former pathway relies on the utilization of complex I for the oxidation of NADH, while the latter is observed when the electron transfer from the reducing substrates NADH or succinate to O_2 occurs by alternative NADH dehydrogenases or SQR enzymes, bypassing complexes I, III and IV. This pathway does not contribute to the generation of a proton motive force and therefore the redox energy released during AOX activity is not conserved for the production of ATP, but is dissipated as heat [138]. In plants, this can be of great importance if the main respiratory chain is impaired by factors such as growth inhibition or exposure to subzero temperatures [139]. As for trypanosomes, free-living cells make more use of the standard complexes III and IV, whereas AOX plays a critical role in the survival of the parasite in its bloodstream form, where the organism makes use of the glycolytic pathway as its major source of ATP [140]. The mechanism whereby electrons are distributed between the two electron transport pathways to oxygen is not fully understood, but may depend on the ubiquinone/ubiquinol ratio.

1.1.5 ATP synthase

The transmembrane potential generated by the respiratory chain complexes is used by F_1F_O-ATP synthases to drive ATP synthesis from ADP and inorganic phosphate (P_i) [141]. These are membrane complexes present in mitochondria, bacteria and chloroplasts. Na^+-dependent ATP synthases can also be found in bacteria and are broadly similar to F_1F_O-ATP synthase with respect to structure and function, although through the generation of a Na^+ ion motive force [142]. Vacuolar-type H^+-ATPases (V-ATPases), present in other eukaryotic intracellular organelles, and the archaeal ATPases (A-ATPases) are also close relatives to the

F_1F_O-ATP synthase. ATP synthases have similar structures, irrespectively of their source. Two major structural domains compose the enzyme, *i*) a membrane-extrinsic F_1 domain, where the catalytic site of the enzyme is located, and *ii*) a membrane-intrinsic F_O domain, responsible for the uptake of protons from the P-side of the membrane (Figure 6).

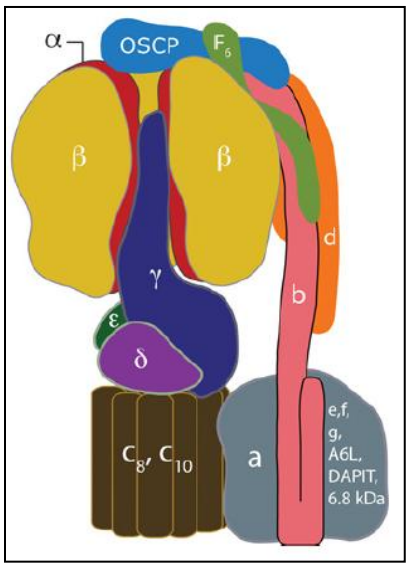

Fig. 6. Representation of the mitochondrial F_1F_O-ATP synthase. The membrane-extrinsic F_1 catalytic domain is located at the upper part of the model and includes the $\alpha_3\beta_3\gamma_1$ rotary motor. This module connects with F_O via subunit γ and a peripheral stalk composed of subunits *OSCP*, *b*, *d* and F_6. F_O domain is responsible for the uptake of protons and bears a *c* ring, with variable *c* subunits, and an associated *a*-subunit which is surrounded by several supernumerary subunits of unidentified roles. Adapted from [1].

The bovine mitochondrial F_1 water-soluble domain is constituted by five different subunits, *α*, *β*, *δ*, *γ* and *ε*, with the stoichiometry $\alpha_3\beta_3\delta_1\gamma_1\varepsilon_1$ (~350 kDa). The $\alpha_3\beta_3\gamma_1$ module represents the central stalk, a rotary motor present in all ATP synthases [143] that is linked to the membrane part of the protein by the *γ*-subunit, which protrudes ~30Å beyond the $\alpha_3\beta_3$ domain, where 3 *α*- and *β*-subunits are alternately arranged [144]. This linkage is reinforced by the *δ*- (known as ε subunit in bacteria and chloroplasts) and *ε*-subunits, the latter having no counterpart in bacterial and chloroplast F_1F_O-ATP synthases [145]. The $\alpha_3\beta_3$ domain is also connected to the F_O domain by the peripheral stalk which, in the case of mitochondria, is composed of subunits *OSCP* (oligomycin sensitivity-conferring protein), *b*, *d* and F_6 [146]. The F_O domain contains a *c* ring, composed of several *c*-subunits (from 8 in the

mammalian mitochondria up to 15 in bacteria and chloroplasts) with one associated *a*-subunit. Other supernumerary subunits that are not essential for cellular growth were described to occur exclusively linked to the mitochondrial ATP synthase F_O domain [147]. Most importantly, *e*- and *g*-subunits, appear to play a major role in the organization of this enzyme in the mitochondrial inner membrane and will be further addressed in the context of the eukaryotic supramolecular assemblies.

The pathway for protons through the F_O domain occurs at the interface of *a*- and *c*-subunits. This proton flow induces a conformational change in the *γ*-subunit that allows the rotation of the F_1 domain, in which each *β* catalytic subunit assumes a different conformation, reflecting different affinities for ATP and ADP plus P_i, leading to ATP synthesis in a process termed "binding change" mechanism. In detail, upon rotation of the *γ*-subunit, one *β* subunit displaying a tight conformation site (T-site) with bound ATP, becomes an open site (O-site), releasing the ATP molecule. Concomitantly, a second β subunit changes from a loose site (L-site), with loosely bound ADP and P_i, to a T-site, where the substrates are tightly bound, allowing ATP synthesis [148]. Since the motors F_1 and F_O are tightly coupled, one complete rotation of the *c* ring causes a complete rotation of the $\alpha_3\beta_3$ domain and thus the formation of three molecules of ATP. In the case of the bovine F_1F_O-ATP synthase, which was proposed to contain 8 *c*-subunits [149], a H^+/ATP ratio of 8/3 would be expected, but since an additional proton is required for adenine nucleotide exchange and phosphate transport across the inner membrane [150], the ratio is corrected to 11/3. This value is also related to the number of ATP molecules synthesized by oxidative phosphorylation for each pair of electrons (P/O ratio), which in the case of mammalian mitochondria is predicted to be 2.7 or 1.6 depending on the electron donor being NADH or succinate, respectively [151].

1.2 Structural and functional organization of aerobic respiratory chains

The solid state model, suggested to explain the structural and functional organization of the mitochondrial aerobic respiratory chain in the membrane was proposed before the isolation and structural analysis of its complexes and is attributed to Keilin and Hartree studies [152] and to the spectrophotometric pioneering studies of Chance and Williams [153], which considered that the mechanism for the electron transfer to dioxygen occurred in one singular cytochrome system, composed of cytochromes *b*, *c*, *a* and a_3, sequentially organized. These catalysts were envisioned as more or less rigidly held together in a framework that would ensure their mutual accessibility and a consequent high catalytic activity.

Shortly after, the isolation and reconstitution of functionally active complexes that participate in the electron transfer process [154,155], as well as the demonstration that the electron transfer from different electron donors mediated by cytochrome *c* and ubiquinone required multiple collisions and occurred across a long range distance, allowed Hackenbrock and colleagues to propose a random collision model in which the respiratory enzymes were not in close contact with each other [156], contradicting any solid state organization of the respiratory chain components. The proposal of this model was based on three fundamental postulates: *i*) all redox components are independent lateral diffusants, from which cytochrome *c* is able to diffuse primarily in three dimensions; *ii*) electron transport is a multicollisional, obstructed, long-range diffusion-coupled kinetic process and *iii*) this process is directly dependent on the redox components' diffusion rates. These observations were supported by the assumption that only 50% of the membrane surface area was occupied by proteins [157], meaning that the respiratory chain complexes and electron carriers would be able to freely diffuse in the membrane independently of each other. In agreement, the fluorescence

recovery after photobleaching (FRAP) technique was used to confirm the existence of lateral diffusion and to determine diffusion coefficients for complexes III, IV as well as cytochrome *c* and ubiquinone [158]. In addition, the rotational mobility of complex IV was detected to be the same either in the presence or absence of complex III and cytochrome *c* [159].

At the same time, experimental evidences revealing that mitochondrial respiratory chain complexes could be found within larger, though dynamic, aggregates, or supercomplexes [160,161], were usually overlooked. In fact, the discovery of bacterial supramolecular assemblies, namely of isolated supercomplexes composed of complexes III and IV from *P. denitrificans* [162] and thermophilic bacterium PS3 [163] was considered a special feature of the prokaryotic respiratory chain. Nevertheless, the later development of a major tool provided strong evidences supporting the existence of a solid state model in the mitochondrial respiratory chain. The solubilization of mammalian or yeast mitochondrial membranes with the mild non-ionic detergent digitonin, and subsequent analysis of the solubilized samples by 1D and 2D Blue Native or Clear Native Polyacrylamide Gel Electrophoresis (BN/CN-PAGE), allowed the discovery of several respiratory chain supercomplexes with distinct complex compositions and stoichiometries [164]. Of special interest, in mammalian mitochondria, a functional supercomplex comprising complexes I, III and IV, was shown to autonomously transfer electrons from NADH to O_2 in the presence of quinones and cytochrome *c* [165], the so-called respirasome. Respirasomes are supercomplexes that contain the necessary respiratory chain complexes to accomplish reduced equivalent electron transfer to oxygen. Other evidences suggesting functional supramolecular associations in the OXPHOS system were also provided by flux control analysis [166,167]. In bovine heart mitochondria it was shown that both complexes I and III exerted rate control on NADH oxidation while a weaker control was exhibited by complex IV, indicating a favorable organization of a I_1+III_2 supercomplex in which complex IV could participate while being concomitantly present in a free form state.

The discovery of supercomplexes in prokaryotic respiratory systems was also achieved through these and other techniques (see [168] for a review), meaning that this type of organization of the respiratory chains is present in every life domain.

The different supercomplex compositions described in both eukaryotic and prokaryotic respiratory chains will be thoroughly discussed in the following sections. The requirements for the establishment of such organizations and their advantages regarding the optimization of the oxidative phosphorylation processes will be addressed in the final sections of this chapter.

1.3 Respiratory chain supercomplexes: an overview

1.3.1 Eukaryotic supercomplexes

i. The $I+III_2+IV_{1-4}$ respirasome

The fundamental features of the supramolecular organization of respiratory chain complexes I, III and IV as a respirasome were revealed in several eukaryotic organisms, the best characterized being the ones described in fungi [169], plants [170,171] and mammalian mitochondria [172,173]. These supramolecular assemblies are present in multiple forms in which up to four copy numbers of complex IV are present. The first structural insight of a $I_1+III_2+IV_1$ respirasome was reported for bovine heart mitochondria, after isolation through electroelution of the BN-PAGE respirasome band and subsequent characterization by transmission electron microscopy [174]. A more refined investigation on this respirasome structure was recently obtained by single particle cryo-electron microscopy analysis, either using amphipol-solubilized supercomplexes [175] or performing tomographic analysis on digitonin-solubilized specimens [172]. By superimposing the tilted view images of the supercomplexes with the available electron

microscopy and X-ray crystal structures of the individual complexes, these authors provided a broader comprehension on the unique interaction between these complexes within the respirasome (Figure 7). Both representations demonstrate that only a few points of direct contact are observed between the three complexes, their matrix portions closer to the membrane being the ones in which the complexes appear to interact.

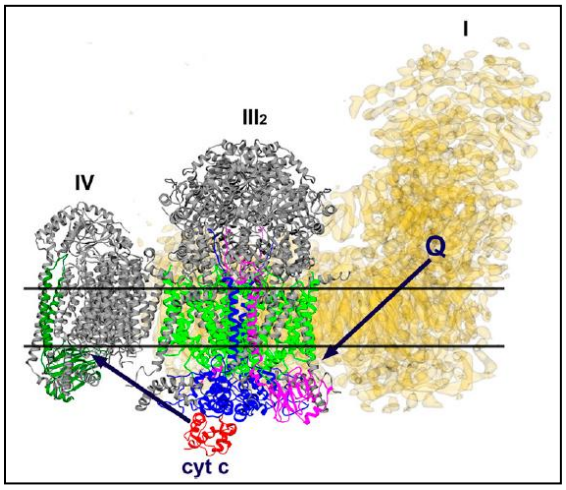

Fig. 7. The I_1+III_2+IV_1 respirasome structure obtained by single particle cryo-electron tomography analysis and superimposition of *Y. lipolytica* complex I and mammalian mitochondrial complexes III_2 and IV structures. Complexes I and III_2 appear to be physiologically linked by the quinone movement, while complexes III_2 and IV cytochrome *c* binding sites are in close proximity, allowing soluble cytochrome *c* to move within a short distance. Black arrows indicate the movement performed by the electron carriers. Adapted from [172].

In detail, complex I ubiquinone binding site and the cytochrome *b* subunit from one complex III monomer appear to face each other at a distance of 13 nm, allowing an efficient electron transfer between both complexes. In the I_1+III_2+IV_1 respirasome, a monomeric complex IV interacts with the remaining monomer of complex III with its convex side, which is the opposite side of the dimer interface observed in the X-ray structure. Specifically, complex III cytochrome *b* and Rieske Fe-S protein subunits are in close proximity with complex IV subunits III, VIa and VIIa, while the soluble cytochrome *c* binding sites on both complexes appear to face each other at a distance of 11 nm, facilitating a putative electron pathway between both complexes [172,175].

ii. The I_{1-2}+III_2 and III_2+IV_{1-4} supercomplexes

In addition to I_1+III_2+IV_{1-4} supercomplexes, several modules of this larger assembly were described in mammalian, plant and fungi mitochondria. In bovine heart mitochondria, the less abundant I_1+III_2 and III_2+IV_1 supercomplexes were obtained using variable digitonin/protein ratios [164,176]. Whether these supercomplexes are degradation products or essential for the assembly of respirasomes in mammalian mitochondria it is still not known. The combination of BN-PAGE data with the calculated stoichiometry of 1:3:6 for bovine heart respiratory complexes I, III, and IV, respectively [177], led the authors to propose a network organization in the bovine inner mitochondrial membrane composed of two different supercomplexes, I_1+III_2+IV_4 and III_2+IV_4, in a 2:1 ratio [177]. This hypothesis was later refined to tentatively assign the regular 26-30 nm intervals of the large 13 x 22 nm particles observed in the electron microscopy analysis of the *Paramecium multimicronucleatum* inner mitochondrial membrane [178], leading to the proposal of a "respiratory string", in which one III_2+IV_4 supercomplex interacts with two $[I_1$+III_2+$IV_4]_2$ respirasomes, the interactions between each supramolecular assembly being mediated by their complex IV dimers [179] (Figure 8).

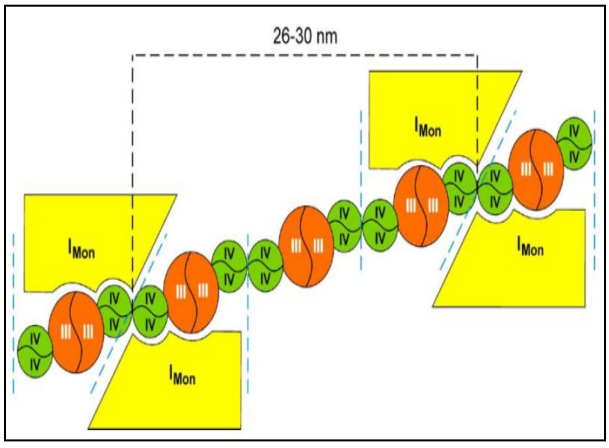

Fig. 8. Respiratory string model proposed for the mammalian mitochondrial respiratory supercomplexes. $[I_1$+III_2+$IV_4]_2$ and III_2+IV_4 supercomplexes are the basic units that constitute this megacomplex and are hypothesized to be linked by complex IV dimeric assemblies provided by each unit, explaining the regular 26-30 nm intervals observed in *P. multimicronucleatum* mitochondria particles. Adapted from [179].

Other respiratory chain supercomplexes that were not detected in mammalian mitochondria were observed in plants and fungi. For instance, although the mammalian mitochondrial complex I is usually found as a monomeric assembly associated with other respiratory chain complexes in the BN-PAGE analysis, in plants and fungi it was also solubilized as a dimeric structure [180-182], either isolated as a I_2 supercomplex [180] or bound to a dimeric complex III in a I_2+III_2 supercomplex [169,182].

In contrast with the mammalian mitochondria, I_1+III_2 supercomplex is the most abundantly detected in plants through BN-PAGE analysis (see [183] for a review), probably due to the presence of a longer complex I hydrophobic module to which complex III is attached [171]. In potato tubers (*Solanum tuberosum*), 2D projection maps of four different OXPHOS supercomplexes were obtained, namely from I_1+III_2, III_2+IV_1, I_1+III_2+IV_1 and I_2+III_2 supercomplexes, allowing the authors to propose a "respiratory string" model different to the one described for the mammalian mitochondria (Figure 9). In detail, this megacomplex organization is represented by several I_2+III_2+IV_2 supercomplex building blocks and the interaction between blocks is mediated by the concave side of each monomeric complex IV [182], which corresponds to its dimeric structure interface, in contrast with the previously described model.

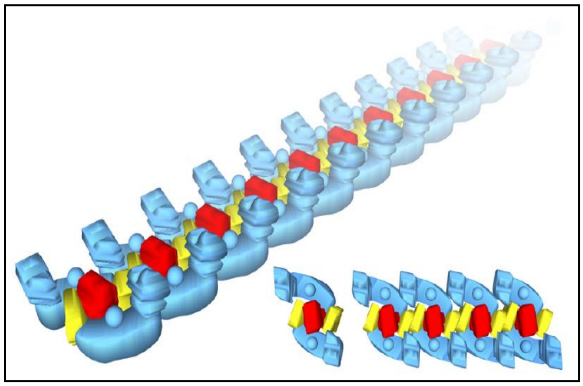

Fig. 9. Schematic representation of the respiratory string model proposed for plant mitochondria. The basic unit for this megacomplex is represented by I_2+III_2+IV_2 supercomplex, which is hypothesized to be linked to identical respirasomes through the monomeric complex IV located on each side of the complex III dimeric assembly. Adapted from [182].

The fungi mitochondrial respiratory chain presents some similarities with the mammalian one with respect to supercomplex composition [180,181]. In addition to the detected I_1+III_2+IV_4 respirasome and the already mentioned I_2, I_1+III_2 and III_2+IV_1 supercomplexes, *N. crassa* respiratory chain was shown to contain a III_2+IV_2 supercomplex, a dimeric complex IV and a unique I_1+IV_1 supercomplex, similarly to what was described for the *Y. lipolytica* respiratory chain [180,184]. In contrast with these organisms, in *S. cerevisiae* the respirasome is absent, since its respiratory chain is devoid of complex I. However, high yields of stable III_2+IV_1 and III_2+IV_2 supercomplexes were detected, the latter being analyzed with further detail through single particle electron microscopy [164,185]. Similarly to the proposed potato tuber respiratory chain I_2+III_2+IV_2 building block, in the *S. cerevisiae* III_2+IV_2 supercomplex, complex IV is attached to complex III_2 as a monomer on two opposite sides, leaving its concave side open for putative protein-protein interactions [185].

Although complex II association in supercomplexes is hardly detectable in BN-PAGE, several studies using different approaches identified this complex as part of higher molecular mass assemblies. In mitochondria of mouse fibroblast cells, complex II was found to be part of a functional respirasome together with complex I, III and IV [165]. Moreover, there are also evidences in *S. cerevisiae* respiratory chain for an interaction between complex II either with complex III [186] or complex IV [167].

The AOXs from plants, fungi and protists were also shown to form supercomplexes with complex III, as in the case of tomato (*Lycopersicon esculentum*) and amoeba (*Acanthamoeba castellanii*) [187] and with supercomplexes I_1+IV_1 and IV_2, as reported in *N. crassa* mutant cells devoid of complex III [188]. In contrast, *Y. lipolytica* AOXs do not seem to associate with other components of the respiratory chain in the logarithmic growth phase, while in the same conditions the external NAD(P)H dehydrogenase NDE2 was shown to interact with the classic cytochrome *c* pathway, specifically with complex IV [184].

Due to the observed variations in the amount and composition of supercomplexes between different cell types, a "plasticity model" was proposed, wherein different combinations of supercomplexes were suggested to be present as a consequence of the cell type or the physiological state encountered [165]. In agreement, supercomplex composition in potato mitochondria was shown to vary with pH and oxygen availability in a dynamic way [189].

iii. The F_1F_O-ATP synthase supramolecular assemblies

In addition to the supramolecular organization of the OXPHOS system, the eukaryotic F_1F_O-ATP synthase was also reported to assemble as dimers and homo-oligomers, namely in mammalian [190], plant [183] and fungi [181,191] mitochondria. F_1F_O-ATP synthase dimers are V-shaped supercomplexes (Figure 10) in which the membrane parts of both monomers are joined in an angle that varies between species and is considerably dependent on the detergent solubilization procedure [183,192,193]. The first characterization of F_1F_O-ATP synthase dimers was reported in the *S. cerevisiae* respiratory chain [194], where the previously mentioned supernumerary *e*- and *g*-subunits, also present in the mammalian enzyme, were described as being essential for its dimeric stability. In addition, the dimeric *a*-subunit was proposed to be the bridging module between two ATP synthase monomers [195].

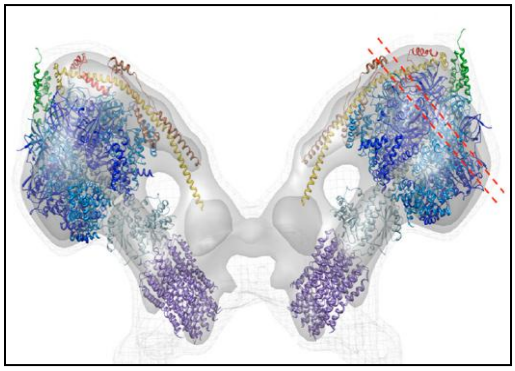

Fig. 10. The F_1F_O-ATP synthase dimeric supercomplex obtained by cryo-electron microscopy analysis and superimposition of *S. cerevisiae* F_1/rotor ring assembly and mammalian mitochondrial peripheral stalk X-ray crystal structures. The V-shaped dimer interface is located in the membrane between the two peripheral stalks. Adapted from [199].

Further characterization of the eukaryotic F_1F_O-ATP synthase through cryo-electron tomography of mitochondria and mitochondrial membranes from six different species [196,197] allowed its identification in two parallel rows, or ribbons, of up to 80 dimers, preferentially located along the highly curved cristae ridges of this organelle. The solubilization and BN-PAGE detection of tetrameric, hexameric, and octameric F_1F_O-ATP synthases, suggested that these oligomers are assembled from ATP synthase dimeric building blocks to form the long ribbons [198]. Of special interest, a tight relationship between ATP synthase oligomerization and cristae morphogenesis could be established in yeast mutants devoid of *e*- and *g*-subunits. In these strains, the oligomerization of ATP synthase is no longer achieved and consequently the small invaginations of the inner mitochondrial membrane disappear. Instead, the membrane appears extended and organized in a number of separate vesicles, with few or no cristae, as an "onion"-like structure, where the ATPase activity is highly reduced [199,200]. Although essential for oligomerization, *e*- and *g*-subunits were never shown to mediate interaction between ATP synthase dimers. Instead, it was proposed that the membrane curvature induced by ATP synthase dimer is sufficient to drive the formation of long dimer rows [199]. These rows are ubiquitous in all mitochondria, including protists [201], but their organization in the membrane varies. While dimer rows in yeast and vertebrates run along ridges of lamellar cristae [196,197], the ones observed in *Polytomella* and *Paramecium* are located around tubular cristae in a helical arrangement [202].

1.3.2 Prokaryotic supercomplexes

Prokaryotic respiratory chains display a great flexibility that is reflected in their ability to cope with several different environmental conditions. This variability is correlated with the ability of promoting different supramolecular organizations to the ones described for the eukaryotic respiratory chains. To date, the isolation of

several supercomplexes has been reported in bacteria and archaea. Although only few representatives have been studied and no structural data is yet available, this apparently conserved evolutionary feature was mainly demonstrated through the same techniques used to isolate eukaryotic supercomplexes, namely BN/CN-PAGE and mass spectrometry analysis of digitonin solubilized membranes, as well as UV-visible spectroscopy analysis and enzymatic activity measurements, among others.

i. Gram negative bacteria

The supercomplexes that most resemble the mitochondrial ones are those reported in *P. denitrificans* respiratory chain. Although presenting different stoichiometries, the authors were able to isolate, through hydroxylapatite chromatography and gel filtration techniques, a fully functional I_1+III_4+IV_4 supercomplex that is, similarly to the mammalian mitochondria respirasome, essential for the stabilization of complex I [162,203]. III_4+IV_4 and III_4+IV_2 supercomplexes were also detected in this organism's multi-branched respiratory chain that comprises also cytochromes *ba*$_3$ quinol oxygen reductase and *cbb*$_3$ oxygen reductase along with other dehydrogenases besides complex I, that were not found associated with other complexes.

Overall, supercomplexes comprising complexes III (*bc*$_1$ complex) and IV (cytochrome *caa*$_3$ oxygen reductase), or analogues, are widespread among the bacterial supramolecular assemblies analyzed so far, revealing a tight regulation of the "canonical" cytochrome *c* pathway, regardless of the alternative pathways available. This is the case for the Gram negative bacterium *Bradyrhizobium japonicum* respiratory chain, where a functional association between *bc*$_1$ complex and cytochrome *cbb*$_3$ oxygen reductase, which belongs to heme-copper oxygen reductases C-family, was reported [204]. Similarly, a supercomplex retaining the quinol:oxygen oxidoreductase activity was reported in *R. marinus*, which is devoid of the typical *bc*$_1$ complex, as previously mentioned [102]. An alternative complex

III (ACIII) was described to play its role in a supercomplex wherein cytochrome *caa*$_3$ oxygen reductase is also present [205].

Of special interest are the supramolecular assemblies described in *Aquifex aeolicus* respiratory chain, where two putative complementary respiratory pathways for sulfur reduction and sulfur oxidation seem to be regulated by two functional supercomplexes [206]. One is a respirasome that concomitantly catalyzes the reduction of oxygen with the oxidation of hydrogen sulfide (H_2S), and is composed of a sulfide quinone reductase, a dimeric *bc*$_1$ complex and a unique cytochrome *ba*$_3$ oxygen reductase that was proposed to oxidize both cytochrome *c* and ubiquinol [207,208]. The other supercomplex assembles a hydrogenase with a sulfur reductase, and couples the reduction of cytoplasmic sulfur with the periplasmic oxidation of molecular hydrogen (H_2) [209].

A unique respiratory chain supercomplex involving both bacterium external and internal membranes was reported in *Acidithiobacillus ferrooxidans* [210,211]. This supercomplex oxidizes Fe(II) through the high molecular mass *c*-type cytochrome *C*$_2$ (Cyc2) located in the external membrane and transfers the electrons to the periplasmic blue copper protein rusticyanin. The electrons can then be transported in two branches within the same supercomplex, *i*) an oxygen reduction "downhill" electron pathway that involves further associations with the internal membrane-bound *c*-type cytochrome *C*$_4$ (Cyc1) and the cytochrome *caa*$_3$ oxygen reductase, or *ii*) a NAD^+ reduction "uphill" pathway where the electrons are transferred to a *bc*$_1$ complex *via* another internal membrane-bound *c*-type cytochrome *C*$_4$ (CycA1).

ii. Gram positive bacteria

As previously mentioned, the thermophilic bacterium PS3 respiratory chain supramolecular assemblies were detected before the development of milder solubilization procedures and subsequent BN/CN-PAGE analysis, implying that the tight regulation of the "canonical" cytochrome *c* pathway in supercomplexes is also observed in Gram positive bacteria [163]. Through immunoprecipitation, gel

filtration analysis and enzymatic activity measurements, the authors were able to isolate a 380 kDa bc_1:caa_3 supercomplex with both TMPD/ascorbate: and cytochrome *c*:oxygen oxidoreductase activities. Since Gram positive bacteria are devoid of external membrane, the cytochrome *c* pathway is commonly dependent on membrane-anchored *c*-type cytochromes, either *via* a transmembrane helix, a lipid moiety or directly fused as integral domains of enzyme subunits [163,212,213]. In *Mycobacterium smegmatis* [214] and *Corynebacterium glutanicum* [215] respiratory chains a supercomplex comprising *bcc* complex and cytochrome aa_3 oxygen reductase was described. These species' genomes do not encode either soluble or independent membrane-bound cytochrome *c*, nevertheless, the c_1 subunit of the classical bc_1 complex includes a binding site for a second heme *c*, hence termed *bcc* complex [216,217]. In addition, 30 extra amino acids containing many charged residues were found to be encoded by *C. glutanicum* cytochrome aa_3 oxygen reductase subunit II gene [216]. These features appear to be of great importance in establishing a viable electron transfer pathway in the absence of a mobile cytochrome *c*, to which a supramolecular organization would be theoretically advantageous.

A unique supercomplex involving F_1F_O-ATP synthase and cytochrome caa_3 oxygen reductase was described in the alkaliphilic *Bacillus pseudofirmus* OF4, using methods of differential scanning calorimetry (DSC) and saturation transfer electron paramagnetic resonance (STEPR) [218].

iii. Archaea

A unique combination between respiratory chain complexes III and IV was also reported for the archaeal domain, namely in *Sulfolobus acidocaldarius* and *Sulfolobus* sp. Strain 7 [104,219,220]. *S. acidocaldarius* supercomplexes SoxABCD and SoxM were described in better detail.

SoxABCD is composed of four subunits, from which two (SoxB and SoxC) contain two *a*-type hemes. SoxA is similar to complex IV subunit II, although

devoid of the binuclear Cu_A centre. SoxB displays similarity with complex IV subunit I and contains the same prosthetic groups, namely the *a*-type heme and the binuclear Cu_B/a_3 catalytic site. SoxC subunit, as previously mentioned, is a homolog of complex III cytochrome *b* subunit, but the di-heme redox component is exclusively composed of *a*-type hemes [104].

SoxM supercomplex is composed of six subunits (SoxEFGHIM) arranged in two functional subcomplexes which are similar to complexes III and IV, linked by the blue copper protein sulfocyanin (SoxE subunit). One subcomplex comprises subunits SoxM and SoxH that contain two *b*-type hemes (*b* and b_3), a Cu_B centre and a binuclear Cu_A centre, being homologous to type A heme-copper oxygen reductases. The other subcomplex is composed of subunits SoxF, a homolog of complex III Rieske Fe-S protein subunit with an attached binuclear [Fe-S] cluster, and SoxG, a structural analog to complex III cytochrome *b* subunit which, similarly to SoxC subunit of SoxABCD supercomplex, comprises two *a*-type hemes [103,221], as previously mentioned. Since *c*-type cytochromes are absent in *S. acidocaldarius* respiratory chain, membrane-anchored sulfocyanin mediates the electron transfer between SoxF and SoxH binuclear Cu_A centre [219].

Finally, functional supercomplexes comprising a membrane-bound hydrogenase and a sulfur reductase, similarly to the already described *A. aeolicus* supramolecular assembly, were reported in three hyperthermophilic archaeons, *Pyrococcus abyssi* [222], *Thermoproteus neutrophilus* [223] and *A. ambivalens* [224].

1.4 Requirements for supramolecular organization

Eukaryotic and prokaryotic respiratory chain complexes' structure and functional integrity are severely influenced by the surrounding membrane composition and arrangement, the interactions established with lipid molecules or other proteins being the major factors that ensure a correct assembly of supramolecular structures. So far, the influence of those key players in the organization of such structures has been extensively studied in mitochondrial supercomplexes and can be correlated in some aspects with the ones reported in prokaryotes.

1.4.1 Lipid-protein interactions

The lipid content of the inner mitochondrial membrane comprises different concentrations of cardiolipin, phosphatidylcholine, phosphatidylethanolamine, phosphatidylinositol and neutral lipids [225]. Of these, the most abundant phospholipid cardiolipin, which is also a major participant in the bacterial membrane [226], has the ability to form dimeric structures that are essential in filling cavities at protein interfaces, thus stabilizing interactions between individual subunits of oligomeric proteins as well as between higher order supramolecular structures (see [227] for a review). In fact, the absolute requirement of this phospholipid for the enzymatic activities of mitochondrial complexes I, III and IV, suggests that it plays an essential role in the electron transfer process [228,229]. In addition, *S. cerevisiae* complex II was shown to require cardiolipin for optimal function and assembly [230]. With respect to respiratory chain supramolecular assemblies, several studies have reported the influence of this phospholipid in maintaining their function and structural arrangement or its importance in the oligomerization of F_1F_O-ATP synthase [231]. The supercomplex III_2+IV_2 reported in the *S. cerevisiae* respiratory chain almost completely dissociates in a mutant strain devoid of cardiolipin, despite the abnormal elevated phosphatidylethanolamine

and phosphatidylglycerol levels [232]. Similarly, concentration levels of mammalian supercomplexes I_1+III_2 and I_1+III_2+IV_1 drastically decreased in Barth syndrome patients whose mitochondria bear a lower cardiolipin content, in contrast with the reported increased levels of monomeric complex IV [233]. As previously mentioned, the mammalian respirasome I_1+III_2+IV_1 structural analysis demonstrated that only a few points of direct contact were observed between the three complexes. Indeed, the authors suggest that the remaining gaps observed at the complexes' interfaces, specially between complexes III_2 and IV, may be occupied by cardiolipin molecules [172].

In prokaryotes, cardiolipin has also been shown to restore the activity of a number of purified respiratory chain complexes such as NDH-1 [234], lactate dehydrogenase [235], SQR [84] and cytochrome *bo*$_3$ oxygen reductase [236]. In addition, cardiolipin molecules were found to be essential for the homo-oligomerization of specific prokaryotic complexes, such as the trimeric and dimeric assemblies of the *E. coli* formate dehydrogenase FDH-N [237] and nitrate reductase A complexes [238], respectively.

1.4.2 Protein-protein interactions

Proteins other than respiratory complexes can also be essential for the assembly and function of respiratory chain supercomplexes. This is the case for the *S. cerevisiae* protein factors Rcf1 and Rcf2, termed respiratory supercomplex factors 1 and 2, respectively, which were shown to independently associate with III_2+IV_1 and III_2+IV_2 supercomplexes [239]. In addition, Rcf1 mammalian homolog, Hig2A, was also found to be associated with mammalian III_2+IV_1 supercomplex while the depletion of this protein was shown to severely decrease all the supercomplexes containing complex IV, including the respirasome I_1+III_2+IV_1 [240]. Interestingly, Rcf1 homologues are also present in prokaryotes, namely in the α-proteobacterium *B. japonicum*. Since this organism respiratory chain bears a

supercomplex involving a cytochrome *cbb*$_3$ oxygen reductase, it was hypothesized that the Rcf1 homolog should play a role in the stabilization or function of the *bc*$_1$:*cbb*$_3$ supercomplex [168].

Further interaction partners that co-assemble with the OXPHOS supercomplexes were also described, namely through the interactions between *i*) *S. cerevisiae* ADP/ATP carrier and III_2+IV_2 supercomplex [241], *ii*) *Arabidopsis thaliana* carbonic anhydrase subunits and complex I [242], and *iii*) mammalian respirasomes and fatty acid β-oxidation complex (FAO) [243].

1.4.3 Membrane microcompartmentalization

Eukaryotic membrane components are often organized in small domains of variable composition and length scale that are essential for the establishment and the heterogeneous distribution of supramolecular assemblies. The general advantage of this microcompartmentalization is to facilitate the diffusion of substrates needed for an efficient electron transfer process as well as to prevent energy losses or futile proton escape (see [244] for a review). The concentration of respiratory chain proteins in specific domains is clearly observed on the inner mitochondrial membrane enlarged surface (cristae), which further organizes in three additional microcompartments with different lipid and protein compositions that define protein functionality [245,246]. Moreover, protein concentration is seen as a determinant factor for supercomplex organization in mitochondria [247]. This functional role of the mitochondrial cristae membrane was recently reported in an attempt to explain the localization of F_1F_O-ATP synthase oligomeric structures along the highly curved cristae ridges and of respiratory chain supercomplexes in the adjacent membrane regions [196]. Davies and colleagues proposed that this conserved arrangement would allow a preferential diffusion of protons along the membrane from the respiratory chain proton-translocating enzymes toward the

proton sinks established by the ATP synthase dimer rows, instead of diffusing equally in multiple directions.

Similarly, the prokaryotic cytoplasmic membrane is also a heterogeneous and highly dynamic structure with defined membrane microenvironments [248]. For instance, several aerobic respiratory chain complexes from *E. coli* and *B. subtilis* were shown to be concentrated in unevenly distributed mobile patches [249,250], leading the authors to propose the existence of prokaryotic compartments specialized in respiratory processes, termed respirazones [251].

1.5 Supercomplex advantages

Several advantages are proposed for the organization of the aerobic respiratory chains in a solid state model. Besides the already mentioned advantage of F_1F_O-ATP synthase ribbons in shaping the inner mitochondrial membrane ultra-structure [196,252], respiratory chain supercomplexes may optimize the oxidative phosphorylation processes by *i*) promotion of substrate channeling with concomitant enhancement of electron transfer rates [247], *ii*) stabilization of individual complexes [173], and *iii*) regulation of reactive oxygen species production [253].

1.5.1 Substrate channeling

The greatest advantage envisioned for the requirement of supramolecular structures in the respiratory chain electron transfer processes is the substrate channeling and confinement of the mobile electron carriers, namely quinones and cytochrome *c*. Although few functional analyses are available regarding this issue, there are indications that such a role may be performed by mammalian mitochondrial and *P. denitrificans* supercomplexes.

In mammalian mitochondria, metabolic flux control analysis of NADH oxidation has provided evidences suggesting that both complexes I and III exhibit high flux control coefficients, supporting the existence of a quinone electron channeling within I_1+III_2 supercomplex [254]. A similar control seems to be exhibited by *P. denitrificans* I_1+III_4+IV_4 respirasome, where a specific enrichment in ubiquinone was demonstrated [203]. Other fully functional respirasomes, namely from mammalian mitochondria, were shown to promote electron transfer from NADH or succinate to oxygen in polarographic analyses [165].

As previously mentioned, in the resolved 3D structures of the bovine heart I_1+III_2+IV_1 respirasome, similar results have indicated that ubiquinone and cytochrome *c* binding sites from complex I and III or complex III and IV, respectively, were separated by short distances (11 to 13 nm) [172,175]. Althoff and colleagues showed that both ubiquinol and cytochrome *c* molecules were present in the respirasome enriched fractions [175]. However, since a detailed knowledge of the interacting sites' molecular structure is still lacking, protein conformational changes or restricted diffusion (microdiffusion) of the redox components within the space between binding sites should not be disregarded.

1.5.2 Stabilization of individual complexes

The observation that supramolecular assemblies are able to increase the stability of individual complexes was mainly provided by the studies in mammalian and *P. denitrificans* respiratory chains [203].

In mammalian mitochondria, free dimeric complex III and monomeric complex IV were always detected in BN-PAGE after solubilization, complex I monomeric assembly being only detected under harsher solubilization conditions [164,176]. In fact, only 14-16% of total bovine mitochondrial complex I, or 10% of the human enzyme, was found in the free form, in the presence of digitonin [177,255], reflecting a possible structural dependence of this complex towards complex III

and IV in the mammalian respiratory chain, under physiological conditions [256]. In agreement, primary genetic assembly defects of human mitochondrial complex III led to a secondary loss of complex I and prevented respirasome formation, confirming that complex I stability and assembly are dependent on the correct assembly of this respiratory chain component [257]. Moreover, this interdependence was recently enlightened in the characterization of the respirasome biosynthetic process, which was demonstrated to be essential for complex I final assembly and activation [255].

In contrast, as previously mentioned, fungi respiratory complex I can be obtained as an isolated stable dimeric assembly (I_2 supercomplex) [180]. In agreement, *N. crassa* and *Podospora anserina* respiratory chain mutants devoid of complex III revealed that the absence of this complex is not correlated with a deficiency in complex I assembly [188] or activity [258].

1.5.3 Reactive oxygen species regulation

Mitochondria are generally regarded as a major source of ROS (see [259] for a review). Within this organelle, respiratory chain complexes I, II and III are considered the main producers of superoxide and derived ROS [260-262], which contribute to mitochondrial disfunction in a wide range of pathologies as well as in redox signaling from this organelle to the rest of the cell [263,264].

Superoxide production from complex I is observed when *i*) ATP is being slowly produced and consequently a high proton motive force and a reduced quinone pool are observed in the OXPHOS process or *ii*) the NADH/NAD^+ ratio in the matrix is elevated. FMN and the [Fe-S] cluster N2 are potential sites for oxygen reduction, hence the potential source of ROS production in complex I [265]. However, it should not be excluded that other [Fe-S] clusters may react with oxygen, due to their negative reduction potential and availability of paramagnetic

states. In addition, superoxide production in complex III occurs at the Q_o binding site and is stimulated by the presence of oxidized ubiquinone [260].

Several studies have reported a role of mitochondrial respiratory chain supercomplexes in limiting ROS production. For example, a dissociation of mammalian I_1+III_2 supercomplexes is directly linked to a concomitant increase of ROS production [266]. Slightly different conformations of complex I are observed when its structure is compared on the isolated form or as part of the mammalian I_1+III_2+IV_1 respirasome [174]. In this context, if complex I is associated within a supramolecular assembly, its FMN-containing subunit may be less prone to interact with oxygen, thus limiting the ROS production under stress conditions. Superoxide production is also observed in prokaryotic cells, but a correlation between supramolecular assemblies and ROS regulation was not yet established.

1.7 References

[1] Walker, J.E. (2013). The ATP synthase: the understood, the uncertain and the unknown. Biochem Soc Trans 41, 1-16.

[2] Boyer, P.D. (1998). ATP synthase--past and future. Biochim Biophys Acta 1365, 3-9.

[3] Schultz, B.E. and Chan, S.I. (2001). Structures and proton-pumping strategies of mitochondrial respiratory enzymes. Annu Rev Biophys Biomol Struct 30, 23-65.

[4] Saraste, M. (1999). Oxidative phosphorylation at the fin de siècle. Science 283, 1488-93.

[5] Mitchell, P. (1966). Chemiosmotic coupling in oxidative and photosynthetic phosphorylation. Biol Rev Camb Philos Soc 41, 445-502.

[6] Pereira, M.M., Bandeiras, T.M., Fernandes, A.S., Lemos, R.S., Melo, A.M.P. and Teixeira, M. (2004). Respiratory chains from aerobic thermophilic prokaryotes. J Bioenerg Biomembr 36, 93-105.

[7] Melo, A.M.P., Bandeiras, T.M. and Teixeira, M. (2004). New insights into type II NAD(P)H:quinone oxidoreductases. Microbiol Mol Biol Rev 68, 603-16.

[8] John, P. and Whatley, F.R. (1975). *Paracoccus denitrificans* and the evolutionary origin of the mitochondrion. Nature 254, 495-8.

[9] de Gier, J.W., Lübben, M., Reijnders, W.N., Tipker, C.A., Slotboom, D.J., van Spanning, R.J., Stouthamer, A.H. and van der Oost, J. (1994). The terminal oxidases of *Paracoccus denitrificans*. Mol Microbiol 13, 183-96.

[10] Rasmusson, A.G., Soole, K.L. and Elthon, T.E. (2004). Alternative NAD(P)H dehydrogenases of plant mitochondria. Annu Rev Plant Biol 55, 23-39.

[11] Verkhovsky, M.I. and Bogachev, A.V. (2010). Sodium-translocating NADH:quinone oxidoreductase as a redox-driven ion pump. Biochim Biophys Acta 1797, 738-46.
[12] Walker, J.E. (1992). The NADH:ubiquinone oxidoreductase (complex I) of respiratory chains. Q Rev Biophys 25, 253-324.
[13] Wikström, M. (1984). Two protons are pumped from the mitochondrial matrix per electron transferred between NADH and ubiquinone. FEBS Lett 169, 300-4.
[14] Carroll, J., Shannon, R.J., Fearnley, I.M., Walker, J.E. and Hirst, J. (2002). Definition of the nuclear encoded protein composition of bovine heart mitochondrial complex I. Identification of two new subunits. J Biol Chem 277, 50311-7.
[15] Ragan, C.I. and Racker, E. (1973). Partial resolution of the enzymes catalyzing oxidative phosphorylation. 28. The reconstitution of the first site of energy conservation. J Biol Chem 248, 2563-9.
[16] Leonard, K., Haiker, H. and Weiss, H. (1987). Three-dimensional structure of NADH: ubiquinone reductase (complex I) from *Neurospora* mitochondria determined by electron microscopy of membrane crystals. J Mol Biol 194, 277-86.
[17] Hofhaus, G., Weiss, H. and Leonard, K. (1991). Electron microscopic analysis of the peripheral and membrane parts of mitochondrial NADH dehydrogenase (complex I). J Mol Biol 221, 1027-43.
[18] Hunte, C., Zickermann, V. and Brandt, U. (2010). Functional modules and structural basis of conformational coupling in mitochondrial complex I. Science 329, 448-51.
[19] Guénebaut, V., Schlitt, A., Weiss, H., Leonard, K. and Friedrich, T. (1998). Consistent structure between bacterial and mitochondrial NADH:ubiquinone oxidoreductase (complex I). J Mol Biol 276, 105-12.
[20] Zickermann, V., Kerscher, S., Zwicker, K., Tocilescu, M.A., Radermacher, M. and Brandt, U. (2009). Architecture of complex I and its implications for electron transfer and proton pumping. Biochim Biophys Acta 1787, 574-83.
[21] Brandt, U. (2006). Energy converting NADH:quinone oxidoreductase (complex I). Annu Rev Biochem 75, 69-92.
[22] Remacle, C., Barbieri, M.R., Cardol, P. and Hamel, P.P. (2008). Eukaryotic complex I: functional diversity and experimental systems to unravel the assembly process. Mol Genet Genomics 280, 93-110.
[23] Chomyn, A., Cleeter, M.W., Ragan, C.I., Riley, M., Doolittle, R.F. and Attardi, G. (1986). *URF6*, last unidentified reading frame of human mtDNA, codes for an NADH dehydrogenase subunit. Science 234, 614-8.
[24] Hirst, J., Carroll, J., Fearnley, I.M., Shannon, R.J. and Walker, J.E. (2003). The nuclear encoded subunits of complex I from bovine heart mitochondria. Biochim Biophys Acta 1604, 135-50.
[25] Angerer, H. et al. (2011). A scaffold of accessory subunits links the peripheral arm and the distal proton-pumping module of mitochondrial complex I. Biochem J 437, 279-88.
[26] Au, H.C., Seo, B.B., Matsuno-Yagi, A., Yagi, T. and Scheffler, I.E. (1999). The *NDUFA1* gene product (MWFE protein) is essential for activity of complex I in mammalian mitochondria. Proc Natl Acad Sci U S A 96, 4354-9.
[27] Friedrich, T. and Scheide, D. (2000). The respiratory complex I of bacteria, archaea and eukarya and its module common with membrane-bound multisubunit hydrogenases. FEBS Lett 479, 1-5.

[28] Finel, M. (1998). Organization and evolution of structural elements within complex I. Biochim Biophys Acta 1364, 112-21.
[29] Mathiesen, C. and Hägerhäll, C. (2003). The 'antiporter module' of respiratory chain complex I includes the MrpC/NuoK subunit -- a revision of the modular evolution scheme. FEBS Lett 549, 7-13.
[30] Albracht, S.P. (1993). Intimate relationships of the large and the small subunits of all nickel hydrogenases with two nuclear-encoded subunits of mitochondrial NADH: ubiquinone oxidoreductase. Biochim Biophys Acta 1144, 221-4.
[31] Mathiesen, C. and Hägerhäll, C. (2002). Transmembrane topology of the NuoL, M and N subunits of NADH:quinone oxidoreductase and their homologues among membrane-bound hydrogenases and bona fide antiporters. Biochim Biophys Acta 1556, 121-32.
[32] Sazanov, L.A. and Hinchliffe, P. (2006). Structure of the hydrophilic domain of respiratory complex I from *Thermus thermophilus*. Science 311, 1430-6.
[33] Baradaran, R., Berrisford, J.M., Minhas, G.S. and Sazanov, L.A. (2013). Crystal structure of the entire respiratory complex I. Nature 494, 443-8.
[34] Moparthi, V.K. and Hägerhäll, C. (2011). The evolution of respiratory chain complex I from a smaller last common ancestor consisting of 11 protein subunits. J Mol Evol 72, 484-97.
[35] Esterházy, D., King, M.S., Yakovlev, G. and Hirst, J. (2008). Production of reactive oxygen species by complex I (NADH:ubiquinone oxidoreductase) from *Escherichia coli* and comparison to the enzyme from mitochondria. Biochemistry 47, 3964-71.
[36] Efremov, R.G., Baradaran, R. and Sazanov, L.A. (2010). The architecture of respiratory complex I. Nature 465, 441-5.
[37] Page, C.C., Moser, C.C., Chen, X. and Dutton, P.L. (1999). Natural engineering principles of electron tunnelling in biological oxidation-reduction. Nature 402, 47-52.
[38] Efremov, R.G. and Sazanov, L.A. (2011). Structure of the membrane domain of respiratory complex I. Nature 476, 414-20.
[39] Belevich, G., Knuuti, J., Verkhovsky, M.I., Wikström, M. and Verkhovskaya, M. (2011). Probing the mechanistic role of the long α-helix in subunit L of respiratory Complex I from *Escherichia coli* by site-directed mutagenesis. Mol Microbiol 82, 1086-95.
[40] Steuber, J., Schmid, C., Rufibach, M. and Dimroth, P. (2000). Na^+ translocation by complex I (NADH:quinone oxidoreductase) of *Escherichia coli*. Mol Microbiol 35, 428-34.
[41] Stolpe, S. and Friedrich, T. (2004). The *Escherichia coli* NADH:ubiquinone oxidoreductase (complex I) is a primary proton pump but may be capable of secondary sodium antiport. J Biol Chem 279, 18377-83.
[42] Batista, A.P., Fernandes, A.S., Louro, R.O., Steuber, J. and Pereira, M.M. (2010). Energy conservation by *Rhodothermus marinus* respiratory complex I. Biochim Biophys Acta 1797, 509-15.
[43] Gemperli, A.C., Dimroth, P. and Steuber, J. (2002). The respiratory complex I (NDH I) from *Klebsiella pneumoniae*, a sodium pump. J Biol Chem 277, 33811-7.
[44] Batista, A.P., Marreiros, B.C. and Pereira, M.M. (2012). The role of proton and sodium ions in energy transduction by respiratory complex I. IUBMB Life 64, 492-8.
[45] Degli Esposti, M. (1998). Inhibitors of NADH-ubiquinone reductase: an overview. Biochim Biophys Acta 1364, 222-35.

[46] Rasmusson, A.G., Svensson, A.S., Knoop, V., Grohmann, L. and Brennicke, A. (1999). Homologues of yeast and bacterial rotenone-insensitive NADH dehydrogenases in higher eukaryotes: two enzymes are present in potato mitochondria. Plant J 20, 79-87.

[47] de Vries, S. and Grivell, L.A. (1988). Purification and characterization of a rotenone-insensitive NADH:Q6 oxidoreductase from mitochondria of *Saccharomyces cerevisiae*. Eur J Biochem 176, 377-84.

[48] Melo, A.M.P., Duarte, M. and Videira, A. (1999). Primary structure and characterisation of a 64 kDa NADH dehydrogenase from the inner membrane of *Neurospora crassa* mitochondria. Biochim Biophys Acta 1412, 282-7.

[49] Uyemura, S.A., Luo, S., Vieira, M., Moreno, S.N. and Docampo, R. (2004). Oxidative phosphorylation and rotenone-insensitive malate- and NADH-quinone oxidoreductases in *Plasmodium yoelii yoelii* mitochondria *in situ*. J Biol Chem 279, 385-93.

[50] Björklöf, K., Zickermann, V. and Finel, M. (2000). Purification of the 45 kDa, membrane bound NADH dehydrogenase of *Escherichia coli* (NDH-2) and analysis of its interaction with ubiquinone analogues. FEBS Lett 467, 105-10.

[51] Gomes, C.M., Bandeiras, T.M. and Teixeira, M. (2001). A new type-II NADH dehydrogenase from the archaeon *Acidianus ambivalens*: characterization and in vitro reconstitution of the respiratory chain. J Bioenerg Biomembr 33, 1-8.

[52] Wierenga, R.K., Terpstra, P. and Hol, W.G. (1986). Prediction of the occurrence of the ADP-binding beta alpha beta-fold in proteins, using an amino acid sequence fingerprint. J Mol Biol 187, 101-7.

[53] Kerscher, S.J. (2000). Diversity and origin of alternative NADH:ubiquinone oxidoreductases. Biochim Biophys Acta 1459, 274-83.

[54] Duarte, M., Peters, M., Schulte, U. and Videira, A. (2003). The internal alternative NADH dehydrogenase of *Neurospora crassa* mitochondria. Biochem J 371, 1005-11.

[55] Melo, A.M.P., Duarte, M., Møller, I.M., Prokisch, H., Dolan, P.L., Pinto, L., Nelson, M.A. and Videira, A. (2001). The external calcium-dependent NADPH dehydrogenase from *Neurospora crassa* mitochondria. J Biol Chem 276, 3947-51.

[56] Carneiro, P., Duarte, M. and Videira, A. (2004). The main external alternative NAD(P)H dehydrogenase of *Neurospora crassa* mitochondria. Biochim Biophys Acta 1608, 45-52.

[57] Carneiro, P., Duarte, M. and Videira, A. (2007). The external alternative NAD(P)H dehydrogenase NDE3 is localized both in the mitochondria and in the cytoplasm of *Neurospora crassa*. J Mol Biol 368, 1114-21.

[58] Goffeau, A. et al. (1996). Life with 6000 genes. Science 274, 546, 563-7.

[59] Velázquez, I. and Pardo, J.P. (2001). Kinetic characterization of the rotenone-insensitive internal NADH: ubiquinone oxidoreductase of mitochondria from *Saccharomyces cerevisiae*. Arch Biochem Biophys 389, 7-14.

[60] Iwata, M., Lee, Y., Yamashita, T., Yagi, T., Iwata, S., Cameron, A.D. and Maher, M.J. (2012). The structure of the yeast NADH dehydrogenase (Ndi1) reveals overlapping binding sites for water- and lipid-soluble substrates. Proc Natl Acad Sci U S A 109, 15247-52.

[61] Luttik, M.A., Overkamp, K.M., Kötter, P., de Vries, S., van Dijken, J.P. and Pronk, J.T. (1998). The *Saccharomyces cerevisiae* NDE1 and NDE2 genes encode separate mitochondrial NADH dehydrogenases catalyzing the oxidation of cytosolic NADH. J Biol Chem 273, 24529-34.

[62] Matsushita, K., Ohnishi, T. and Kaback, H.R. (1987). NADH-ubiquinone oxidoreductases of the *Escherichia coli* aerobic respiratory chain. Biochemistry 26, 7732-7.

[63] Yagi, T. (1986). Purification and characterization of NADH dehydrogenase complex from *Paracoccus denitrificans*. Arch Biochem Biophys 250, 302-11.

[64] Bergsma, J., Strijker, R., Alkema, J.Y., Seijen, H.G. and Konings, W.N. (1981). NADH dehydrogenase and NADH oxidation in membrane vesicle from *Bacillus subtilis*. Eur J Biochem 120, 599-606.

[65] Deckert, G. et al. (1998). The complete genome of the hyperthermophilic bacterium *Aquifex aeolicus*. Nature 392, 353-8.

[66] Nakamura, Y. et al. (2002). Complete genome structure of the thermophilic cyanobacterium *Thermosynechococcus elongatus* BP-1. DNA Res 9, 123-30.

[67] Kawarabayasi, Y. et al. (2001). Complete genome sequence of an aerobic thermoacidophilic crenarchaeon, *Sulfolobus tokodaii* strain7. DNA Res 8, 123-40.

[68] Kawashima, T. et al. (2000). Archaeal adaptation to higher temperatures revealed by genomic sequence of *Thermoplasma volcanium*. Proc Natl Acad Sci U S A 97, 14257-62.

[69] Cook, S.A. and Shiemke, A.K. (2002). Evidence that a type-2 NADH:quinone oxidoreductase mediates electron transfer to particulate methane monooxygenase in *Methylococcus capsulatus*. Arch Biochem Biophys 398, 32-40.

[70] Nakayama, Y., Hayashi, M. and Unemoto, T. (1998). Identification of six subunits constituting Na^+-translocating NADH-quinone reductase from the marine *Vibrio alginolyticus*. FEBS Lett 422, 240-2.

[71] Zhou, W., Bertsova, Y.V., Feng, B., Tsatsos, P., Verkhovskaya, M.L., Gennis, R.B., Bogachev, A.V. and Barquera, B. (1999). Sequencing and preliminary characterization of the Na^+-translocating NADH:ubiquinone oxidoreductase from *Vibrio harveyi*. Biochemistry 38, 16246-52.

[72] Skulachev, V.P. (1989). The sodium cycle: a novel type of bacterial energetics. J Bioenerg Biomembr 21, 635-47.

[73] Lancaster, C.R. (2002). Succinate:quinone oxidoreductases: an overview. Biochim Biophys Acta 1553, 1-6.

[74] Lancaster, C.R. (2013). The di-heme family of respiratory complex II enzymes. Biochim Biophys Acta 1827, 679-87.

[75] Cecchini, G. (2003). Function and structure of complex II of the respiratory chain. Annu Rev Biochem 72, 77-109.

[76] Sun, F., Huo, X., Zhai, Y., Wang, A., Xu, J., Su, D., Bartlam, M. and Rao, Z. (2005). Crystal structure of mitochondrial respiratory membrane protein complex II. Cell 121, 1043-57.

[77] Hägerhäll, C. (1997). Succinate: quinone oxidoreductases. Variations on a conserved theme. Biochim Biophys Acta 1320, 107-41.

[78] Nakamura, K. et al. (1996). Two hydrophobic subunits are essential for the heme *b* ligation and functional assembly of complex II (succinate-ubiquinone oxidoreductase) from *Escherichia coli*. J Biol Chem 271, 521-7.

[79] Yu, L., Xu, J.X., Haley, P.E. and Yu, C.A. (1987). Properties of bovine heart mitochondrial cytochrome b_{560}. J Biol Chem 262, 1137-43.

[80] Oyedotun, K.S., Yau, P.F. and Lemire, B.D. (2004). Identification of the heme axial ligands in the cytochrome b_{562} of the *Saccharomyces cerevisiae* succinate dehydrogenase. J Biol Chem 279, 9432-9.

[81] Lemma, E., Hägerhäll, C., Geisler, V., Brandt, U., von Jagow, G. and Kröger, A. (1991). Reactivity of the *Bacillus subtilis* succinate dehydrogenase complex with quinones. Biochim Biophys Acta 1059, 281-5.
[82] Hägerhäll, C. and Hederstedt, L. (1996). A structural model for the membrane-integral domain of succinate: quinone oxidoreductases. FEBS Lett 389, 25-31.
[83] Hederstedt, L. (1999). Respiration without O_2. Science 284, 1941-2.
[84] Yankovskaya, V. et al. (2003). Architecture of succinate dehydrogenase and reactive oxygen species generation. Science 299, 700-4.
[85] Schäfer, G., Anemüller, S. and Moll, R. (2002). Archaeal complex II: 'classical' and 'non-classical' succinate:quinone reductases with unusual features. Biochim Biophys Acta 1553, 57-73.
[86] Kolaj-Robin, O., O'Kane, S.R., Nitschke, W., Léger, C., Baymann, F. and Soulimane, T. (2011). Biochemical and biophysical characterization of succinate: quinone reductase from *Thermus thermophilus*. Biochim Biophys Acta 1807, 68-79.
[87] Lancaster, C.R. (2002). *Wolinella succinogenes* quinol:fumarate reductase-2.2-A resolution crystal structure and the E-pathway hypothesis of coupled transmembrane proton and electron transfer. Biochim Biophys Acta 1565, 215-31.
[88] Hederstedt, L. (2002). Succinate:quinone oxidoreductase in the bacteria *Paracoccus denitrificans* and *Bacillus subtilis*. Biochim Biophys Acta 1553, 74-83.
[89] Iverson, T.M., Luna-Chavez, C., Cecchini, G. and Rees, D.C. (1999). Structure of the *Escherichia coli* fumarate reductase respiratory complex. Science 284, 1961-6.
[90] Lemos, R.S., Fernandes, A.S., Pereira, M.M., Gomes, C.M. and Teixeira, M. (2002). Quinol:fumarate oxidoreductases and succinate:quinone oxidoreductases: phylogenetic relationships, metal centres and membrane attachment. Biochim Biophys Acta 1553, 158-70.
[91] Hamann, N., Bill, E., Shokes, J.E., Scott, R.A., Bennati, M. and Hedderich, R. (2009). The CCG-domain-containing subunit SdhE of succinate:quinone oxidoreductase from *Sulfolobus solfataricus* P2 binds a [4Fe-4S] cluster. J Biol Inorg Chem 14, 457-70.
[92] Lemos, R.S., Gomes, C.M. and Teixeira, M. (2001). *Acidianus ambivalens* Complex II typifies a novel family of succinate dehydrogenases. Biochem Biophys Res Commun 281, 141-50.
[93] Zhang, J., Frerman, F.E. and Kim, J.J. (2006). Structure of electron transfer flavoprotein-ubiquinone oxidoreductase and electron transfer to the mitochondrial ubiquinone pool. Proc Natl Acad Sci U S A 103, 16212-7.
[94] Nielsen, F.S., Rowland, P., Larsen, S. and Jensen, K.F. (1996). Purification and characterization of dihydroorotate dehydrogenase A from *Lactococcus lactis*, crystallization and preliminary X-ray diffraction studies of the enzyme. Protein Sci 5, 852-6.
[95] Crofts, A.R. (2004). The cytochrome bc_1 complex: function in the context of structure. Annu Rev Physiol 66, 689-733.
[96] Zhang, Z. et al. (1998). Electron transfer by domain movement in cytochrome bc_1. Nature 392, 677-84.
[97] Iwata, S. et al. (1998). Complete structure of the 11-subunit bovine mitochondrial cytochrome bc_1 complex. Science 281, 64-71.
[98] Berry, E.A., Guergova-Kuras, M., Huang, L.S. and Crofts, A.R. (2000). Structure and function of cytochrome *bc* complexes. Annu Rev Biochem 69, 1005-75.

[99] Berry, E.A., Huang, L.S., Saechao, L.K., Pon, N.G., Valkova-Valchanova, M. and Daldal, F. (2004). X-Ray Structure of Rhodobacter Capsulatus Cytochrome *bc* (1): Comparison with its Mitochondrial and Chloroplast Counterparts. Photosynth Res 81, 251-75.

[100] Abergel, C., Nitschke, W., Malarte, G., Bruschi, M., Claverie, J.M. and Giudici-Orticoni, M.T. (2003). The structure of *Acidithiobacillus ferrooxidans c*(4)-cytochrome: a model for complex-induced electron transfer tuning. Structure 11, 547-55.

[101] Kramer, D.M., Nitschke, W. and Cooley, J.W. (2009) The cytochrome bc_1 and related *bc* complexes: The Rieske/Cytochrome *b* Complex as the Functional Core of a Central Electron/Proton Transfer Complex. Advances in Photosynthesis and Respiration 28, 451-473.

[102] Pereira, M.M., Carita, J.N. and Teixeira, M. (1999). Membrane-bound electron transfer chain of the thermohalophilic bacterium *Rhodothermus marinus*: a novel multihemic cytochrome *bc*, a new complex III. Biochemistry 38, 1268-75.

[103] Komorowski, L., Verheyen, W. and Schäfer, G. (2002). The archaeal respiratory supercomplex SoxM from *S. acidocaldarius* combines features of quinole and cytochrome *c* oxidases. Biol Chem 383, 1791-9.

[104] Lübben, M., Kolmerer, B. and Saraste, M. (1992). An archaebacterial terminal oxidase combines core structures of two mitochondrial respiratory complexes. EMBO J 11, 805-12.

[105] Mitchell, P. (1975). The protonmotive Q cycle: a general formulation. FEBS Lett 59, 137-9.

[106] Crofts, A.R. (2004). The Q-cycle - A Personal Perspective. Photosynth Res 80, 223-43.

[107] Brandt, U. (1996). Bifurcated ubihydroquinone oxidation in the cytochrome bc_1 complex by proton-gated charge transfer. FEBS Lett 387, 1-6.

[108] Ohnishi, T. and Trumpower, B.L. (1980). Differential effects of antimycin on ubisemiquinone bound in different environments in isolated succinate . cytochrome *c* reductase complex. J Biol Chem 255, 3278-84.

[109] von Jagow, G. and Ohnishi, T. (1985). The chromone inhibitor stigmatellin--binding to the ubiquinol oxidation center at the C-side of the mitochondrial membrane. FEBS Lett 185, 311-5.

[110] Crofts, A.R., Barquera, B., Gennis, R.B., Kuras, R., Guergova-Kuras, M. and Berry, E.A. (1999). Mechanism of ubiquinol oxidation by the *bc*(1) complex: different domains of the quinol binding pocket and their role in the mechanism and binding of inhibitors. Biochemistry 38, 15807-26.

[111] Swierczek, M., Cieluch, E., Sarewicz, M., Borek, A., Moser, C.C., Dutton, P.L. and Osyczka, A. (2010). An electronic bus bar lies in the core of cytochrome bc_1. Science 329, 451-4.

[112] Pereira, M.M., Santana, M. and Teixeira, M. (2001). A novel scenario for the evolution of haem-copper oxygen reductases. Biochim Biophys Acta 1505, 185-208.

[113] Chang, H.Y., Hemp, J., Chen, Y., Fee, J.A. and Gennis, R.B. (2009). The cytochrome ba_3 oxygen reductase from *Thermus thermophilus* uses a single input channel for proton delivery to the active site and for proton pumping. Proc Natl Acad Sci U S A 106, 16169-73.

[114] Buschmann, S., Warkentin, E., Xie, H., Langer, J.D., Ermler, U. and Michel, H. (2010). The structure of cbb_3 cytochrome oxidase provides insights into proton pumping. Science 329, 327-30.
[115] Tsukihara, T. et al. (1996). The whole structure of the 13-subunit oxidized cytochrome *c* oxidase at 2.8 A. Science 272, 1136-44.
[116] Iwata, S., Ostermeier, C., Ludwig, B. and Michel, H. (1995). Structure at 2.8 A resolution of cytochrome *c* oxidase from *Paracoccus denitrificans*. Nature 376, 660-9.
[117] Noor, M.R. and Soulimane, T. (2013). Structure of *caa*(3) cytochrome *c* oxidase--a nature-made enzyme-substrate complex. Biol Chem 394, 579-91.
[118] Yoshikawa, S., Muramoto, K. and Shinzawa-Itoh, K. (2011). Proton-pumping mechanism of cytochrome *c* oxidase. Annu Rev Biophys 40, 205-23.
[119] Stanicová, J., Sedlák, E., Musatov, A. and Robinson, N.C. (2007). Differential stability of dimeric and monomeric cytochrome *c* oxidase exposed to elevated hydrostatic pressure. Biochemistry 46, 7146-52.
[120] Michel, H., Behr, J., Harrenga, A. and Kannt, A. (1998). Cytochrome *c* oxidase: structure and spectroscopy. Annu Rev Biophys Biomol Struct 27, 329-56.
[121] Hendler, R.W., Pardhasaradhi, K., Reynafarje, B. and Ludwig, B. (1991). Comparison of energy-transducing capabilities of the two- and three-subunit cytochromes aa_3 from *Paracoccus denitrificans* and the 13-subunit beef heart enzyme. Biophys J 60, 415-23.
[122] Yoshikawa, S. et al. (1998). Redox-coupled crystal structural changes in bovine heart cytochrome *c* oxidase. Science 280, 1723-9.
[123] Popović, D.M. (2013). Current advances in research of cytochrome *c* oxidase. Amino Acids 45, 1073-87.
[124] Puustinen, A., Finel, M., Virkki, M. and Wikström, M. (1989). Cytochrome *o* (*bo*) is a proton pump in *Paracoccus denitrificans* and *Escherichia coli*. FEBS Lett 249, 163-7.
[125] Bloch, D., Belevich, I., Jasaitis, A., Ribacka, C., Puustinen, A., Verkhovsky, M.I. and Wikström, M. (2004). The catalytic cycle of cytochrome *c* oxidase is not the sum of its two halves. Proc Natl Acad Sci U S A 101, 529-33.
[126] Konstantinov, A.A., Siletsky, S., Mitchell, D., Kaulen, A. and Gennis, R.B. (1997). The roles of the two proton input channels in cytochrome *c* oxidase from *Rhodobacter sphaeroides* probed by the effects of site-directed mutations on time-resolved electrogenic intraprotein proton transfer. Proc Natl Acad Sci U S A 94, 9085-90.
[127] Lee, H.M., Das, T.K., Rousseau, D.L., Mills, D., Ferguson-Miller, S. and Gennis, R.B. (2000). Mutations in the putative H-channel in the cytochrome *c* oxidase from *Rhodobacter sphaeroides* show that this channel is not important for proton conduction but reveal modulation of the properties of heme *a*. Biochemistry 39, 2989-96.
[128] Palmer, G. (1993). Current issues in the chemistry of cytochrome *c* oxidase. J Bioenerg Biomembr 25, 145-51.
[129] Cooper, C.E. and Brown, G.C. (2008). The inhibition of mitochondrial cytochrome oxidase by the gases carbon monoxide, nitric oxide, hydrogen cyanide and hydrogen sulfide: chemical mechanism and physiological significance. J Bioenerg Biomembr 40, 533-9.

[130] Borisov, V.B., Gennis, R.B., Hemp, J. and Verkhovsky, M.I. (2011). The cytochrome *bd* respiratory oxygen reductases. Biochim Biophys Acta 1807, 1398-413.
[131] Jünemann, S. (1997). Cytochrome *bd* terminal oxidase. Biochim Biophys Acta 1321, 107-27.
[132] Osborne, J.P. and Gennis, R.B. (1999). Sequence analysis of cytochrome *bd* oxidase suggests a revised topology for subunit I. Biochim Biophys Acta 1410, 32-50.
[133] Cunningham, L., Pitt, M. and Williams, H.D. (1997). The *cioAB* genes from *Pseudomonas aeruginosa* code for a novel cyanide-insensitive terminal oxidase related to the cytochrome *bd* quinol oxidases. Mol Microbiol 24, 579-91.
[134] Azarkina, N., Siletsky, S., Borisov, V., von Wachenfeldt, C., Hederstedt, L. and Konstantinov, A.A. (1999). A cytochrome bb'-type quinol oxidase in *Bacillus subtilis* strain 168. J Biol Chem 274, 32810-7.
[135] Vanlerberghe, G.C. and McIntosh, L. (1997). Alternative Oxidase: From Gene to Function. Annu Rev Plant Physiol Plant Mol Biol 48, 703-734.
[136] Albury, M.S., Elliott, C. and Moore, A.L. (2009). Towards a structural elucidation of the alternative oxidase in plants. Physiol Plant 137, 316-27.
[137] Shiba, T. et al. (2013). Structure of the trypanosome cyanide-insensitive alternative oxidase. Proc Natl Acad Sci U S A 110, 4580-5.
[138] Moore, A.L., Bonner, W.D. and Rich, P.R. (1978). The determination of the proton-motive force during cyanide-insensitive respiration in plant mitochondria. Arch Biochem Biophys 186, 298-306.
[139] Wagner, A.M., Krab, K., Wagner, M.J. and Moore, A.L. (2008). Regulation of thermogenesis in flowering Araceae: the role of the alternative oxidase. Biochim Biophys Acta 1777, 993-1000.
[140] Chaudhuri, M., Ott, R.D. and Hill, G.C. (2006). Trypanosome alternative oxidase: from molecule to function. Trends Parasitol 22, 484-91.
[141] Boyer, P.D. (1997). The ATP synthase--a splendid molecular machine. Annu Rev Biochem 66, 717-49.
[142] Dimroth, P. (1997). Primary sodium ion translocating enzymes. Biochim Biophys Acta 1318, 11-51.
[143] Walker, J.E. et al. (1985). Primary structure and subunit stoichiometry of F_1-ATPase from bovine mitochondria. J Mol Biol 184, 677-701.
[144] Abrahams, J.P., Leslie, A.G., Lutter, R. and Walker, J.E. (1994). Structure at 2.8 A resolution of F_1-ATPase from bovine heart mitochondria. Nature 370, 621-8.
[145] Walker, J.E., Runswick, M.J. and Saraste, M. (1982). Subunit equivalence in *Escherichia coli* and bovine heart mitochondrial F_1F_0 ATPases. FEBS Lett 146, 393-6.
[146] Collinson, I.R., van Raaij, M.J., Runswick, M.J., Fearnley, I.M., Skehel, J.M., Orriss, G.L., Miroux, B. and Walker, J.E. (1994). ATP synthase from bovine heart mitochondria. In vitro assembly of a stalk complex in the presence of F_1-ATPase and in its absence. J Mol Biol 242, 408-21.
[147] Walker, J.E., Lutter, R., Dupuis, A. and Runswick, M.J. (1991). Identification of the subunits of F_1F_0-ATPase from bovine heart mitochondria. Biochemistry 30, 5369-78.
[148] Bianchet, M.A., Hullihen, J., Pedersen, P.L. and Amzel, L.M. (1998). The 2.8-A structure of rat liver F_1-ATPase: configuration of a critical intermediate in ATP synthesis/hydrolysis. Proc Natl Acad Sci U S A 95, 11065-70.

[149] Watt, I.N., Montgomery, M.G., Runswick, M.J., Leslie, A.G. and Walker, J.E. (2010). Bioenergetic cost of making an adenosine triphosphate molecule in animal mitochondria. Proc Natl Acad Sci U S A 107, 16823-7.
[150] Nury, H., Dahout-Gonzalez, C., Trézéguet, V., Lauquin, G.J., Brandolin, G. and Pebay-Peyroula, E. (2006). Relations between structure and function of the mitochondrial ADP/ATP carrier. Annu Rev Biochem 75, 713-41.
[151] Ferguson, S.J. (2010). ATP synthase: from sequence to ring size to the P/O ratio. Proc Natl Acad Sci U S A 107, 16755-6.
[152] Keilin, D. and Hartree, E.F. (1947). Activity of the cytochrome system in heart muscle preparations. Biochem J 41, 500-2.
[153] Chance, B. and Williams, G.R. (1955). A method for the localization of sites for oxidative phosphorylation. Nature 176, 250-4.
[154] Hatefi, Y., Haavik, A.G., Fowler, L.R. and Griffiths, D.E. (1962). Studies on the electron transfer system. XLII. Reconstitution of the electron transfer system. J Biol Chem 237, 2661-9.
[155] Hatefi, Y., Haavik, A.G. and Griffiths, D.E. (1962). Studies on the electron transfer system. XL. Preparation and properties of mitochondrial DPNH-coenzyme Q reductase. J Biol Chem 237, 1676-80.
[156] Hackenbrock, C.R., Chazotte, B. and Gupte, S.S. (1986). The random collision model and a critical assessment of diffusion and collision in mitochondrial electron transport. J Bioenerg Biomembr 18, 331-68.
[157] Sowers, A.E. and Hackenbrock, C.R. (1981). Rate of lateral diffusion of intramembrane particles: measurement by electrophoretic displacement and rerandomization. Proc Natl Acad Sci U S A 78, 6246-50.
[158] Gupte, S., Wu, E.S., Hoechli, L., Hoechli, M., Jacobson, K., Sowers, A.E. and Hackenbrock, C.R. (1984). Relationship between lateral diffusion, collision frequency, and electron transfer of mitochondrial inner membrane oxidation-reduction components. Proc Natl Acad Sci U S A 81, 2606-10.
[159] Kawato, S., Sigel, E., Carafoli, E. and Cherry, R.J. (1981). Rotation of cytochrome oxidase in phospholipid vesicles. Investigations of interactions between cytochrome oxidases and between cytochrome oxidase and cytochrome bc_1 complex. J Biol Chem 256, 7518-27.
[160] Hochman, J., Ferguson-Miller, S. and Schindler, M. (1985). Mobility in the mitochondrial electron transport chain. Biochemistry 24, 2509-16.
[161] Ozawa, T., Tanaka, M., Suzuki, H. and Nishikimi, M. (1987). Structure and function of mitochondria: their organization and disorders. Brain Dev 9, 76-81.
[162] Berry, E.A. and Trumpower, B.L. (1985). Isolation of ubiquinol oxidase from *Paracoccus denitrificans* and resolution into cytochrome bc_1 and cytochrome c-aa_3 complexes. J Biol Chem 260, 2458-67.
[163] Sone, N., Sekimachi, M. and Kutoh, E. (1987). Identification and properties of a quinol oxidase super-complex composed of a bc_1 complex and cytochrome oxidase in the thermophilic bacterium PS3. J Biol Chem 262, 15386-91.
[164] Schägger, H. and Pfeiffer, K. (2000). Supercomplexes in the respiratory chains of yeast and mammalian mitochondria. EMBO J 19, 1777-83.
[165] Acín-Pérez, R., Fernández-Silva, P., Peleato, M.L., Pérez-Martos, A. and Enriquez, J.A. (2008). Respiratory active mitochondrial supercomplexes. Mol Cell 32, 529-39.

[166] Bianchi, C., Genova, M.L., Parenti Castelli, G. and Lenaz, G. (2004). The mitochondrial respiratory chain is partially organized in a supercomplex assembly: kinetic evidence using flux control analysis. J Biol Chem 279, 36562-9.

[167] Boumans, H., Grivell, L.A. and Berden, J.A. (1998). The respiratory chain in yeast behaves as a single functional unit. J Biol Chem 273, 4872-7.

[168] Magalon, A., Arias-Cartin, R. and Walburger, A. (2012). Supramolecular organization in prokaryotic respiratory systems. Adv Microb Physiol 61, 217-66.

[169] Krause, F., Scheckhuber, C.Q., Werner, A., Rexroth, S., Reifschneider, N.H., Dencher, N.A. and Osiewacz, H.D. (2004). Supramolecular organization of cytochrome *c* oxidase- and alternative oxidase-dependent respiratory chains in the filamentous fungus *Podospora anserina*. J Biol Chem 279, 26453-61.

[170] Krause, F., Reifschneider, N.H., Vocke, D., Seelert, H., Rexroth, S. and Dencher, N.A. (2004). "Respirasome"-like supercomplexes in green leaf mitochondria of spinach. J Biol Chem 279, 48369-75.

[171] Dudkina, N.V., Eubel, H., Keegstra, W., Boekema, E.J. and Braun, H.P. (2005). Structure of a mitochondrial supercomplex formed by respiratory-chain complexes I and III. Proc Natl Acad Sci U S A 102, 3225-9.

[172] Dudkina, N.V., Kudryashev, M., Stahlberg, H. and Boekema, E.J. (2011). Interaction of complexes I, III, and IV within the bovine respirasome by single particle cryoelectron tomography. Proc Natl Acad Sci U S A 108, 15196-200.

[173] Acín-Pérez, R., Bayona-Bafaluy, M.P., Fernández-Silva, P., Moreno-Loshuertos, R., Pérez-Martos, A., Bruno, C., Moraes, C.T. and Enríquez, J.A. (2004). Respiratory complex III is required to maintain complex I in mammalian mitochondria. Mol Cell 13, 805-15.

[174] Schäfer, E., Dencher, N.A., Vonck, J. and Parcej, D.N. (2007). Three-dimensional structure of the respiratory chain supercomplex $I_1III_2IV_1$ from bovine heart mitochondria. Biochemistry 46, 12579-85.

[175] Althoff, T., Mills, D.J., Popot, J.L. and Kühlbrandt, W. (2011). Arrangement of electron transport chain components in bovine mitochondrial supercomplex $I_1III_2IV_1$. EMBO J 30, 4652-64.

[176] Schägger, H. (2002). Respiratory chain supercomplexes of mitochondria and bacteria. Biochim Biophys Acta 1555, 154-9.

[177] Schägger, H. and Pfeiffer, K. (2001). The ratio of oxidative phosphorylation complexes I-V in bovine heart mitochondria and the composition of respiratory chain supercomplexes. J Biol Chem 276, 37861-7.

[178] Allen, R.D., Schroeder, C.C. and Fok, A.K. (1989). An investigation of mitochondrial inner membranes by rapid-freeze deep-etch techniques. J Cell Biol 108, 2233-40.

[179] Wittig, I., Carrozzo, R., Santorelli, F.M. and Schägger, H. (2006). Supercomplexes and subcomplexes of mitochondrial oxidative phosphorylation. Biochim Biophys Acta 1757, 1066-72.

[180] Marques, I., Dencher, N.A., Videira, A. and Krause, F. (2007). Supramolecular organization of the respiratory chain in *Neurospora crassa* mitochondria. Eukaryot Cell 6, 2391-405.

[181] Nübel, E., Wittig, I., Kerscher, S., Brandt, U. and Schägger, H. (2009). Two-dimensional native electrophoretic analysis of respiratory supercomplexes from *Yarrowia lipolytica*. Proteomics 9, 2408-18.

[182] Bultema, J.B., Braun, H.P., Boekema, E.J. and Kouril, R. (2009). Megacomplex organization of the oxidative phosphorylation system by structural analysis of respiratory supercomplexes from potato. Biochim Biophys Acta 1787, 60-7.

[183] Dudkina, N.V., Heinemeyer, J., Sunderhaus, S., Boekema, E.J. and Braun, H.P. (2006). Respiratory chain supercomplexes in the plant mitochondrial membrane. Trends Plant Sci 11, 232-40.

[184] Guerrero-Castillo, S., Vázquez-Acevedo, M., González-Halphen, D. and Uribe-Carvajal, S. (2009). In *Yarrowia lipolytica* mitochondria, the alternative NADH dehydrogenase interacts specifically with the cytochrome complexes of the classic respiratory pathway. Biochim Biophys Acta 1787, 75-85.

[185] Heinemeyer, J., Braun, H.P., Boekema, E.J. and Kouril, R. (2007). A structural model of the cytochrome *c* reductase/oxidase supercomplex from yeast mitochondria. J Biol Chem 282, 12240-8.

[186] Bruel, C., Brasseur, R. and Trumpower, B.L. (1996). Subunit 8 of the *Saccharomyces cerevisiae* cytochrome bc_1 complex interacts with succinate-ubiquinone reductase complex. J Bioenerg Biomembr 28, 59-68.

[187] Navet, R., Jarmuszkiewicz, W., Douette, P., Sluse-Goffart, C.M. and Sluse, F.E. (2004). Mitochondrial respiratory chain complex patterns from *Acanthamoeba castellanii* and *Lycopersicon esculentum*: comparative analysis by BN-PAGE and evidence of protein-protein interaction between alternative oxidase and complex III. J Bioenerg Biomembr 36, 471-9.

[188] Duarte, M. and Videira, A. (2009). Effects of mitochondrial complex III disruption in the respiratory chain of *Neurospora crassa*. Mol Microbiol 72, 246-58.

[189] Ramírez-Aguilar, S.J. et al. (2011). The composition of plant mitochondrial supercomplexes changes with oxygen availability. J Biol Chem 286, 43045-53.

[190] Krause, F., Reifschneider, N.H., Goto, S. and Dencher, N.A. (2005). Active oligomeric ATP synthases in mammalian mitochondria. Biochem Biophys Res Commun 329, 583-90.

[191] Couoh-Cardel, S.J., Uribe-Carvajal, S., Wilkens, S. and García-Trejo, J.J. (2010). Structure of dimeric F_1F_0-ATP synthase. J Biol Chem 285, 36447-55.

[192] Minauro-Sanmiguel, F., Wilkens, S. and García, J.J. (2005). Structure of dimeric mitochondrial ATP synthase: novel F_0 bridging features and the structural basis of mitochondrial cristae biogenesis. Proc Natl Acad Sci U S A 102, 12356-8.

[193] Thomas, D. et al. (2008). Supramolecular organization of the yeast F_1Fo-ATP synthase. Biol Cell 100, 591-601.

[194] Arnold, I., Pfeiffer, K., Neupert, W., Stuart, R.A. and Schägger, H. (1998). Yeast mitochondrial F_1F_0-ATP synthase exists as a dimer: identification of three dimer-specific subunits. EMBO J 17, 7170-8.

[195] Wittig, I., Velours, J., Stuart, R. and Schägger, H. (2008). Characterization of domain interfaces in monomeric and dimeric ATP synthase. Mol Cell Proteomics 7, 995-1004.

[196] Davies, K.M., Strauss, M., Daum, B., Kief, J.H., Osiewacz, H.D., Rycovska, A., Zickermann, V. and Kühlbrandt, W. (2011). Macromolecular organization of ATP synthase and complex I in whole mitochondria. Proc Natl Acad Sci U S A 108, 14121-6.

[197] Strauss, M., Hofhaus, G., Schröder, R.R. and Kühlbrandt, W. (2008). Dimer ribbons of ATP synthase shape the inner mitochondrial membrane. EMBO J 27, 1154-60.

[198] Wittig, I. and Schägger, H. (2005). Advantages and limitations of clear-native PAGE. Proteomics 5, 4338-46.

[199] Davies, K.M., Anselmi, C., Wittig, I., Faraldo-Gómez, J.D. and Kühlbrandt, W. (2012). Structure of the yeast F_1Fo-ATP synthase dimer and its role in shaping the mitochondrial cristae. Proc Natl Acad Sci U S A 109, 13602-7.

[200] Arselin, G., Vaillier, J., Salin, B., Schaeffer, J., Giraud, M.F., Dautant, A., Brèthes, D. and Velours, J. (2004). The modulation in subunits *e* and *g* amounts of yeast ATP synthase modifies mitochondrial cristae morphology. J Biol Chem 279, 40392-9.

[201] Lapaille, M. et al. (2010). Atypical subunit composition of the chlorophycean mitochondrial F_1F_O-ATP synthase and role of Asa7 protein in stability and oligomycin resistance of the enzyme. Mol Biol Evol 27, 1630-44.

[202] Dudkina, N.V., Sunderhaus, S., Braun, H.P. and Boekema, E.J. (2006). Characterization of dimeric ATP synthase and cristae membrane ultrastructure from *Saccharomyces* and *Polytomella* mitochondria. FEBS Lett 580, 3427-32.

[203] Stroh, A., Anderka, O., Pfeiffer, K., Yagi, T., Finel, M., Ludwig, B. and Schägger, H. (2004). Assembly of respiratory complexes I, III, and IV into NADH oxidase supercomplex stabilizes complex I in *Paracoccus denitrificans*. J Biol Chem 279, 5000-7.

[204] Keefe, R.G. and Maier, R.J. (1993). Purification and characterization of an O_2-utilizing cytochrome-*c* oxidase complex from *Bradyrhizobium japonicum* bacteroid membranes. Biochim Biophys Acta 1183, 91-104.

[205] Refojo, P.N., Teixeira, M. and Pereira, M.M. (2010). The alternative complex III of *Rhodothermus marinus* and its structural and functional association with *caa*$_3$ oxygen reductase. Biochim Biophys Acta 1797, 1477-82.

[206] Prunetti, L., Infossi, P., Brugna, M., Ebel, C., Giudici-Orticoni, M.T. and Guiral, M. (2010). New functional sulfide oxidase-oxygen reductase supercomplex in the membrane of the hyperthermophilic bacterium *Aquifex aeolicus*. J Biol Chem 285, 41815-26.

[207] Prunetti, L., Brugna, M., Lebrun, R., Giudici-Orticoni, M.T. and Guiral, M. (2011). The elusive third subunit IIa of the bacterial B-type oxidases: the enzyme from the hyperthermophile *Aquifex aeolicus*. PLoS One 6, e21616.

[208] Gao, Y., Meyer, B., Sokolova, L., Zwicker, K., Karas, M., Brutschy, B., Peng, G. and Michel, H. (2012). Heme-copper terminal oxidase using both cytochrome *c* and ubiquinol as electron donors. Proc Natl Acad Sci U S A 109, 3275-80.

[209] Guiral, M., Tron, P., Aubert, C., Gloter, A., Iobbi-Nivol, C. and Giudici-Orticoni, M.T. (2005). A membrane-bound multienzyme, hydrogen-oxidizing, and sulfur-reducing complex from the hyperthermophilic bacterium *Aquifex aeolicus*. J Biol Chem 280, 42004-15.

[210] Castelle, C., Guiral, M., Malarte, G., Ledgham, F., Leroy, G., Brugna, M. and Giudici-Orticoni, M.T. (2008). A new iron-oxidizing/O_2-reducing supercomplex spanning both inner and outer membranes, isolated from the extreme acidophile *Acidithiobacillus ferrooxidans*. J Biol Chem 283, 25803-11.

[211] Bird, L.J., Bonnefoy, V. and Newman, D.K. (2011). Bioenergetic challenges of microbial iron metabolisms. Trends Microbiol 19, 330-40.

[212] Sone, N. and Toh, H. (1994). Membrane-bound *Bacillus* cytochromes *c* and their phylogenetic position among bacterial class I cytochromes *c*. FEMS Microbiol Lett 122, 203-10.

[213] von Wachenfeldt, C. and Hederstedt, L. (1993). Physico-chemical characterisation of membrane-bound and water-soluble forms of *Bacillus subtilis* cytochrome *c*-550. Eur J Biochem 212, 499-509.

[214] Megehee, J.A., Hosler, J.P. and Lundrigan, M.D. (2006). Evidence for a cytochrome *bcc*-aa_3 interaction in the respiratory chain of *Mycobacterium smegmatis*. Microbiology 152, 823-9.

[215] Niebisch, A. and Bott, M. (2003). Purification of a cytochrome *bc*-aa_3 supercomplex with quinol oxidase activity from *Corynebacterium glutamicum*. Identification of a fourth subunity of cytochrome aa_3 oxidase and mutational analysis of diheme cytochrome c_1. J Biol Chem 278, 4339-46.

[216] Sakamoto, J., Shibata, T., Mine, T., Miyahara, R., Torigoe, T., Noguchi, S., Matsushita, K. and Sone, N. (2001). Cytochrome *c* oxidase contains an extra charged amino acid cluster in a new type of respiratory chain in the amino-acid-producing Gram-positive bacterium *Corynebacterium glutamicum*. Microbiology 147, 2865-71.

[217] Niebisch, A. and Bott, M. (2001). Molecular analysis of the cytochrome bc_1-aa_3 branch of the *Corynebacterium glutamicum* respiratory chain containing an unusual diheme cytochrome c_1. Arch Microbiol 175, 282-94.

[218] Liu, X., Gong, X., Hicks, D.B., Krulwich, T.A., Yu, L. and Yu, C.A. (2007). Interaction between cytochrome caa_3 and F_1F_0-ATP synthase of alkaliphilic *Bacillus pseudofirmus* OF4 is demonstrated by saturation transfer electron paramagnetic resonance and differential scanning calorimetry assays. Biochemistry 46, 306-13.

[219] Lübben, M., Arnaud, S., Castresana, J., Warne, A., Albracht, S.P. and Saraste, M. (1994). A second terminal oxidase in *Sulfolobus acidocaldarius*. Eur J Biochem 224, 151-9.

[220] Iwasaki, T., Matsuura, K. and Oshima, T. (1995). Resolution of the aerobic respiratory system of the thermoacidophilic archaeon, *Sulfolobus* sp. strain 7. I. The archaeal terminal oxidase supercomplex is a functional fusion of respiratory complexes III and IV with no *c*-type cytochromes. J Biol Chem 270, 30881-92.

[221] Komorowski, L., Anemüller, S. and Schäfer, G. (2001). First expression and characterization of a recombinant CuA-containing subunit II from an archaeal terminal oxidase complex. J Bioenerg Biomembr 33, 27-34.

[222] Dirmeier, R., Keller, M., Frey, G., Huber, H. and Stetter, K.O. (1998). Purification and properties of an extremely thermostable membrane-bound sulfur-reducing complex from the hyperthermophilic *Pyrodictium abyssi*. Eur J Biochem 252, 486-91.

[223] Laska, S. and Kletzin, A. (2000). Improved purification of the membrane-bound hydrogenase-sulfur-reductase complex from thermophilic archaea using epsilon-aminocaproic acid-containing chromatography buffers. J Chromatogr B Biomed Sci Appl 737, 151-60.

[224] Laska, S., Lottspeich, F. and Kletzin, A. (2003). Membrane-bound hydrogenase and sulfur reductase of the hyperthermophilic and acidophilic archaeon *Acidianus ambivalens*. Microbiology 149, 2357-71.

[225] Fleischer, S., Brierley, G., Klowen, H. and Slautterback, D.B. (1962). Studies of the electron transfer system. 47. The role of phospholipids in electron transfer. J Biol Chem 237, 3264-72.

[226] Schlame, M. (2008). Cardiolipin synthesis for the assembly of bacterial and mitochondrial membranes. J Lipid Res 49, 1607-20.

[227] Hunte, C. (2005). Specific protein-lipid interactions in membrane proteins. Biochem Soc Trans 33, 938-42.
[228] Fry, M. and Green, D.E. (1981). Cardiolipin requirement for electron transfer in complex I and III of the mitochondrial respiratory chain. J Biol Chem 256, 1874-80.
[229] Robinson, N.C. (1993). Functional binding of cardiolipin to cytochrome *c* oxidase. J Bioenerg Biomembr 25, 153-63.
[230] Schwall, C.T., Greenwood, V.L. and Alder, N.N. (2012). The stability and activity of respiratory Complex II is cardiolipin-dependent. Biochim Biophys Acta 1817, 1588-96.
[231] Acehan, D., Malhotra, A., Xu, Y., Ren, M., Stokes, D.L. and Schlame, M. (2011). Cardiolipin affects the supramolecular organization of ATP synthase in mitochondria. Biophys J 100, 2184-92.
[232] Zhang, M., Mileykovskaya, E. and Dowhan, W. (2002). Gluing the respiratory chain together. Cardiolipin is required for supercomplex formation in the inner mitochondrial membrane. J Biol Chem 277, 43553-6.
[233] McKenzie, M., Lazarou, M., Thorburn, D.R. and Ryan, M.T. (2006). Mitochondrial respiratory chain supercomplexes are destabilized in Barth Syndrome patients. J Mol Biol 361, 462-9.
[234] Thomson, J.W. and Shapiro, B.M. (1981). The respiratory chain NADH dehydrogenase of *Escherichia coli*. Isolation of an NADH:quinone oxidoreductase from membranes and comparison with the membrane-bound NADH:dichlorophenolindophenol oxidoreductase. J Biol Chem 256, 3077-84.
[235] Tanaka, Y., Anraku, Y. and Futai, M. (1976). *Escherichia coli* membrane D-lactate dehydrogenase. Isolation of the enzyme in aggregated from and its activation by Triton X-100 and phospholipids. J Biochem 80, 821-30.
[236] Kita, K., Konishi, K. and Anraku, Y. (1984). Terminal oxidases of *Escherichia coli* aerobic respiratory chain. I. Purification and properties of cytochrome b_{562}-*o* complex from cells in the early exponential phase of aerobic growth. J Biol Chem 259, 3368-74.
[237] Jormakka, M., Törnroth, S., Byrne, B. and Iwata, S. (2002). Molecular basis of proton motive force generation: structure of formate dehydrogenase-N. Science 295, 1863-8.
[238] Bertero, M.G., Rothery, R.A., Palak, M., Hou, C., Lim, D., Blasco, F., Weiner, J.H. and Strynadka, N.C. (2003). Insights into the respiratory electron transfer pathway from the structure of nitrate reductase A. Nat Struct Biol 10, 681-7.
[239] Strogolova, V., Furness, A., Robb-McGrath, M., Garlich, J. and Stuart, R.A. (2012). Rcf1 and Rcf2, members of the hypoxia-induced gene 1 protein family, are critical components of the mitochondrial cytochrome bc_1-cytochrome *c* oxidase supercomplex. Mol Cell Biol 32, 1363-73.
[240] Chen, Y.C. et al. (2012). Identification of a protein mediating respiratory supercomplex stability. Cell Metab 15, 348-60.
[241] Stuart, R.A. (2009). Chapter 11 Supercomplex organization of the yeast respiratory chain complexes and the ADP/ATP carrier proteins. Methods Enzymol 456, 191-208.
[242] Sunderhaus, S. et al. (2006). Carbonic anhydrase subunits form a matrix-exposed domain attached to the membrane arm of mitochondrial complex I in plants. J Biol Chem 281, 6482-8.

[243] Wang, Y., Mohsen, A.W., Mihalik, S.J., Goetzman, E.S. and Vockley, J. (2010). Evidence for physical association of mitochondrial fatty acid oxidation and oxidative phosphorylation complexes. J Biol Chem 285, 29834-41.
[244] Busch, K.B., Deckers-Hebestreit, G., Hanke, G.T. and Mulkidjanian, A.Y. (2013). Dynamics of bioenergetic microcompartments. Biol Chem 394, 163-88.
[245] Chance, B. (1965). Reaction of oxygen with the respiratory chain in cells and tissues. J Gen Physiol 49, Suppl:163-95.
[246] Stoeckenius, W. (1966). Morphological observations on mitochondria and related structures. Ann N Y Acad Sci 137, 641-2.
[247] Lenaz, G. and Genova, M.L. (2010). Structure and organization of mitochondrial respiratory complexes: a new understanding of an old subject. Antioxid Redox Signal 12, 961-1008.
[248] Li, G. and Young, K.D. (2012). Isolation and identification of new inner membrane-associated proteins that localize to cell poles in *Escherichia coli*. Mol Microbiol 84, 276-95.
[249] Lenn, T., Leake, M.C. and Mullineaux, C.W. (2008). Clustering and dynamics of cytochrome *bd*-I complexes in the *Escherichia coli* plasma membrane *in vivo*. Mol Microbiol 70, 1397-407.
[250] Johnson, A.S., van Horck, S. and Lewis, P.J. (2004). Dynamic localization of membrane proteins in *Bacillus subtilis*. Microbiology 150, 2815-24.
[251] Lenn, T., Leake, M.C. and Mullineaux, C.W. (2008). Are *Escherichia coli* OXPHOS complexes concentrated in specialized zones within the plasma membrane? Biochem Soc Trans 36, 1032-6.
[252] Boekema, E.J. and Braun, H.P. (2007). Supramolecular structure of the mitochondrial oxidative phosphorylation system. J Biol Chem 282, 1-4.
[253] Diaz, F., Enríquez, J.A. and Moraes, C.T. (2012). Cells lacking Rieske iron-sulfur protein have a reactive oxygen species-associated decrease in respiratory complexes I and IV. Mol Cell Biol 32, 415-29.
[254] Bianchi, C., Fato, R., Genova, M.L., Parenti Castelli, G. and Lenaz, G. (2003). Structural and functional organization of Complex I in the mitochondrial respiratory chain. Biofactors 18, 3-9.
[255] Moreno-Lastres, D., Fontanesi, F., García-Consuegra, I., Martín, M.A., Arenas, J., Barrientos, A. and Ugalde, C. (2012). Mitochondrial complex I plays an essential role in human respirasome assembly. Cell Metab 15, 324-35.
[256] Lenaz, G. and Genova, M.L. (2009). Structural and functional organization of the mitochondrial respiratory chain: a dynamic super-assembly. Int J Biochem Cell Biol 41, 1750-1772.
[257] Schägger, H., de Coo, R., Bauer, M.F., Hofmann, S., Godinot, C. and Brandt, U. (2004). Significance of respirasomes for the assembly/stability of human respiratory chain complex I. J Biol Chem 279, 36349-53.
[258] Sellem, C.H., Marsy, S., Boivin, A., Lemaire, C. and Sainsard-Chanet, A. (2007). A mutation in the gene encoding cytochrome c_1 leads to a decreased ROS content and to a long-lived phenotype in the filamentous fungus *Podospora anserina*. Fungal Genet Biol 44, 648-58.
[259] Turrens, J.F. (2003). Mitochondrial formation of reactive oxygen species. J Physiol 552, 335-44.
[260] Bleier, L. and Dröse, S. (2012). Superoxide generation by complex III: From mechanistic rationales to functional consequences. Biochim Biophys Acta 1827, 1320-31.

[261] Quinlan, C.L., Orr, A.L., Perevoshchikova, I.V., Treberg, J.R., Ackrell, B.A. and Brand, M.D. (2012). Mitochondrial complex II can generate reactive oxygen species at high rates in both the forward and reverse reactions. J Biol Chem 287, 27255-64.

[262] Lenaz, G., Fato, R., Genova, M.L., Bergamini, C., Bianchi, C. and Biondi, A. (2006). Mitochondrial Complex I: structural and functional aspects. Biochim Biophys Acta 1757, 1406-20.

[263] Balaban, R.S., Nemoto, S. and Finkel, T. (2005). Mitochondria, oxidants, and aging. Cell 120, 483-95.

[264] Dröge, W. (2002). Free radicals in the physiological control of cell function. Physiol Rev 82, 47-95.

[265] Murphy, M.P. (2009). How mitochondria produce reactive oxygen species. Biochem J 417, 1-13.

[266] Maranzana, E., Barbero, G., Falasca, A.I., Lenaz, G. and Genova, M.L. (2013). Mitochondrial Respiratory Supercomplex Association Limits Production of Reactive Oxygen Species from Complex I. Antioxid Redox Signal 19, 1469-80.

[267] Hirst, J. (2010). Towards the molecular mechanism of respiratory complex I. Biochem J 425, 327-39.

Chapter 1

Part II – Supramolecular organizations in the aerobic respiratory chain of *Escherichia coli*

Chapter 2

Introducing the Escherichia coli *aerobic respiratory chain*

2.1 Escherichia coli *aerobic respiratory chain*

Escherichia coli is a facultative anaerobic, Gram negative bacterium, that contains a flexible respiratory chain bearing alternative pathways in response to different environmental conditions, exploiting a wide variety of electron donors as well as terminal electron acceptors. The respiratory chain of this organism has been intensively studied since the early 60s of the last century [1-3]. *E. coli* aerobic respiratory chain comprises three major primary dehydrogenases, a succinate:quinone oxidoreductase (SQR) [4] and two NADH dehydrogenases, a type I NADH:quinone oxidoreductase (NDH-1) and a type II NADH:quinone oxidoreductase (NDH-2) [5] (Figure 1). In addition, *E. coli* aerobic respiratory chain expresses three quinol oxygen reductases, cytochrome bo_3 [6] and type I and II cytochromes *bd* oxygen reductases [7,8], that accomplish the electron transfer from ubiquinol-8 to O_2. Other enzymes such as lactate, formate (FDH-O) and glycerol-1-phosphate dehydrogenases, as well as tryptophan [W] repressor-binding protein (WrbA) or the quinone oxidoreductases YhdH and QOR may also participate at the electron input site of this oxygen respiring process [8,9]

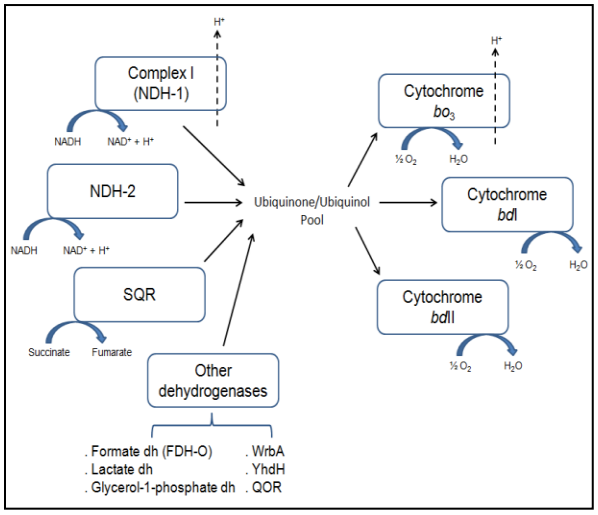

Fig. 1. *E. coli* aerobic respiratory chain. Electrons from the oxidation of reducing substrates NADH and succinate by complexes NDH-1 or NDH-2 and SQR, respectively, are transferred via ubiquinone-8 through cytochromes bo_3, *bd*I or *bd*II oxygen reductases to O_2. Concomitantly, proton translocation from the bacterial cytoplasm to the periplasmic space occurs in complex NDH-1 and cytochrome bo_3 oxygen reductase. Other dehydrogenases, such as formate dehydrogenase (FDH-O) are also present. Adapted from [8,9].

i. NADH:ubiquinone oxidoreductase (NDH-1)

NDH-1 is the major proton-translocating complex present in the *E. coli* aerobic respiratory chain. It is an L-shaped integral membrane complex of ~537 kDa containing a hydrophilic peripheral arm that protrudes into the cytoplasm and one hydrophobic membrane embedded arm [10]. While in most bacterial complexes I, the minimal functional unit of the enzyme generally consists of 14 different subunits, *E. coli* NDH-1 assembles only 13 subunits termed NuoA-N encoded by the *nuoA-N* operon, where *nuoC* and *nuoD* are fused [11] (see Table 1 from Chapter 1). The six peripheral subunits NuoB, CD, E, F, G and I build the peripheral arm and contain the known redox groups, namely one FMN and nine [Fe-S] clusters, of which eight have identifiable EPR signals [12-17]. The membrane arm domain contains the remaining subunits and its structure was recently determined at 3 Å resolution [18]. The three highly similar subunits NuoL, M and N were shown to contain, each, 14 conserved transmembrane helices and a putative proton-translocation channel, in agreement with the composition and function of the Na^+/H^+ antiporter complex (Mrp) subunits, as previously mentioned [19].

ii. Alternative NADH:ubiquinone oxidoreductase (NDH-2)

E. coli NDH-2 consists of a single polypeptidic chain of 48 kDa, encoded by *ndh* gene, that interacts with the N-side of the cytoplasmic membrane by at least a C-terminal amphipatic α-helix [20]. This protein contains a non-covalently bound flavin cofactor FAD [21], does not translocate protons across the membrane and is not able of oxidizing deamino-NADH [22].

Although *E. coli* NDH-2 X-ray crystal structure is still missing, a structural model was created based on sequence similarity using the flavoenzyme NAD(P)H peroxidase as template [23], a member of the SCOP-family “FAD/NAD-linked

reductases". It was suggested that the redox active parts of both protein cofactors, the nicotinamide ring of NADH and the isoalloxazine ring of FADH, are oriented in parallel, in close proximity to each other, and surrounded by highly conserved amino acidic residues. In fact, the recently solved X-ray crystal structure of *S. cerevisiae* type II NADH dehydrogenase (Ndi1) confirmed that the NAD^+ nicotinamide ring stacks at a distance of 3.1 Å on the *re*-face of the isoalloxazine ring of the FAD cofactor [24]. Although the C-terminal domain of FAD/NAD-linked reductases was shown to be involved in dimerization [23], which is further corroborated by the isolation and structural characterization of functional dimeric NDH-2 proteins in other organisms [24,25], the *E. coli* NDH-2 was never shown to form a functional dimer or to establish protein-protein interactions.

iii. Succinate:ubiquinone oxidoreductase (SQR)

E. coli SQR is a 121 kDa complex that comprises four subunits encoded by *sdhABCD* operon. Similarly to the mammalian complex II, it bears a type-C membrane domain composed of two membrane subunits (SqrC and SqrD) that accommodate one *b*-type heme (b_P), in addition to the highly conserved hydrophilic subunits SqrA and SqrB, where a covalently bound FAD cofactor, and three [Fe-S] clusters ($[2Fe\text{-}2S]^{2+/1+}$, $[4Fe\text{-}4S]^{2+/1+}$ and $[3Fe\text{-}4S]^{1+/0}$) are located, respectively [26]. As in many Gram negative bacteria, the *E. coli* genome contains two operons for complex II-like enzymes, one of them encoding a fumarate reductase (QFR), which bears a type-D hydrophobic domain with no *b*-type hemes [27] and is predominantly expressed under microaerophilic and anaerobic conditions, in contrast with SQR, that is expressed aerobically [28,29]. Interestingly, both enzymes share the ability to interact with ubiquinone (UQ) and menaquinol (MQH_2) and can even replace each other *in vivo*, if conditions for their expression are provided [30,31]. *E. coli* SQR X-ray crystal structure was solved at a resolution of 2.6 Å showing a trimeric structure with a total molecular mass of 360 kDa (Figure 2) [26]. The tightly packed arrangement of SQR monomers in

such a supramolecular assembly led the authors to propose it to be physiologically relevant.

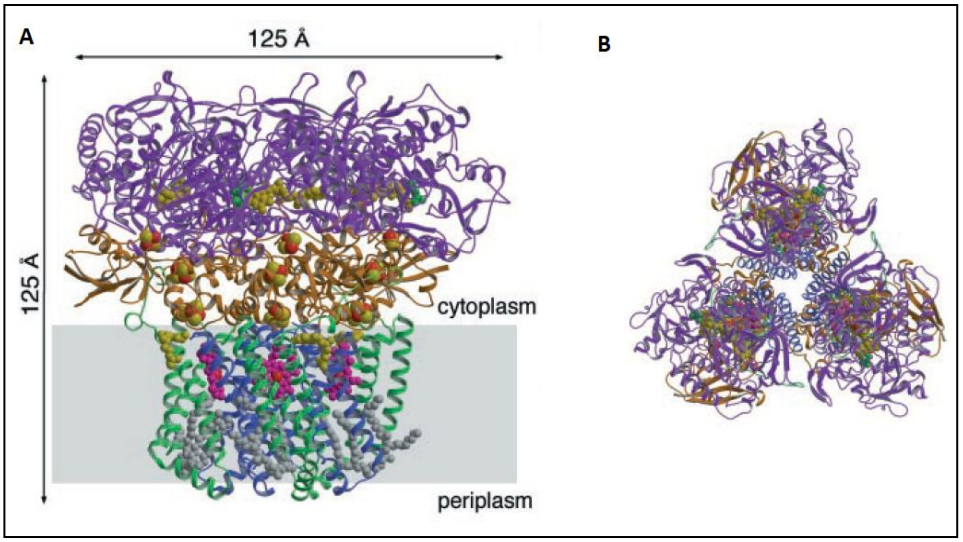

Fig. 2. *E. coli* SQR trimeric 3D structure, viewed parallel to the membrane (A) or from the cytoplasm along the membrane normal (B). Subunits SqrA and SqrB, shown in purple and orange, respectively, protrude into the cytoplasm and harbor a covalently bound FAD cofactor (gold) and three [Fe-S] clusters (red and yellow, for Fe and S atoms, respectively). The hydrophobic module comprises subunits SqrC and SqrD, shown in green and blue, respectively, wherein a *b*-type heme (magenta) is present, along with several cardiolipin molecules (grey). Adapted from [26].

A cardiolipin molecule was found to be engulfed in the SqrC and SqrD interface of each SQR monomer, above heme b_P, where it occupies the position of *b*-type heme (b_D) usually observed in type-A and –B hydrophobic domains [32]. The role of cardiolipin in the trimer formation of SqrABCD remains unclear but was suggested to stabilize these membrane-embedded proteins while being not essential for heme *b* integrity [33,34].

Whether cardiolipin is essential for the establishment of the prokaryotic supercomplexes described in chapter I, it is still not known. In fact, *E. coli* aerobic respiratory chain supercomplexes, which will be thoroughly analyzed in the next chapters, were not disrupted in membranes devoid of cardiolipin (Sousa et al., unpublished results).

iv. Aerobic formate dehydrogenase (FDH-O)

The *E. coli* genome encodes three formate dehydrogenase (FDH) isoenzymes (see [35] for a review), FDH-N, FDH-H and FDH-O, the latter being the only one synthesized in the presence of oxygen [36], and is encoded by the *fdoGHI* operon [37]. FDH-O structure and function are still poorly understood, however, this enzyme displays high sequence similarity with FDH-N, whose structural and functional characterization is well established [38], allowing the prediction of a similar structure for FDH-O [35,37].

The composition of FDH-O should comprise three different subunits, *i*) the 110 kDa selenopolypeptide FdoG [36], that shares 77% identity and 87% similarity with the FdnG counterpart, as calculated by CLUSTAL W [39]; *ii*) FdoH (75% identity and 85% similarity with FdnH) and *iii*) FdoI subunits (46% identity and 66% similarity with FdnI). In addition, the enzyme should contain five [Fe-S] clusters and two *b*-type hemes (b_P and b_C, for periplasm and cytoplasm, respectively) that couple the oxidation of formate with the reduction of ubiquinone [38,40]. In agreement with their sequence similarity, FDH-O and FDH-N are also capable of reducing dichlorophenol indophenol (DCPIP) in the presence of phenazine methosulfate (PMS) and formate [41]. Interestingly, FDH-N is packed as a trimer in a "mushroom"-like shape with a total molecular mass of 510 kDa, the interface between monomers being occupied by cardiolipin molecules [38].

v. Cytochrome bo_3 oxygen reductase

E. coli cytochrome bo_3 oxygen reductase is a quinol oxygen reductase with a predicted molecular mass of 142 kDa that belongs to the superfamily of heme-copper oxygen reductases (A-family), as the mitochondrial complex IV [42]. This complex couples the oxidation of ubiquinol molecules with the reduction of O_2 to water, concomitantly with the translocation of four protons across the cytoplasmic

membrane for each ubiquinol molecule oxidized [43]. Cytochrome bo_3 oxygen reductase X-ray crystal structure was solved at a resolution of 3.5 Å, showing to be composed of four different subunits (CyoABCD) encoded by the genes *cyoABCD* (Figure 3) [44]. CyoB (subunit I), the catalytic core of this enzyme, contains 15 transmembrane helices that assemble the ubiquinol binding site, the redox centres (heme *b*, heme o_3 and Cu_B) and the two proton-translocating pathways (K and D) [44,45]. CyoA (subunit II) forms part of the entry site for the K proton-translocating pathway and contains two transmembrane helices and a large periplasmic domain [46]. In contrast with mitochondrial complex IV, subunit II does not contain a binuclear Cu_A centre or a cytochrome *c* binding site. Instead, heme *b* receives electrons directly from a liposoluble ubiquinol-8 molecule, hence the name cytochrome bo_3 quinol oxygen reductase [47].

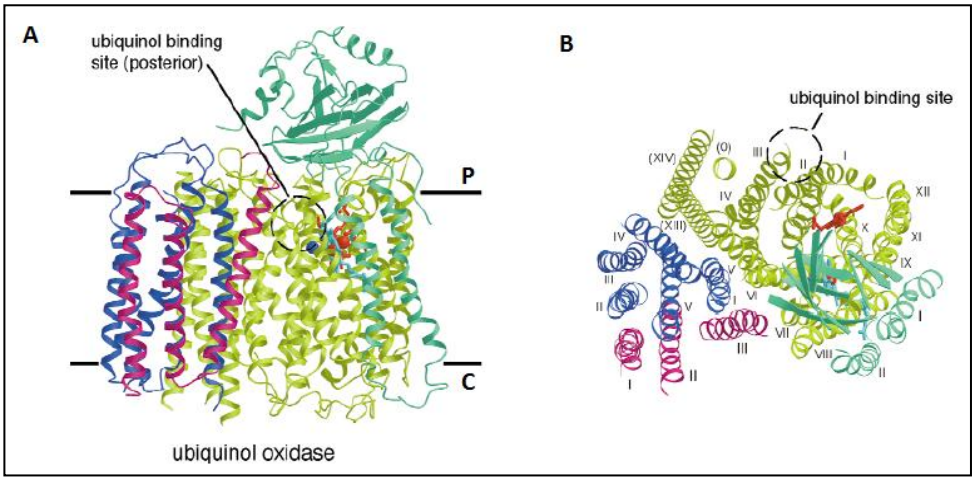

Fig. 3. Overall 3D structure of cytochrome bo_3 quinol oxygen reductase, viewed parallel to the membrane (A) or along the membrane normal from the periplasmic side (B). Subunit CyoB, shown in yellow, harbors the ubiquinol binding site as well as the redox centres heme *b* (red), heme o_3 (light blue) and Cu_B (blue sphere). CyoA, CyoC and CyoD subunits are represented in yellow, green, blue and pink, respectively. P and C stand for periplasm and cytoplasm, respectively. Adapted from [44].

CyoC (subunit III) may be regarded as important for the structural integrity of the redox sites and in the delivery of O_2 [48], while CyoD (subunit IV) function remains elusive. The *cyo* operon contains an additional gene, *cyoE*, which encodes for a

membrane-located farnesyl transferase that is involved in heme *o* synthesis [49]. Interestingly, cardiolipin was shown to stimulate ubiquinol:cytochrome bo_3 oxidoreductase activity of the purified complex [50]. Since cytochrome bo_3 oxygen reductase was detected as a homodimeric complex of 320 kDa in *E. coli* intact cells resolved by BN-PAGE [51], cardiolipin may be required for the establishment of such assemblies.

vi. Type I and II cytochrome *bd* oxygen reductases

E. coli cytochrome *bd*I oxygen reductase is a 100 kDa quinol oxygen reductase that assembles two polypeptides, CydA and CydB, which are encoded by the *cydAB* genes [52]. This complex contains a low spin *b*-type heme (b_{558}), a high spin *b*-type heme (b_{595}), and a *d*-type heme (high spin chlorin) [53,54]. Heme b_{558} is located on CydA (subunit I), whereas hemes b_{595} and *d* are likely to be in the area of both subunits' interface [55]. It has been proposed that these two hemes form a di-heme site involved in binding, activation and reduction of O_2 [56,57], while the low-spin heme b_{558} transfers electrons from the natural electron donor ubiquinol-8 towards the di-heme site [58]. This electron transfer is concomitant with the vectorial movement of protons across the membrane from the cytoplasm to the di-heme active site, which is located on the opposite side of the membrane. Thus, it is suggested that one transmembrane proton-conducting pathway is assembled in *bd*-type oxygen reductases, to convey protons from the cytoplasm to the heme b_{595}/heme *d* site for H_2O production. In agreement, several highly conserved polar or ionizable residues have been postulated to be part of this putative proton channel [59,60].

E. coli cytochrome *bd*II oxygen reductase, encoded by the *appBC* genes [61], is still poorly understood. However, this complex displays high similarity with the cytochrome *bd*I oxygen reductase. Subunits AppC and CydA display the highest identity and similarity, 78% and 60%, respectively, as calculated by CLUSTAL W [39], whereas subunits AppB and CydB presented 74% identity and 60% similarity,

suggesting that both proteins may contain similar structures. In agreement, cytochrome *bd*II oxygen reductase assembles identical prosthetic groups and spectral properties [7], and *appB* gene fusion studies suggested that its encoded subunit is inserted in the same orientation as CydB [61]. Moreover, cytochrome *bd*II oxygen reductase was shown to compensate for the loss of cytochrome *bd*I activity under conditions of respiratory stress, corroborating the high metabolic flexibility of *E. coli*.

The structural differences between cytochrome bo_3 and *bd*-type oxygen reductases are reflected in their affinity towards O_2. *E. coli* cytochrome *bd*I oxygen reductase is induced under microaerophilic conditions and has a high affinity for oxygen (K_M = 0.27 µM) whereas cytochrome bo_3 oxygen reductase has a lower affinity (K_M = 6.05 µM) and is predominant under high aeration conditions [62]. It appears that cytochrome *bd*II oxygen reductase is induced under microaerophilic conditions, by carbon and phosphate starvation [61,63], and has been proposed to function as an electron sink in the presence of high NADH concentrations [9].

vii. Bioenergetic efficiency of *E. coli* aerobic respiratory chain

The stoichiometry of protons translocated for each electron transferred has been determined for the described complexes (Figure 4). NDH-1 and cytochrome bo_3 oxygen reductase translocate protons over the membrane, resulting in a H^+/e^- stoichiometry of 2 for each complex [64,65]. Cytochrome *bd*I oxygen reductase does not translocate protons from the cytoplasm to the periplasm. However, the net electron transfer of its reaction, which requires the oxidation of ubiquinol and the uptake of protons from the cytoplasmic side of the membrane for water production, results in proton translocation with a H^+/e^- stoichiometry of 1 [47]. Similarly, cytochrome *bd*II oxygen reductase mechanism was found to be identical to that of cytochrome *bd*I oxygen reductase, where a H^+/e^- stoichiometry of 1 was proposed [66], which is in agreement with the strong sequence similarity observed between the two enzymes. In contrast, NDH-2 and SQR are non-electrogenic

enzymes (H^+/e^- = 0) [22,67] and no information is available regarding the eventual proton translocation generated by FDH-O.

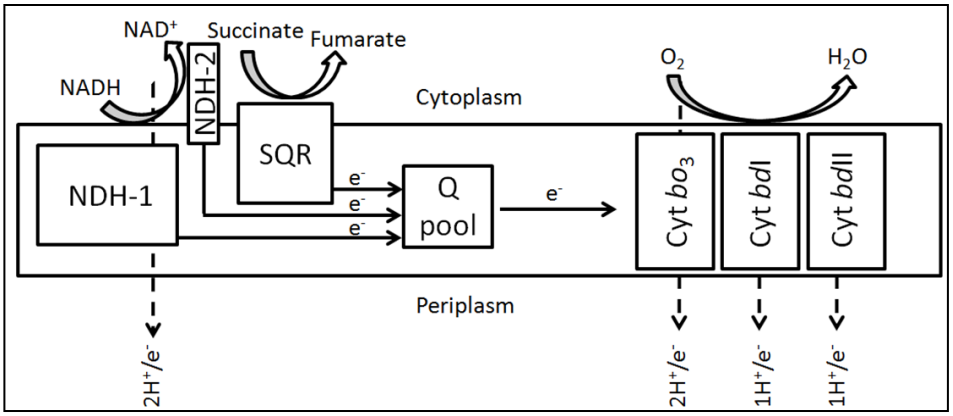

Fig. 4. *E. coli* aerobic respiratory chain enzymes and their proton-translocation properties. NDH-1 and cytochrome bo_3 oxygen reductase exhibit the highest H^+/e^- stoichiometry (2 H^+/e^-), whereas SQR and NDH-2 do not translocate protons to the periplasm. Information regarding FDH-O is not yet available. Cyt, cytochrome; Q, quinone. Adapted from [9,66,67].

The *E. coli* and mitochondrial F_1F_O-ATP synthases have a related overall structure [68]. The main differences rely on the supernumerary subunits, which are exclusively linked to the mitochondrial enzyme, and on the number of *c*-subunits that compose the F_O domain, which in the *E. coli* enzyme was proposed to be 10 [69]. As previously mentioned, the number of *c*-subunits determines the H^+/ATP as well as the P/O ratios of a given pathway [70]. Therefore, since *E. coli* has a truncated electron transport chain, different ratios are obtained. The transfer of 2 electrons through the *E. coli* proton-translocating NDH-1 and cytochrome bo_3 oxygen reductase yields $8H^+/2e^-$, with a maximum P/O ratio of 2.4. In contrast, use of the *E. coli* NDH-2 and cytochrome *bd* oxygen reductases decreases the $H^+/2e^-$ to 2, yielding 0.6 ATP molecules. This difference illustrates that an organism such as *E. coli* may not always be seeking to maximize the stoichiometry of ATP production.

2.2 References

[1] Hendler, R.W. and Burgess, A.H. (1972). Respiration and protein synthesis in *Escherichia coli* membrane-envelope fragments. VI. Solubilization and characterization of the electron transport chain. J Cell Biol 55, 266-81.

[2] Ingledew, W.J. and Poole, R.K. (1984). The respiratory chains of *Escherichia coli*. Microbiol Rev 48, 222-71.

[3] Price, C.E. and Driessen, A.J. (2010). Biogenesis of membrane bound respiratory complexes in *Escherichia coli*. Biochim Biophys Acta 1803, 748-66.

[4] Kasahara, M. and Anraku, Y. (1974). Succinate dehydrogenase of *Escherichia coli* membrane vesicles. Activation and properties of the enzyme. J Biochem 76, 959-66.

[5] Bragg, P.D. and Hou, C. (1967). Reduced nicotinamide adenine dinucleotide oxidation in *Escherichia coli* particles. II. NADH dehydrogenases. Arch Biochem Biophys 119, 202-8.

[6] Minagawa, J., Mogi, T., Gennis, R.B. and Anraku, Y. (1992). Identification of heme and copper ligands in subunit I of the cytochrome *bo* complex in *Escherichia coli*. J Biol Chem 267, 2096-104.

[7] Sturr, M.G., Krulwich, T.A. and Hicks, D.B. (1996). Purification of a cytochrome bd terminal oxidase encoded by the *Escherichia coli app* locus from a delta *cyo* delta *cyd* strain complemented by genes from *Bacillus firmus* OF4. J Bacteriol 178, 1742-9.

[8] Unden, G. and Bongaerts, J. (1997). Alternative respiratory pathways of *Escherichia coli*: energetics and transcriptional regulation in response to electron acceptors. Biochim Biophys Acta 1320, 217-34.

[9] Bekker, M., de Vries, S., Ter Beek, A., Hellingwerf, K.J. and de Mattos, M.J. (2009). Respiration of *Escherichia coli* can be fully uncoupled via the nonelectrogenic terminal cytochrome *bd*-II oxidase. J Bacteriol 191, 5510-7.

[10] Friedrich, T. and Böttcher, B. (2004). The gross structure of the respiratory complex I: a Lego System. Biochim Biophys Acta 1608, 1-9.

[11] Friedrich, T. (1998). The NADH:ubiquinone oxidoreductase (complex I) from *Escherichia coli*. Biochim Biophys Acta 1364, 134-46.

[12] Nakamaru-Ogiso, E., Yano, T., Ohnishi, T. and Yagi, T. (2002). Characterization of the iron-sulfur cluster coordinated by a cysteine cluster motif (CXXCXXXCX27C) in the Nqo3 subunit in the proton-translocating NADH-quinone oxidoreductase (NDH-1) of *Thermus thermophilus* HB-8. J Biol Chem 277, 1680-8.

[13] Nakamaru-Ogiso, E., Matsuno-Yagi, A., Yoshikawa, S., Yagi, T. and Ohnishi, T. (2008). Iron-sulfur cluster N5 is coordinated by an HXXXCXXCXXXXXC motif in the NuoG subunit of *Escherichia coli* NADH:quinone oxidoreductase (complex I). J Biol Chem 283, 25979-87.

[14] Nakamaru-Ogiso, E., Yano, T., Yagi, T. and Ohnishi, T. (2005). Characterization of the iron-sulfur cluster N7 (N1c) in the subunit NuoG of the proton-translocating NADH-quinone oxidoreductase from *Escherichia coli*. J Biol Chem 280, 301-7.

[15] Velazquez, I., Nakamaru-Ogiso, E., Yano, T., Ohnishi, T. and Yagi, T. (2005). Amino acid residues associated with cluster N3 in the NuoF subunit of the proton-translocating NADH-quinone oxidoreductase from *Escherichia coli*. FEBS Lett 579, 3164-8.

[16] Uhlmann, M. and Friedrich, T. (2005). EPR signals assigned to Fe/S cluster N1c of the *Escherichia coli* NADH:ubiquinone oxidoreductase (complex I) derive from cluster N1a. Biochemistry 44, 1653-8.

[17] Narayanan, M., Gabrieli, D.J., Leung, S.A., Elguindy, M.M., Glaser, C.A., Saju, N., Sinha, S.C. and Nakamaru-Ogiso, E. (2013). Semiquinone and cluster N6 signals in His-tagged proton-translocating NADH:ubiquinone oxidoreductase (complex I) from *Escherichia coli*. J Biol Chem 288, 14310-9.

[18] Efremov, R.G. and Sazanov, L.A. (2011). Structure of the membrane domain of respiratory complex I. Nature 476, 414-20.

[19] Mathiesen, C. and Hägerhäll, C. (2002). Transmembrane topology of the NuoL, M and N subunits of NADH:quinone oxidoreductase and their homologues among membrane-bound hydrogenases and bona fide antiporters. Biochim Biophys Acta 1556, 121-32.

[20] Villegas, J.M., Volentini, S.I., Rintoul, M.R. and Rapisarda, V.A. (2011). Amphipathic C-terminal region of *Escherichia coli* NADH dehydrogenase-2 mediates membrane localization. Arch Biochem Biophys 505, 155-9.

[21] Jaworowski, A., Mayo, G., Shaw, D.C., Campbell, H.D. and Young, I.G. (1981). Characterization of the respiratory NADH dehydrogenase of *Escherichia coli* and reconstitution of NADH oxidase in ndh mutant membrane vesicles. Biochemistry 20, 3621-8.

[22] Matsushita, K., Ohnishi, T. and Kaback, H.R. (1987). NADH-ubiquinone oxidoreductases of the *Escherichia coli* aerobic respiratory chain. Biochemistry 26, 7732-7.

[23] Schmid, R. and Gerloff, D.L. (2004). Functional properties of the alternative NADH:ubiquinone oxidoreductase from *E. coli* through comparative 3-D modelling. FEBS Lett 578, 163-8.

[24] Iwata, M., Lee, Y., Yamashita, T., Yagi, T., Iwata, S., Cameron, A.D. and Maher, M.J. (2012). The structure of the yeast NADH dehydrogenase (Ndi1) reveals overlapping binding sites for water- and lipid-soluble substrates. Proc Natl Acad Sci U S A 109, 15247-52.

[25] Fang, J. and Beattie, D.S. (2002). Novel FMN-containing rotenone-insensitive NADH dehydrogenase from Trypanosoma brucei mitochondria: isolation and characterization. Biochemistry 41, 3065-72.

[26] Yankovskaya, V. et al. (2003). Architecture of succinate dehydrogenase and reactive oxygen species generation. Science 299, 700-4.

[27] Iverson, T.M., Luna-Chavez, C., Cecchini, G. and Rees, D.C. (1999). Structure of the *Escherichia coli* fumarate reductase respiratory complex. Science 284, 1961-6.

[28] Maklashina, E., Cecchini, G. and Dikanov, S.A. (2013). Defining a direction: electron transfer and catalysis in *Escherichia coli* complex II enzymes. Biochim Biophys Acta 1827, 668-78.

[29] Park, S.J., Tseng, C.P. and Gunsalus, R.P. (1995). Regulation of succinate dehydrogenase (*sdhCDAB*) operon expression in *Escherichia coli* in response to carbon supply and anaerobiosis: role of ArcA and Fnr. Mol Microbiol 15, 473-82.

[30] Maklashina, E., Berthold, D.A. and Cecchini, G. (1998). Anaerobic expression of *Escherichia coli* succinate dehydrogenase: functional replacement of fumarate reductase in the respiratory chain during anaerobic growth. J Bacteriol 180, 5989-96.

[31] Guest, J.R. (1981). Partial replacement of succinate dehydrogenase function by phage- and plasmid-specified fumarate reductase in *Escherichia coli*. J Gen Microbiol 122, 171-9.

[32] Hägerhäll, C. and Hederstedt, L. (1996). A structural model for the membrane-integral domain of succinate: quinone oxidoreductases. FEBS Lett 389, 25-31.

[33] Ruprecht, J., Yankovskaya, V., Maklashina, E., Iwata, S. and Cecchini, G. (2009). Structure of *Escherichia coli* succinate:quinone oxidoreductase with an occupied and empty quinone-binding site. J Biol Chem 284, 29836-46.

[34] Ruprecht, J., Iwata, S., Rothery, R.A., Weiner, J.H., Maklashina, E. and Cecchini, G. (2011). Perturbation of the quinone-binding site of complex II alters the electronic properties of the proximal [3Fe-4S] iron-sulfur cluster. J Biol Chem 286, 12756-65.

[35] Sawers, G. (1994). The hydrogenases and formate dehydrogenases of *Escherichia coli*. Antonie Van Leeuwenhoek 66, 57-88.

[36] Sawers, G., Heider, J., Zehelein, E. and Böck, A. (1991). Expression and operon structure of the *sel* genes of *Escherichia coli* and identification of a third selenium-containing formate dehydrogenase isoenzyme. J Bacteriol 173, 4983-93.

[37] Plunkett, G., Burland, V., Daniels, D.L. and Blattner, F.R. (1993). Analysis of the *Escherichia coli* genome. III. DNA sequence of the region from 87.2 to 89.2 minutes. Nucleic Acids Res 21, 3391-8.

[38] Jormakka, M., Törnroth, S., Byrne, B. and Iwata, S. (2002). Molecular basis of proton motive force generation: structure of formate dehydrogenase-N. Science 295, 1863-8.

[39] Thompson, J.D., Higgins, D.G. and Gibson, T.J. (1994). CLUSTAL W: improving the sensitivity of progressive multiple sequence alignment through sequence weighting, position-specific gap penalties and weight matrix choice. Nucleic Acids Res 22, 4673-80.

[40] Giordano, G., Grillet, L., Rosset, R., Dou, J.H., Azoulay, E. and Haddock, B.A. (1978). Characterization of an *Escherichia coli* K12 mutant that is sensitive to chlorate when grown aerobically. Biochem J 176, 553-61.

[41] Pommier, J., Mandrand, M.A., Holt, S.E., Boxer, D.H. and Giordano, G. (1992). A second phenazine methosulphate-linked formate dehydrogenase isoenzyme in *Escherichia coli*. Biochim Biophys Acta 1107, 305-13.

[42] Pereira, M.M., Santana, M. and Teixeira, M. (2001). A novel scenario for the evolution of haem-copper oxygen reductases. Biochim Biophys Acta 1505, 185-208.

[43] Puustinen, A., Finel, M., Virkki, M. and Wikström, M. (1989). Cytochrome *o* (*bo*) is a proton pump in *Paracoccus denitrificans* and *Escherichia coli*. FEBS Lett 249, 163-7.

[44] Abramson, J. et al. (2000). The structure of the ubiquinol oxidase from *Escherichia coli* and its ubiquinone binding site. Nat Struct Biol 7, 910-7.

[45] Namslauer, A. and Brzezinski, P. (2004). Structural elements involved in electron-coupled proton transfer in cytochrome *c* oxidase. FEBS Lett 567, 103-10.

[46] Brändén, M., Tomson, F., Gennis, R.B. and Brzezinski, P. (2002). The entry point of the K-proton-transfer pathway in cytochrome *c* oxidase. Biochemistry 41, 10794-8.

[47] Puustinen, A., Finel, M., Haltia, T., Gennis, R.B. and Wikström, M. (1991). Properties of the two terminal oxidases of *Escherichia coli*. Biochemistry 30, 3936-42.

[48] Yoshikawa, S. et al. (1998). Redox-coupled crystal structural changes in bovine heart cytochrome *c* oxidase. Science 280, 1723-9.

[49] Saiki, K., Mogi, T. and Anraku, Y. (1992). Heme *O* biosynthesis in *Escherichia coli*: the *cyoE* gene in the cytochrome *bo* operon encodes a protoheme IX farnesyltransferase. Biochem Biophys Res Commun 189, 1491-7.

[50] Kita, K., Konishi, K. and Anraku, Y. (1984). Terminal oxidases of *Escherichia coli* aerobic respiratory chain. I. Purification and properties of cytochrome b_{562}-*o* complex from cells in the early exponential phase of aerobic growth. J Biol Chem 259, 3368-74.

[51] Stenberg, F., von Heijne, G. and Daley, D.O. (2007). Assembly of the cytochrome bo_3 complex. J Mol Biol 371, 765-73.

[52] Trumpower, B.L. and Gennis, R.B. (1994). Energy transduction by cytochrome complexes in mitochondrial and bacterial respiration: the enzymology of coupling electron transfer reactions to transmembrane proton translocation. Annu Rev Biochem 63, 675-716.

[53] Miller, M.J., Hermodson, M. and Gennis, R.B. (1988). The active form of the cytochrome d terminal oxidase complex of *Escherichia coli* is a heterodimer containing one copy of each of the two subunits. J Biol Chem 263, 5235-40.

[54] Lorence, R.M., Koland, J.G. and Gennis, R.B. (1986). Coulometric and spectroscopic analysis of the purified cytochrome *d* complex of *Escherichia coli*: evidence for the identification of "cytochrome a_1" as cytochrome b_{595}. Biochemistry 25, 2314-21.

[55] Newton, G. and Gennis, R.B. (1991). *In vivo* assembly of the cytochrome *d* terminal oxidase complex of *Escherichia coli* from genes encoding the two subunits expressed on separate plasmids. Biochim Biophys Acta 1089, 8-12.

[56] Borisov, V., Arutyunyan, A.M., Osborne, J.P., Gennis, R.B. and Konstantinov, A.A. (1999). Magnetic circular dichroism used to examine the interaction of *Escherichia coli* cytochrome *bd* with ligands. Biochemistry 38, 740-50.

[57] Hill, J.J., Alben, J.O. and Gennis, R.B. (1993). Spectroscopic evidence for a heme-heme binuclear center in the cytochrome *bd* ubiquinol oxidase from *Escherichia coli*. Proc Natl Acad Sci U S A 90, 5863-7.

[58] Belevich, I., Borisov, V.B., Zhang, J., Yang, K., Konstantinov, A.A., Gennis, R.B. and Verkhovsky, M.I. (2005). Time-resolved electrometric and optical studies on cytochrome bd suggest a mechanism of electron-proton coupling in the di-heme active site. Proc Natl Acad Sci U S A 102, 3657-62.

[59] Borisov, V.B., Belevich, I., Bloch, D.A., Mogi, T. and Verkhovsky, M.I. (2008). Glutamate 107 in subunit I of cytochrome *bd* from *Escherichia coli* is part of a transmembrane intraprotein pathway conducting protons from the cytoplasm to the heme b_{595}/heme *d* active site. Biochemistry 47, 7907-14.

[60] Osborne, J.P. and Gennis, R.B. (1999). Sequence analysis of cytochrome *bd* oxidase suggests a revised topology for subunit I. Biochim Biophys Acta 1410, 32-50.

[61] Dassa, J., Fsihi, H., Marck, C., Dion, M., Kieffer-Bontemps, M. and Boquet, P.L. (1991). A new oxygen-regulated operon in *Escherichia coli* comprises the genes for a putative third cytochrome oxidase and for pH 2.5 acid phosphatase (*appA*). Mol Gen Genet 229, 341-52.

[62] Mason, M.G., Shepherd, M., Nicholls, P., Dobbin, P.S., Dodsworth, K.S., Poole, R.K. and Cooper, C.E. (2009). Cytochrome *bd* confers nitric oxide resistance to *Escherichia coli*. Nat Chem Biol 5, 94-6.

[63] Atlung, T., Knudsen, K., Heerfordt, L. and Brøndsted, L. (1997). Effects of sigmaS and the transcriptional activator AppY on induction of the *Escherichia coli hya* and *cbdAB*-appA operons in response to carbon and phosphate starvation. J Bacteriol 179, 2141-6.

[64] Leif, H., Sled, V.D., Ohnishi, T., Weiss, H. and Friedrich, T. (1995). Isolation and characterization of the proton-translocating NADH: ubiquinone oxidoreductase from *Escherichia coli*. Eur J Biochem 230, 538-48.

[65] Wikström, M., Bogachev, A., Finel, M., Morgan, J.E., Puustinen, A., Raitio, M., Verkhovskaya, M. and Verkhovsky, M.I. (1994). Mechanism of proton translocation by the respiratory oxidases. The histidine cycle. Biochim Biophys Acta 1187, 106-11.

[66] Borisov, V.B., Murali, R., Verkhovskaya, M.L., Bloch, D.A., Han, H., Gennis, R.B. and Verkhovsky, M.I. (2011). Aerobic respiratory chain of *Escherichia coli* is not allowed to work in fully uncoupled mode. Proc Natl Acad Sci U S A 108, 17320-4.

[67] Cecchini, G., Maklashina, E., Yankovskaya, V., Iverson, T.M. and Iwata, S. (2003). Variation in proton donor/acceptor pathways in succinate:quinone oxidoreductases. FEBS Lett 545, 31-8.

[68] Walker, J.E. (2013). The ATP synthase: the understood, the uncertain and the unknown. Biochem Soc Trans 41, 1-16.

[69] Ballhausen, B., Altendorf, K. and Deckers-Hebestreit, G. (2009). Constant c10 ring stoichiometry in the *Escherichia coli* ATP synthase analyzed by cross-linking. J Bacteriol 191, 2400-4.

[70] Ferguson, S.J. (2010). ATP synthase: from sequence to ring size to the P/O ratio. Proc Natl Acad Sci U S A 107, 16755-6.

Chapter 3

Escherichia coli *aerobic respiratory chain is organized in supercomplexes*

Summary

The organization of respiratory chain complexes in supercomplexes has been shown in the mitochondria of several eukaryotes and in the cell membranes of some bacteria. These supercomplexes are suggested to be important for oxidative phosphorylation efficiency and to prevent the formation of reactive oxygen species.

Here we describe, for the first time, the identification of supramolecular organizations in the aerobic respiratory chain of *Escherichia coli*, including a trimer of succinate dehydrogenase. Furthermore, two heterooligomerizations have been shown: one resulting from the association of the NADH:quinone oxidoreductases NDH-1 and NDH-2, and another composed of cytochrome bo_3 quinol:oxygen reductase, cytochrome *bd* quinol:oxygen reductase and formate dehydrogenase (*fdo*). These results are supported by blue native-electrophoresis, mass spectrometry and kinetic data of wild type and mutant *E. coli* strains.

This chapter was published in

***Biochimie* 93, 2011, p. 418-25.**

Supramolecular organizations in the aerobic respiratory chain of *Escherichia coli*

Pedro M.F. Sousa, Sara T.N. Silva, Brian L. Hood, Nuno Charro, João N. Carita, Fátima Vaz, Deborah Penque, Thomas P. Conrads and Ana M.P. Melo.

- Pedro M.F. Sousa performed all the experiments reported in this chapter, with the exception of mass spectrometry analysis, in collaboration with Sara T.N. Silva and Ana M.P. Melo.
- Nuno Charro, Fátima Vaz and Deborah Penque were responsible for the MALDI-TOF/TOF MS analysis.
- Brian L. Hood and Thomas P. Conrads performed the LC-MS/MS analysis.

3.1 Introduction

The respiratory chain of eukaryotic cells is located in the inner mitochondrial membrane, where a set of membrane proteins (complexes I-IV) and small electron carriers (ubiquinone and cytochrome *c*) mediate electron transfer from reducing substrates like NADH and succinate to oxygen. Coupled to the redox reactions, complexes I (type I NADH:ubiquinone oxidoreductase or NDH-1), III (ubiquinol:cytochrome *c* oxidoreductase) and IV (cytochrome *c*:oxygen oxidoreductase) translocate protons from the matrix to the intermembrane space, generating a proton motive force that will enable ATP synthase to synthesize ATP, along with the reflux of protons to the matrix. In contrast to complexes I, III and IV, complex II (succinate:ubiquinone oxidoreductase, SDH) does not translocate protons [1].

Similarly, bacterial aerobic respiratory chains are assembled in the cytoplasmic membrane, through which proton translocation occurs from the cytoplasm to the periplasmic space. Unlike mitochondria, bacteria may have type I, II and III NADH:quinone oxidoreductases [2], together with different types of oxygen reductases, such as cytochrome *bd*-like oxygen reductases and heme-copper oxygen reductases, the latter being either cytochrome *c*/high potential iron-sulfur protein (HiPIP)/blue-copper protein (e.g. sulfocyanin) or quinol:oxygen reductases [3].

The aerobic respiratory chain of *Escherichia coli* comprises type I and II NADH:quinone oxidoreductases, succinate:quinone oxidoreductase, and at least two quinol:oxygen oxidoreductases, cytochromes *bd* and bo_3, all enzymes being differentially expressed in response to the oxygen tension of the culture medium and growth phase [4,5].

Supramolecular organization of respiratory chains has been recently extensively reported for all life domains, challenging the random diffusion model [6] and providing new evidence in strong support of the “solid state” model proposed by

Chance and Williams [7]. In eukaryotes, supercomplexes formed by complexes I, III and IV, the so-called respirasomes, have been observed in mitochondria of bovine heart [8-10], mouse liver [11], potato tuber [12,13], *Neurospora crassa* [14] and *Yarrowia lipolytica* [15]. Associations of complexes III and IV have also been described in these organisms, as well as in *Saccharomyces cerevisiae*, that lacks complex I, and for which a mitochondrial dehydrogenase supercomplex has been proposed [16].

Respiratory chain supercomplexes have also been described in archaea and bacteria. It was reported that *Sulfolobus* sp. strain 7 has a terminal oxygen reductase supercomplex, resulting from the functional fusion of complexes III and IV, containing cytochromes of the *b* and *a* types, and a Rieske-type iron-sulfur protein [17,18]. A mitochondrial-like respirasome was identified in *Paraccocus denitrificans* [19] and supramolecular associations of complexes III and IV were detected in *P. denitrificans* [19,20], *Corynebacterium glutamicum* [21], and *Bacillus* PS3 [22,23].

Although little is known regarding a possible interaction between ATP synthase and respiratory proton translocating complexes, the interaction between the caa_3 oxygen reductase and the ATP synthase of *Bacillus pseudofirmus* has been suggested [24]. Furthermore, oligomers of ATP synthase have been reported in bovine heart mitochondria and seem to shape the inner membrane cristae [25]. In *S. cerevisiae*, dimeric ATP synthase complexes were characterized and proposed to influence the assembly of the complex III-IV supercomplex, providing further evidence for a close relation between ATP synthase and the electron transport complexes [26].

In spite of the fact that the functional relevance of such organizations requires further clarification, there is clear consensus regarding the benefits it may bring to oxidative phosphorylation in the enhancement of electron transfer, sequestration (or diminished formation) of reactive oxygen species, induction of mitochondrial cristae shape and structural stabilization of individual complexes [15,19,27-29].

To date, evidence to support the existence of supercomplexes in the aerobic respiratory chain of *E. coli* is lacking. Indeed, it has been suggested that since it contains a detergent stable complex I and is devoid of complex III, such supramolecular organization is not necessary [19]. Nevertheless, co-localization of oxidative phosphorylation complexes has been suggested [30].

Here, we present evidence for the presence of two supercomplexes, one formed by complex I and the type II NADH:quinone oxidoreductase (NDH-2), and another comprised of cytochromes bo_3 and *bd* quinol:oxygen reductases and a protein with NADH:NBT oxidoreductase activity, that has been identified by mass spectrometry to be the aerobic formate dehydrogenase. Moreover, the trimer of succinate dehydrogenase was observed for the first time in solubilized membranes of this bacterium.

3.2 Materials and Methods

Solubilized membrane preparation

E. coli K-12 (ATCC 23716) and selected respiratory chain mutants were grown manually in Luria-Bertani medium adjusted to pH 7, at 37°C, under vigorous agitation, the volume of cultures corresponding to one fifth of the total volume of the flasks, and harvested at early stationary phase. Upon suspension in MES 50 mM pH 6.0 [31] and disruption in a French press (6000 psi), cells were submitted to low speed centrifugation (14000 x *g*, 15 min) to remove intact cells and cell debris and the supernatant was ultracentrifuged (138000 x *g*, 2 h) to separate the soluble from the membrane fraction. The isolated membrane fraction was aliquoted, frozen in liquid nitrogen and stored at -80°C.

Membrane protein concentration was determined by the BCA assay [32]. Membrane solubilization trials were performed using several detergents (Triton X-100, DDM and digitonin) with variable detergent/protein ratios and analyzed by BN-PAGE (Appendix – Fig. 1). Solubilization was performed in a buffer containing NaCl 50 mM, aminocaproic acid 5 mM, EDTA 1 mM, PMSF 2 mM and imidazole/HCl 50 mM pH 6, on ice for 15 min and vortexing each 3 min, followed by centrifugation (14000 x *g*, 30 min). A ratio of 6 g of digitonin per g of protein was found to be the best solubilization condition that preserved protein-protein interactions within the respiratory chain complexes and therefore used for the subsequent work herein described.

Electrophoretic techniques

Proteins from the solubilized membranes (150 µg per lane) were resolved by BN-PAGE [33-35].

The activities of NADH:NBT and succinate:NBT oxidoreductase were detected *in gel* [36] as well as *b*-type hemes [37]. Solubilized membranes (12.5 mg) were also applied on top of continuous sucrose gradients (0.3 – 1.5 M and 1 – 1.5 M) in a buffer containing 15 mM Tris/HCl pH 7, 20 mM KCl and 0.2% digitonin, resolved by ultra-centrifugation at 4°C (20 h, 150000 x *g*) [38] and 1 mL fractions were collected, frozen in liquid nitrogen and stored at -80°C.

Spectroscopic techniques

Spectroscopic characterization of intact or solubilized wild type membranes was performed by UV-visible absorption spectroscopy. Spectra were recorded with the as-isolated membranes or gradient fractions (oxidized state) and upon reduction by the addition of trace quantities of sodium dithionite powder. To obtain the CO-reduced spectrum, dithionite-reduced samples were incubated with CO gas for 2-3 min before spectral acquisition. The pyridine-hemochrome method [39] was used to quantify the type *b* hemes present in the above mentioned samples.

Catalytic activities

NADH:potassium ferricyanide and succinate:DCPIP oxidoreductase activities were spectrophotometricaly measured in solubilized membranes and in sucrose gradient fractions. NADH:ferricyanide oxidoreductase activity was determined following oxidation of NADH at 340 nm (ε_{NADH} = 6.22 mM^{-1} cm^{-1}) in a reaction buffer containing 100 mM MOPS pH 7.2, 250 µM NADH and 250 µM $K_3[Fe(CN)_6]$ [40]. Succinate:DCPIP oxidoreductase activity was monitored by following the PMS-coupled reduction of DCPIP at 578 nm at 37°C (ε_{DCPIP} = 20.5 mM^{-1} cm^{-1}). The reaction mixture contained 100 mM MOPS pH 7.2, 0.05 mM PMS, 0.05 mM DCPIP and 20 µM succinate [41].

Oxygen consumption rates due to NADH, succinate and quinol oxidation were polarographically determined in a Rank Broths oxygen electrode (Hansatech) at 37°C, in intact membranes, sucrose gradient fractions and NADH:NBT oxidoreductase positive bands. NADH and succinate oxidation were measured in a buffer containing 50 mM MOPS pH 7.2 and 250 µM NADH or 20 mM succinate, respectively. Quinol:oxygen oxidoreductase activity was monitored in a reaction mixture containing 100 mM MOPS pH 7.2, 50 mM KCl, 0.5 mM EDTA, 5.7 mM dithiothreitol, and 80 µM coenzyme Q_1. Specific inhibitors of the respiratory chain complexes such as rotenone (200 µM), piericidin A (2 µM), malonate (15 mM), and KCN (0.5 mM or 2.5 mM) were used. All reactions were initiated by addition of membranes (0.1 mg) or gradient fractions (40 µL).

Mass spectrometry

Proteins from digitonin-solubilized membranes were resolved by BN-PAGE and bands revealing NADH:NBT oxidoreductase activity were excised for digestion and MS analysis [42]. Tryptic peptides were deposited on a 192-well MALDI plate with 5 mg/mL α-CHCA (LaserBiolabs, 1:1) in 0.1% trifluoroacetic acid/ 60% acetonitrile (v/v) and MS analysis was performed on a MALDI-TOF/TOF MS (ABI 4700 Proteomics Analyzer, Applied Biosystems). Internal calibration, data acquisition, processing and interpretation and database search were performed according to standard criteria [43].

In addition, *in gel* digestion was performed and peptide extracts were resuspended in 0.1% trifluoroacetic acid and analyzed by reversed-phase liquid chromatography (Ultimate 3000, Dionex Corporation, Sunnyvale, CA) coupled online to a linear ion trap MS (LTQ-XL, ThermoFisher Scientific, San Jose, CA). Separations were performed using a 75 µm i.d. x 360 o.d. x 20 cm long fused silica capillary columns (Polymicro Technologies, Phoenix, AZ) slurry packed in-house with 5 µm, 300 Å pore size C-18 silica-bonded stationary phase (Jupiter,

Phenomenex, Torrance, CA). Following sample injection onto a C-18 precolumn (Dionex), the column was washed for 3 min with mobile phase A (2% acetonitrile, 0.1% formic acid) at a flow rate of 30 µL/min. Peptides were eluted using a linear gradient of 1% mobile phase B (0.1% formic acid in acetonitrile)/minute for 40 min, then to 95% B in an additional 10 min, all at a constant flow rate of 200 nL/min. Column washing was performed at 95% B for 15 min for all analyses, after which the column was re-equilibrated with mobile phase A prior to subsequent injections.

The MS was operated in data-dependent MS/MS mode in which each full MS scan was followed by seven MS/MS scans performed in the linear ion trap (LIT) where the seven most abundant peptide molecular ions were selected for collision-induced dissociations (CID), using a normalized collision energy of 35%. Data were collected over a broad precursor ion selection scan range of *m/z* 375-1800 and dynamic exclusion was enabled to minimize redundant selection of peptides previously selected for CID. Tandem mass spectra were searched against the UniProt-derived-*E. coli* protein database (6/10 release) from the European Bioinformatics Institute (http://www.ebi.ac.uk/integr8), using SEQUEST (ThermoFisher Scientific). Additionally, peptides were searched for dynamic methionine oxidation (15.995 amu). Peptides were considered legitimately identified if they met specific charge state and proteolytic cleavage-dependent cross correlation scores of 1.9 for $[M+H]^{1|}$, 2.2 for $[M+2H]^{2|}$ and 3.5 for $[M+3H]^{3|}$ and a minimum delta correlation of 0.08.

3.3 Results and Discussion

Characterization of the *E. coli* aerobic respiratory chain activities

Supramolecular organizations involving the NADH:quinone oxidoreductase activity were investigated in the *E. coli* K-12 aerobic respiratory chain, which was thoroughly characterized prior to supercomplex detection.

UV-visible absorption spectra of the *E. coli* solubilized membranes were recorded in the oxidized and dithionite-reduced states and upon incubation with CO. The difference spectrum (spectrum of the dithionite-reduced state minus that of the oxidized state) indicates the presence of hemes *b* (maxima at 416 and 560 nm) and hemes *d* (shoulder at 441 nm, maxima at 631 nm and trough at 651 nm) (Fig. 1A). Furthermore, the difference spectrum of the dithionite-reduced membranes incubated with CO minus the spectrum of the dithionite-reduced membranes revealed the presence of hemes *o* (maxima at 416 and 567 nm and trough at 430 nm) and *d* (shoulder at 420 and maxima at 642 nm and trough at 430, 442, 560 and 622 nm) (Fig. 1B), indicating that both cytochromes bo_3 and *bd* oxygen reductases were expressed [4,44].

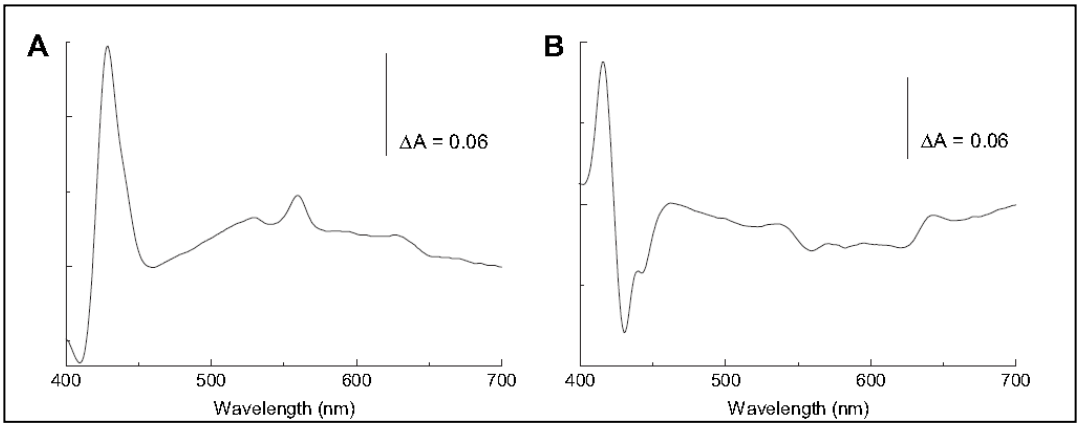

Fig. 1. UV-visible absorption spectra of triton X-100 *E. coli* membranes. Spectral acquisition was performed to the as-isolated membranes (oxidized state) and after the addition of sodium dithionite (reduced state). The dithionite-reduced samples were incubated with CO to obtain the CO spectrum. Shown are difference spectra representing dithionite-reduced minus oxidized (**A**) and CO-reduced minus dithionite-reduced (**B**).

The study of the aerobic respiratory chain activities, performed polarographically with an oxygen electrode, resulted in the detection of NADH:oxygen oxidoreductase activity [2,45]. NADH oxidation was only 70% inhibited by two complex I inhibitors (rotenone and piericidin A), suggesting the presence of another NADH dehydrogenase (NDH-2) as has been previously described for the

E. coli electron transfer chain [46]. A malonate-sensitive succinate:oxygen oxidoreductase activity was also measured, suggesting the presence of SDH [47]. Both NADH and succinate oxidoreductase activities were nearly completely inhibited by KCN (Table 1), which is known to inhibit heme-copper oxygen reductases [3], like cytochrome *bo*$_3$. In addition, a high rate of KCN sensitive quinol:oxygen oxidoreductase activity was observed (Table 1).

Table 1
Substrate:oxygen oxidoreductase activities of the *E. coli* aerobic respiratory chain, at 37°C. The results are an average of three assays with -80°C frozen/thawed membranes.

	Activity nmol O_2 min^{-1} mg^{-1}	Inhibition (%)
NADH	1284 ± 24	
KCN	40 ± 9	97
Succinate	283 ± 4	
KCN	6 ± 0,6	98
Quinol	4248 ± 67	
KCN	0	100

Identification of supramolecular organizations in the aerobic respiratory chain of *E. coli*

i) Detection of supercomplexes by electrophoretic techniques

The solubilized membrane fraction was resolved by BN-PAGE and, after staining for NADH:NBT and succinate:NBT oxidoreductase artificial activities, 4 bands with NADH:NBT oxidoreductase activity (bands 1-4), and 2 bands with activity of succinate:NBT oxidoreductase (bands 5 and 6) were apparent (Fig. 2). In addition, heme staining allowed the detection of another band (band 7). The

apparent molecular mass of bands 1-7 was estimated from the BN-PAGE in reference to molecular markers extracted from bovine heart mitochondria [48] and the molecular mass of the individual respiratory chain complexes was deduced from their primary structures (Table 2).

Bands 5 and 6, with apparent molecular masses of 305 ± 14 and 128 ± 2 kDa, respectively, most likely correspond to the trimeric and monomeric forms of SDH (Fig. 2B). It is noteworthy that the *E. coli* enzyme has been reported to crystallize as a trimer and this oligomerization of the protein was suggested to have physiological relevance [49]. Band 7, detected by heme staining (Fig. 2C), may be attributed to the dimer of cytochrome bo_3 oxygen reductase, previously observed in *E. coli* intact cells resolved by BN-PAGE [50], due to the proximity of the estimated masses (320 kDa vs. 316 ± 12 kDa). This is the first time that it is identified in solubilized membranes, indicating that the solubilization conditions used in this investigation serve to preserve these inter-complex interactions.

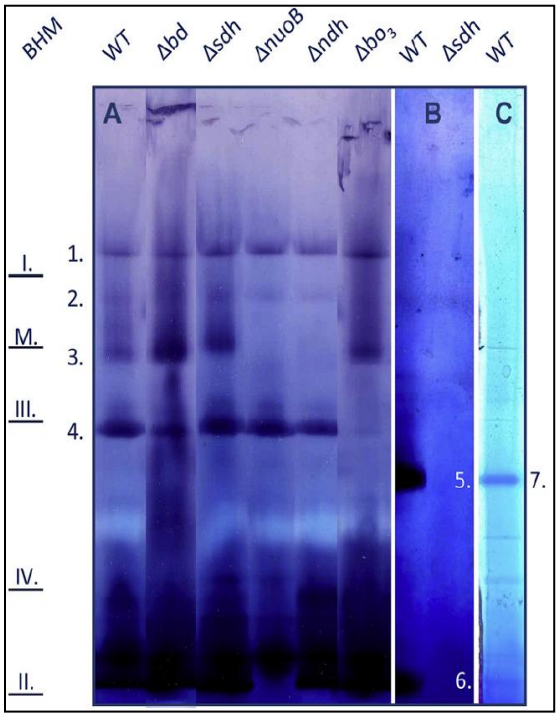

Fig. 2. *In gel* analyses of *E. coli* supercomplexes. Membrane fractions of *E. coli* and bovine heart mitochondria were solubilized with digitonin and resolved by BN-PAGE. **A**. Detection of NADH:NBT oxidoreductase activity in wild type and respiratory chain mutant strains. **B**. The activity of succinate:NBT oxidoreductase as detected in the wild type and SDH deletion strains. This activity was tested in the other respiratory chain mutants, bands 5 and 6 were also detected (data not shown). **C**. Heme staining of wild type membranes. Band 7 was observed in membranes of all mutants (data not shown). BHM – bovine heart mitochondria, I, II, III, IV and M stand for the mitochondrial complexes I-IV, and the ATP synthase, respectively, with molecular masses of 1000, 123, 482, 205 and 597 kDa.

The assignment of bands 1-4 (Fig. 2A) is more complex, since none of the estimated molecular masses fall within those as deduced from the amino acid sequence of complex I, suggesting that at least some of these bands may correspond to respiratory chain supercomplexes.

Table 2
Primary sequence deduced and BN-PAGE estimated molecular masses in kDa of respiratory chain components. The estimated molecular masses are the average of at least 3 BN-PAGE experiments. Band numbering refers to Figure 2.

	DMM[a]	NADH:NBT[b]	Succinate:NBT[b]	Heme staining
NDH-1	537			
NDH-2	48			
SDH	121			
Cytochrome bo_3	142			
Cytochrome *bd*	99			
Fdo	205			
Band 1		991 ± 17		
Band 2		797 ± 11		
Band 3		606 ± 5		
Band 4		432 ± 7		
Band 5			305 ± 14	
Band 6			128 ± 2	
Band 7				316 ± 12

[a] DMM – deduced molecular mass.
[b] oxidoreductase activity.

The quinol:oxygen oxidoreductase activity of bands 1-4 was determined by means of an oxygen electrode. The activity of band 7, already assigned to cytochrome bo_3, was used as a positive control. In contrast with the low quinol oxidation activity exhibited by bands 1-3, bands 4 and 7 exhibited high rates due to oxygen consumption, which were inhibited by addition of KCN, indicating the presence of oxygen reductases in these bands (Fig. 3).

To assign bands 1-4 (Fig. 2A) to *E. coli* respiratory chain components and enumerate the composition of these supercomplexes, the activity NADH:NBT oxidoreductase was detected in the solubilized membrane fraction of *E. coli* strains wherein cytochrome bo_3 (ML20S2), cytochrome *bd* (ML15A),

succinate:quinone oxidoreductase (DW35), complex I (ann021), and NDH-2 (ann001) were deleted.

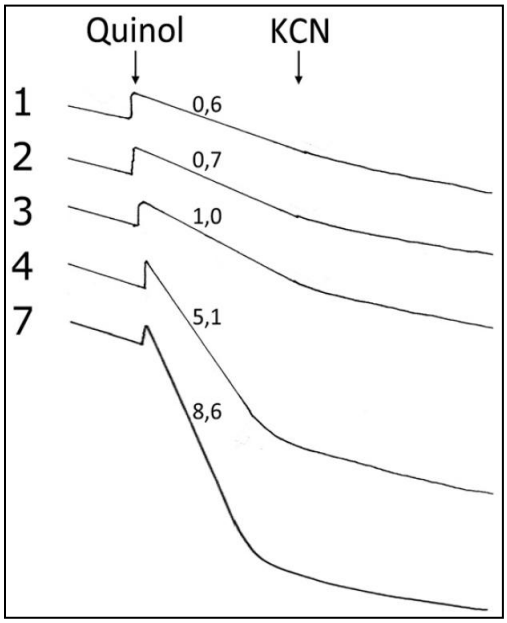

Fig. 3. Quinol:oxygen oxidoreductase activity of NADH:NBT oxidoreductase stained bands. Sets of 6 bands 1, 2, 3, 4 and 7 were excised from the BN-PAGE, placed in the oxygen electrode chamber and assayed for quinol:oxygen oxidoreductase activity. The rates of quinol oxidation activity are presented in nmol O_2 min^{-1} $band^{-1}$ after subtraction of the rates due to oxygen consumption before substrate addition. All activities are fully inhibited by the heme-copper oxidase inhibitor KCN.

The activities of bands 1 and 2 were not affected by any of the referred gene deletions, suggesting that the proteins responsible for the NADH:NBT oxidoreductase activity in these bands do not arise from the aerobic electron transfer chain of this bacterium. Band 1 was analyzed by MALDI-TOF/TOF and identified as pyruvate dehydrogenase (data not shown), further corroborating this suggestion. In contrast, the activity of band 3 is absent in those strains mutant in complex I and NDH-2, and the activity of band 4 is lacking in the membranes prepared from the cytochrome *bo_3* mutant strain. These results indicate the presence of a supramolecular organization involving NADH:quinone oxidoreductases of *E. coli* electron transport chain in band 3. Moreover, the apparent mass of band 3 (606 ± 5 kDa) agrees well with the sum of the individual masses of NDH-1 and NDH-2 (586 kDa). A physical association of both enzymes is supported by the fact that in the absence of NDH-2, a 48 kDa-polypeptide, band 3 is not detected. The presence of complex I in band 3 was further corroborated

by MS. In a preliminary approach, MALDI-TOF/TOF allowed the identification of 2 peptides of NuoB [sequences R.QADLMVVAGTCFTKMAPVIQR.L + oxidation of M (residues 92-112) and R.IAVTNLR.T (residues 209-215)]. To refine and improve this identification, the band was also analyzed by LC-MS/MS, which identified several peptides of subunits Nuo A, B, CD, F, G, H, I and L (Table 3).

Table 3
LC-MS/MS of bands 3 and 4 in Fig. 2.

Band	Enzyme	Subunit	Gene	UniProt Accession	Peptides identified
3	NADH-quinone oxidoreductase	NuoCD	nuoCD	P33599	19
		NuoG	nuoG	P33602	15
		NuoI	nuoI	P0AFD6	8
		NuoB	nuoB	P0AFC7	7
		NuoH	nuoH	P0AFD4	5
		NuoF	nuoF	P31979	5
		NuoA	nuoA	P0AFC3	3
		NuoL	nuoL	P33607	3
4	Formate dehydrogenase-O	FdoG	fdoG	P32176	61
		FdoH	fdoH	P0AAJ5	7
		FdoI	fdoI	P0AEL0	4
	bo$_3$ oxygen reductase	Subunit I	cyoB	P0ABI8	3
		Subunit II	cyoA	P0ABJ1	3
	bd oxygen reductase	Subunit I	cydA	P0ABJ9	11

Band 4 is absent from the cells of the strain deleted in the *bo*$_3$ oxygen reductase, thus indicating the presence of a NADH oxidase supercomplex. To identify the partner of cytochrome *bo*$_3$ in this supercomplex, band 4 was also analyzed by LC-MS/MS. As expected, peptides originating from subunits I and II of *bo*$_3$ oxygen reductase were identified, along with peptides from subunit I of cytochrome *bd*. This result correlates with the observation that the intensity of band 4 is considerably reduced in the strain devoid of cytochrome *bd* and this decrease in intensity is reproducible. In addition, several peptides from the three components of the aerobic membrane-bound formate dehydrogenase, FdoG, H and I, were

also identified (Table 3). This enzyme catalyzes the reversible oxidation of formate coupled to the reduction of NAD^+.

The aerobic formate dehydrogenase of *E. coli* has been suggested to oxidize formate from the cytoplasm [51] and to be able of transferring electrons to terminal oxygen reductases, *via* ubiquinone [52]. The co-localization of the 3 enzymes in band 4 and the absence or reduction of the NADH:NBT oxidoreductase activity in the membranes of the *E. coli* strains devoid of cytochrome bo_3 or *bd*, respectively, suggests the assembly of a formate oxidase supercomplex, with a stoichiometry of 1:1:1, which is further supported by the estimated mass of band 4, 432 ± 7 kDa, in agreement with the sum of the 3 enzymatic components of the supercomplex hypothesized herein, 446 kDa. It is tempting to speculate that in the cytochrome *bd* mutant strain, band 4 may account for a formate oxidase supercomplex where the cytochrome *bd* unit was replaced by a second molecule of cytochrome bo_3 in a 1:2 stoichiometry, a supramolecular organization with a molecular mass in close proximity to that of the corresponding wild type supercomplex. The proposed respiratory chain supercomplex could provide an alternative pathway to generate the proton motive force to drive ATP synthesis or secondary transport in aerobic conditions.

ii) Sucrose gradient analysis of *E. coli* membranes

An alternative procedure to resolve *E. coli* respiratory chain components according to their molecular mass was also performed using a sucrose gradient (0.3 – 1.5 M) centrifugation of the solubilized membranes. The resolved gradient was divided in 1 mL fractions (F1-F9 from highest to lowest molecular mass, respectively) and the respiratory chain activities with artificial electron acceptors, the oxygen consumption rates and heme *b* content were determined. NADH:$K_3[Fe(CN)_6]$ oxidoreductase activity was present throughout the gradient fractions being maximal in fraction 1. Such distribution may be explained by the

presence of type I and II NADH:quinone oxidoreductases as monomers, homodimers or combined with other respiratory chain complexes in supercomplexes. Recently, Muster *et al.* [53] suggested that there may be a population of respiratory chain complexes that is not assembled in supercomplexes, based on *in vivo* data obtained from living HeLa cells. Succinate:DCPIP oxidoreductase activity was also maximal in fraction 1 but also significant in fractions 6 and 8, probably accounting for the trimeric and monomeric forms of the SDH complex, respectively (Fig. 4B).

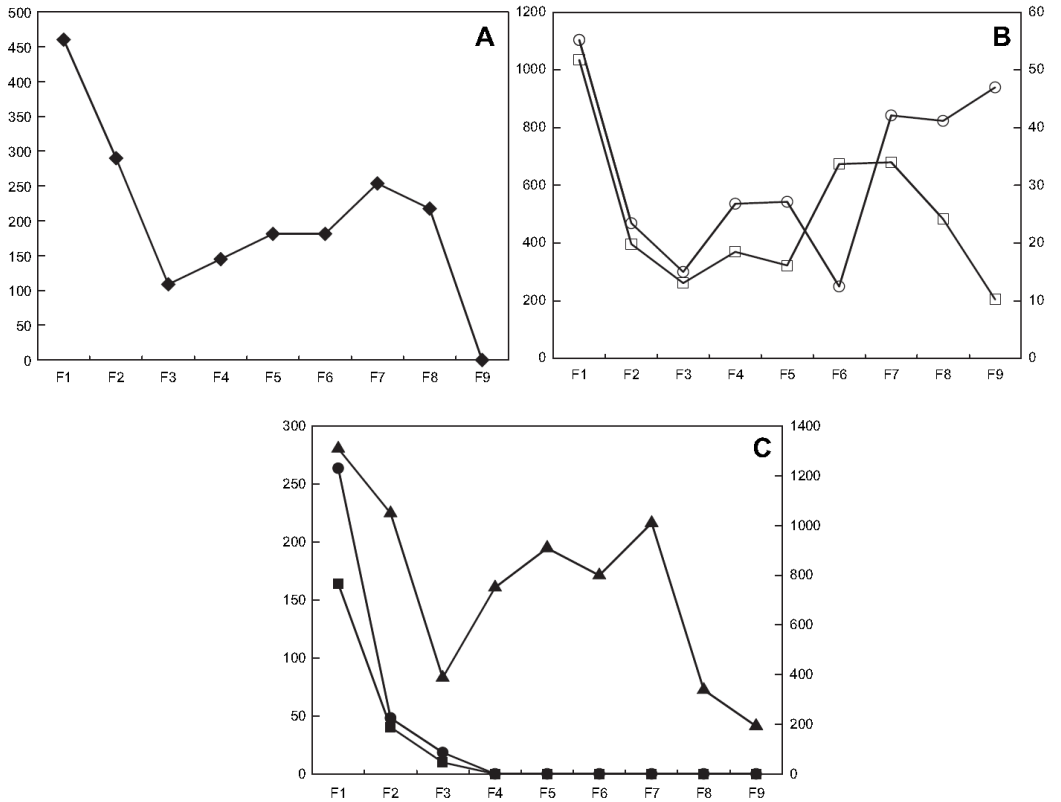

Fig. 4. Characterization of 0.3-1.5 M sucrose gradient fractions. The sucrose gradient fractions were investigated polarographically with respect to their substrate:oxygen oxidoreductase activity, and their heme *b* content was spectrophotometricaly assessed measuring the pyridine-hemochrome formation. The artificial activities NADH:$K_3[Fe(CN)_6]$ and succinate:DCPIP oxidoreductase were also measured. **A**. Pyridine-hemochrome content (nM). **B**. NADH:$K_3[Fe(CN)_6$, open balls, ($nmol_{NADH}$ mL^{-1} min^{-1}) and succinate:DCPIP oxidoreductase activities, open squares, ($nmol_{DCPIP}$ mL^{-1} min^{-1}). **C**. NADH: (filled balls, primary axis), succinate: (filled squares, primary axis) and quinol: (filled triangles, secondary axis) oxygen oxidoreductase activities ($nmol_{O_2}$ mL^{-1} min^{-1}).

The amount of *b*-type hemes is maximal in fraction 1, followed by fractions 6-8, although present in other fractions (Fig. 4A). Considering that *E. coli* bo_3, *bd* quinol:oxygen reductases and SDH are heme *b*-containing proteins, the distribution of hemes *b* in several gradient fractions may also result from the different oligomerization states of these enzymes, as well as from their supramolecular association with other complexes.

Oxygen consumption due to NADH or succinate oxidation was only present in fractions 1 and 2, being significantly higher in fraction 1 (Fig. 4C). These activities were more than 90% inhibited by KCN, indicating that a complete respiratory chain is operative. Quinol:oxygen oxidoreductase activity was also evident in the sucrose gradient fractions. In this case, the activity was distributed throughout the gradient, the activity of which was also maximal in fraction 1, and completely inhibited by KCN (Fig. 4C). The results from the analysis of the sucrose gradient fractions further support the notion that the *E. coli* aerobic respiratory chain is organized in a supramolecular fashion.

A refined sucrose gradient (1-1.5 M) fractionation was performed showing that NADH and succinate:oxygen oxidoreductase activities were maximal in fraction 4, thus excluding the possibility of the results obtained in the wider range-gradient being explained by protein aggregation (Fig. 5). The latter results were corroborated by the observation that NADH and succinate:oxygen oxidoreductase activities of *E. coli* membranes and fraction 1 of the 0.3-1.5 M sucrose gradient were eliminated in the presence of 0.025% Triton X-100, while the activities of the individual enzymes were retained, as assessed by the spectrophotometric measurement of NADH:ferricyanide and succinate:DCPIP oxidoreductase activities. This observation indicates that the presence of intact respiratory chain modules, upon digitonin solubilization, does not result from protein aggregation but from inter-complex interactions, which, although preserved upon digitonin solubilization, are disrupted by the subsequent addition of the harsher detergent Triton X-100.

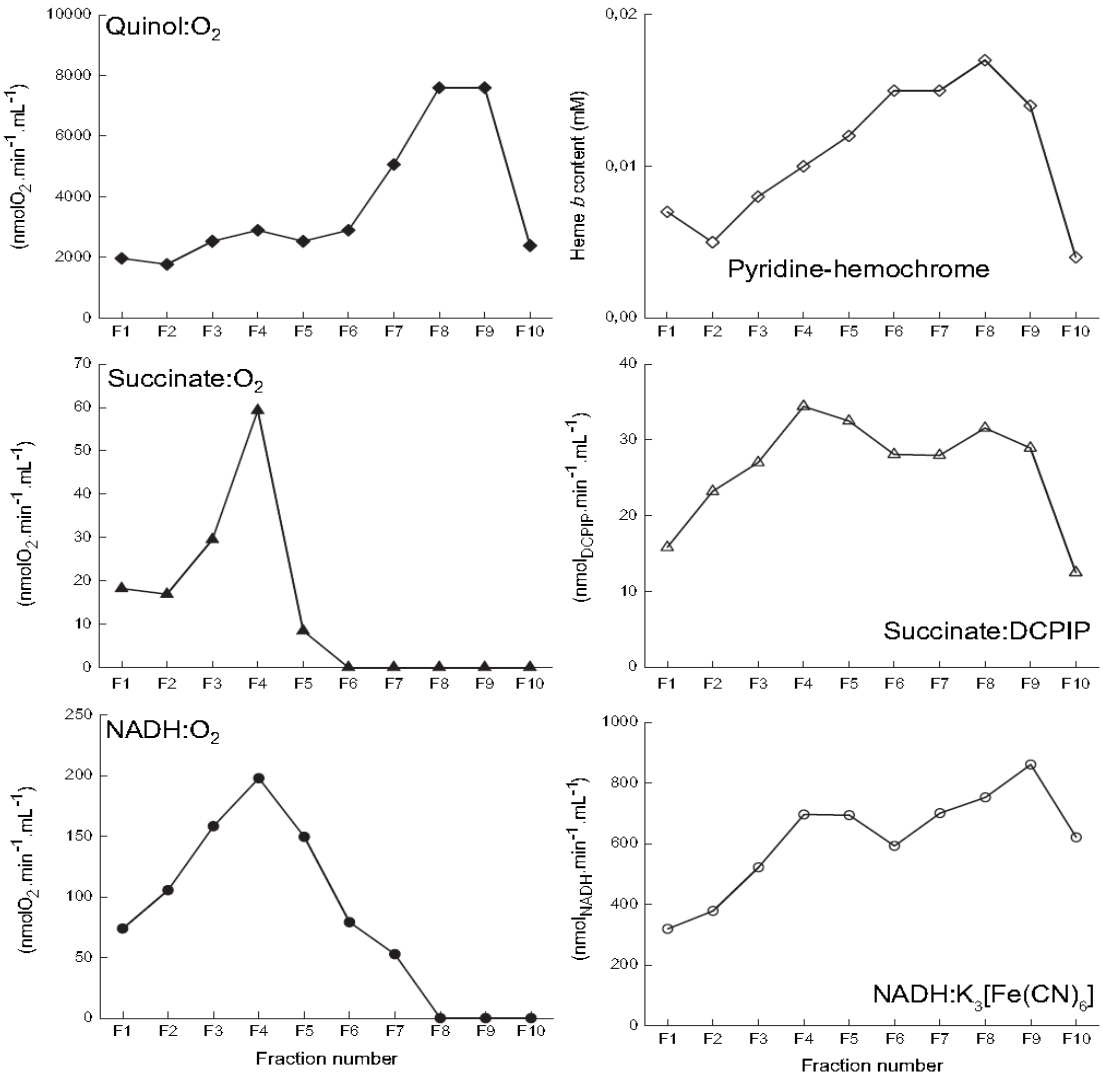

Fig. 5. Resolution of digitonin-solubilized *E. coli* membranes by sucrose gradient centrifugation. The gradient fractions were analyzed as in Fig. 4. The highest succinate: and NADH:oxygen oxidoreductase activities were observed in fraction 4, where quinol:oxygen oxidoreductase activity was also present (left side). Fraction 4 also contains type *b* hemes, presumably from cytochrome bo_3 oxygen reductase and succinate:ubiquinone oxidoreductase, and succinate:DCPIP and NADH:$K_3[Fe(CN)_6]$ oxidoreductase activities (right side).

3.4 Conclusion

Here is provided for the first time evidence for the presence of supercomplexes in the aerobic respiratory chain of *E. coli*, namely a supercomplex formed by NDH-1 and NDH-2, and a second representing the assembly of formate dehydrogenase with the oxygen reductases bo_3 and *bd*. In the context of prokaryotes, the supramolecular associations of the aerobic respiratory chain reported to date involved only cytochrome *c*:oxygen oxidoreductases, similarly to those present in mitochondria, namely the aa_3 cytochrome *c*:oxygen oxidoreductase in the *P. denitrificans* respirasome and the caa_3:cytochrome *c*:oxygen oxidoreductase in *Bacillus* PS3. It is, thus, noteworthy that this is the first report of supercomplexes involving enzymes such as type II NADH:quinone oxidoreductase, the *bd* and bo_3 quinol:oxygen reductases, and the aerobic formate dehydrogenase, thereby providing further evidence that supramolecular organization of the respiratory chain complexes is a widespread strategy to optimize oxidative phosphorylation.

3.5 Acknowledgments

We are greatly indebted to Drs. Miguel Teixeira and Lígia Saraiva for continuous suggestions during the work presented and critical review of this manuscript. The authors would like to thank Drs. Robert Gennis, Thorsten Friedrich and Joel Weiner for the *E. coli* strains ML20S2 and ML15A, ann001 and ann021, and DW35, respectively. Isabel Palos and Paula Alves, from IICT, and Patricia Gomes-Alves, from INSA are acknowledged for excellent technical assistance. The present research was funded by Fundação para a Ciência e a Tecnologia (FCT) (PTDC/BIA-PRO/67105/2006 to AMPM), FCT/Poly-Annual Funding and FEDER/Saúde XXI Programs to DP (Portugal); PS and NC received grants from FCT (SFRH/BD/46553/2008, SFRH/27906/2006, respectively), SS is the recipient of a BI grant in the frame of the financing project.

3.6 References

[1] Hatefi, Y. (1985). The mitochondrial electron transport and oxidative phosphorylation system. Annu Rev Biochem 54, 1015-69.

[2] Melo, A.M.P., Bandeiras, T.M. and Teixeira, M. (2004). New insights into type II NAD(P)H:quinone oxidoreductases. Microbiol Mol Biol Rev 68, 603-16.

[3] Pereira, M.M., Bandeiras, T.M., Fernandes, A.S., Lemos, R.S., Melo, A.M.P. and Teixeira, M. (2004). Respiratory chains from aerobic thermophilic prokaryotes. J Bioenerg Biomembr 36, 93-105.

[4] Kita, K., Konishi, K. and Anraku, Y. (1984). Terminal oxidases of *Escherichia coli* aerobic respiratory chain. II. Purification and properties of cytochrome b_{558}-*d* complex from cells grown with limited oxygen and evidence of branched electron-carrying systems. J Biol Chem 259, 3375-81.

[5] Unden, G. and Bongaerts, J. (1997). Alternative respiratory pathways of *Escherichia coli*: energetics and transcriptional regulation in response to electron acceptors. Biochim Biophys Acta 1320, 217-34.

[6] Hackenbrock, C.R., Chazotte, B. and Gupte, S.S. (1986). The random collision model and a critical assessment of diffusion and collision in mitochondrial electron transport. J Bioenerg Biomembr 18, 331-68.

[7] Chance, B. and Williams, G.R. (1955). A method for the localization of sites for oxidative phosphorylation. Nature 176, 250-4.

[8] Bianchi, C., Genova, M.L., Parenti Castelli, G. and Lenaz, G. (2004). The mitochondrial respiratory chain is partially organized in a supercomplex assembly: kinetic evidence using flux control analysis. J Biol Chem 279, 36562-9.

[9] Schäfer, E., Dencher, N.A., Vonck, J. and Parcej, D.N. (2007). Three-dimensional structure of the respiratory chain supercomplex $I_1III_2IV_1$ from bovine heart mitochondria. Biochemistry 46, 12579-85.

[10] Schägger, H. and Pfeiffer, K. (2001). The ratio of oxidative phosphorylation complexes I-V in bovine heart mitochondria and the composition of respiratory chain supercomplexes. J Biol Chem 276, 37861-7.

[11] Acín-Pérez, R., Fernández-Silva, P., Peleato, M.L., Pérez-Martos, A. and Enriquez, J.A. (2008). Respiratory active mitochondrial supercomplexes. Mol Cell 32, 529-39.

[12] Bultema, J.B., Braun, H.P., Boekema, E.J. and Kouril, R. (2009). Megacomplex organization of the oxidative phosphorylation system by structural analysis of respiratory supercomplexes from potato. Biochim Biophys Acta 1787, 60-7.

[13] Eubel, H., Heinemeyer, J. and Braun, H.P. (2004). Identification and characterization of respirasomes in potato mitochondria. Plant Physiol 134, 1450-9.

[14] Marques, I., Dencher, N.A., Videira, A. and Krause, F. (2007). Supramolecular organization of the respiratory chain in *Neurospora crassa* mitochondria. Eukaryot Cell 6, 2391-405.

[15] Nübel, E., Wittig, I., Kerscher, S., Brandt, U. and Schägger, H. (2009). Two-dimensional native electrophoretic analysis of respiratory supercomplexes from *Yarrowia lipolytica*. Proteomics 9, 2408-18.

[16] Grandier-Vazeille, X., Bathany, K., Chaignepain, S., Camougrand, N., Manon, S. and Schmitter, J.M. (2001). Yeast mitochondrial dehydrogenases are associated in a supramolecular complex. Biochemistry 40, 9758-69.

[17] Iwasaki, T., Matsuura, K. and Oshima, T. (1995). Resolution of the aerobic respiratory system of the thermoacidophilic archaeon, Sulfolobus sp. strain 7. I. The archaeal terminal oxidase supercomplex is a functional fusion of respiratory complexes III and IV with no *c*-type cytochromes. J Biol Chem 270, 30881-92.

[18] Iwasaki, T., Wakagi, T., Isogai, Y., Iizuka, T. and Oshima, T. (1995). Resolution of the aerobic respiratory system of the thermoacidophilic archaeon, Sulfolobus sp. strain 7. II. Characterization of the archaeal terminal oxidase subcomplexes and implication for the intramolecular electron transfer. J Biol Chem 270, 30893-901.

[19] Stroh, A., Anderka, O., Pfeiffer, K., Yagi, T., Finel, M., Ludwig, B. and Schägger, H. (2004). Assembly of respiratory complexes I, III, and IV into NADH oxidase supercomplex stabilizes complex I in *Paracoccus denitrificans*. J Biol Chem 279, 5000-7.

[20] Berry, E.A. and Trumpower, B.L. (1985). Isolation of ubiquinol oxidase from *Paracoccus denitrificans* and resolution into cytochrome bc_1 and cytochrome c-aa_3 complexes. J Biol Chem 260, 2458-67.

[21] Niebisch, A. and Bott, M. (2003). Purification of a cytochrome bc-aa_3 supercomplex with quinol oxidase activity from *Corynebacterium glutamicum*. Identification of a fourth subunity of cytochrome aa_3 oxidase and mutational analysis of diheme cytochrome c_1. J Biol Chem 278, 4339-46.

[22] Sone, N., Sekimachi, M. and Kutoh, E. (1987). Identification and properties of a quinol oxidase super-complex composed of a bc_1 complex and cytochrome oxidase in the thermophilic bacterium PS3. J Biol Chem 262, 15386-91.

[23] Tanaka, T., Inoue, M., Sakamoto, J. and Sone, N. (1996). Intra- and inter-complex cross-linking of subunits in the quinol oxidase super-complex from thermophilic *Bacillus* PS3. J Biochem 119, 482-6.

[24] Liu, X., Gong, X., Hicks, D.B., Krulwich, T.A., Yu, L. and Yu, C.A. (2007). Interaction between cytochrome caa_3 and F_1F_0-ATP synthase of alkaliphilic *Bacillus pseudofirmus* OF4 is demonstrated by saturation transfer electron paramagnetic resonance and differential scanning calorimetry assays. Biochemistry 46, 306-13.

[25] Strauss, M., Hofhaus, G., Schröder, R.R. and Kühlbrandt, W. (2008). Dimer ribbons of ATP synthase shape the inner mitochondrial membrane. EMBO J 27, 1154-60.

[26] Stuart, R.A. (2008). Supercomplex organization of the oxidative phosphorylation enzymes in yeast mitochondria. J Bioenerg Biomembr 40, 411-7.

[27] Boekema, E.J. and Braun, H.P. (2007). Supramolecular structure of the mitochondrial oxidative phosphorylation system. J Biol Chem 282, 1-4.

[28] Lenaz, G., Fato, R., Formiggini, G. and Genova, M.L. (2007). The role of Coenzyme Q in mitochondrial electron transport. Mitochondrion 7 Suppl, S8-33.

[29] Schägger, H. (2002). Respiratory chain supercomplexes of mitochondria and bacteria. Biochim Biophys Acta 1555, 154-9.

[30] Lenn, T., Leake, M.C. and Mullineaux, C.W. (2008). Clustering and dynamics of cytochrome *bd*-I complexes in the *Escherichia coli* plasma membrane *in vivo*. Mol Microbiol 70, 1397-407.

[31] Leif, H., Sled, V.D., Ohnishi, T., Weiss, H. and Friedrich, T. (1995). Isolation and characterization of the proton-translocating NADH: ubiquinone oxidoreductase from *Escherichia coli*. Eur J Biochem 230, 538-48.

[32] Smith, P.K. et al. (1985). Measurement of protein using bicinchoninic acid. Anal Biochem 150, 76-85.

[33] Krause, F. and Seelert, H. (2008). Detection and analysis of protein-protein interactions of organellar and prokaryotic proteomes by blue native and colorless native gel electrophoresis. Curr Protoc Protein Sci Chapter 19, Unit 19.18.

[34] Schägger, H. and von Jagow, G. (1991). Blue native electrophoresis for isolation of membrane protein complexes in enzymatically active form. Anal Biochem 199, 223-31.

[35] Wittig, I., Braun, H.P. and Schägger, H. (2006). Blue native PAGE. Nat Protoc 1, 418-28.

[36] Zerbetto, E., Vergani, L. and Dabbeni-Sala, F. (1997). Quantification of muscle mitochondrial oxidative phosphorylation enzymes via histochemical staining of blue native polyacrylamide gels. Electrophoresis 18, 2059-64.

[37] Holland, V., Saunders, B., Rose, F. and Walpole, A. (1974). A safer substitute for benzidine in the detection of blood. Tetrahedron 30, 3299-3302.

[38] Dudkina, N.V., Eubel, H., Keegstra, W., Boekema, E.J. and Braun, H.P. (2005). Structure of a mitochondrial supercomplex formed by respiratory-chain complexes I and III. Proc Natl Acad Sci U S A 102, 3225-9.

[39] Berry, E.A. and Trumpower, B.L. (1987). Simultaneous determination of hemes *a*, *b*, and *c* from pyridine hemochrome spectra. Anal Biochem 161, 1-15.

[40] Hatefi, Y. (1978). Preparation and properties of NADH: ubiquinone oxidoreductase (complex I), EC 1.6.5.3. Methods Enzymol 53, 11-4.

[41] Hatefi, Y. (1978). Resolution of complex II and isolation of succinate dehydrogenase (EC 1.3.99.1). Methods Enzymol 53, 27-35.

[42] Bensalem, N. et al. (2007). High sensitivity identification of membrane proteins by MALDI TOF-MASS spectrometry using polystyrene beads. J Proteome Res 6, 1595-602.

[43] Gomes-Alves, P., Couto, F., Pesquita, C., Coelho, A.V. and Penque, D. (2010). Rescue of F508del-CFTR by RXR motif inactivation triggers proteome modulation associated with the unfolded protein response. Biochim Biophys Acta 1804, 856-65.

[44] Kita, K., Konishi, K. and Anraku, Y. (1984). Terminal oxidases of *Escherichia coli* aerobic respiratory chain. I. Purification and properties of cytochrome b_{562}-*o* complex from cells in the early exponential phase of aerobic growth. J Biol Chem 259, 3368-74.

[45] Friedrich, T. et al. (1994). Two binding sites of inhibitors in NADH: ubiquinone oxidoreductase (complex I). Relationship of one site with the ubiquinone-binding site of bacterial glucose:ubiquinone oxidoreductase. Eur J Biochem 219, 691-8.

[46] Bragg, P.D. and Hou, C. (1967). Reduced nicotinamide adenine dinucleotide oxidation in *Escherichia coli* particles. II. NADH dehydrogenases. Arch Biochem Biophys 119, 202-8.

[47] Maklashina, E. and Cecchini, G. (1999). Comparison of catalytic activity and inhibitors of quinone reactions of succinate dehydrogenase (Succinate-ubiquinone oxidoreductase) and fumarate reductase (Menaquinol-fumarate oxidoreductase) from *Escherichia coli*. Arch Biochem Biophys 369, 223-32.

[48] Wittig, I., Beckhaus, T., Wumaier, Z., Karas, M. and Schägger, H. (2010). Mass estimation of native proteins by blue native electrophoresis: principles and practical hints. Mol Cell Proteomics 9, 2149-61.

[49] Yankovskaya, V. et al. (2003). Architecture of succinate dehydrogenase and reactive oxygen species generation. Science 299, 700-4.

[50] Stenberg, F., von Heijne, G. and Daley, D.O. (2007). Assembly of the cytochrome bo_3 complex. J Mol Biol 371, 765-73.

[51] Benoit, S., Abaibou, H. and Mandrand-Berthelot, M.A. (1998). Topological analysis of the aerobic membrane-bound formate dehydrogenase of *Escherichia coli*. J Bacteriol 180, 6625-34.

[52] Sawers, G., Heider, J., Zehelein, E. and Böck, A. (1991). Expression and operon structure of the *sel* genes of *Escherichia coli* and identification of a third selenium-containing formate dehydrogenase isoenzyme. J Bacteriol 173, 4983-93.

[53] Muster, B., Kohl, W., Wittig, I., Strecker, V., Joos, F., Haase, W., Bereiter-Hahn, J. and Busch, K. (2010). Respiratory chain complexes in dynamic mitochondria display a patchy distribution in life cells. PLoS One 5, 11-25.

Chapter 4

The aerobic respiratory chain of Escherichia coli*: from genes to supercomplexes*

Summary

In spite of the large number of reports on the aerobic respiratory chain of *Escherichia coli*, from gene transcription regulation to enzyme kinetics and structural studies, an integrative perspective of this pathway is yet to be produced. Here, a multi-level analysis of the aerobic respiratory chain of *E. coli* was performed to find correlations between gene transcription, enzyme activity, growth dynamics, and supercomplex formation and composition. The transcription level of all genes encoding the aerobic respiratory chain of *E. coli* varied significantly in response to bacterial growth. Coordinated expression patterns were observed between the genes encoding NADH:quinone oxidoreductase and complex I (NDH-1), alternative NADH:quinone oxidoreductase (NDH-2) and cytochrome *bd*I, and also between *sdhA* and *appC*, encoding succinate dehydrogenase and cytochrome *bd*II, respectively. In general, the rates of the respiratory chain activities increased from mid-exponential to late-stationary phase, with no significant further variation occurring until the mid-stationary phase. Multi-level correlations between gene transcription, enzyme activity and growth dynamics were also found in this study. The previously reported NADH dehydrogenase and formate:oxygen oxidoreductase supercomplexes of *E. coli* were already assembled at mid-exponential phase and remained throughout growth. A new succinate oxidase supercomplex composed of succinate dehydrogenase and cytochrome *bd*II was identified, in agreement with the suggestion provided by the coordinated transcription of *sdhA* and *appC*.

This chapter was published in

***Microbiology* 158, 2012, p. 2408-18.**

The aerobic respiratory chain of *Escherichia coli*: from genes to supercomplexes

Pedro M.F. Sousa, Marco A.M. Videira, Andreas Bohn, Brian L. Hood, Thomas P. Conrads, Luis F. Goulao and Ana M.P. Melo.

- Pedro M.F. Sousa performed all the experiments reported in this chapter, with the exception of mass spectrometry and statistical analyses, in collaboration with Marco A.M. Videira and Ana M.P. Melo.
- Andreas Bohn and Luis F. Goulao were responsible for the statistical analyses integrating data from the bacterial growth, enzymatic activities and transcription profiles.
- Brian L. Hood and Thomas P. Conrads performed the LC-MS/MS analysis.

4.1 Introduction

The respiratory chains of the facultatively anaerobic, Gram negative bacterium *Escherichia coli* have been intensively studied since the early 60s of the last century [1-3]. Many studies of the structure, kinetics and transcriptional regulation of both the aerobic and anaerobic electron transfer chains, which consider either the whole pathway or the individual enzymes, have been reported separately, but an overall analysis of the respiratory pathway is lacking.

The aerobic electron transfer chain of *E. coli* is located in the cytosolic membrane and comprises three major primary dehydrogenases, e.g. a succinate:quinone oxidoreductase (SDH) [4] and two NADH dehydrogenases (see [5] for a review), a type I NADH:quinone oxidoreductase (complex I or NDH-1), a type II NADH:quinone oxidoreductase (NDH-2) [6], and three ubiquinol:oxygen oxidoreductases, cytochromes bo_3 [7], *bd*I and *bd*II [8,9]. The apparent redundancy of the NADH dehydrogenases and oxygen reductases, which is also observed in other prokaryotes, may provide this bacterium with the required robustness to adjust to a wide range of environmental conditions [10], like temperature, carbon source or oxygen availability.

The supramolecular organization of the aerobic respiratory chain in supercomplexes has already been studied (see [11] for a review), namely in bacteria such as *Paraccocus denitrificans* [12] and *Aquifex aeolicus* [13], and more recently in the cytoplasmic membrane of *E. coli* [14]. In the last, supercomplexes composed by NDH-1 and NDH-2, and by the aerobic formate dehydrogenase (FdoGHI) [15] and cytochrome bo_3 have been described.

The expression of the genes encoding the aerobic respiratory chain of *E. coli* depends on external factors, such as oxygen availability [16], *via* the two-component ArcBA system (anoxic redox control), which senses oxygen availability and triggers gene transcription [17,18], or the type of electron acceptors available,

and this determines the transcription of the terminal reductases, for instance via the fumarate nitrate regulator, FNR [19].

In addition, the expression of respiratory chain components varies according to the phase of bacterial growth [20], due to the effect of many other transcriptional regulators [21], whose expression is also dependent on the growth phase. Examples include Fis [22], Rpos (RNA polymerase sigma factor) and IHF (integration host factor) [9].

In the present work, we have performed a quantitative analysis of the transcription and activity of the *E. coli* aerobic respiratory chain components in the mid-exponential (mid-log; ML), as well as the early (ES), mid- (MS) and late stationary (LS) phases of growth, to generate a comprehensive view of the events involving the aerobic respiratory chain pathway during the growth of this bacterium. Furthermore, the timing of assembly of respiratory chain supercomplexes during the growth of *E. coli* was investigated.

4.2 Methods

Bacterial growth

Wild-type *E. coli* K-12 (ATCC 23716) cells were grown aerobically in Luria-Bertani (LB) medium [23] in 500 mL flasks with 100 mL bacterial culture, at 37°C and 150 r.p.m. An overnight inoculum was prepared, 1% of which was used to inoculate a new culture to be monitored. Bacterial growth was monitored by following OD_{600}, leading to the generation of a typical growth curve from at least three independent cultures, and allowing the determination of the ML, ES, MS and LS (Fig. 1). Growth curves were fitted with the Richards growth model, using the package "grofit" for the R Language for Statistical Computing [24]. Samples from ML, ES, MS and LS were harvested and used for RNA isolation and membrane preparation. The pH was monitored at harvesting steps presenting a variation of 1 pH unit; it was determined as 6.8, 7.3, 7.8 and 7.8 at ML, ES, MS and LS, respectively.

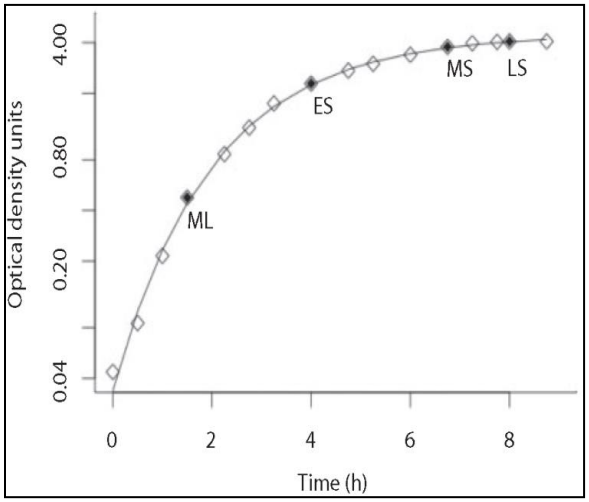

Fig. 1. Aerobic growth of *E. coli* K-12 in LB medium monitored following OD_{600}. The line represents the best-fit curve to the Richards growth model for the experimental data represented by the symbols. Under the given conditions, the *E. coli* K-12 strain presented a maximum value of 4.49 ± 0.09 optical density units (ODU) and growth rate of 0.79 ± 0.02 ODU h^{-1}. Filled symbols correspond to times of sampling for subsequent studies, namely at ML, ES, MS and LS phases of growth, corresponding to OD_{600} 0.5, 2.2, 3.8 and 4, respectively.

Membrane preparation, solubilization and analysis

Cells from *E. coli* were suspended in 50 mM MES, pH 6.0, disrupted in a French press (6000 psi; 414 MPa), and submitted to a low-speed centrifugation (14000 x *g*, 15 min) to pellet intact cells and cell debris. The supernatant was then ultracentrifuged (138000 x *g*, 2 h), and the membrane fraction was obtained in the pellet, suspended in the same buffer, aliquoted, frozen in liquid nitrogen and stored at -80°C until used. Protein concentration was determined using the bicinchoninic acid (BCA) protein assay from Pierce [25]. Membrane solubilization was performed with 6 g digitonin per gram of protein, in a buffer containing 50 mM NaCl, 5 mM aminocaproic acid, 1 mM EDTA, 2 mM PMSF and 50 mM imidazole/HCl, pH 6, as previously described [14]. Solubilized membranes (150 µg per lane) were resolved in a 3-10% acrylamide gradient blue native-PAGE (BN-PAGE) gel [26-28], and NADH:NBT (nitro blue tetrazolium) and succinate:NBT oxidoreductase activities were detected in the gel [29].

Solubilized membranes (12.5 mg) were also applied to the top of a continuous sucrose gradient (0.3-1.5 M) in a buffer containing 15 mM Tris/HCl, pH 7, 20 mM KCl and 0.2% digitonin, resolved by ultracentrifugation at 4°C (20 h, 150000 x *g*) [14,30] and collected in 1 mL fractions.

Membrane samples (50 or 100 µg) were resolved by SDS-PAGE [31], transferred onto a PVDF membrane essentially according to [32], and detected with polyclonal antibodies against subunits of respiratory chain complexes.

RNA isolation, cDNA synthesis and quantitative real-time PCR (qRT-PCR)

RNA was extracted from 2.4 x 10^9 cells harvested at ML, ES, MS and LS using the Aurum Total RNA Mini kit (Bio-Rad), essentially following the manufacturer's instructions with the exception that the period of incubation with DNase I was extended to 45 min.

Isolated RNA was analyzed by agarose gel electrophoresis, and spectrophotometricaly in a NanoDrop instrument (Thermo) using the rations A_{260}/A_{280} and A_{260}/A_{230}, and the 350-220 nm absorption spectrum to assess integrity and purity. The absence of DNA in the purified RNA samples was also verified by PCR with primers nuoCDrev and nuoCDfwd (Table 1).

Reverse transcription and qRT-PCR were performed with the iScript Select cDNA Synthesis kit (Bio-Rad) and SsoFast EvaGreen Supermix (Bio-Rad), respectively, following the manufacturer's instructions, and using 1 µg RNA and 200 ng cDNA as appropriate. Purity and concentration of cDNA were evaluated as described for RNA.

qRT-PCR data were collectively analyzed to determine relative gene expression, using the Pfaffl method with correction for primer efficiency of amplification [33].

Table 1
Oligonucleotides used in qRT-PCR experiments, genes whose expression was analyzed and encoded proteins.

Gene	Oligonucleotide	Sequence (5′–3′)	Protein
appC	AppCRev	GAAAGCCAGTTGTCCTGTGGTT	Cytochrome *bd*II O_2 reductase
	AppCFwd	GGTGGTTTATGACCGAGTTTGG	
cydA	CydBRev	GTCGGTAGAACCAGAACGCAGT	Cytochrome *bd*I O_2 reductase
	CydAFwd	GTTATCGGCCTGAAAGAGCTGA	
cyoB	CyoBRev	GTTTATGGTCGACGGAGGTCAG	Cytochrome bo_3 O_2 reductase
	CyoBFwd	TGGCATTATTTTGGGAGGTCTG	
ndh	NdhRev	ACACCTGGCGTATTGAAATCGT	NDH-2
	NdhFwd	CGAGAAAGGTGAACTGCTGGTT	
nuoCD	NuoCDfwd	TTCGGGTGACCGTCGAAAGT	NDH-1
	NuoCDrev	CCCGGGTAATTTGCGCCTGTCGGCA	
nuoF	NuoFRev	CGGAGATGAGCATACCTTCCAC	NDH-1
	NuoFwd	GCTGTGTAATGCCGATGAAATG	
16S rRNA	16SRev	TACCGCGGCTGCTGGCAC	Ribosome
	16SFwd	TGGAGAGTTTGATCCTGGCTCAG	
sdhA	SdhARev	CAACCACATCTTCGCCTTTCTC	SDH
	SdhAFwd	ATTCCGGTTATCCCAACCTGTC	

Primer design, optimization and efficiency

The primers used in qRT-PCR experiments (Table 1) were designed using the Primer3 algorithm [34], and the reaction conditions were previously optimized in PCRs with genomic DNA. Primer efficiency was determined by qRT-PCR of five sequential dilutions of cDNA. The obtained threshold cycles were plotted against the log values of the corresponding cDNA concentrations, and primer efficiency was calculated based on the trend line slope.

Enzyme activities

NADH:potassium ferricyanide and succinate:DCPIP (dichlorophenol indophenol) oxidoreductase activities were determined spectrophotometricaly by following the oxidation of deamino-NADH (DA-NADH) and NADH at 340 nm (ε_{NADH}=6.22 mM^{-1} cm^{-1}), in a reaction buffer containing 100 mM MOPS, pH 7.2, 250 µM DA-NADH or NADH and 250 µM $K_3[Fe(CN)_6]$ [35], and by following the phenazine methosulfate (PMS)-coupled reduction of DCPIP at 578 nm at 37°C (ε_{DCPIP}=20.5 mM^{-1} cm^{-1}), in a reaction mixture containing 100 mM MOPS, pH 7.2, 0.05 mM PMS, 0.05 mM DCPIP and 20 mM succinate [36], respectively.

Oxygen uptake due to (DA)-NADH, succinate and quinol oxidation was monitored in a Rank Broths oxygen electrode (Hansatech) at 37°C. The oxidation of NADH and succinate was measured in a buffer containing 50 mM MOPS, pH 7.2, and 1 mM NADH or 20 mM succinate, respectively. Quinol:oxygen oxidoreductase activity was assayed in a reaction mixture containing 100 mM MOPS, pH 7.2, 50 mM KCl, 0.5 mM EDTA, 5.7 mM DTT and 80 µM coenzyme Q_1. All assays were ended by the addition of 0.5 or 2.5 mM KCN, an inhibitor of heme-copper oxygen reductases.

Liquid chromatography-tandem mass spectrometry (LC-MS/MS)

Bands with succinate:NBT oxidoreductase activity resulting from BN-PAGE analysis of digitonin-solubilized membranes were excised from the gel, *in gel* digestion was performed, and peptides were extracted and vacuum-dried. The sucrose gradient fractions were buffer-exchanged into 25 mM ammonium bicarbonate, pH 7.5, using Amicon Ultra-0.5 centrifugal filters (10 kDa MWCO, Millipore) through three consecutive concentration and resuspension cycles. Samples were loaded onto a 1D-PAGE gel and electrophoresed briefly to run the proteins into the stacking gel. Bands were excised and treated as above. Tryptic peptides were resuspended in 0.1% (v/v) trifluoroacetic acid and analyzed by nanoflow liquid chromatography (Easy-nLC, Thermo Fisher Scientific) coupled online with an LTQ Orbitrap XL mass spectrometer (Thermo Fisher Scientific). All of the samples were resolved on a 100 µm inner diameter x 360 µm outer diameter x 20 cm long capillary column (Polymicro Technologies), which was slurry-packed in house with a 5 µm, 30 nm pore-size C-18 silica-bonded stationary phase (Jupiter, Phenomenex). Following precolumn and analytical column equilibration, each sample was loaded onto a 2 cm reversed-phase (C-18) precolumn (Thermo Fisher Scientific) at 2 µL min^{-1} for 6 min with mobile phase A [0.1% (v/v) formic acid in water]. Peptides were eluted at a constant flow rate of 200 nL min^{-1} by development of a linear gradient of 0.33% min^{-1} mobile phase B (0.1% formic acid in acetonitrile) for 120 min and then to 95% B for an additional 15 min. The column was washed for 15 min at 95% B and then quickly brought to 100% A for the next sample injection. The LTQ-Orbitrap XL mass spectrometer was configured to collect high-resolution (R=60000 at *m/z* 400) broadband mass spectra (*m/z* 375-1800) using the lock mass feature for the polydimethylcyclosiloxane (PCM) ion generated in the electrospray process (*m/z* 445.12002).

Protein identification

Tandem mass spectra were searched against UniProt *Escherichia coli* protein databases (07/2011) from the European Bioinformatics Institute (http://www.ebi.ac.uk/integr8/EBI-Integr8-HomePage.do;jsessionid=624E6C5BA9--22A73EC29EF3F7F4262E02) using Mascot Daemon (Matrix Science). The data were searched with a precursor mass tolerance of 10 p.p.m. and a fragment ion tolerance of 0.8 Da. Methionine oxidation (+ 15.99592 Da) was set as a dynamic modification, and a maximum of two missed cleavages were allowed. An automatic decoy search was performed on all raw files, and peptides were filtered using an ion score cut-off of 25, resulting in a false peptide discovery rate of <1%. In cases where peptides were identified in more than one protein sequence in the database, protein identifications were compiled based on the highest score UniProt accession number listed in the protein match results for each peptide.

Statistical analyses

The correlations between growth, enzyme activities and transcription fold changes were estimated by the Kendall rank correlation coefficient, τ [37]. This coefficient can be interpreted as the probability of two observables having the same sequence of ranks. Perfect correlation between two variables is given by $\tau=1$, indicating an identical sequence of ranks, e.g. 4-3-2-1, in both variables. Perfect anti-correlation is given by $\tau=-1$, which can be obtained, e.g. by having a rank sequence 4-3-2-1 in one variable and 1-2-3-4 in the other one. The ranks of each observable were determined by pairwise *t* tests for the equality of mean values at each time point. In the case of a non-significant difference, a tie of ranks was assumed. The corresponding *t* values were corrected for ties, yielding the Kendall τ_c correlation coefficient [38]. For simplicity, τ is referred to throughout this paper, though in practice the corrected correlation coefficient, τ_c, was computed.

Besides the perfect (anti-)correlations with $\tau=\pm1$, results with $0.9\leq|\tau|<1$ were considered as almost perfect. For correlations between time series with four points, $|\tau|=\pm0.667$ indicates that the rank sequences of both series were in perfect concordance with the exception of a single pair of values. Therefore, values in the range $0.667\leq|\tau|<0.9$ were accepted as weak correlations.

4.3 Results

Growth curve and sampling

The aerobic respiratory chain of *E. coli* was studied during bacterial growth, with the purpose of investigating the timing of assembly of its supercomplexes, and to establish eventual correlations between their composition, and gene transcription and enzyme activity profiles.

The aerobic growth curve of *E. coli* K-12 in LB medium was obtained, and times of sampling for further analysis covering all growth stages were established, namely ML, ES, MS and LS (Fig. 1).

Transcription analysis of respiratory chain components

The relative expression of genes encoding the aerobic electron transfer chain enzymes (Table 1) was analyzed by qRT-PCR, in mRNA extracted from aerobically grown *E. coli* at the above-mentioned stages, to establish the transcription variation profile of its components. Primer efficiencies were determined and used in the calculation of relative expression ratios, allowing the comparison of transcript abundance between the different genes [33].

Notable variations in the amounts of respiratory chain transcripts were observed as growth progressed (Fig. 2). According to the variation profile of gene

transcription, two groups emerged. One was composed of *nuoF*, *ndh* and *cydA*, which presented the highest levels of transcripts at ML, and decreased in the subsequent phases of growth. It is noteworthy that *nuoF* and *cydA* are the most abundant transcripts at ML. The second group comprised *appC*, *cyoB* and *sdhA*, whose transcriptional levels were minimal at ML. In the next stages of growth, *sdhA* and *appC* displayed a similar variation profile (Fig. 2).

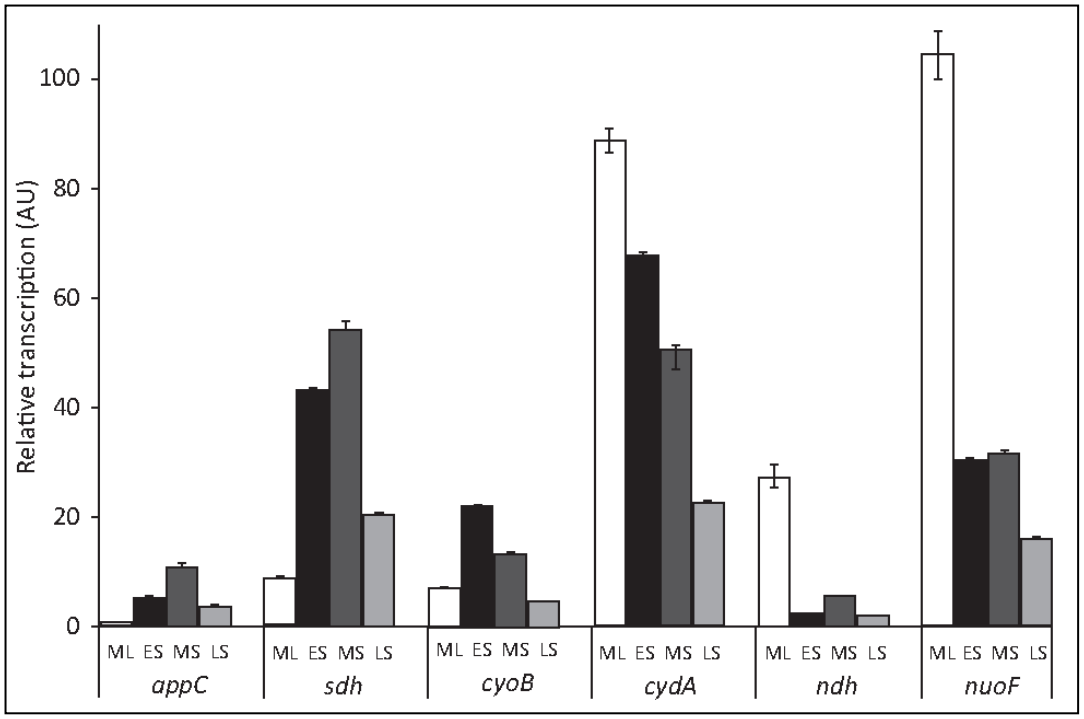

Fig. 2. Relative transcription levels between each aerobic respiratory chain gene and the most expressed gene/condition (ML-NuoF), normalized to the 16 rRNA reference gene. The assays were conducted in triplicate biological samples. The relative amount of each transcript was calculated using the Pfaffl method with correction for efficiency of primer amplification, to allow comparison of the relative expression between the different genes investigated. Error bars, $_{SEM}$, calculated following the rules of error propagation [55]. White, black, dark-grey and light-grey bars correspond to ML, ES, MS and LS, respectively.

The similarities in temporal development of gene transcription during bacterial growth were quantified by Kendall's τ coefficient. Almost perfect positive

correlations were observed between *nuoF* and *cydA* (Fig. 3). Moreover, a weaker but still important positive correlation between the expression of *ndh* and *cydA* was in evidence. The transcription of *sdhA* and *appC* genes presented a perfect positive correlation (τ=1; Fig. 3). The expression of *cyoB* did not correlate with any of the respiratory chain genes analyzed.

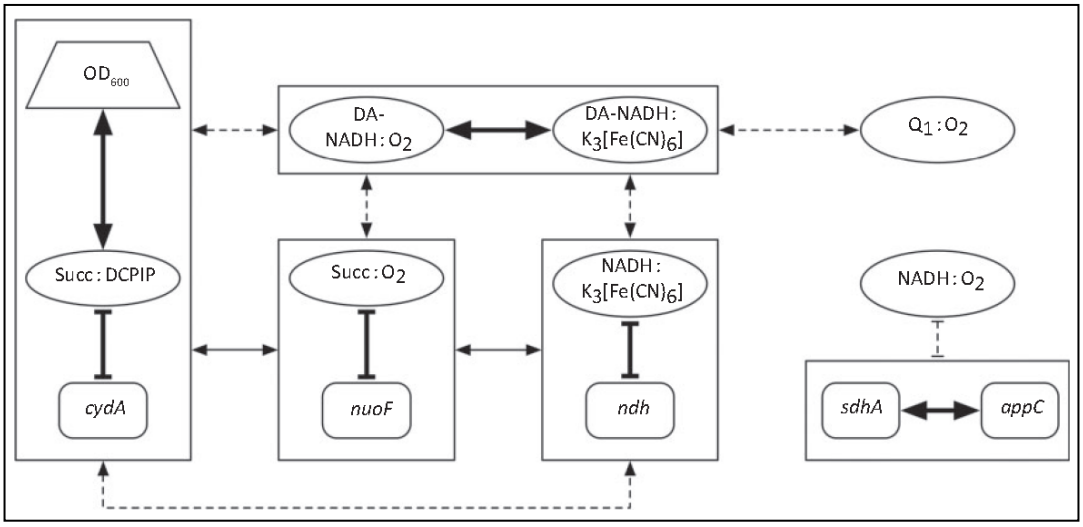

Fig. 3. Integrated view of bacterial growth (OD_{600}), transcription and activity profile of the *E. coli* respiratory chain through mapping of important correlations estimated by the Kendall rank correlation coefficient τ (see Methods). Thick black lines, $|\tau|=1$; solid lines, $0.9 \leq |\tau| < 1$; dashed lines, $0.67 \leq |\tau| < 0.9$. Arrow end points, positive correlation; bar end points, negative correlation. Boxes around several of the elements indicate that all connected correlation arrows apply equally to the contained elements.

Enzyme activity and protein content of respiratory chain components

Respiratory chain activities were determined for the individual enzymes and the whole electron transfer pathway, in membranes isolated from *E. coli* cells harvested at the selected stages of growth, namely ML, ES, MS and LS.

The rate of oxygen consumption due to NADH oxidation, which accounts for the two NADH dehydrogenases and the three quinol:oxygen reductases, did not present dramatic changes during growth, being slightly smaller at MS than during the rest of growth (Fig. 4a). This activity was ~90% inhibited by KCN at all growth

stages. In contrast, when using the NDH-1 specific substrate DA-NADH, the rate of oxygen consumption was minimal at ML, doubled at ES and remained unchanged until the end of growth. KCN inhibition of the oxygen uptake due to DA-NADH oxidation was ~80%, presenting a decrease of 10% in comparison with NADH oxidation. In addition, at each growth stage, the rate of oxygen consumption by *E. coli* membranes respiring DA-NADH was less than half than when NADH was the respiratory substrate (Fig. 4a). NDH-1 and NDH-2 activities, or NDH-1 activity alone, were assessed by measuring NADH: or DA-NADH:$K_3[Fe(CN)_6]$ oxidoreductase activity, respectively. Both activities nearly doubled from ML to ES phase and remained constant until LS phase (Fig. 4c).

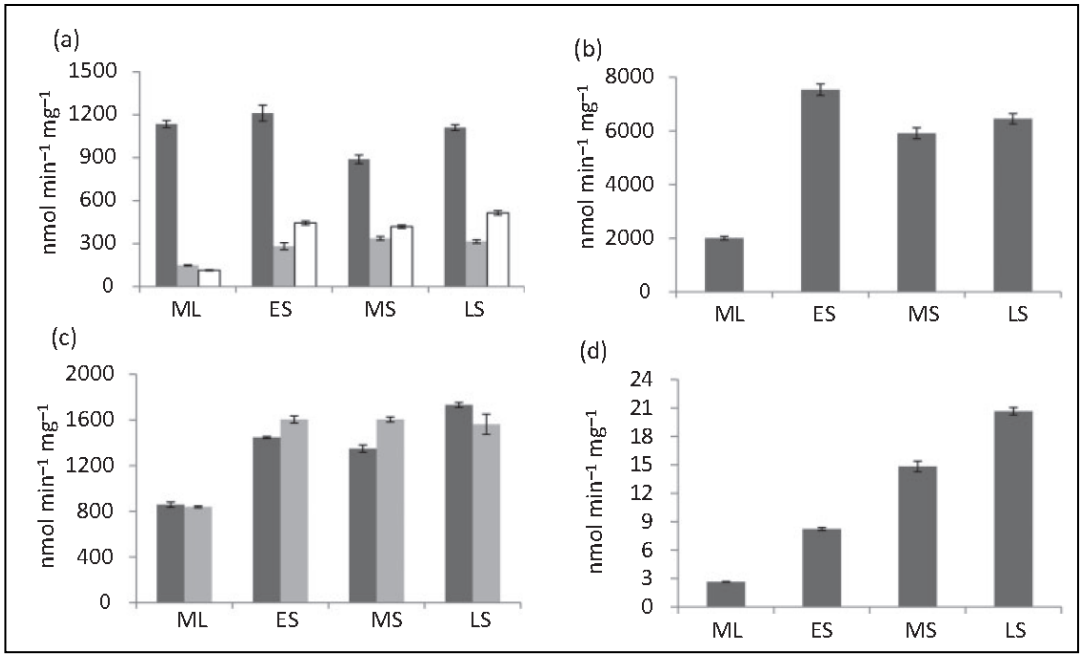

Fig. 4. The oxidation rate of respiratory chain substrates in the membranes of *E. coli* varies according to the growth stage. Oxidoreductase activities were expressed as specific activity. Nevertheless, when the total activities were calculated, the variation profiles were similar (data not shown). (**a**) Oxidoreductase activities: NADH, dark grey; DA-NADH, light grey; succinate:O_2, white. (**b**) Ubiquinol:O_2 oxidoreductase activity. (**c**) Oxidoreductase activities: NADH:$K_3[Fe(CN)_6]$, dark grey; DA-NADH:$K_3[Fe(CN)_6]$, light grey. (**d**) Succinate:DCPIP oxidoreductase activity.

Succinate:O_2 oxidoreductase activity, as observed for the activities described above, was minimal at ML, increased about four time to ES, and remained constant until the end of growth (Fig. 4a). Succinate:DCPIP oxidoreductase activity was also lower at ML, but increased progressively during growth, reaching seven times the initial rate at LS (Fig. 4d). A significant difference between the rates of succinate oxidation by DCPIP and oxygen was observed, which was reported earlier by Hendler & Burgess [1].

Quinol:O_2 oxidoreductase activity, which accounts for cytochromes *bd*I, *bd*II and *bo*$_3$ oxygen reductases, was minimal at ML, rising more than three times at ES, and did not vary significantly during the next stages of growth (Fig. 4b). This activity was always completely inhibited by KCN.

Variation in the amounts of respiratory chain enzymes during growth was assessed in Western blots of SDS-PAGE-resolved *E. coli* membranes probed with polyclonal antibodies against succinate dehydrogenase, cytochrome *bd*I and NDH-1 subunits. The amount of succinate dehydrogenase increased from ML to ES, and remained constant throughout stationary phase, according to the intensity of cross-reactivity against SdhA subunit. Cytochrome *bd*I, in agreement with the literature [39], is predominant in stationary phase and nearly absent in the exponential phase, based on the immunodecoration of the CydB subunit. The content of NDH-1 was higher at ES, although the overall variation was not substantial, as inferred from the detection of the NuoI subunit (Fig. 5).

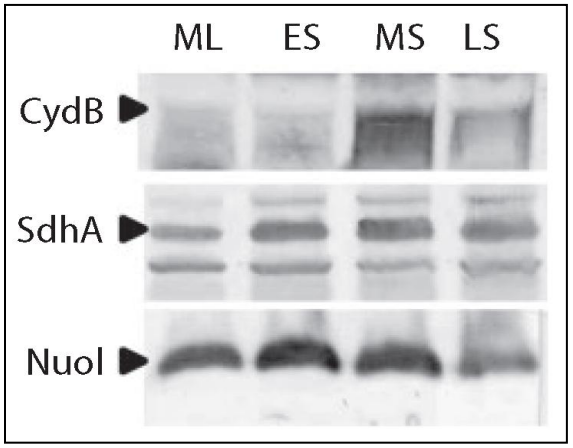

Fig. 5. Immunoblot of *E. coli* membranes harvested at ML, ES, MS and LS. *E. coli* membranes were detected with polyclonal antibodies against the cytochrome *bd*I of *E. coli*, the SdhA subunit of *Bacillus subtilis* succinate dehydrogenase and the NuoI subunit of the *E. coli* NDH-1. Membrane proteins (100 or 50 µg) were used to detect the CydB subunit of cytochrome *bd*I oxygen reductase, or SdhA and NuoI, respectively.

Correlation between bacterial growth, enzyme activity and gene expression

Envisaging the acquisition of an integrated picture of respiratory chain-related events during growth, the full set of data obtained via the different methodological approaches was analyzed using the Kendall τ correlation coefficient (Fig. 3).

With the exception of the NADH:O_2 oxidoreductase activity, all other primary dehydrogenase activities analyzed were positively correlated with each other. Perfect positive correlations were verified between the DA-NADH:O_2 and DA-NADH:K_3[$Fe(CN)_6$] oxidoreductase activities, and almost perfect correlations between succinate:O_2 and succinate:DCPIP, and succinate:O_2 and NADH:K_3[$Fe(CN)_6$] oxidoreductase activities (Fig. 3). The remaining dehydrogenase activities presented weak, but important, positive correlations between each other. Quinol:oxygen oxidoreductase activity also showed a positive correlation with DA-NADH:O_2 and DA-NADH:K_3[$Fe(CN)_6$] oxidoreductase activities. Furthermore, all dehydrogenase activities, with the exception of NADH:O_2 oxidoreductase, showed positive correlations with the progression of growth, as inferred from OD_{600}. The OD_{600} values, in turn, correlated negatively with the expression of *nuoF*, *ndh* and *cydA*. With the exception of *cyoB*, a negative correlation between the transcription profiles of all genes encoding the respiratory chain and enzyme activities was observed. In detail, *sdhA* and *appC* expression correlated negatively with NADH:O_2 oxidoreductase activity, while the expression of *nuoF*, *cydA* and *ndh* exhibited a negative correlation with the remaining oxidoreductase activities, including succinate oxidoreductase (Fig. 3).

Supramolecular assemblies

The presence of the supercomplexes of the *E. coli* respiratory chain described previously [14] was studied during bacterial growth to establish the growth phase in which these supramolecular structures are assembled. With this purpose, BN-

PAGE resolved membranes obtained from cells collected at ML, ES, MS and LS were probed for NADH:NBT and succinate:NBT oxidoreductase activities (Fig. 6). The presence of the already described NDH-1:NDH-2 (band 3) and the formate:O_2 oxidoreductase supercomplexes (band 4) [14] was observed throughout growth (Fig. 6a). Furthermore, a new band was detected with NADH:NBT oxidoreductase activity, identified as band 2a, which was absent from *E. coli* strains devoid of NDH-1 or NDH-2, Δ*nuoB* and Δ*ndh-2* mutants, respectively, indicating that these enzymes are part of this newly detected supercomplex (Fig. 6c). Mass spectrometry analysis of this band (Table S1, [40]) confirmed that it contains NDH-1 and NDH-2.

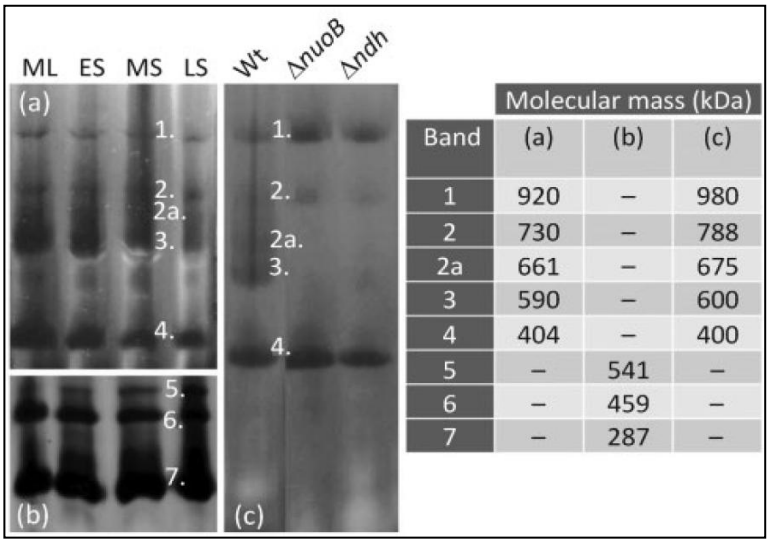

Band	Molecular mass (kDa) (a)	(b)	(c)
1	920	–	980
2	730	–	788
2a	661	–	675
3	590	–	600
4	404	–	400
5	–	541	–
6	–	459	–
7	–	287	–

Fig. 6. Respiratory chain supercomplexes are present at all stages of *E. coli* growth. Detection of NADH:NBT (a, c) and succinate:NBT (b) oxidoreductase activities performed in BN-PAGE-resolved membranes of *E. coli* K-12 prepared from cells harvested at ML, ES, MS and LS (a, b). In addition, NADH:NBT oxidoreductase activity was detected in membranes of *E. coli* K12 and mutant strains devoid of NDH-1 (Δ*nuoB*) and NDH-2 (Δ*ndh*) from cells collected at LS (c). Bands 1, 3 and 4 were previously sequenced [14]. Peptides from NDH-1 and NDH-2 were retrieved from LC-MS/MS analysis of band 2a, and of SDH in bands 5 and 6. The molecular mass of the detected bands was estimated using known membrane protein markers from bovine or chicken heart mitochondria, as described elsewhere [56].

Besides the trimeric (band 7) and monomeric forms of SDH (data not shown), two new homo- or hetero-oligomerizations of this enzyme were visualized by *in gel*

activity of succinate:NBT oxidoreductase activity in membranes resolved by BN-PAGE (Fig. 6b, bands 5 and 6), which were also observed in membranes harvested from ML to LS. Peptides of SDH subunits A and B were identified in bands 5-7 upon mass spectrometry analysis (Table S1, [40]).

Possible partners of the new oligomerizations containing NDH-1 and NDH-2, and SDH, were investigated by detecting NADH: and succinate:NBT oxidoreductase activities in membranes of *E. coli* strains devoid of cytochromes *bo*3, *bd*I and *bd*II quinol:oxygen reductases, of *yhcB*, a novel homo-multimeric complex of the *E. coli* inner membrane whose function remains to be determined [41], and of the transcriptional regulator ArcA [42]. However, the mutants generated the same bands as those observed in the wild-type strain upon detection of NADH: and succinate:NBT oxidoreductase activity, thus ruling out the suggested associations (data not shown).

sdhA and *appC* transcription presented a perfect positive correlation (Fig. 2). To investigate an eventual supramolecular association of SDH and cytochrome *bd*II, membranes from the MB37 strain of *E. coli*, where complex I, and *bd*I and bo_3 cytochrome oxidases are inactivated [43], were solubilized, resolved in a 1.5-0.3 M sucrose gradient, and characterized regarding the distribution of succinate:oxygen and quinol:oxygen oxidoreductase activities. As expected, the quinol:oxygen oxidoreductase activity was present from the heaviest to lightest gradient fractions. In contrast, succinate:oxygen oxidoreductase activity was only observed in the heaviest fractions, F1 and F2 (Fig. 7). Upon detergent solubilization, the detection of this activity is only possible if inter-complex interactions are preserved between succinate dehydrogenase and an oxygen reductase, thus indicating the presence of a succinate oxidase supercomplex. Since the sole oxygen reductase expressed in strain MB37 is cytochrome *bd*II, the assembly of a supercomplex containing SDH and cytochrome *bd*II was confirmed. Furthermore, direct molecular evidence of the presence of SDH and cytochrome *bd*II in fractions F1 and F2 of the MB37 gradient was obtained by LC-MS/MS analysis of these fractions. Peptides of all subunits of each complex (SdhABCD and AppAB) were identified in these

fractions (Table S2, [40]), confirming the composition of the supercomplex identified here, which contains SDH and cytochrome *bd*II, as suggested by the correlation observed between the gene transcription data.

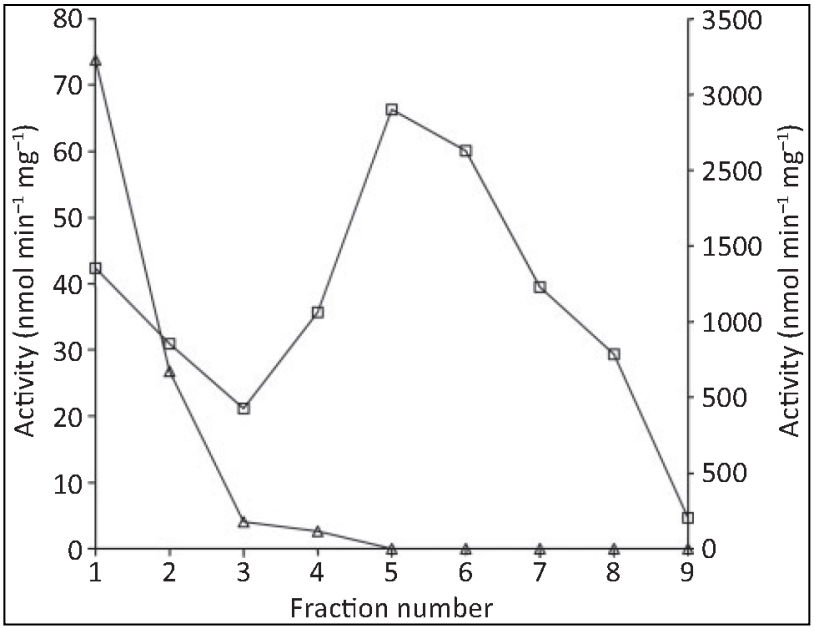

Fig. 7. Analysis of succinate:oxygen and quinol:oxygen oxidoreductase activity in fractions of sucrose gradient-resolved membranes from strain MB37. Membranes were solubilized with digitonin and resolved in a 1.5-0.3 M sucrose gradient. Fraction 1 exhibited succinate:oxygen oxidoreductase activity, which was more than 70% inhibited by 2.5 mM KCN. Squares – quinol:O_2 oxidoreductase activity (right-hand axis) and triangles – succinate:O_2 oxidoreductase activity (left-hand axis).

4.4 Discussion

The work presented herein used an innovative approach in integrating data corresponding to different levels of cell metabolism, growth dynamics, gene expression, protein expression and activity, and supramolecular assembly to provide a global overview of the aerobic respiratory pathway of *E. coli*.

Notable differences in the relative expression of genes encoding aerobic respiratory chain components were observed: changes of almost one order of

magnitude from one growth stage to the next were detected, being generally more pronounced in the transition from ML to ES, and from MS to LS (Fig. 2). The possibility that, besides the growth phase, the variation of oxygen concentration during growth also affected gene expression should not be disregarded. Although there is always some oxygen present during growth [44], it is likely that growth at the later stages of growth (MS and LS) is limited by the oxygen supply. The transcription level variation of *sdhA*, *cyoB* and *cydA* genes during growth did not follow the trend described for progressive oxygen concentration decrease reported by Rolfe *et al.* [18]. It can thus be assumed that although the oxygen concentration in the cultures was low, it was almost unchanged during the sample collection period.

In an array constructed with cDNA prepared from mRNA from *E. coli* K-12/MG1655 cells grown aerobically in minimal medium M9 supplemented with glucose [45], other authors verified that globally there are no dramatic variations in gene expression between the exponential and ES phases. However, in agreement with our results, the genes involved in the aerobic respiratory chain presented a decrease in expression from ML to stationary phase.

The transcription of the NADH dehydrogenases encoding genes *nuoF* and *ndh* was positively correlated (Fig. 3), in agreement with the previously identified NADH dehydrogenase supercomplex that contains NDH-1 and NDH-2 [14]. The abundance of *nuoF* transcripts was always larger than that of *ndh*, in agreement with earlier studies [20]; in addition, and in agreement with those authors, the relative expression of *ndh* was highest at ML.

The relative expression of *cydA* also displayed a positive correlation with *nuoF* and *ndh*, suggesting that cytochrome *bd*I could be a preferential intermediate in oxygen reduction by the electrons that result from NADH oxidation by the NADH dehydrogenase supercomplex. The progressive decrease of the transcription level of *cydA* is in contradiction with earlier reports, in which the expression of the *cyd* operon increased when *E. coli* cultures entered the stationary phase, presumably due to decreased oxygen availability [46]. However, this could still be explained by

considering that this gene is negatively regulated by the histone-like protein H-NS under aerobic conditions [47], and that this repressor is antagonized by Fis, which is abundant at the early exponential phase [48].

Perfect positive correlation was observed between the transcription profiles of *sdhA* and *appC*, suggesting an alternative electron transfer pathway composed of succinate:quinone oxidoreductase and cytochrome *bd*II oxygen reductase. This suggestion was further supported by the detection of succinate:oxygen oxidoreductase activity in fractions 1 and 2 of the *E. coli* MB37 strain sucrose gradient (Fig. 7), in which cytochrome *bd*II is the sole oxygen reductase present, and was confirmed by MS analysis of the above-mentioned fractions.

We have recently described a supramolecular assembly of formate dehydrogenase (Fdo) and cytochrome bo_3 in the respiratory chain of *E. coli* [14]. The existence of these selective associations of the respiratory chain may account for the apparent redundancy of the respiratory chain enzymes observed in this bacterium and others. In terms of energy conservation, these combinations produce proton motive forces with different H^+/e^- ratios, having a value of 3 in the case of the association of NDH-1 (2 H^+/e^-), NDH-2 (0 H^+/e^-) and cytochrome *bd*I (1 H^+/e^-) [49], and of 1 in the case of SDH (0 H^+/e^-) [50] and cytochrome *bd*II (1 H^+/e^-) [51]. Concerning the association between formate dehydrogenase and cytochrome bo_3, and considering that there is no information about the eventual proton motive force generated by formate dehydrogenase, the H^+/e^- ratio will be at least 2 [52]. In light of the available knowledge, there is no reasonable hypothesis to explain the physiological significance of *E. coli* supercomplexes described.

Enzyme activities were also analyzed by searching for correlations in their rate variation profile during bacterial growth. With the exception of NADH:oxygen oxidoreductase activity, the respiratory chain activities presented positive correlations with each other (Fig. 3). NADH:oxygen oxidoreductase activity is an outlier to this group, a fact that could be related to the presence of other enzymes with NADH:oxygen oxidoreductase activity (e.g. WrbA, YhdH and QOR; [43]) in the respiratory chain of *E. coli*.

It is worth mentioning that the highest transcription levels of *nuoF* and *ndh* observed at ML did not lead to a higher NADH and DA-NADH oxidoreductase activity or NDH-1 content. In fact, it was at LS that most genes presented lower transcription levels, but eventual corresponding decreases in enzyme activities were not observed. Such discrepancies between gene expression and enzyme activity could be due to partial mRNA degradation, a mechanism that result in modulation of gene transcription and which is widespread in bacteria [53]. Another explanation could be regulation at the transcriptional level, as proposed by Kramer *et al.* [54], which seems to be the case for cytochrome *bd*I, whose protein levels are maximal at stationary phase. According to those authors, cytochrome *bd*I-encoding genes have multiple levels of regulation, namely the transcriptional (see above) and translational levels. The primary dehydrogenase whose transcripts are most abundant at ES and MS is SDH, suggesting that it plays an important metabolic role during entry into stationary phase that is not necessarily related to the electron transfer chain.

Moreover, the negative correlations observed between the expression of *sdhA* and *appC* and NADH:O_2 oxidoreductase activity, and between that of *nuoF*, *cydA* and *ndh* and the remaining oxidoreductase activities (Fig. 3), including succinate oxidoreductase, suggest that the aerobic respiratory chain of *E. coli* is a multi-level tightly regulated pathway.

4.5 Conclusions

This is believed to be the first comprehensive study of the aerobic respiratory chain of *E. coli* during bacterial growth, from gene transcription to enzyme activity and supramolecular organization.

Correlations between the aerobic respiratory chain components of this bacterium were observed at two levels: gene transcription and enzyme activity. The established correlations allowed the association of *nuoF*, *ndh* and *cydA* in one

group and of *sdhA* and *appC* in another, representing preferential enzyme partners in the electron transfer chain of *E. coli*, at least partially organized in supercomplexes, and these predictions were supported by experimental data.

Furthermore, multi-level correlations were identified that related gene expression to enzyme activity and growth dynamics, suggesting a tight and complex regulation of the aerobic respiratory pathway.

It was shown that the previously described NADH dehydrogenase and formate:oxygen oxidoreductase supercomplexes are already formed at ML and are present until stationary phase (Fig. 6a). A novel supramolecular assembly containing succinate dehydrogenase and cytochrome *bd*II was described.

4.6 Acknowledgements

The authors thank Drs Thorsten Friedrich (University of Freiburg) and Robert Gennis (University of Illinois at Urbana-Champaign) for the *E. coli* strains ann001 and ann021 and NuoI antiserum, and ML20S2, ML15A and cytochrome *bd*, respectively. Dr Lars Hederstedt (Lund University) and the *E. coli* Genetic Stock Center are also acknowledged for the SdhA antiserum, and for JW09601, JW55391 and JW43641 strains, respectively. Isabel Palos, Andreia Mósca, Filipe Santos and Sara Silva are acknowledged for excellent technical assistance. The present research was funded by Fundação para a Ciência e a Tecnologia (FCT) (PTDC/BIA-PRO/67105/2006 to A.M.P.M. and Pest-OE/EQB/LA0004/2011). P.S. is a recipient of the FCT grant SFRH/BD/46553/2008.

4.7 References

[1] Hendler, R.W. and Burgess, A.H. (1972). Respiration and protein synthesis in *Escherichia coli* membrane-envelope fragments. VI. Solubilization and characterization of the electron transport chain. J Cell Biol 55, 266-81.

[2] Ingledew, W.J. and Poole, R.K. (1984). The respiratory chains of *Escherichia coli*. Microbiol Rev 48, 222-71.

[3] Price, C.E. and Driessen, A.J. (2010). Biogenesis of membrane bound respiratory complexes in *Escherichia coli*. Biochim Biophys Acta 1803, 748-66.

[4] Kasahara, M. and Anraku, Y. (1974). Succinate dehydrogenase of *Escherichia coli* membrane vesicles. Activation and properties of the enzyme. J Biochem 76, 959-66.

[5] Melo, A.M.P., Bandeiras, T.M. and Teixeira, M. (2004). New insights into type II NAD(P)H:quinone oxidoreductases. Microbiol Mol Biol Rev 68, 603-16.

[6] Bragg, P.D. and Hou, C. (1967). Reduced nicotinamide adenine dinucleotide oxidation in *Escherichia coli* particles. II. NADH dehydrogenases. Arch Biochem Biophys 119, 202-8.

[7] Minagawa, J., Mogi, T., Gennis, R.B. and Anraku, Y. (1992). Identification of heme and copper ligands in subunit I of the cytochrome *bo* complex in *Escherichia coli*. J Biol Chem 267, 2096-104.

[8] Sturr, M.G., Krulwich, T.A. and Hicks, D.B. (1996). Purification of a cytochrome bd terminal oxidase encoded by the *Escherichia coli app* locus from a delta *cyo* delta *cyd* strain complemented by genes from *Bacillus firmus* OF4. J Bacteriol 178, 1742-9.

[9] Unden, G. and Bongaerts, J. (1997). Alternative respiratory pathways of *Escherichia coli*: energetics and transcriptional regulation in response to electron acceptors. Biochim Biophys Acta 1320, 217-34.

[10] Pereira, M.M., Bandeiras, T.M., Fernandes, A.S., Lemos, R.S., Melo, A.M.P. and Teixeira, M. (2004). Respiratory chains from aerobic thermophilic prokaryotes. J Bioenerg Biomembr 36, 93-105.

[11] Dudkina, N.V., Kouril, R., Peters, K., Braun, H.P. and Boekema, E.J. (2010). Structure and function of mitochondrial supercomplexes. Biochim Biophys Acta 1797, 664-70.

[12] Stroh, A., Anderka, O., Pfeiffer, K., Yagi, T., Finel, M., Ludwig, B. and Schägger, H. (2004). Assembly of respiratory complexes I, III, and IV into NADH oxidase supercomplex stabilizes complex I in *Paracoccus denitrificans*. J Biol Chem 279, 5000-7.

[13] Prunetti, L., Infossi, P., Brugna, M., Ebel, C., Giudici-Orticoni, M.T. and Guiral, M. (2010). New functional sulfide oxidase-oxygen reductase supercomplex in the membrane of the hyperthermophilic bacterium *Aquifex aeolicus*. J Biol Chem 285, 41815-26.

[14] Sousa, P.M.F. et al. (2011). Supramolecular organizations in the aerobic respiratory chain of *Escherichia coli*. Biochimie 93, 418-425.

[15] Benoit, S., Abaibou, H. and Mandrand-Berthelot, M.A. (1998). Topological analysis of the aerobic membrane-bound formate dehydrogenase of *Escherichia coli*. J Bacteriol 180, 6625-34.

[16] Gunsalus, R.P. (1992). Control of electron flow in *Escherichia coli*: coordinated transcription of respiratory pathway genes. J Bacteriol 174, 7069-74.
[17] Bekker, M., Alexeeva, S., Laan, W., Sawers, G., Teixeira de Mattos, J. and Hellingwerf, K. (2010). The ArcBA two-component system of *Escherichia coli* is regulated by the redox state of both the ubiquinone and the menaquinone pool. J Bacteriol 192, 746-54.
[18] Rolfe, M.D. et al. (2011). Transcript profiling and inference of *Escherichia coli* K-12 ArcA activity across the range of physiologically relevant oxygen concentrations. J Biol Chem 286, 10147-54.
[19] Spiro, S. and Guest, J.R. (1990). FNR and its role in oxygen-regulated gene expression in *Escherichia coli*. FEMS Microbiol Rev 6, 399-428.
[20] Wackwitz, B., Bongaerts, J., Goodman, S.D. and Unden, G. (1999). Growth phase-dependent regulation of *nuoA-N* expression in *Escherichia coli* K-12 by the Fis protein: upstream binding sites and bioenergetic significance. Mol Gen Genet 262, 876-83.
[21] Keseler, I.M. et al. (2011). EcoCyc: a comprehensive database of *Escherichia coli* biology. Nucleic Acids Res 39, D583-90.
[22] Jackson, L., Blake, T. and Green, J. (2004). Regulation of *ndh* expression in *Escherichia coli* by Fis. Microbiology 150, 407-13.
[23] Lennox, E.S. (1955). Transduction of linked genetic characters of the host by bacteriophage P1. Virology 1, 190-206.
[24] Kahm, M., Hasenbrink, G., Lichtenberg-Frate, H., Ludwig, J. and Kschischo, M. (2010). Grofit: fitting biological growth curves with R. J Stat Softw 33, 1-21.
[25] Smith, P.K. et al. (1985). Measurement of protein using bicinchoninic acid. Anal Biochem 150, 76-85.
[26] Krause, F. and Seelert, H. (2008). Detection and analysis of protein-protein interactions of organellar and prokaryotic proteomes by blue native and colorless native gel electrophoresis. Curr Protoc Protein Sci Chapter 19, Unit 19.18.
[27] Schägger, H. and von Jagow, G. (1991). Blue native electrophoresis for isolation of membrane protein complexes in enzymatically active form. Anal Biochem 199, 223-31.
[28] Wittig, I., Braun, H.P. and Schägger, H. (2006). Blue native PAGE. Nat Protoc 1, 418-28.
[29] Zerbetto, E., Vergani, L. and Dabbeni-Sala, F. (1997). Quantification of muscle mitochondrial oxidative phosphorylation enzymes via histochemical staining of blue native polyacrylamide gels. Electrophoresis 18, 2059-64.
[30] Dudkina, N.V., Eubel, H., Keegstra, W., Boekema, E.J. and Braun, H.P. (2005). Structure of a mitochondrial supercomplex formed by respiratory-chain complexes I and III. Proc Natl Acad Sci U S A 102, 3225-9.
[31] Laemmli, U.K. (1970). Cleavage of structural proteins during the assembly of the head of bacteriophage T4. Nature 227, 680-5.
[32] Towbin, H., Staehelin, T. and Gordon, J. (1979). Electrophoretic transfer of proteins from polyacrylamide gels to nitrocellulose sheets: procedure and some applications. Proc Natl Acad Sci U S A 76, 4350-4.
[33] Pfaffl, M.W. (2001). A new mathematical model for relative quantification in real-time RT-PCR. Nucleic Acids Res 29, e45.
[34] Rozen, S. and Skaletsky, H. (2000). Primer3 on the WWW for general users and for biologist programmers. Methods Mol Biol 132, 365-86.

[35] Hatefi, Y. (1978). Preparation and properties of NADH: ubiquinone oxidoreductase (complex I), EC 1.6.5.3. Methods Enzymol 53, 11-4.
[36] Hatefi, Y. (1978). Resolution of complex II and isolation of succinate dehydrogenase (EC 1.3.99.1). Methods Enzymol 53, 27-35.
[37] Kendall, M. (1938). A new measure of rank correlation. Biometrika 30, 81-89.
[38] Abdi, H. (2007) Kendall Rank Correlation. In Encyclopedia of Measurement and Statistics, pp. 508-510. Sage, Thousand Oaks, CA.
[39] Kita, K., Konishi, K. and Anraku, Y. (1984). Terminal oxidases of *Escherichia coli* aerobic respiratory chain. II. Purification and properties of cytochrome b_{558}-*d* complex from cells grown with limited oxygen and evidence of branched electron-carrying systems. J Biol Chem 259, 3375-81.
[40] Sousa, P.M.F., Videira, M.A., Bohn, A., Hood, B.L., Conrads, T.P., Goulao, L.F. and Melo, A.M.P. (2012). The aerobic respiratory chain of *Escherichia coli*: from genes to supercomplexes. Microbiology 158, 2408-18.
[41] Maddalo, G. et al. (2011). Systematic analysis of native membrane protein complexes in *Escherichia coli*. J Proteome Res 10, 1848-59.
[42] Bekker, M., Teixeira de Mattos, M.J. and Hellingwerf, K.J. (2006). The role of two-component regulation systems in the physiology of the bacterial cell. Sci Prog 89, 213-42.
[43] Bekker, M., de Vries, S., Ter Beek, A., Hellingwerf, K.J. and de Mattos, M.J. (2009). Respiration of *Escherichia coli* can be fully uncoupled via the nonelectrogenic terminal cytochrome *bd*-II oxidase. J Bacteriol 191, 5510-7.
[44] Van Sujidam, J., Kossen, N. and Joha, A. (1978). Model for oxygen transfer in a shake flask. Biotechnol Bioeng 20, 1695-1709.
[45] Wei, Y., Lee, J.M., Richmond, C., Blattner, F.R., Rafalski, J.A. and LaRossa, R.A. (2001). High-density microarray-mediated gene expression profiling of *Escherichia coli*. J Bacteriol 183, 545-56.
[46] Georgiou, C.D., Dueweke, T.J. and Gennis, R.B. (1988). Regulation of expression of the cytochrome *d* terminal oxidase in *Escherichia coli* is transcriptional. J Bacteriol 170, 961-6.
[47] Govantes, F., Orjalo, A.V. and Gunsalus, R.P. (2000). Interplay between three global regulatory proteins mediates oxygen regulation of the *Escherichia coli* cytochrome *d* oxidase (*cydAB*) operon. Mol Microbiol 38, 1061-73.
[48] Falconi, M., Higgins, N.P., Spurio, R., Pon, C.L. and Gualerzi, C.O. (1993). Expression of the gene encoding the major bacterial nucleotide protein H-NS is subject to transcriptional auto-repression. Mol Microbiol 10, 273-82.
[49] Puustinen, A., Finel, M., Haltia, T., Gennis, R.B. and Wikström, M. (1991). Properties of the two terminal oxidases of *Escherichia coli*. Biochemistry 30, 3936-42.
[50] Cecchini, G., Maklashina, E., Yankovskaya, V., Iverson, T.M. and Iwata, S. (2003). Variation in proton donor/acceptor pathways in succinate:quinone oxidoreductases. FEBS Lett 545, 31-8.
[51] Borisov, V.B., Murali, R., Verkhovskaya, M.L., Bloch, D.A., Han, H., Gennis, R.B. and Verkhovsky, M.I. (2011). Aerobic respiratory chain of *Escherichia coli* is not allowed to work in fully uncoupled mode. Proc Natl Acad Sci U S A 108, 17320-4.
[52] Puustinen, A., Finel, M., Virkki, M. and Wikström, M. (1989). Cytochrome *o* (*bo*) is a proton pump in *Paracoccus denitrificans* and *Escherichia coli*. FEBS Lett 249, 163-7.

[53] Bastet, L., Dubé, A., Massé, E. and Lafontaine, D.A. (2011). New insights into riboswitch regulation mechanisms. Mol Microbiol 80, 1148-54.

[54] Kramer, G. et al. (2010). Proteome-wide alterations in *Escherichia coli* translation rates upon anaerobiosis. Mol Cell Proteomics 9, 2508-16.

[55] Vandesompele, J., De Preter, K., Pattyn, F., Poppe, B., Van Roy, N., De Paepe, A. and Speleman, F. (2002). Accurate normalization of real-time quantitative RT-PCR data by geometric averaging of multiple internal control genes. Genome Biol 3, RESEARCH0034.

[56] Wittig, I., Beckhaus, T., Wumaier, Z., Karas, M. and Schägger, H. (2010). Mass estimation of native proteins by blue native electrophoresis: principles and practical hints. Mol Cell Proteomics 9, 2149-61.

Chapter 5

The formate:oxygen oxidoreductase supercomplex of Escherichia coli *aerobic respiratory chain*

Summary

The *Escherichia coli* formate:oxygen oxidoreductase supercomplex (FdOx) was investigated with respect to function and composition. Formate oxidoreductase activity was detected in blue native polyacrylamide gel electrophoresis (BN-PAGE) resolved membranes of *E. coli*, which were also capable of cyanide sensitive formate:oxygen oxidoreductase activity. The latter was compromised in strains devoid of specific oxygen reductases, particularly, in those devoid of cytochrome bo_3 or *bd*I. A principal component analysis (PCA) integrating *E. coli* aerobic respiratory chain gene transcription, enzyme activity and growth dynamics was performed, correlating formate:oxygen oxidoreductase activity and the transcription of the genes encoding cytochromes bo_3 and *bd*I, and corroborating previous evidence that associated these complexes in FdOx.

This chapter was published in

***FEBS Lett.* 587, 2013, p. 2559-2564**

The formate:oxygen oxidoreductase supercomplex of *Escherichia coli* aerobic respiratory chain

Pedro M.F. Sousa, Marco A.M. Videira and Ana M.P. Melo.

- Pedro M.F. Sousa performed all the experiments reported in this chapter, in collaboration with Marco A.M. Videira and Ana M.P. Melo.
- Luis Goulao provided valuable insights regarding the PCA analysis and is mentioned in the acknowledgments section.

5.1 Introduction

The association of respiratory chain enzymes in supramolecular structures called supercomplexes is widespread in nature, being widely characterized in eukaryotic organisms both from the functional and structural point of view. Such organizations favor the efficiency of the oxidative phosphorylation systems, mainly due to substrate channeling and avoidance of reactive oxygen species production [1-3]. Prokaryotic respiratory chain supercomplexes have been described for a large set of microorganisms, from archaea to Gram positive and Gram negative bacteria [4-6]. In *Escherichia coli*, three supramolecular associations have been proposed: (i) the NADH oxidoreductase, (ii) the succinate:oxygen oxidoreductase and (iii) the formate:oxygen oxidoreductase (FdOx) supercomplexes, according to gel based techniques and mass spectrometry evidences [7,8]. The later was unexpected since formate dehydrogenases (FDHs) and oxygen reductases were hardly related.

E. coli synthesizes three distinct membrane-associated formate dehydrogenase isoenzymes, two expressed under anaerobic conditions, FDH-H and FDH-N, and FDH-O, synthesized in the presence of oxygen or nitrate [9]. FDH-O and FDH-N are encoded by *fdoGHI* and *fdnGHI* genes. The catalytic subunits FdoG and FdnG, 110 kDa selenopolypeptides, display the highest identity and similarity, 76% and 87%, respectively, as calculated by CLUSTAL W [10] and carry out the formate-dependent reduction of dichlorophenol indophenol (DCPIP) in the presence of phenazine methosulfate (PMS) [11]. Similarly, FdoH and FdnH presented 75% identity and 85% similarity. The close relation between subunits G and H suggests that these enzymes may have similar structures.

In the present article, FdOx was investigated with respect to its function. Formate:oxygen oxidoreductase activity and the transcription of *fdoG*, the gene encoding FDH-O subunit G, was analyzed over growth. In addition,

formate:oxygen oxidoreductase activity was studied in selected oxygen reductase mutants, to infer the importance of each *E. coli* oxygen reductase in FdOx.

5.2 Materials and Methods

Bacterial growth, cDNA synthesis and quantitative real-time PCR (qRT-PCR)

Cells from different *E. coli* strains, namely wild-type (K12), *Δbo*$_3$ (ML20S2), *ΔbdI* (ML15A), *ΔbdII* (JW0960-1) and *ΔfdoI* (JW3863) were grown aerobically and, as appropriate, harvested at mid-logarithmic (ML), early-stationary (ES), mid-stationary (MS) and late-stationary (LS) phases for RNA isolation [8] and membrane preparation [7]. The pH was monitored at harvesting steps presenting a variation of 1 pH unit and oxygen availability was ensured by growing cells under vigorous agitation in a volume corresponding to one fifth of the total volume of the flasks [8].

cDNA was synthesized and qRT-PCR experiments were performed according with [8], using oligonucleotides for *fdoG* 5'GGTGTACGACAACCCCAATGAT and 5'GGATCAGCCATTCCAGTTTGTC.

Membrane preparation, solubilization and blue native polyacrylamide gel electrophoresis (BN-PAGE) analysis

High yields of *E. coli* inner membranes were obtained after a two-step sucrose gradient purification procedure [12], solubilized with digitonin and resolved by a 3-10% acrylamide gradient BN-PAGE. Selected lanes were further resolved in a 2D-BN-PAGE (3-10%) after incubation with 0.02% dodecyl-β-D-maltoside (DDM) and 0.05% sodium deoxycholate [13], or in harsher conditions to allow subcomplex

dissociation, 0.04% DDM and 0.1% sodium deoxycholate. NADH: [7] and formate:NBT oxidoreductase [14] artificial activities were detected *in gel*.

Enzyme activities

Enzyme activities, namely NADH:, succinate: and reduced coenzyme UQ_1 (hereon designated ubiquinol):oxygen oxidoreductase, were measured polarographicaly as previously described [8]. In addition, formate:oxygen oxidoreductase activity was also measured in a reaction buffer containing 100 mM MOPS pH 7.2, 30 mM sodium formate and *E. coli* membranes (20 µg) from wild-type and selected respiratory chain mutant strains. The reactions were stopped by the addition of 0.5 or 2.5 mM KCN. Moreover, the same activity was tested for wild-type *E. coli* membranes harvested at different aerobic growth phases, namely ML, ES, MS and LS.

To characterize the enzyme kinetics of FDH-O, formate:oxygen oxidoreductase activity was tested using different concentrations of sodium formate (0.1 - 30 mM). The experiments were performed using 20 µg of *E. coli* wild-type membranes harvested at LS phase and three replicates of each assay were acquired. The Lineweaver-Burk plot [15] was obtained to determine the Michaelis Menten constant (K_M) and maximal velocity (V_{MAX}) of formate oxidation.

Principal component analysis (PCA)

Data from relative gene transcription, enzyme activity and growth dynamics were standardized and a pair-wised correlation matrix was calculated and subjected to eigenvalue decomposition to identify orthogonal components of the original matrix and generate a principal component analysis (PCA) [16] bi-plot, using the NTsys-PC version 2.20e) software package [17]. A minimum-spanning tree was calculated in order to facilitate the visualization of the distances between

operational units. Shorter distances reflect higher correlation between each component.

5.3 Results

Electrophoretic analysis of subcomplex composition of FdOx

To characterize FdOx, membranes from *E. coli* were resolved in a BN-PAGE and stained for NADH: (N) and formate:NBT (F) oxidoreductase activities. Bands N and F, with identical molecular masses (432 ± 7 kDa) were detected (Fig. 1).

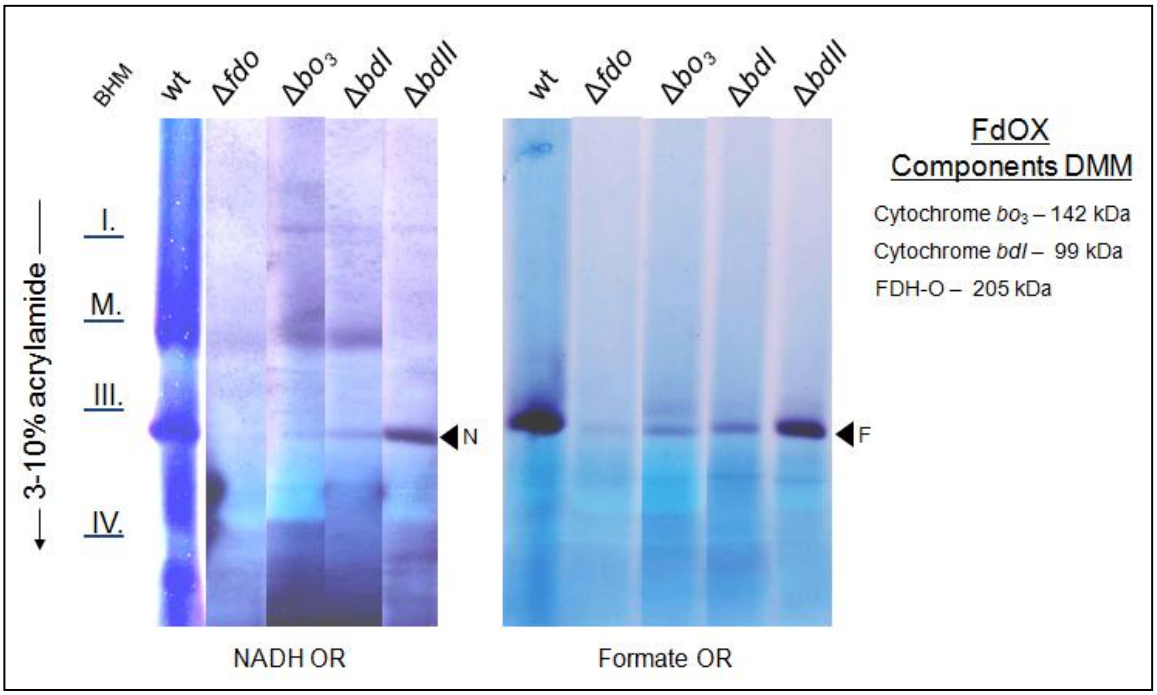

Fig. 1. *In* gel detection of the *E. coli* FdOx. Membranes from *E. coli* wild-type strain and respiratory chain mutants were resolved by BN-PAGE and the artificial oxidoreductase (OR) activities of NADH: (N) and formate:NBT (F) were detected. Digitonin solubilized bovine heart mitochondrial (BHM) complexes I, III, IV and the ATP synthase (M), were used as molecular mass markers, with 1000, 482, 205 and 597 kDa, respectively [24]. The deduced molecular masses (DMM) of FdOx individual complexes were calculated according with their amino acid sequences.

Additionally, to confirm the presence of the individual complexes in FdOx, the same procedure was applied in membranes from *E. coli* strains where FDH-O and cytochromes bo_3, *bd*I and *bd*II were disrupted. Bands N and F were identified in *ΔbdII* with similar intensity to that registered for the wild-type strain, but nearly absent in the remaining mutants, thus indicating that cytochromes bo_3 and *bd*I oxygen reductases are important at least for the assembly of FdOx (Fig. 1), as previously suggested [7]. A 2D BN-PAGE was performed to investigate the dissociation of FdOx in smaller subcomplexes (Fig. 2). NADH:NBT and formate:NBT oxidoreductase activities co-localized, in bands N and F1. In addition, the formate:NBT oxidoreductase activity allowed the identification of a subcomplex of FdOx, which retained formate:NBT oxidoreductase activity, in a smaller band, F2 (Fig. 2B).

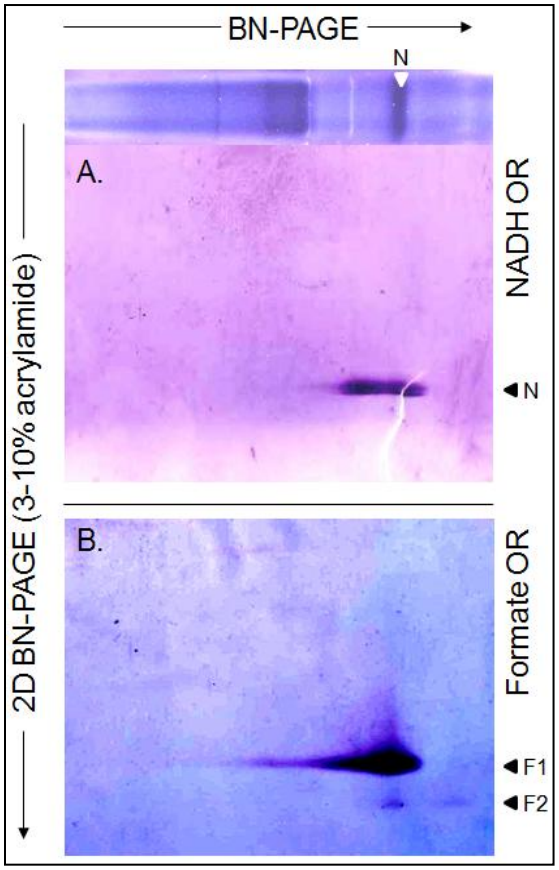

Fig. 2. Identification of FdOx supercomplex by 2D BN-PAGE. Lanes derived from the first dimension BN-PAGE were resolved in a second dimension BN-PAGE and detected for NADH: (A) and formate:NBT oxidoreductase (B) activities, retrieving bands N and F1 corresponding to FdOx, and a smaller subcomplex with formate:NBT oxidoreductase activity, F2.

Characterization of FdOx activity

Membranes of wild-type and selected aerobic respiratory chain mutants, namely *Δbo*$_3$, *ΔbdI*, *Δfdo* and *ΔbdII* of *E. coli,* were investigated by means of an oxygen electrode. The rates of oxygen uptake due to NADH, succinate and ubiquinol oxidation increased in membranes where cytochromes *bo*$_3$ or *bd*I were deleted, comparatively with the wild-type (Fig. 3 A-C). These activities were at least 80% inhibited by KCN, being completely inhibited when ubiquinol was used as substrate. It is noteworthy that succinate:oxygen oxidoreductase activity was severely impaired in the absence of cytochrome *bd*II, indicating the importance of this terminal oxygen reductase when succinate is oxidized, in agreement with the proposed supercomplex composed of SDH and cytochrome *bd*II [8].

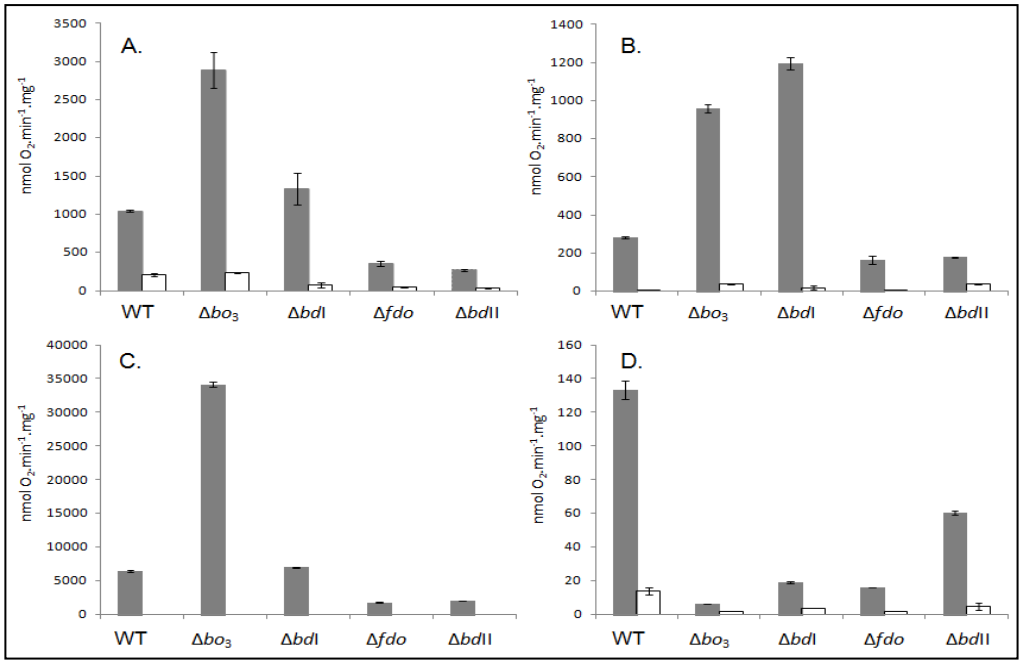

Fig. 3. Oxidation rate of respiratory chain substrates in *E. coli* membranes of wild-type, *Δbo*$_3$, *ΔbdI*, *Δfdo* and *ΔbdII* strains. Oxygen consumption was measured upon NADH (A), succinate (B), ubiquinol (UQ_1) (C) and formate addition (D) (nmol $O_2.min^{-1}.mg^{-1}$) on *E. coli* (grey bars). The addition of KCN (white bars) inhibited oxygen consumption by at least 80%, this inhibition being complete when UQ_1 was used as substrate. 90% of formate:oxygen oxidoreductase inhibition by KCN was displayed in both wild-type and *ΔbdII*

In contrast, formate:oxygen oxidoreductase activity was higher in membranes from wild-type and cytochrome *bd*II mutant strains (Fig. 3D), displaying a KCN inhibition of 90%, and was barely detectable in *Δbo*$_3$, *ΔbdI* and *Δfdo* membranes, corroborating evidences from BN-PAGE (Fig. 1) and mass spectrometry results [7]. This is the first time that cyanide sensitive formate:oxygen oxidoreductase activity was detected in *E. coli* membranes.

FdOx activity was monitored during wild-type *E. coli* aerobic growth at ML, ES, MS and LS phases. Formate:oxygen oxidoreductase activity was maximal at ML and ES growth stages, decreased about 20% at MS and dropped to nearly 25% at LS. 90% of KCN inhibition was displayed in all growth stages (Fig. 4A).

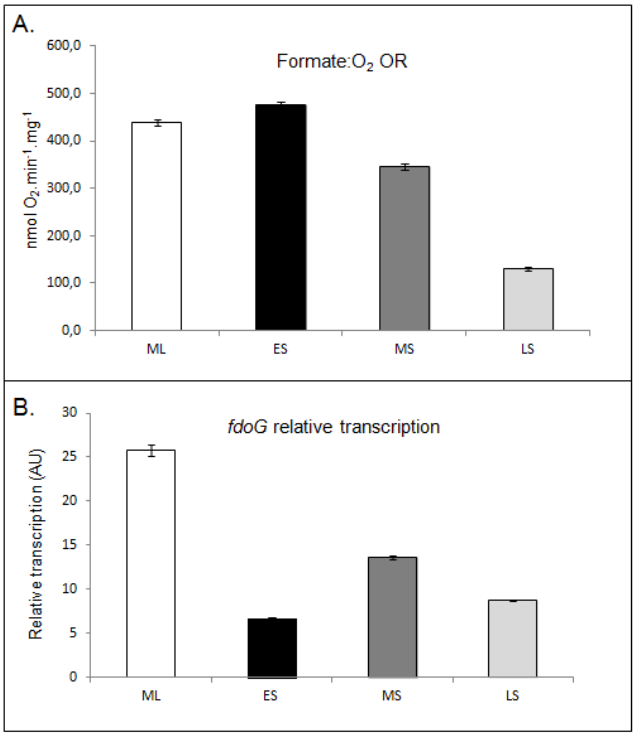

Fig. 4. Formate:oxygen oxidoreductase activity (A) and *fdoG* relative transcription (B) during aerobic growth. *E. coli* wild-type membranes were harvested at mid-logarithmic (white), early-stationary (black), mid-stationary (dark-grey) and late-stationary (light-grey) growth phases. Relative transcription levels of *fdoG* along the aerobic growth were analyzed together with the dataset reported for other *E. coli* aerobic respiratory chain components [8]. The transcription of *fdoG* at each curve point was normalized to the 16S rRNA reference gene and calculated in function of the most expressed gene/condition of the whole dataset, ML-*nuoF* [8].

The kinetics of FdOx was investigated in *E. coli* membranes establishing the apparent K_M and V_{MAX} of formate oxidation, at pH 7.2, by measuring the rate of formate oxidation in response to a range of formate concentrations. Lineweaver-Burk plots were generated and the kinetic parameters calculated according with [15] (Fig. 5). The K_M of formate oxidation was 169 ± 21 µM and the corresponding V_{MAX} 117 ± 15 nmol O_2.min^{-1}.mg^{-1}. The K_M value is of the same order of magnitude of FDH-N K_M (120 µM) [11] being reasonable to assume that it may play the same physiological role of the anaerobic counterpart at neutral pH, suggested to oxidize the formate excreted from the cytoplasm and compartmentalized in the periplasm [18].

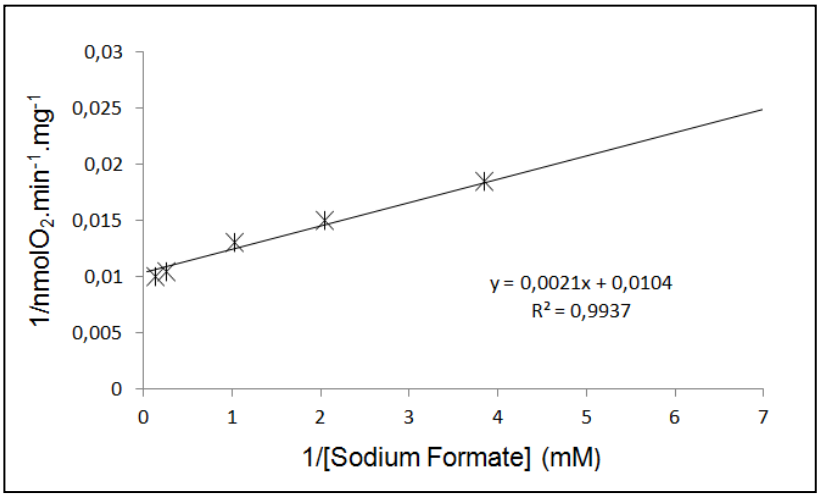

Fig. 5. Lineweaver-Burk plot of formate oxidation by FdOx supercomplex, at pH 7.2. K_M and V_{MAX} were of 169 ± 21 µM and 117 ± 15 nmol O_2.min^{-1}.mg^{-1}, respectively.

Integrative analysis of FdOx: bacterial growth, enzyme activity and gene transcription

In order to evaluate the prevalence of FDH-O along the *E. coli* aerobic growth and to compare the variation of *fdoG* transcription profile with that of other *E. coli*

aerobic respiratory chain genes [8], the relative transcription of *fdoG* was analyzed by qRT-PCR at ML, ES, MS and LS growth stages. *fdoG* transcription levels were maximal at ML, dropping to 25% at ES, increasing to 50% at MS and dropping again to 33% at LS growth stage (Fig. 4B), similarly to *ndh* relative transcription profile [8]. Interestingly, the growth stage where *fdoG* relative transcription values were lowest, ES, presented the highest values of oxygen consumption due to formate oxidation in *E. coli* wild-type membranes (Fig. 4A). Such variation is in agreement with what is observed when comparing the relative transcription of *nuoF* and *ndh* genes with the oxygen consumption profile over growth due to NADH oxidation [8].

A PCA bi-plot was acquired from the activity and transcription data of FdOx and *fdoG* and the dataset obtained in [8] (Fig. 6).

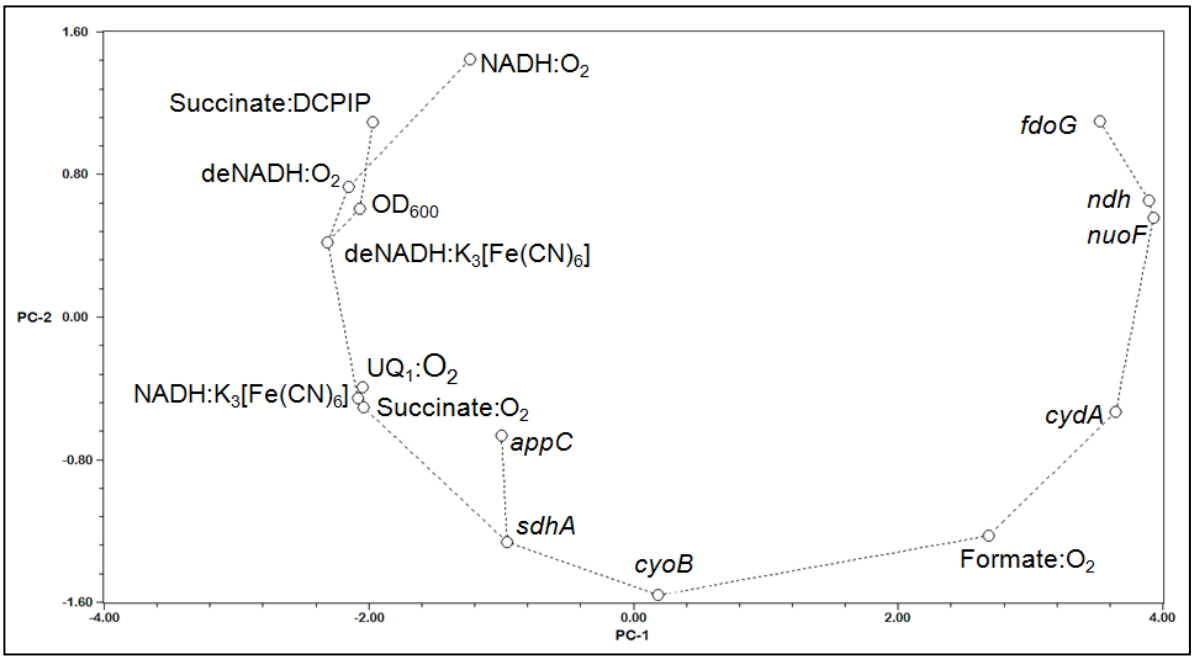

Fig. 6. PCA applied to relative gene transcription, enzyme activity and growth dynamics values of *E. coli* aerobic respiratory chain. The first two principal components account for 92.8% of the total variation, from which PC-1 and PC-2 correspond to 67.9% and 24.9% of variance, respectively. A minimum-length spanning tree connecting the nearest variables based on the correlation matrix is superimposed.

fdoG relative transcription and FdOx activity were negatively correlated with the growth progress (OD_{600}), as deduced by their relative position in the PCA bi-plot. Moreover, the activity profile of FdOx along growth is not correlated with the other oxygen oxidoreductase activities, namely succinate:, ubiquinol: and NADH:oxygen oxidoreductase activities (see [8]). Finally, according to the PCA and supported by the minimum-length spanning tree and apart from the strong positive correlation confirmed between *ndh* and *nuoF* [8], the nearest variables connecting *fdoG* gene were *cydA*, formate:oxygen oxidoreductase activity and *cyoB*, in agreement with the composition and enzymatic activity of the supercomplex herein characterized.

5.4 Discussion

This work provided evidences to support the existence of a functional FdOx supercomplex with cyanide sensitive formate:oxygen oxidoreductase activity in the aerobic respiratory chain of *E. coli*. BN-PAGE (Figs. 1 and 2) analysis and the positive correlation established between the formate:O_2 oxidoreductase activity and the transcription of *cyoB* and *cydA* genes, which encode subunits of bo_3 and *bd*I oxygen reductases (Fig. 6), respectively, confirmed that FdOx supercomplex is composed of these three complexes. In addition, it was demonstrated that bo_3 and *bd*I oxygen reductases are crucial for FdOx activity (Fig. 3D).

A supramolecular structure like FdOx may contribute to the generation of a proton motive force from the oxidation of formate, with energy conservation, since bo_3 and *bd*I oxygen reductases are electrogenic [19]. In fact, cytochrome bo_3 is the only proton-pumping oxygen reductase present in the *E. coli* respiratory chain [20].

Previous reports suggested that FDH-O is synthesized in the presence of oxygen [9] and able of formate oxidation in whole cells when oxygen is present [9,21], very likely via FdOx, at the light of the findings presented herein. Formate is a highly reducing compound ($E_{m,7}$ -420 mV) and under aerobic conditions FDH-O is the best candidate to prevent formate accumulation in cells. Furthermore, the

assembly of the aerobic formate dehydrogenase and bo_3 and *bd*I oxygen reductases in a functional supercomplex is in agreement with older evidences that suggest ubiquinone, rather than menaquinone, to be the electron acceptor of formate oxidation [22].

As previously mentioned, the catalytic subunit G of FDH-N is highly similar to that of FDH-O, thus being reasonable to expect that the FDH-O active site faces the periplasmic side of the cytoplasmic membrane as it was proposed in the structure of FDH-N [23].

5.5 Acknowledgments

The authors would like to thank Dr. Robert Gennis for the generous gift of the E. coli mutant strains ML20S2 and ML15A, and *E. coli* Genetic Stock Center for supplying E. coli JW0960-1 and JW3863 strains. Dr. Luis Goulao is acknowledged for helpful discussions regarding the PCA analysis and the statistic results. Micaela Sousa, Elisabete Lopes and Isabel Palos are acknowledged for excellent technical assistance. P.S. is a recipient of the FCT Grant SFRH/BD/46553/2008.

5.6 References

[1] Lenaz, G. and Genova, M.L. (2009). Mobility and function of coenzyme Q (ubiquinone) in the mitochondrial respiratory chain. Biochim Biophys Acta 1787, 563-73.

[2] Diaz, F., Enríquez, J.A. and Moraes, C.T. (2012). Cells lacking Rieske iron-sulfur protein have a reactive oxygen species-associated decrease in respiratory complexes I and IV. Mol Cell Biol 32, 415-29.

[3] Lenaz, G. and Genova, M.L. (2012). Supramolecular organisation of the mitochondrial respiratory chain: a new challenge for the mechanism and control of oxidative phosphorylation. Adv Exp Med Biol 748, 107-44.

[4] Iwasaki, T., Matsuura, K. and Oshima, T. (1995). Resolution of the aerobic respiratory system of the thermoacidophilic archaeon, Sulfolobus sp. strain 7. I. The archaeal terminal oxidase supercomplex is a functional fusion of respiratory complexes III and IV with no *c*-type cytochromes. J Biol Chem 270, 30881-92.

[5] Sone, N., Sekimachi, M. and Kutoh, E. (1987). Identification and properties of a quinol oxidase super-complex composed of a bc_1 complex and cytochrome oxidase in the thermophilic bacterium PS3. J Biol Chem 262, 15386-91.

[6] Berry, E.A. and Trumpower, B.L. (1985). Isolation of ubiquinol oxidase from *Paracoccus denitrificans* and resolution into cytochrome bc_1 and cytochrome c-aa_3 complexes. J Biol Chem 260, 2458-67.

[7] Sousa, P.M.F. et al. (2011). Supramolecular organizations in the aerobic respiratory chain of *Escherichia coli*. Biochimie 93, 418-425.

[8] Sousa, P.M.F., Videira, M.A., Bohn, A., Hood, B.L., Conrads, T.P., Goulao, L.F. and Melo, A.M.P. (2012). The aerobic respiratory chain of *Escherichia coli*: from genes to supercomplexes. Microbiology 158, 2408-18.

[9] Sawers, G., Heider, J., Zehelein, E. and Böck, A. (1991). Expression and operon structure of the *sel* genes of *Escherichia coli* and identification of a third selenium-containing formate dehydrogenase isoenzyme. J Bacteriol 173, 4983-93.

[10] Thompson, J.D., Higgins, D.G. and Gibson, T.J. (1994). CLUSTAL W: improving the sensitivity of progressive multiple sequence alignment through sequence weighting, position-specific gap penalties and weight matrix choice. Nucleic Acids Res 22, 4673-80.

[11] Sawers, G. (1994). The hydrogenases and formate dehydrogenases of *Escherichia coli*. Antonie Van Leeuwenhoek 66, 57-88.

[12] Stenberg, F., Chovanec, P., Maslen, S.L., Robinson, C.V., Ilag, L.L., von Heijne, G. and Daley, D.O. (2005). Protein complexes of the *Escherichia coli* cell envelope. J Biol Chem 280, 34409-19.

[13] Wittig, I., Braun, H.P. and Schägger, H. (2006). Blue native PAGE. Nat Protoc 1, 418-28.

[14] Enoch, H.G. and Lester, R.L. (1975). The purification and properties of formate dehydrogenase and nitrate reductase from *Escherichia coli*. J Biol Chem 250, 6693-705.

[15] Lineweaver, H. and Burk, D. (1934) The determination of enzyme dissociation constants. J Am Chem Soc 56, 658-666.

[16] Jolliffe, I.T. (2002) Principal Component Analysis, Springer. New York, USA.

[17] Rohlf, F.J. (2005) NTSYS-pc, Numerical taxonomy and multivariate analysis system. Exeter Software, Setauket, New York, USA.

[18] Sawers, R.G. (2005). Formate and its role in hydrogen production in *Escherichia coli*. Biochem Soc Trans 33, 42-6.

[19] Puustinen, A., Finel, M., Haltia, T., Gennis, R.B. and Wikström, M. (1991). Properties of the two terminal oxidases of *Escherichia coli*. Biochemistry 30, 3936-42.

[20] Puustinen, A., Finel, M., Virkki, M. and Wikström, M. (1989). Cytochrome *o* (*bo*) is a proton pump in *Paracoccus denitrificans* and *Escherichia coli*. FEBS Lett 249, 163-7.

[21] Pinsent, J. (1954). The need for selenite and molybdate in the formation of formic dehydrogenase by members of the coli-aerogenes group of bacteria. Biochem J 57, 10-6.

[22] Giordano, G., Grillet, L., Rosset, R., Dou, J.H., Azoulay, E. and Haddock, B.A. (1978). Characterization of an *Escherichia coli* K12 mutant that is sensitive to chlorate when grown aerobically. Biochem J 176, 553-61.

[23] Jormakka, M., Törnroth, S., Byrne, B. and Iwata, S. (2002). Molecular basis of proton motive force generation: structure of formate dehydrogenase-N. Science 295, 1863-8.

[24] Wittig, I., Beckhaus, T., Wumaier, Z., Karas, M. and Schägger, H. (2010). Mass estimation of native proteins by blue native electrophoresis: principles and practical hints. Mol Cell Proteomics 9, 2149-61.

Part III – Supramolecular organizations in the aerobic respiratory chain of *Bacillus subtilis*

Chapter 6

Introducing the Bacillus subtilis *aerobic respiratory chain*

Chapter 6

6.1 Bacillus subtilis *aerobic respiratory chain*

Bacillus subtilis is a mesophilic, Gram positive bacterium, that inhabits the soil and is able to grow in the presence of oxygen or under anoxic conditions, employing either a fermentative metabolism or using nitrate or nitrite as the terminal electron acceptors of an electron transfer respiratory chain [1]. The aerobic respiratory chain of this organism comprises several dehydrogenases, namely a type II NADH:quinone oxidoreductase (NDH-2) (see [2] for a review), succinate:quinone oxidoreductase (SQR) [3] and glycerol-3-phosphate dehydrogenase [4], acting as electron entry points for menaquinone reduction (Figure 1).

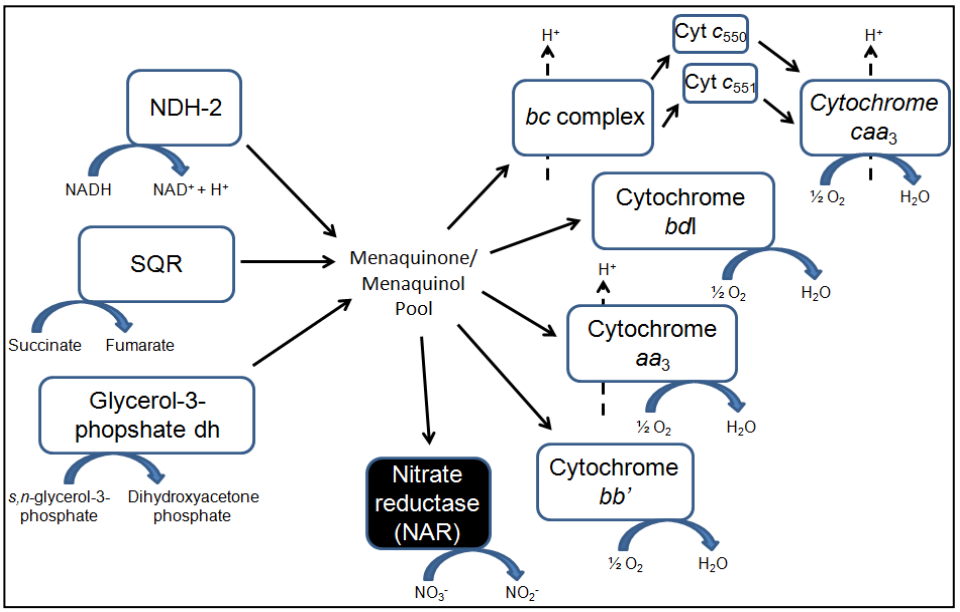

Fig. 1. *B. subtilis* aerobic respiratory chain. Electrons from the oxidation of NADH, succinate and *s*,*n*-glycerol-3-phosphate by NDH-2, SQR and glycerol-3-phosphate dehydrogenase enzymes, respectively, are transferred via menaquinone to O_2 through four different branches. Under low oxygen concentration conditions, an alternative electron transfer pathway is provided by the respiratory nitrate reductase (NAR), highlighted in black to distinguish the terminal electron acceptor nitrate. Adapted from [4,5,7-11,17,22,42].

B. subtilis contains a branched respiratory chain, the oxygen respiring branches being composed of a cytochrome *c* pathway where *bc* complex [5] and caa_3 oxygen reductase [6] operate, and three quinol oxygen reductase pathways involving cytochromes *bd* [7], aa_3 [8] or *bb'* [9] menaquinol oxygen reductases. Strikingly, no freely soluble *c*-type cytochromes are detected in *B. subtilis* aerobic respiratory chain. Instead, two cytoplasmic membrane-anchored *c*-type cytochromes, c_{550} or c_{551}, were suggested to mediate the electron transfer occurring in the cytochrome *c* pathway [10,11]. A nitrate respiring branch is suggested to operate also in the respiratory chain of *B. subtilis* grown under low oxygen concentration conditions [12], through the expression of a membrane-anchored respiratory nitrate reductase (NAR), which is also assembled under anaerobic conditions [13].

i. Primary dehydrogenases

Type-II NADH-dehydrogenase (NDH-2)

B. subtilis 168 genome contains three putative NDH-2 encoding genes, *yjlD*, *yutJ* and *yumB*, the corresponding transcripts' primary structure sharing 44%, 41% and 40% sequence similarity with the *E. coli* NDH-2, respectively, as calculated by CLUSTAL W [14]. Additionally, *E. coli* NDH-2 and *B. subtilis* putative NDH-2 enzymes share the two -GXGXXG- consensus motifs involved in noncovalently binding of NAD(P)H and FAD [2]. YjlD (also termed Ndh) has been reported to be a membrane-associated protein, whose expression is abolished under anaerobic conditions [15], thus being tempting to assign it as the *B. subtilis* aerobic respiratory chain NDH-2. In fact, this enzyme was suggested to correspond to the one reported by Bergsma and colleagues, who purified and characterized a type-II NADH dehydrogenase from *B. subtilis* strain W23 [16,17]. These authors have shown that, similarly to the *E. coli* enzyme, the NDH-2 of *B. subtilis* strain W23, with an apparent molecular mass of 64 kDa, is a single, membrane-associated

polypeptide containing a flavin cofactor FAD, its catalytic activity being specific for NADH [17]. Noteworthy, *yjlD* transcription is directly regulated by a redox-sensing protein, Rex (also termed YdiH), the activity of which is regulated by the $NADH/NAD^+$ ratio, thus suggesting that *B. subtilis* YjlD and Rex form a regulatory loop to maintain the balance of the cytoplasmic $NADH/NAD^+$ ratio in cells grown in the presence of oxygen [18].

Succinate:quinone oxidoreductase (SQR)

B. subtilis SQR is a 116 kDa complex that contains three subunits encoded by *sdhCAB* operon. SqrA and SqrB hydrophilic subunits are highly conserved between different organisms and contain a covalently bound FAD cofactor and three [Fe-S] clusters. SqrC subunit represents the membrane domain and assembles two *b*-type hemes (b_D and b_P), a feature exclusive of the type-B SQRs membrane domain [19]. The two hemes have different optical and EPR spectral properties [20] and are essential for the enzyme assembly [21].

Although the *B. subtilis* SQR X-ray crystal structure is still missing, this enzyme bears significant amino acid sequence similarity with the *W. succinogenes* quinol:fumarate oxidoreductase (QFR) [22], the structure of which, solved at a 2.2 Å resolution, revealed to be a dimer [23]. SqrA, SqrB and SqrC share 44%, 44% and 31% sequence similarity with *W. succinogenes* QfrA, QfrB and QfrC, respectively, as calculated by CLUSTAL W [14]. In fact, *B. subtilis* SQR is a bifunctional enzyme also active as QFR [24]. It is thus reasonable to expect that both proteins may share similar structures. In agreement, *W. succinogenes* QFR was shown to contain a type-B hydrophobic domain assembling the same prosthetic groups.

The reaction catalyzed by the *B. subtilis* SQR requires an endergonic electron transfer, from the oxidation of succinate to the reduction of menaquinone, due to the more negative reduction potential of menaquinone (-75 mV) which, in contrast with ubiquinone, is lower than the succinate reduction potential (+30 mV).

Therefore, this electron transfer is suggested to be coupled with the uptake of two protons from the inner wall zone to the menaquinone binding site [25,26], which was shown to be near heme b_D, in agreement with the binding location of the menaquinone-like inhibitor HQNO [27].

ii. The cytochrome *c* branch

B. subtilis respiratory chain cytochrome *c* branch comprises a *bc* complex and a cytochrome caa_3 oxygen reductase, that mediate the electron transfer from the oxidation of menaquinol to the reduction of oxygen, yielding water. In addition, *B. subtilis* aerobic respiratory chain expresses two distinct *c*-type cytochromes anchored to the cytoplasmic membrane, cytochrome c_{550} being attached by an N-terminal transmembrane segment [10] and cytochrome c_{551} being linked by a diacyl glycerol tail [11].

B. subtilis bc complex (Qcr) is a unique proton-translocating menaquinol:cytochrome *c* oxidoreductase related to bc_1 and b_6f complexes [5]. It is a 73 kDa complex encoded by *qcrABC* operon that contains three subunits, QcrA, QcrB and QcrC. QcrA is a transmembrane subunit similar to Rieske type iron-sulfur proteins, bearing the conserved amino acid residues present in the $[2Fe\text{-}2S]^{2+/1+}$ cluster binding site, similarly to what is observed in the mitochondrial bc_1 complex Rieske [Fe-S] subunit. QcrB subunit resembles the cytochrome *b* subunit from b_6f complexes of photosynthetic organisms. For example, the cytochrome *b* subunit from the photosynthetic eukaryote *Cyanophora paradoxa* b_6f complex shares 44% and 63% identity and similarity, respectively, with the *B. subtilis* QcrB subunit, as calculated by CLUSTAL W [14]. Moreover, QcrB subunit was also shown to display high similarity with the cytochrome *b* subunit N-terminal domain of the canonical bc_1 complex [5]. QcrB subunit assembles two *b*-type hemes of low and high reduction potentials, b_L and b_H, respectively, the latter suggested to be covalently linked to the polypeptide in the *B. subtilis bc* complex, through mutagenesis studies [28]. The third subunit, QcrC, comprises *i*) a highly

hydrophobic N-terminal domain similar to the subunit IV of the cyanobacteria b_6f complex and to the cytochrome *b* subunit C-terminal domain of the canonical bc_1 complex; and ii) a C-terminal domain, the amino acid sequence of which contains a -CXYCH- heme *c* binding motif, thus suggesting that QcrC contains a covalently attached cytochrome *c* [5].

B. subtilis cytochrome caa_3 oxygen reductase is a 145 kDa complex encoded by *ctaCDEF* operon that belongs to the heme-copper oxygen reductases A-family, similarly to the mitochondrial complex IV, described in Chapter 1, or the *P. denitrificans* cytochrome aa_3 oxygen reductase [29]. *ctaC*, *ctaD*, *ctaE* and *ctaF* encode subunits II (CtaC), I (CtaD), III (CtaE) and IV (CtaF), respectively [30], of which subunits I and II contain all the redox groups of the enzyme. Subunit II assembles a binuclear Cu_A centre and, in contrast with the mitochondrial complex IV, harbors an extension of approximately 100 amino acids in the C-terminal sequence with a consensus -CXXCH- heme *c* binding motif [30], similarly to the *R. marinus* cytochrome caa_3 oxygen reductase [31]. Nevertheless, the reactivity of the *B. subtilis* caa_3 enzyme with oxygen was shown to be identical to that of the mitochondrial complex IV [32]. Subunit I assembles one *a*-type heme and a binuclear complex consisting of a second *a*-type heme (a_3) together with Cu_B. It shares the conserved amino acid residues of D and K proton channels with the subunit I of the eukaryotic complex IV [29]. Thus, *B. subtilis* caa_3 enzyme is suggested to catalyze the sequential transfer of four electrons from cytochrome *c* to O_2, yielding two water molecules. This reaction requires the uptake of four protons from the N-side of the membrane as well as the translocation of four protons to the inner wall zone [33].

It is currently unknown whether the electron transfer within the cytochrome *c* branch is mediated by the covalently bound *c*-type cytochromes present in *bc* complex and caa_3 oxygen reductase or through the membrane-bound cytochromes c_{550} and c_{551}. Noteworthy, mutants devoid of either membrane-bound *c*-type cytochrome showed no apparent phenotypic differences [34], and the *c*-type cytochrome from caa_3 oxygen reductase was proposed to be the only one

required for electron transfer in this terminal oxygen reductase [35], suggesting that the cytochrome *c* branch electron transfer may not require these specific membrane-bound cytochromes to operate.

iii. The quinol oxygen reductase branches

Three quinol oxygen reductases are present in *B. subtilis* aerobic respiratory chain, namely cytochrome *bd*, *bb'* and aa_3 menaquinol oxygen reductases, from which the latter is the only quinol oxygen reductase present that belongs to the heme-copper oxygen reductases superfamily [29]. These enzymes directly catalyze the electron transfer from the oxidation of menaquinol to the reduction of O_2, yielding water.

Cytochrome aa_3 menaquinol oxygen reductase belongs to the heme-copper oxygen reductases family A and is therefore related with the mitochondrial complex IV, the *B. subtilis* cytochrome caa_3 oxygen reductase or the *E. coli* cytochrome bo_3 quinol oxygen reductase complex previously described [36]. Its catalytic reaction requires the concomitant translocation of four protons to the inner wall zone for each menaquinol molecule oxidized. It is a 147 kDa complex containing four subunits encoded by the *qoxABCD* operon, QoxA (subunit II), QoxB (subunit I), QoxC (subunit III) and QoxD (subunit IV). Subunit I contains all the redox groups [37,38] and displays high similarity with the corresponding subunit from *B. subtilis* cytochrome caa_3 oxygen reductase (66%) and *E. coli* cytochrome bo_3 quinol oxygen reductase (69%), as calculated by CLUSTAL W [14]. Thus, like subunit I of the *B. subtilis* cytochrome caa_3 oxygen reductase, cytochrome aa_3 menaquinol oxygen reductase QoxB subunit assembles two *a*-type hemes, *a* and a_3, together with a copper atom, Cu_B. In contrast with mitochondrial complex IV, the subunit II of this enzyme does not contain a binuclear Cu_A centre or a cytochrome *c* binding site, similarly to *E. coli* cytochrome bo_3 quinol oxygen reductase. Instead, the heme *a* receives electrons directly from

a liposoluble menaquinol molecule [36]. Subunits III and IV do not contain prosthetic groups and are not essential for the enzyme activity [38].

The genome of *B. subtilis* contains genes for two potential cytochrome *bd*-type menaquinol oxygen reductases, namely *cydABCD* and *ythABC* [39].

The *cydABCD* operon encodes a cytochrome *bd* menaquinol oxygen reductase, where *cydAB* constitute the structural genes encoding subunits CydA and CydB and *cydCD* encode a putative ATP-binding cassette (ABC) type of transporter and is required for the assembly and expression of a functional cytochrome *bd* complex [7]. CydA and CydB subunits display 52% and 50% similarity with the *E. coli* cytochrome *bd*I quinol oxygen reductase corresponding subunits, respectively, as calculated by CLUSTAL W [14], thus being expected to perform a similar reaction to that described in chapter 2.

The *ythABC* gene cluster was proposed to encode a second *bd*-type menaquinol oxygen reductase in *B. subtilis* respiratory chain [40]. *ythA* and *ythB* translated sequences are closely related to the subunits I and II of *Bacillus stearothermophilus* cytochrome *bd* quinol oxygen reductase [41], respectively. However, direct experimental evidence for the presence of this terminal oxygen reductase in *B. subtilis* respiratory chain is still missing.

A third *bd*-type menaquinol oxygen reductase, cytochrome *bb*' menaquinol oxygen reductase, was identified through spectroscopic analysis and shown to be unrelated with *ythABC* [9]. Azarkina and colleagues analyzed a *B. subtilis* mutant strain (LUH27) devoid of cytochrome aa_3 oxygen reductase, SQR and cytochrome caa_3 oxygen reductase and were able to identify a menaquinol oxygen reductase of the *bd*-type in which the *d*-type heme was completely missing, being replaced by a high spin *b*-type heme. Since the genes encoding such an oxygen reductase have not been identified in *B. subtilis* genome, the authors proposed that the cytochrome *bd* menaquinol oxygen reductase encoded by *cydABCD* would be the one responsible for incorporating a *b*-type heme instead of a *d*-type heme, for unknown reasons. However, it is possible that this oxygen reductase may be encoded by other *B. subtilis* genes for which the function remains elusive.

iv. Respiratory nitrate reductase (NAR)

When external oxygen is limited, *B. subtilis* can still grow in the presence of oxygen using an alternative electron acceptor such as nitrate, by expressing a respiratory nitrate reductase complex (NAR) [42], which is also assembled under anaerobic conditions [12]. *B. subtilis* NAR is a 241 kDa membrane complex encoded by *narGHJI* operon that contains three subunits, NarG, NarH and NarI. Its structure and function are still poorly understood, however, this enzyme displays high sequence similarity with *E. coli* NAR, the structure and function of which are well established [43]. Comparing the amino acid sequences of proteins encoded by *narGHJI* with those of *E. coli* NAR indicated that NarH subunit displays the highest identity and similarity, 55% and 73%, respectively, as calculated by CLUSTAL W [14]. Similarly, NarG subunits of both enzymes display 50% identity and 68% similarity, whereas NarI subunits identity and similarity were calculated to be 32% and 55%, respectively.

Thus, through analogy with the *E. coli* enzyme, *B. subtilis* NarG subunit, is likely the catalytic subunit that promotes the reduction of nitrate to nitrite in the cytoplasm, with the concomitant uptake of two protons from the cytoplasm, yielding water [43]. *B. subtilis* NarH subunit amino acid sequence contains an arrangement of cysteine residues typical of [Fe-S] clusters. In agreement, the *E. coli* NarH subunit assembles three $[4Fe\text{-}4S]^{2+/1+}$ and one $[3Fe\text{-}4S]^{1+/0}$ clusters, sequentially positioned [43]. *E. coli* NarI is an integral membrane subunit that assembles two *b*-type hemes (b_D and b_P) where the ubiquinol binding site is located.

In the *E. coli* NAR complex, NarI subunit receives two electrons from ubiquinol, with the concomitant translocation of two protons to the inner wall zone, transfers the electrons first to the [Fe-S] clusters of NarH subunit, and then to the [Fe-S] cluster of NarG subunit. The electrons finally reach the molybdenum cofactor in NarG subunit, where nitrate is reduced to nitrite [44].

Considering the similarities displayed by *E. coli* and *B. subtilis* NAR enzymes, it is expected that both proteins may share identical structures and, consequently, catalytic function.

B. subtilis narGHJI operon encodes a fourth polypeptide, NarJ, which was suggested to be required for the enzyme assembly [13] and is unrelated with the *E. coli* NarJ protein.

v. Bioenergetic efficiency of *B. subtilis* respiratory chain

Since *B. subtilis* does not possess a proton-translocating NADH dehydrogenase, the bioenergetic efficiency of its aerobic respiratory chain is solely dependent on the expression of the enzymes present in the cytochrome *c* or the quinol oxygen reductase branches, which couple electron transfer with the generation of an electrochemical proton gradient. As previously mentioned, the use of a particular oxygen reductase for energy generation is governed primarily by the environmental conditions such as the availability of oxygen or of a carbon source like glucose [45]. The main electron flow in *B. subtilis* grown in the presence of glucose and oxygen is *via* cytochrome aa_3 menaquinol oxygen reductase [37]. In fact, mutant stains devoid of cytochrome aa_3 menaquinol oxygen reductase presented a significantly reduced growth, in comparison with the *B. subtilis* wild type, suggesting that this enzyme may be the most important terminal oxygen reductase expressed during the exponential growth phase [40]. In contrast, cytochrome *bd* menaquinol oxygen reductase appears to be expressed mainly at low oxygen concentrations [7]. Nevertheless, it has been demonstrated that the expression of at least one menaquinol oxygen reductase, either cytochrome aa_3 or *bd* menaquinol oxygen reductases, is essential for *B. subtilis* growth in the presence of oxygen [40]. The cytochrome *c* branch is undetectable in *B. subtilis* cells grown in the presence of glucose [46], but is expressed during growth on nonfermentable carbon sources [47]. The expression of *bc* complex is induced at the end of the exponential growth phase and reduces as the bacteria undergoes

sporulation [5]. On the other hand, at least one heme-copper oxygen reductase, either cytochrome aa_3 menaquinol oxygen reductase or cytochrome caa_3 oxygen reductase, is required for efficient sporulation [40]. As previously mentioned, *B. subtilis* expresses a respiratory NAR complex under low oxygen concentration conditions. Although outside the scope of the aerobic respiratory chain, this enzyme potentially represents an alternative pathway for the reduction of menaquinol in the presence of nitrate and oxygen.

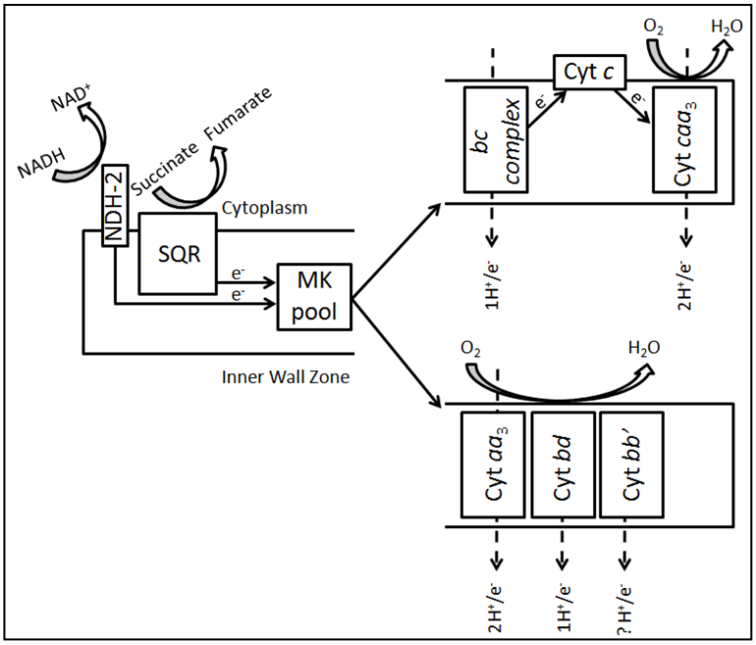

Fig. 2. *B. subtilis* aerobic respiratory chain enzymes and their proton-translocation properties. The cytochrome *c* branch, containing *bc* complex and cytochrome caa_3 oxygen reductase, exhibits the highest H^+/e^- stoichiometry (3 H^+/e^-), whereas SDH and NDH-2 do not translocate protons to the inner wall zone. Information regarding cytochrome *bb'* menaquinol oxygen reductase is not yet available. Cyt, cytochrome; MK, menaquinone. Adapted from [17,26,33].

Depending on the respiratory chain expressed enzymes, between 1 and 3 protons may be translocated per transported electron in *B. subtilis* grown in the presence of oxygen (Figure 2). *B. subtilis* aerobic respiratory chain using the cytochrome *c* branch results in proton translocation with a H^+/e^- stoichiometry of 3,

considering that *bc* complex and cytochrome *caa*$_3$ oxygen reductase translocate 1 and 2 protons, respectively, for each transferred electron. On the other hand, use of the menaquinol oxygen reductase branch may reflect a H^+/e^- stoichiometry of 2 or 1, if oxygen is reduced *via* cytochrome *aa*$_3$ or *bd* menaquinol oxygen reductases, respectively [33]. Information regarding the H^+/e^- stoichiometry of *B. subtilis* cytochrome *bb*' menaquinol oxygen reductase is still not available, however, through analogy with its corresponding counterpart, it is expected to be 1 [48]. Similarly, there is no information regarding the potential H^+/e^- stoichiometry promoted by the *B. subtilis* NAR complex. Nevertheless, the close related *E. coli* NAR complex was suggested to bear a H^+/e^- stoichiometry of 1 [44], being reasonable to assume a similar value for the *B. subtilis* enzyme.

Bacillus subtilis F_1F_O-ATP synthase structure is still unknown but the arrangement of its encoding genes in the *atp* encoding operon is highly similar to that of *Escherichia coli* F_1F_O-ATP synthase [49]. Although no information is available regarding *B. subtilis* F_1F_O-ATP synthase number of *c*-subunits, which would allow an accurate determination of the H^+/ATP as well as the P/O ratios of a given pathway [50], model predictions of the estimated P/O ratio based on the genomic analysis of *B. subtilis* electron transport enzymes and the experimental data available for each protein revealed a maximal P/O ratio of 1.33 for glucose-grown *B. subtilis* aerobic respiratory chain [45]. This in agreement with the predicted H^+/e^- stoichiometry of 2 for the cytochrome *aa*$_3$ menaquinol oxygen reductase pathway, which is the main oxygen reductase expressed in the presence of glucose [37].

Besides being required for ATP synthesis, the electrochemical proton gradient appears to be essential as a driving force for SQR, which, as previously mentioned, catalyzes a reversed electron transfer when oxidizing succinate to fumarate using menaquinone as electron acceptor [25].

vi. The composition of *B. subtilis* respiratory chain supercomplexes

The supramolecular organization of *B. subtilis* respiratory chain was recently analyzed in cells grown under aerobic conditions in a medium supplied with 3% succinate [51]. Using two different electrophoretic techniques (BN and CN-PAGE) to resolve wild type *B. subtilis* digitonin solubilized membranes, Oca and colleagues suggested the presence of several respiratory chain supercomplexes through heme staining and *in gel* activities, followed by mass spectrometry analysis. These authors suggested that the *B. subtilis* aerobic respiratory chain comprises supercomplexes of high molecular mass containing: *i*) *bc* complex and caa_3 oxygen reductase, in which F_1F_O-ATP synthase peptides were also identified as well as the membrane-anchored cytochrome c_{550}; *ii*) the dimeric assembly of SQR together with the respiratory NAR; *iii*) SQR and cytochrome aa_3 menaquinol oxygen reductase and *iv*) cytochrome aa_3 menaquinol oxygen reductase together with F_1-ATP synthase. In the same study, NDH-2 was detected within a low molecular mass band likely corresponding to its monomeric form and most of the F_1F_O-ATP synthase was found in the monomeric state.

As these studies relied mostly on the electrophoretic analyses of wild type *B. subtilis* solubilized membranes, information regarding the supramolecular structures assembled in specific respiratory chain mutants, which allows for a better comprehension of their composition, stoichiometry and catalytic function is still missing. In the following chapter we address these questions and provide further evidences regarding the supramolecular composition of the *B. subtilis* respiratory chain.

6.2 References

[1] Nakano, M.M. and Zuber, P. (1998). Anaerobic growth of a "strict aerobe" (*Bacillus subtilis*). Annu Rev Microbiol 52, 165-90.

[2] Melo, A.M.P., Bandeiras, T.M. and Teixeira, M. (2004). New insights into type II NAD(P)H:quinone oxidoreductases. Microbiol Mol Biol Rev 68, 603-16.

[3] Lemma, E., Hägerhäll, C., Geisler, V., Brandt, U., von Jagow, G. and Kröger, A. (1991). Reactivity of the *Bacillus subtilis* succinate dehydrogenase complex with quinones. Biochim Biophys Acta 1059, 281-5.

[4] Morbidoni, H.R., de Mendoza, D. and Cronan, J.E. (1995). Synthesis of *sn*-glycerol 3-phosphate, a key precursor of membrane lipids, in *Bacillus subtilis*. J Bacteriol 177, 5899-905.

[5] Yu, J., Hederstedt, L. and Piggot, P.J. (1995). The cytochrome *bc* complex (menaquinone:cytochrome *c* reductase) in *Bacillus subtilis* has a nontraditional subunit organization. J Bacteriol 177, 6751-60.

[6] Bengtsson, J., Tjalsma, H., Rivolta, C. and Hederstedt, L. (1999). Subunit II of *Bacillus subtilis* cytochrome *c* oxidase is a lipoprotein. J Bacteriol 181, 685-8.

[7] Winstedt, L., Yoshida, K., Fujita, Y. and von Wachenfeldt, C. (1998). Cytochrome *bd* biosynthesis in *Bacillus subtilis*: characterization of the *cydABCD* operon. J Bacteriol 180, 6571-80.

[8] De Vrij, W., Azzi, A. and Konings, W.N. (1983). Structural and functional properties of cytochrome *c* oxidase from *Bacillus subtilis* W23. Eur J Biochem 131, 97-103.

[9] Azarkina, N., Siletsky, S., Borisov, V., von Wachenfeldt, C., Hederstedt, L. and Konstantinov, A.A. (1999). A cytochrome *bb*'-type quinol oxidase in *Bacillus subtilis* strain 168. J Biol Chem 274, 32810-7.

[10] von Wachenfeldt, C. and Hederstedt, L. (1990). *Bacillus subtilis* 13-kilodalton cytochrome c-$_{550}$ encoded by *cccA* consists of a membrane-anchor and a heme domain. J Biol Chem 265, 13939-48.

[11] Bengtsson, J., Rivolta, C., Hederstedt, L. and Karamata, D. (1999). *Bacillus subtilis* contains two small *c*-type cytochromes with homologous heme domains but different types of membrane anchors. J Biol Chem 274, 26179-84.

[12] Bohin, J.P., Bohin, A. and Schaeffer, P. (1976). Increased nitrate reductase A activity as a sign of membrane alteration in early blocked asporogenous mutants of *Bacillus subtilis*. Biochimie 58, 99-108.

[13] Hoffmann, T., Troup, B., Szabo, A., Hungerer, C. and Jahn, D. (1995). The anaerobic life of *Bacillus subtilis*: cloning of the genes encoding the respiratory nitrate reductase system. FEMS Microbiol Lett 131, 219-25.

[14] Thompson, J.D., Higgins, D.G. and Gibson, T.J. (1994). CLUSTAL W: improving the sensitivity of progressive multiple sequence alignment through sequence weighting, position-specific gap penalties and weight matrix choice. Nucleic Acids Res 22, 4673-80.

[15] Marino, M., Hoffmann, T., Schmid, R., Möbitz, H. and Jahn, D. (2000). Changes in protein synthesis during the adaptation of *Bacillus subtilis* to anaerobic growth conditions. Microbiology 146 (Pt 1), 97-105.

[16] Bergsma, J., Strijker, R., Alkema, J.Y., Seijen, H.G. and Konings, W.N. (1981). NADH dehydrogenase and NADH oxidation in membrane vesicle from *Bacillus subtilis*. Eur J Biochem 120, 599-606.

[17] Bergsma, J., Van Dongen, M.B. and Konings, W.N. (1982). Purification and characterization of NADH dehydrogenase from *Bacillus subtilis*. Eur J Biochem 128, 151-7.

[18] Gyan, S., Shiohira, Y., Sato, I., Takeuchi, M. and Sato, T. (2006). Regulatory loop between redox sensing of the NADH/NAD(+) ratio by Rex (YdiH) and oxidation of NADH by NADH dehydrogenase Ndh in *Bacillus subtilis*. J Bacteriol 188, 7062-71.

[19] Hägerhäll, C. (1997). Succinate: quinone oxidoreductases. Variations on a conserved theme. Biochim Biophys Acta 1320, 107-41.

[20] Hägerhäll, C., Aasa, R., von Wachenfeldt, C. and Hederstedt, L. (1992). Two hemes in *Bacillus subtilis* succinate:menaquinone oxidoreductase (complex II). Biochemistry 31, 7411-21.

[21] Hederstedt, L. and Rutberg, L. (1980). Biosynthesis and membrane binding of succinate dehydrogenase in *Bacillus subtilis*. J Bacteriol 144, 941-51.

[22] Hederstedt, L. (2002). Succinate:quinone oxidoreductase in the bacteria *Paracoccus denitrificans* and *Bacillus subtilis*. Biochim Biophys Acta 1553, 74-83.

[23] Lancaster, C.R., Kröger, A., Auer, M. and Michel, H. (1999). Structure of fumarate reductase from *Wolinella succinogenes* at 2.2 A resolution. Nature 402, 377-85.

[24] Schnorpfeil, M., Janausch, I.G., Biel, S., Kröger, A. and Unden, G. (2001). Generation of a proton potential by succinate dehydrogenase of *Bacillus subtilis* functioning as a fumarate reductase. Eur J Biochem 268, 3069-74.

[25] Schirawski, J. and Unden, G. (1998). Menaquinone-dependent succinate dehydrogenase of bacteria catalyzes reversed electron transport driven by the proton potential. Eur J Biochem 257, 210-5.

[26] Lancaster, C.R. et al. (2005). Experimental support for the "E pathway hypothesis" of coupled transmembrane e^- and H^+ transfer in dihemic quinol:fumarate reductase. Proc Natl Acad Sci U S A 102, 18860-5.

[27] Smirnova, I.A., Hägerhäll, C., Konstantinov, A.A. and Hederstedt, L. (1995). HOQNO interaction with cytochrome *b* in succinate:menaquinone oxidoreductase from *Bacillus subtilis*. FEBS Lett 359, 23-6.

[28] Yu, J. and Le Brun, N.E. (1998). Studies of the cytochrome subunits of menaquinone:cytochrome *c* reductase (*bc* complex) of *Bacillus subtilis*. Evidence for the covalent attachment of heme to the cytochrome *b* subunit. J Biol Chem 273, 8860-6.

[29] Pereira, M.M., Santana, M. and Teixeira, M. (2001). A novel scenario for the evolution of haem-copper oxygen reductases. Biochim Biophys Acta 1505, 185-208.

[30] Saraste, M., Metso, T., Nakari, T., Jalli, T., Lauraeus, M. and Van der Oost, J. (1991). The *Bacillus subtilis* cytochrome-*c* oxidase. Variations on a conserved protein theme. Eur J Biochem 195, 517-25.

[31] Santana, M., Pereira, M.M., Elias, N.P., Soares, C.M. and Teixeira, M. (2001). Gene cluster of *Rhodothermus marinus* high-potential iron-sulfur Protein: oxygen oxidoreductase, a *caa*(3)-type oxidase belonging to the superfamily of heme-copper oxidases. J Bacteriol 183, 687-99.

[32] Hill, B.C. (1996). Stopped-flow, laser-flash photolysis studies on the reactions of CO and O_2 with the cytochrome caa_3 complex from *Bacillus subtilis*: conservation of electron transfer pathways from cytochrome *c* to O_2. Biochemistry 35, 6136-43.

[33] Trumpower, B.L. and Gennis, R.B. (1994). Energy transduction by cytochrome complexes in mitochondrial and bacterial respiration: the enzymology of coupling electron transfer reactions to transmembrane proton translocation. Annu Rev Biochem 63, 675-716.

[34] von Wachenfeldt, C. and Hederstedt, L. (1992). Molecular biology of *Bacillus subtilis* cytochromes. FEMS Microbiol Lett 79, 91-100.

[35] Andrews, D., Mattatall, N.R., Arnold, D. and Hill, B.C. (2005). Expression, purification, and characterization of the CuA-cytochrome *c* domain from subunit II of the *Bacillus subtilis* cytochrome caa_3 complex in *Escherichia coli*. Protein Expr Purif 42, 227-35.

[36] Yi, S.M., Narasimhulu, K.V., Samoilova, R.I., Gennis, R.B. and Dikanov, S.A. (2010). Characterization of the semiquinone radical stabilized by the cytochrome $aa_{3\text{-}600}$ menaquinol oxidase of *Bacillus subtilis*. J Biol Chem 285, 18241-51.

[37] Santana, M., Kunst, F., Hullo, M.F., Rapoport, G., Danchin, A. and Glaser, P. (1992). Molecular cloning, sequencing, and physiological characterization of the *qox* operon from *Bacillus subtilis* encoding the $aa_{3\text{-}600}$ quinol oxidase. J Biol Chem 267, 10225-31.

[38] Lemma, E., Schägger, H. and Kröger, A. (1993). The menaquinol oxidase of *Bacillus subtilis* W23. Arch Microbiol 159, 574-8.

[39] Kunst, F. et al. (1997). The complete genome sequence of the gram-positive bacterium *Bacillus subtilis*. Nature 390, 249-56.

[40] Winstedt, L. and von Wachenfeldt, C. (2000). Terminal oxidases of *Bacillus subtilis* strain 168: one quinol oxidase, cytochrome *aa*(3) or cytochrome *bd*, is required for aerobic growth. J Bacteriol 182, 6557-64.

[41] Sakamoto, J., Koga, E., Mizuta, T., Sato, C., Noguchi, S. and Sone, N. (1999). Gene structure and quinol oxidase activity of a cytochrome *bd*-type oxidase from *Bacillus stearothermophilus*. Biochim Biophys Acta 1411, 147-58.

[42] LaCelle, M., Kumano, M., Kurita, K., Yamane, K., Zuber, P. and Nakano, M.M. (1996). Oxygen-controlled regulation of the flavohemoglobin gene in *Bacillus subtilis*. J Bacteriol 178, 3803-8.

[43] Bertero, M.G., Rothery, R.A., Palak, M., Hou, C., Lim, D., Blasco, F., Weiner, J.H. and Strynadka, N.C. (2003). Insights into the respiratory electron transfer pathway from the structure of nitrate reductase A. Nat Struct Biol 10, 681-7.

[44] Garland, P.B., Downie, J.A. and Haddock, B.A. (1975). Proton translocation and the respiratory nitrate reductase of *Escherichia coli*. Biochem J 152, 547-59.

[45] Sauer, U. and Bailey, J.E. (1999). Estimation of P-to-O ratio in *Bacillus subtilis* and its influence on maximum riboflavin yield. Biotechnol Bioeng 64, 750-4.

[46] Lauraeus, M., Haltia, T., Saraste, M. and Wikström, M. (1991). *Bacillus subtilis* expresses two kinds of haem-*a*-containing terminal oxidases. Eur J Biochem 197, 699-705.

[47] Liu, X. and Taber, H.W. (1998). Catabolite regulation of the *Bacillus subtilis ctaBCDEF* gene cluster. J Bacteriol 180, 6154-63.

[48] Borisov, V.B., Gennis, R.B., Hemp, J. and Verkhovsky, M.I. (2011). The cytochrome *bd* respiratory oxygen reductases. Biochim Biophys Acta 1807, 1398-413.

[49] Santana, M., Ionescu, M.S., Vertes, A., Longin, R., Kunst, F., Danchin, A. and Glaser, P. (1994). *Bacillus subtilis* F_0F_1 ATPase: DNA sequence of the *atp* operon and characterization of *atp* mutants. J Bacteriol 176, 6802-11.

[50] Ferguson, S.J. (2010). ATP synthase: from sequence to ring size to the P/O ratio. Proc Natl Acad Sci U S A 107, 16755-6.

[51] García Montes de Oca, L.Y., Chagolla-López, A., González de la Vara, L., Cabellos-Avelar, T., Gómez-Lojero, C. and Gutiérrez Cirlos, E.B. (2012). The composition of the *Bacillus subtilis* aerobic respiratory chain supercomplexes. J Bioenerg Biomembr 44, 473-86.

Chapter 7

The *bc*:*caa*$_3$ supercomplexes from the Gram positive bacterium *Bacillus subtilis* respiratory chain: a megacomplex organization?

Summary

The respiratory chain of some prokaryotes was shown to be organized in supercomplexes. This association has been proposed to improve enzyme stability and the overall efficiency of the oxidative phosphorylation process. Here, we have revisited recent data on the supercomplexes of *Bacillus subtilis* respiratory chain, by means of 1D and 2D-BN-PAGE, sucrose gradient fractionation of solubilized membranes, and mass spectrometry analysis of BN-PAGE bands detected *in gel* for succinate and cytochrome *c* oxidoreductase activities. The cytochrome bc:caa3 oxygen oxidoreductase supercomplex was observed in different stoichiometries, (*bc*)$_4$:(*caa*$_3$)$_2$, (*bc*)$_2$:(*caa*$_3$)$_4$ and 2[(*bc*)$_2$:(*caa*$_3$)$_4$], suggesting for the first time the string association model of supercomplexes in a Gram positive bacterium. In addition, the presence of a succinate:quinone oxidoreductase:nitrate reductase supercomplex was confirmed by the co-localized succinate:nitroblue tetrazolium and methyl viologen:nitrate oxidoreductase activities detected *in gel* and corroborated by LC-MS/MS analysis.

This chapter was published in

***Arch. Biochem. Biophys.* 537, 2013, p. 153-160**

The *bc*:*caa*$_3$ supercomplexes from the Gram positive bacterium *Bacillus subtilis* respiratory chain: a megacomplex organization?

Pedro M.F. Sousa, Marco A.M. Videira, Filipe A.S. Santos, Brian L. Hood, Thomas P. Conrads and Ana M.P. Melo.

- Pedro M.F. Sousa performed all the experiments reported in this chapter, with the exception of mass spectrometry analysis, in collaboration with Marco A.M. Videira, Filipe A.S. Santos and Ana M.P. Melo.
- Brian L. Hood and Thomas P. Conrads performed the LC-MS/MS analysis.

7.1 Introduction

Bacillus subtilis is a rod-shaped Gram positive bacterium commonly found in soil. Although it has previously been classified as an obligate aerobe, it was demonstrated that *B. subtilis* can also grow in anaerobic conditions by fermentation, or using nitrate as the terminal acceptor of an electron transfer respiratory chain [1].

The aerobic respiratory chain of *B. subtilis*, like that of other Gram positive bacteria, is located in the cytoplasmic membrane, and its most peculiar characteristic relies in the absence of a freely soluble *c*-type cytochrome. In fact, *B. subtilis* contains two distinct *c*-type cytochromes anchored to the cytoplasmic membrane: cytochrome *c*-550 attached to the membrane by an N-terminal transmembrane segment [2], and cytochrome *c*-551 anchored to the membrane by a diacyl glycerol tail [3]. This aerobic respiratory chain essentially contains a type II NADH:quinone oxidoreductase (see [4] for a review), which is membrane associated and has a FAD co-factor [5] and a succinate:quinone oxidoreductase (SQR) [6] of the B type (see [7] for a review), acting as electron entry points for menaquinone reduction. The electron transfer from menaquinol to oxygen may occur via four distinct pathways involving: (i) *bc* menaquinol:cytochrome *c* oxidoreductase (*bc* complex) [8], cytochrome *c*-550 or *c*-551 and *caa*$_3$ cytochrome *c*:oxygen oxidoreductase (*caa*$_3$ oxygen reductase) [9]; (ii) *aa*$_3$ menaquinol:oxygen oxidoreductase (*aa*$_3$ oxygen reductase) [10]; (iii) *bd* menaquinol:oxygen oxidoreductase (*bd* oxygen reductase) [11] or (iv) *bb*' menaquinol:oxygen oxidoreductase (*bb*' oxygen reductase) [12]. It is worth mentioning that *B. subtilis* *bc* complex (Qcr) has an unusual composition. It contains a Rieske-type iron-sulfur protein (QcrA), a cytochrome *b* subunit (QcrB) similar to *b*$_6$*f* complexes and a third subunit, QcrC, similar to *b*$_6$*f* complexes' subunit IV in the N-terminus, and a cytochrome *c* in the C-terminal region [8,13].

The organization of the oxidative phosphorylation complexes in supramolecular structures called supercomplexes has been recently reported in eukaryotes and prokaryotes. These were proposed to play important roles in (i) enhancing electron transfer rates by promoting substrate channeling [14], (ii) the regulation of reactive oxygen species production [15], (iii) the stabilization of individual complexes [16], (iv) influencing inner mitochondrial membrane ultra-structure [17] and (v) enlarging the protein insertion capacity of the inner mitochondrial membrane [18].

In mitochondria, respirasomes, or supercomplexes comprising NADH:ubiquinone oxidoreductase (complex I), ubiquinol:cytochrome *c* oxidoreductase (bc_1 complex or complex III) and cytochrome *c*:oxygen oxidoreductase (complex IV) have been reported in plants, fungi and animals (e.g. [19-21]). Moreover, supercomplexes containing only complexes I+III [19,21] or III+IV [22] were also identified. Dimers of ATP synthase were observed in mitochondria from fungi, plants and mammals [17,19], nevertheless, to date, there is no evidence of a physical association of this enzyme with other mitochondrial oxidative phosphorylation complex.

Aerobic respiratory chain supercomplexes have also been described in the cytoplasmic membrane of bacteria and archaea [23]. In Gram negative bacteria, a homolog of the mitochondrial respirasome was reported in *Paracoccus denitrificans* [24]. Furthermore, in the *Escherichia coli* aerobic respiratory chain NADH oxidoreductase [25], formate:oxygen oxidoreductase [25,26] and succinate:oxygen oxidoreductase [27] supercomplexes were identified. In addition, a sulfide:oxygen oxidoreductase supercomplex was characterized in *Aquifex aeolicus* [28]. Supercomplexes composed of bc_1 and caa_3 or bc_1 and aa_3 complexes were described in the Gram positive bacteria PS3 [29] and *Corynebacterium glutamicum* [30], respectively. It is noteworthy that a supercomplex composed of the bc_1 complex, cytochrome *c* and the aa_3 oxygen oxidoreductase was also found in *P. denitrificans* [31]. In contrast with the mitochondrial enzyme, an interaction between the prokaryotic ATP synthase and caa_3 oxygen reductase was observed in *B. pseudofirmus* [32].

A description of *B. subtilis* respiratory chain supercomplexes was recently reported [33]. In this work, we present new data and revisit the proposed supramolecular organization. Namely, the stoichiometry of supercomplexes composed of the *bc* complex and the *caa*$_3$ oxygen reductase is discussed, and the SQR:nitrate reductase (NAR) supercomplex is further characterized by means of *in gel* activity detection.

7.2 Methods

Cell growth and solubilized membrane preparation

B. subtilis 168 (wild type) and single mutant strains where the genes coding for cytochrome *aa*$_3$ oxygen reductase [9], *bc* complex [13], *caa*$_3$ oxygen oxidoreductase [9] or SQR [34] were disrupted (Table 1) were manually grown in LB medium adjusted to pH 7, at 37ºC, under vigorous agitation. The culture volume corresponded to a fifth of the total flask volume, to ensure the presence of oxygen throughout growth [35]. Cells were harvested when the cultures reached the stationary phase. Cultures were inoculated with 1% of an overnight pre-inoculum.

Table 1
List of *B. subtilis* strains used in this work.

This work	Strain (*B. subtilis*)	Genotype	Source or references
Wild type	168	*trpC2*	BGSC[#]
Δ*bc*	LUH51	*trpC2 ΔqcrB::neo*	[13]
Δ*caa*$_3$	LUH15	*trpC2 ΔctaCD::ble*	[9]
Δ*aa*$_3$	LUH14	*trpC2 ΔqoxABCD::kan*	[9]
Δsqr	LUH16	*trpC2 ΔsdhCAB::ble*	[34]

[#] *Bacillus* Genetic Stock Center, Ohio State University, Columbus.

Cells were suspended in 50 mM MOPS pH 7.0 and disrupted in a French press (6000 psi), centrifuged at 14,000*g*, 15 min, to remove intact cells and cell debris, and the supernatant was ultra-centrifuged (138,000*g*, 2 h). The pellet containing the isolated membrane fraction, here after designated by crude membranes, was aliquoted, frozen in liquid nitrogen and stored at -80 ºC until further use. Alternatively, cells were chemically treated with lysozyme, to obtain wall-free plasma membranes, according to [36] with the following modifications: 10 g of cells were washed in 600 mL 50 mM KH_2PO_4 pH7.5 and traces of PMSF. Membrane protein concentration was determined by the bicinchoninic acid protein assay (BIO-RAD) [37].

Membranes obtained by either method were solubilized by adding digitonin in a ratio of 5 g of detergent per g of protein in a buffer containing 50 mM NaCl, 5 mM aminocaproic acid, 1 mM ethylenediamine tetraacetic acid, 2 mM PMSF and 50 mM imidazole/HCl pH 7. After 15 min on ice and vortexing every 3 min, the suspension was centrifuged (14,000*g*, 30 min). The supernatant constituted the solubilized membranes.

Electrophoretic techniques

Solubilized membranes from *B. subtilis* strains (300 µg per lane) were resolved by BN-PAGE essentially as described in [38-40]. When 2D-BN-PAGE was performed, 1 mg of solubilized membrane protein was loaded in a twice thicker 1D gel. The unstained lane was excised, placed between two glass plates separated by a single spacer and resolving and concentration gels were poured and let polymerize. In frame with the 1D gel lane, one or two wells were inserted to load molecular mass markers.

ATP synthase [41], methyl viologen:nitrate oxidoreductase [42], succinate:NBT oxidoreductase and cytochrome *c* oxidoreductase activities were detected *in gel*

[43]. In addition, hemes of *b* and *c* types were also detected after heme staining [44].

In detail, detection of ATPase activity was performed by immersion of the gel strips in a reaction buffer containing 270 mM glycine, 35 mM Tris/HCl pH 8.4 for 3 hours, at room temperature, followed by the addition of 14 mM $MgSO_4$, 0.2% $Pb(NO_3)_2$ and 8mM ATP. White colored bands formed on a dark background, upon overnight incubation.

Nitrate reductase activity was performed under anaerobic conditions at room temperature. The gel strips were incubated in a solution containing 50 mM sodium phosphate pH 8.0 and 2 mM methyl viologen, previously degassed and deaerated with argon for 15 minutes. At this point, the strips were transferred to the anaerobic chamber and the viologen dye in the solution was reduced with sodium dithionite. White bands were detected 30 min after the addition of 40 mM KNO_3.

Cytochrome *caa*$_3$ oxygen reductase was visualized by the detection of cytochrome *c* oxidoreductase activity, at 37°C, following the incubation of gel strips in a 50 mM sodium phosphate pH 7.4 buffer containing 2.5 mM 3,3'-diaminobenzidine, 1 mg/mL cytochrome *c* from equine heart, 220 mM sucrose and 2 µg/mL catalase, for 6 h.

Sucrose gradient analysis

Solubilized membranes (12.5 mg) were applied on top of continuous sucrose gradients (0.73-1.5 M) in a buffer containing 15 mM Tris/HCl pH 7, 20 mM KCl and 0.2 % digitonin and resolved by ultra-centrifugation at 4 ºC (20 h, 150,000*g*) [25]; 1 mL fractions were collected, frozen in liquid nitrogen and stored at -80ºC.

Spectroscopic techniques

UV-visible absorption spectra of TX-100-solubilized wild type membranes (0.025% v/v) were recorded with the as-isolated membranes (oxidized state) and

with membranes to which trace amounts of sodium dithionite powder was added (reduced state). Dithionite-reduced samples were incubated with CO gas for 2-3 min to obtain the *CO-reduced* spectrum [25].

Catalytic activities

Oxygen consumption rates by *B. subtilis* crude and plasma membranes, by sucrose gradient fractions and by cytochrome caa_3 oxygen oxidoreductase active bands were measured polarographicaly essentially according to [27]. NADH: and succinate:oxygen oxidoreductase activities were measured in a buffer containing 50 mM MOPS pH 7.2 and 250 µM NADH or 20 mM succinate, respectively. Ubiquinol:oxygen oxidoreductase activity was monitored in a reaction mixture containing 100 mM MOPS pH 7.2, 50 mM KCl, 0.5 mM EDTA, 5.7 mM dithiothreitol, and 80 µM coenzyme Q1. Oxygen consumption in the presence of 2/10mM TMPD/ascorbate was followed in 20 mM Tris/HCl pH 7.5. Specific inhibitors of the respiratory chain complexes such as malonate (15 mM), antimycin A (0.4 µM) and KCN (0.5 mM or 2.5 mM) were used when appropriate. All reactions were initiated by the addition of protein sample. Oxygen consumption by gel slices presumably containing cytochrome caa_3 oxygen reductase was analyzed according to [25].

Liquid chromatography-tandem mass spectrometry

Bands or spots detected by succinate:NBT oxidoreductase or cytochrome *c* oxidoreductase activities in the 2D-BN-PAGE were excised for digestion and liquid chromatography-tandem mass spectrometry analysis. Tryptic peptides were resuspended in 25 mM ammonium bicarbonate pH 7.6 and analyzed by nanoflow liquid chromatography (Easy-nLC, ThermoFisher Scientific, San Jose, CA, USA) coupled online with an LTQ-Orbitrap XL MS (ThermoFisher Scientific). All the samples were resolved on a 100 µm I.D. × 360 µm O.D. × 20 cm long capillary

column (Polymicro Technologies, Phoenix, AZ, USA), which was slurry packed in house with 5 µm, 30 nm pore size C-18 silica-bonded stationary phase (Jupiter, Phenomenex, Torrance, CA, USA). Following pre-column and analytical column equilibration, each sample was loaded onto a 2 cm reversed-phase (C-18) precolumn (ThermoFisher Scientific) at 3 µL/min for 10 min with mobile phase A (0.1% (v/v) formic acid in water). Peptides were eluted at a constant flow rate of 200 nL/min using a linear gradient of mobile phase B (0.1% formic acid in acetonitrile) up to 40% over 15 min and then to 95% B for an additional 10 min. The column was washed for 10 min at 95% B and quickly brought to 100% A for the next sample injection. The LTQ-Orbitrap XL MS was configured to collect high resolution (R=60,000 at m/z 400) broadband mass spectra (m/z 375-1800) using the lock mass feature for the polydimethylcyclosiloxane (PCM) ion generated in the electrospray process (m/z 445.12002).

Protein identification

Tandem mass spectra were searched against UniProt *B. subtilis* protein databases (08/2012) from the Universal Protein Resource (UniProt) (http://www.uniprot.org) using Mascot Daemon (Matrix Science Inc., Boston, MA, USA). The data were searched with a precursor mass tolerance of 10 ppm and a fragment ion tolerance of 0.6 Da. Methionine oxidation (+15.99492 Da) was set as a dynamic modification and a maximum of two missed cleavages were allowed. An automatic decoy search was performed on all raw files and peptides were filtered using an ion score cutoff of 20 resulting in a false peptide discovery rate of <1%.

7.3 Results and discussion

Respiratory chain activities of the *B. subtilis* membranes

The respiratory chain activities of membranes from *B. subtilis* 168 strain (wild type) grown in LB in Erlenmeyer flasks were thoroughly characterized, prior to the investigation of supramolecular assembly of the respiratory chain complexes.

UV-visible absorption spectra of the *B. subtilis* solubilized membranes were recorded in the oxidized and dithionite-reduced states. The redox difference spectrum (the subtraction of the spectra of the oxidized samples from those of the reduced samples) indicated the presence of *a*, *b*, *c* and *d*-type cytochromes as judged by the maxima at 441 and 600 nm (heme *a*), 430 and 560 nm (heme *b*), 550 nm (heme *c*), and finally at 631 nm (hemes *d*) (Fig. 1A). The spectrum of the dithionite-reduced membranes incubated with CO minus the spectrum of the dithionite-reduced membranes was also calculated (Fig. 1B).

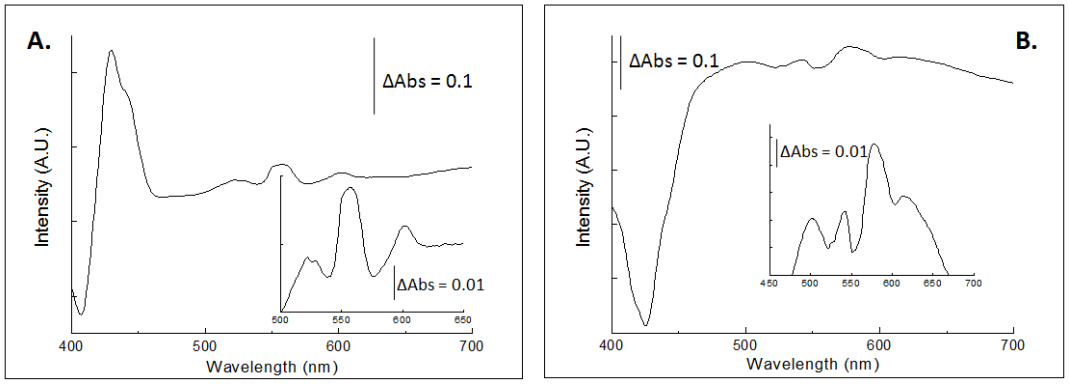

Fig. 1. Room temperature UV-Visible absorption spectra of *B. subtilis* membranes solubilized with TX-100. Spectral acquisition was performed to the as-isolated membranes (oxidized state) and after the addition of sodium dithionite (reduced state). The dithionite-reduced samples were incubated with CO to obtain the CO spectrum. (A) Difference spectra of dithionite-reduced minus oxidized membranes and (B) *CO-reduced* minus dithionite-reduced spectra.

A trough was observed at 602 nm and a shoulder at 544 nm, corroborating previous indications of the presence of *a*-type hemes [45]. The observed peaks were compatible with the presence of the *bc* complex (Qcr) [8], the *caa*$_3$ oxygen reductase and the *aa*$_3$ [45], *bd* [11] and *bb*' [12] menaquinol:oxygen oxidoreductases, as well as of the SQR [46], which in *B. subtilis* contains two *b*-type hemes in a single transmembrane subunit.

Respiratory chain activities were monitored polarographicaly (NADH:, succinate:, reduced coenzyme Q_1 (ubiquinol): and TMPD/ascorbate:oxygen oxidoreductase) by means of an oxygen electrode, confirming the presence of the *B. subtilis* NADH:quinone oxidoreductase, succinate:quinone oxidoreductase, *bc* complex and *caa*$_3$ oxygen reductase (Table 2). While NADH: and ubiquinol:oxygen oxidoreductase activities were almost fully inhibited by KCN, the inhibition of succinate oxidation by this compound was only about 50%, suggesting that the oxidation of this substrate occurs via non-heme copper oxygen reductase like cytochrome *bb*' and *bd*. This is in coherence with the UV-visible absorption spectra, corroborating that besides cytochromes *aa*$_3$ and *caa*$_3$, the oxygen reductases *bd* and *bb*' may also be operating. In addition, TMPD/ascorbate:oxygen oxidoreductase activity was fully inhibited by KCN.

Table 2
Respiratory chain activities of *B. subtilis* wild type membranes. The rates shown are the average of three independent growth and membrane preparation experiments, and the corresponding standard error is presented. For each oxygen consumption experiment, three replicates were acquired.

		Inhibition* (%)	
substrate:oxygen oxidoreductase activity	rate (nmol.min^{-1}.mg^{-1})	antimycin A	KCN
NADH	24.6 ± 2.0	8	88
Succinate	17.9 ± 0.3	21	47
Ubiquinol	13.8 ± 2.3	32	89
TMPD/ascorbate	2426.1 ± 71.4	n.a.	100

*the activities were measured after a 10-min pre-incubation with the adequate inhibitor.

Supramolecular organizations of *B. subtilis* respiratory chain

To pursue the investigation of inter-complex interactions among the complexes of *B. subtilis* respiratory chain and its eventual organization in supercomplexes, a mild detergent like digitonin is often used, which allows an efficient extraction of the enzymes preserving protein-protein interactions and enzyme activity [22]. In the work presented herein, *B. subtilis* membranes were solubilized with digitonin and the solubilized material retained ubiquinol: and TMPD/ascorbate:oxygen oxidoreductase activity (data not shown).

Solubilized plasma membranes from *B. subtilis* wild type were resolved by BN-PAGE and analyzed for ATP hydrolysis, one of the activities carried out by ATP synthase, and succinate, nitrate and cytochrome *c* oxidoreductase (OR) activities, revealing three (A1-3), two (S1-2), two (N1-2) and four (C1-4) bands, respectively (Fig. 2A). In addition, heme-staining (HS) was performed allowing the detection of five bands (H1-5) (Fig. 2A).

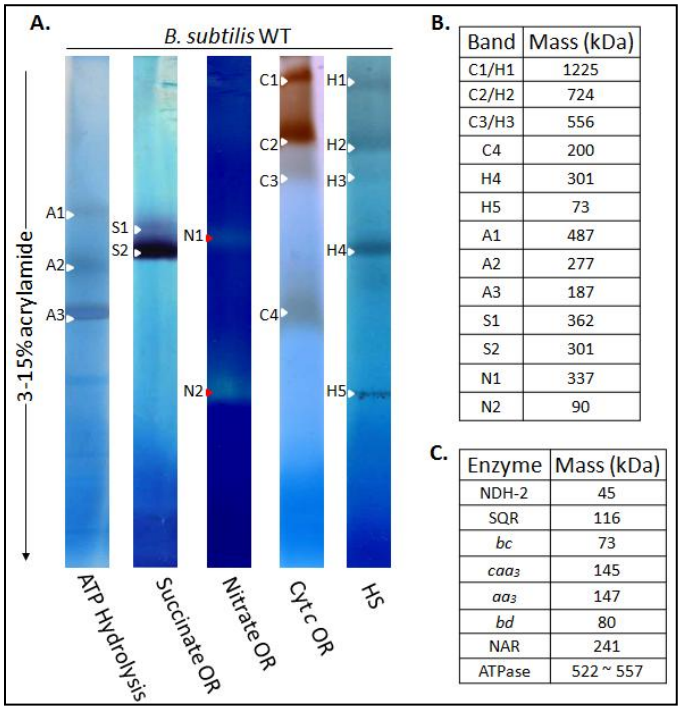

B.

Band	Mass (kDa)
C1/H1	1225
C2/H2	724
C3/H3	556
C4	200
H4	301
H5	73
A1	487
A2	277
A3	187
S1	362
S2	301
N1	337
N2	90

C.

Enzyme	Mass (kDa)
NDH-2	45
SQR	116
bc	73
caa_3	145
aa_3	147
bd	80
NAR	241
ATPase	522 ~ 557

Fig. 2. *In* gel activity detection of wild type *B. subtilis* respiratory chain complexes. Digitonin solubilized membranes from wild type *B. subtilis* were resolved by BN-PAGE in a linear 3%-15% acrylamide gradient. Detection of ATP synthase (A1-A3), succinate:NBT (S1-S2), methyl viologen:nitrate (N1-N2) and cytochrome *c* (bands C1-C4) oxidoreductase activities and heme staining (H1-H5) (A). Deduced apparent molecular masses of the identified bands in reference to bovine heart mitochondria respiratory chain complexes [54] (B). Calculated molecular masses of *B. subtilis* respiratory chain complexes (C).

The apparent molecular masses of the above mentioned bands was estimated (Fig. 2B) and compared with the molecular masses of the individual respiratory chain complexes as deduced from their amino acid sequences (Fig. 2C). Bands detected with ATP hydrolysis assay were assigned to the intact F_1F_0 enzyme (A1) and smaller subcomplexes of this complex (A2-3). In fact, considering their estimated molecular masses, A2 and A3 were tentatively attributed to F1 and a F1 subcomplex, respectively. Band S2, the lowest molecular mass band produced upon succinate:NBT oxidoreductase activity, likely corresponds to the dimer of SQR, based on its significant amino acid sequence similarity with the *Wolinella succinogenes* quinol:fumarate reductase [47], which crystallizes as a dimer [48]. Noteworthy, the *B. subtilis* SQR is a bifunctional enzyme also active as QFR [49]. Moreover, band S2 was sequenced by MALDI-TOF/TOF, SdhA and SdhB being the only significant hits retrieved (data not shown).

Bands S1, N1, C1-C3 and H1-H3, were identified by succinate:NBT, methyl viologen:nitrate and cytochrome *c* oxidoreductase activities, and also by heme-staining, respectively. These bands presented a molecular mass larger than the individual respiratory complexes, and are thus likely to correspond to supercomplexes.

Bands N1 and S1, with similar molecular masses, may correspond to the supercomplex $(SQR)_2$:NAR previously proposed [33]. The previous evidences were based on MS results, the work presented herein being the first where the nitrate reductase activity of $(SQR)_2$:NAR was observed. In addition, band N1 was not produced in the membranes of a *B. subtilis* strain where SQR was disrupted (Fig. 3), confirming that the observed nitrate reductase activity resulted from a supercomplex involving NAR and SQR. *B. subtilis* growth is known to be highly adaptable to the oxygen availability in the environment, and the high positive midpoint redox potential of nitrate (E^0= +430 mV) makes it the preferential terminal electron acceptor under low oxygen concentration conditions [1], which may be relevant considering that the growth medium used in this work, LB, contains relatively high amounts of nitrate [50]. $(SQR)_2$:NAR supercomplex may, thus, have

an important role in maintaining a viable respiratory chain when oxygen concentration fluctuations occur in the environment.

B. subtilis strains devoid of *bc* or caa_3 complexes did not produce bands C1, C2 or C3 after *in gel* detection of cytochrome *c* reductase activity, suggesting that both complexes are present in these bands (Fig. 3). In addition, band C4 was observed in every mutant strains investigated, with the exception of Δcaa_3, indicating the presence of cytochrome caa_3 oxygen reductase in this band, probably in the dimeric form, given its estimated molecular mass (Fig. 2C and Fig. 3). Bands H1-3 detected with heme staining had molecular masses identical to bands C1-3, in agreement with the fact that the latter are composed of heme-containing proteins.

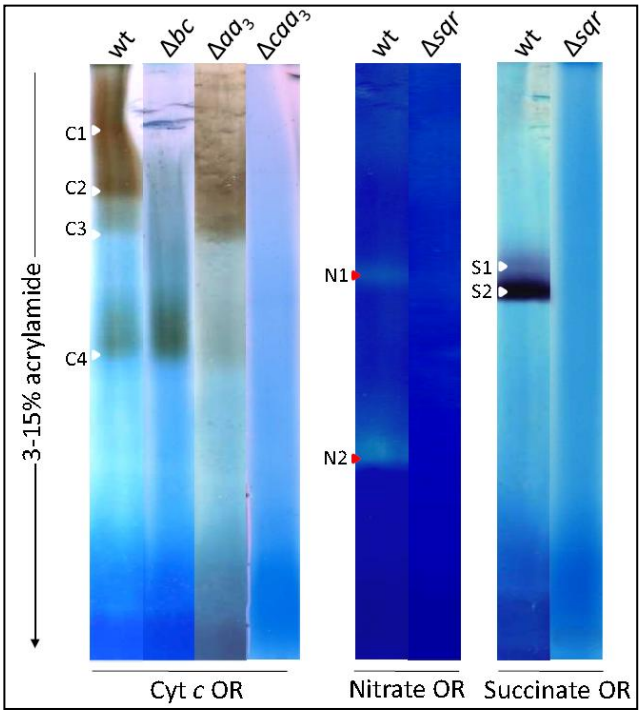

Fig. 3. *In gel* activity detection of BN-PAGE resolved *B. subtilis* membranes from wild type and respiratory chain mutant strains. Cytochrome *c* (C1-4), methyl viologen:nitrate (N1-2) and succinate:NBT (S1-2) oxidoreductase activities. Bands C1-3 were absent from the membranes of *Δbc* and Δcaa_3, however, membranes of the strain devoid of aa_3 oxygen reductase produced bands C2 and C3. The dimeric form of caa_3 oxygen reductase (C4) was identified in all strains except in Δcaa_3. Bands N1-2 and S1-2 were absent in the membranes of *Δsqr*.

Solubilized membranes of *B. subtilis* were also resolved in a sucrose gradient (0.73-1.5M) by ultracentrifugation. Fractions F1-F9, from highest to lowest molecular mass, were collected, resolved by BN-PAGE and analyzed for succinate:NBT and cytochrome *c* oxidoreductase activities (Fig. 4A) or studied with respect to oxygen consumption due to TMPD/ascorbate oxidation (Fig. 4B). The highest TMPD/ascorbate:oxygen oxidoreductase activity was observed in fractions 4-8 (Fig. 4A), in agreement with the intensity of bands C1-3 (Fig. 4B). Band S2, attributed to the SQR dimer, was detected in fractions 4-8. The smear observed above band S2 in fractions 4-7 may be due to the presence of S1 (Fig. 2A). Maximal activity of succinate:DCPIP oxidoreductase was retrieved from fraction 6.

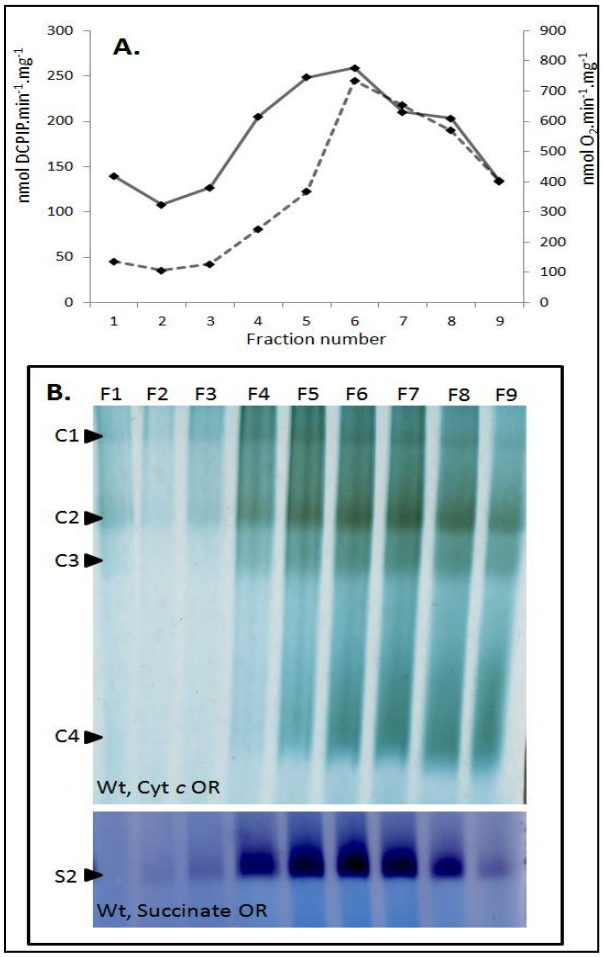

Fig. 4. Sucrose gradient analysis of wild type *B. subtilis* digitonin solubilized membranes. TMPD/ascorbate:oxygen (solid line) and succinate:DCPIP oxidoreductase activities (dashed line) (A). *In gel* activity detection of cytochrome *c* (C1-4) and succinate:NBT oxidoreductase activities (S2) (B).

Identification of *B. subtilis* supercomplexes composition

A 2D-BN-PAGE of wild type *B. subtilis* membranes was performed to observe supercomplex dissociation into the monomeric or oligo-homomeric forms of the respiratory complexes. Detection of cytochrome *c* oxidoreductase activity showed that bands C1-4 resolved into several spots with masses similar or smaller than those estimated to the bands detected with the same activity in the 1D-BN-PAGE (Fig. 5A).

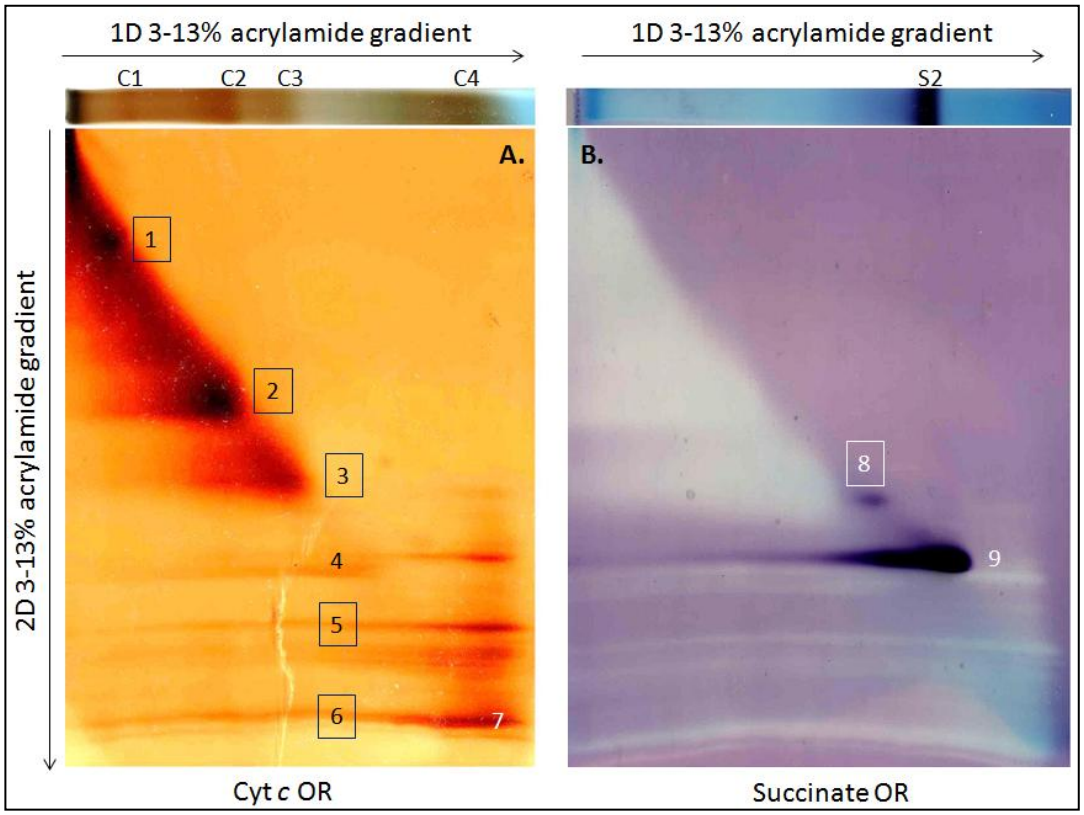

Fig. 5. 2D BN-PAGE of wild type *B. subtilis* membranes previously resolved by 1D BN-PAGE. Cytochrome *c* oxidoreductase *in gel* detection (A) and succinate:NBT oxidoreductase activity (B). Spots 1-3, 5, 6 and 8 were analyzed by LC/MS-MS.

Selected spots detected with this activity in the 2D-BN-PAGE (1-3, 5, 6) were sequenced by LC-MS/MS to elucidate the supercomplexes composition (Table 3).

Spots picked from bands C1-C3 contained peptides of *bc* and *caa*$_3$ complexes, corroborating previous indications of a *bc*:*caa*$_3$ supercomplex in the respiratory chains of *Bacillus* strains [29,33]. Furthermore, spots from bands C2 and C3 also contained cytochrome *aa*$_3$ oxygen reductase peptides (Table 3). Nevertheless, and considering that bands C2 and C3 were detected in *B. subtilis* membranes devoid of *aa*$_3$ oxygen reductase (Fig. 3), this terminal oxygen reductase is not part of the *bc*:*caa*$_3$ supercomplexes.

Table 3
LC-MS/MS analysis of 2D BN-PAGE spots derived from BN-PAGE bands C1-C3, identified in wild type *B. subtilis* membranes.

Band	Enzyme	Subunit	Gene	UniProt Accession	Peptides Identified
C1	Menaquinol:cytochrome *c* oxidoreductase (*b*$_6$*c*$_1$ complex)	A	qcrA	E8VAQ3	22
		B	qcrB	E8VAQ2	17
		C	qcrC	E8VAQ1	14
	caa$_3$ cytochrome *c*:oxygen oxidoreductase (*caa*$_3$ oxygen reductase)	C	ctaC	E8VKN3	28
		E	ctaE	E8VKN5	12
C2	Menaquinol:cytochrome *c* oxidoreductase (*b*$_6$*c*$_1$ complex)	C	qcrC	E8VAQ1	25
		B	qcrB	E8VAQ2	24
		A	qcrA	E8VAQ3	8
	caa$_3$ cytochrome *c*:oxygen oxidoreductase (*caa*$_3$ oxygen reductase)	C	ctaC	E8VKN3	31
		E	ctaE	E8VKN5	12
	aa$_3$ menaquinol:oxygen oxidoreductase (*aa*$_3$ oxygen reductase)	B	qoxB	E8VEN3	41
		A	qoxA	E8VEN2	17
C3	Menaquinol:cytochrome *c* oxidoreductase (*b*$_6$*c*$_1$ complex)	A	qcrA	E8VAQ3	58
		C	qcrC	E8VAQ1	31
		B	qcrB	E8VAQ2	30
	caa$_3$ cytochrome *c*:oxygen oxidoreductase (*caa*$_3$ oxygen reductase)	C	ctaC	E8VKN3	38
		E	ctaE	E8VKN5	12
	aa$_3$ menaquinol:oxygen oxidoreductase (*aa*$_3$ oxygen reductase)	B	qoxB	E8VEN3	23
		A	qoxA	E8VEN2	20

Succinate:NBT oxidoreductase activity was also detected in *B. subtilis* membranes resolved by 2D-BN-PAGE, revealing two different spots 8 and 9 (Fig. 5B). Spot 9, of lower molecular mass, was attributed to the dimer of SQR as previously mentioned. Spot 8, expected to correspond to the part of band S1 that retained the $(SQR)_2$:NAR supercomplex assembly, in spite of DDM exposure, upon LC-MS/MS sequencing, was confirmed to contain SQR and NAR peptides (Table 3), corroborating results from the 1D-BN-PAGE of wild type and *Δsqr* strains (Fig. 2A and 3) and in coherence with the previous findings by Oca et al. [33].

Stoichiometry analysis of *bc*:*caa*$_3$ supercomplexes

Bands C1-3 were shown to be composed of the same proteins, *bc* and *caa*$_3$ complexes (Table 3) suggesting a different stoichiometry of the *bc*:*caa*$_3$ supercomplex in each band. The estimated molecular masses of C1-3 and the deduced molecular masses of b_6c_1 and *caa*$_3$ complexes were compared allowing the attribution of $[(bc)_2:(caa_3)_4]_2$, $(bc)_2:(caa_3)_4$ and $(bc)_4:(caa_3)_2$ stoichiometries to bands C1, C2 and C3, respectively (Fig. 2). This intricate organization suggests that *B. subtilis* aerobic respiratory chain is organized in a string-like megacomplex, as proposed in plant and mammalian mitochondria [19,51] and never previously suggested in prokaryotes.

TMPD/ascorbate oxygen oxidoreductase activity was determined in bands C1-4. The highest rate of oxygen consumption was verified in band C1 or $[(bc)_2:(caa_3)_4]_2$ supercomplex, decreasing in the lighter forms of the supercomplex and in the dimer (Fig. 6). KCN inhibition varied likewise. These results suggest that most of the cytochrome *caa*$_3$ oxygen reductase present in the cell is assembled in the megacomplex.

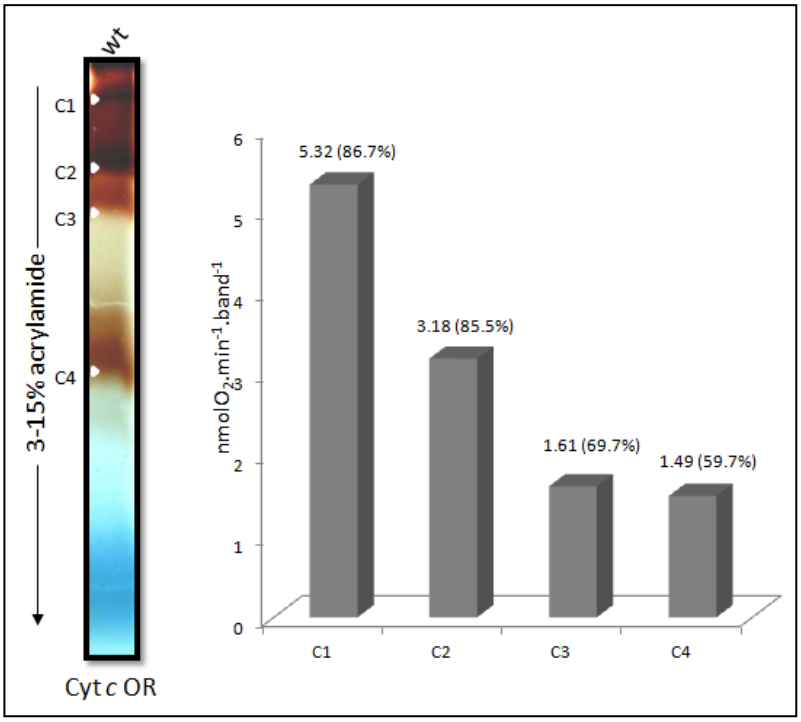

Fig. 6. Detection of TMPD/ascorbate:oxygen oxidoreductase activity on BN-PAGE bands C1-C4. The resulting activity values were plotted after subtraction of the rates due to oxygen consumption before substrate addition. Between brackets is represented the inhibition by the addition of 0.5 mM KCN.

7.4 Conclusion

The data presented herein provided evidences for a new oligomerization of the *bc*:*caa*$_3$ supercomplex as inferred from the *in gel* activity detection in wild type and strains devoid of *bc* complex and *caa*$_3$ oxygen reductase (Fig. 3), and corroborated by mass spectrometry analysis (Fig. 5A, Table 3). This was the first evidence for the presence of a respiratory chain string in prokaryotes, by the identification of different stoichiometries of the *bc*:*caa*$_3$ supercomplex in *B. subtilis*. Such megacomplex organization of the respiratory chain may contribute for a higher efficiency of electron transfer, bypassing the requirement of cytochromes *c*-

550 and *c*-551, by the additional *c*-type cytochrome present in the *bc* and the caa_3 complexes. It is noteworthy that *c*-type cytochrome in caa_3 oxygen reductase was proposed to be the only one required for electron transfer in this terminal oxygen reductase [52]. In agreement, the addition of cytochrome *c*-551 was shown not to enhance the quinol oxidase activity of similar supercomplexes in PS3 [53].

7.5 Acknowledgements

We are greatly indebted to Dr Miguel Teixeira for continuous support. The authors would like to thank Dr Lars Hederstedt for the generous gift of the *B. subtilis* mutant strains. Tiago David, Elisabete Lopes and Isabel Palos are acknowledged for excellent technical assistance. PS is recipient of the FCT Grant SFRH/BD/46553/2008.

7.6 References

[1] Nakano, M.M. and Zuber, P. (1998). Anaerobic growth of a "strict aerobe" (*Bacillus subtilis*). Annu Rev Microbiol 52, 165-90.

[2] von Wachenfeldt, C. and Hederstedt, L. (1990). *Bacillus subtilis* 13-kilodalton cytochrome c_{-550} encoded by *cccA* consists of a membrane-anchor and a heme domain. J Biol Chem 265, 13939-48.

[3] Bengtsson, J., Rivolta, C., Hederstedt, L. and Karamata, D. (1999). *Bacillus subtilis* contains two small *c*-type cytochromes with homologous heme domains but different types of membrane anchors. J Biol Chem 274, 26179-84.

[4] Melo, A.M.P., Bandeiras, T.M. and Teixeira, M. (2004). New insights into type II NAD(P)H:quinone oxidoreductases. Microbiol Mol Biol Rev 68, 603-16.

[5] Bergsma, J., Van Dongen, M.B. and Konings, W.N. (1982). Purification and characterization of NADH dehydrogenase from *Bacillus subtilis*. Eur J Biochem 128, 151-7.

[6] Lemma, E., Hägerhäll, C., Geisler, V., Brandt, U., von Jagow, G. and Kröger, A. (1991). Reactivity of the *Bacillus subtilis* succinate dehydrogenase complex with quinones. Biochim Biophys Acta 1059, 281-5.

[7] Pereira, M.M., Bandeiras, T.M., Fernandes, A.S., Lemos, R.S., Melo, A.M.P. and Teixeira, M. (2004). Respiratory chains from aerobic thermophilic prokaryotes. J Bioenerg Biomembr 36, 93-105.

[8] Yu, J., Hederstedt, L. and Piggot, P.J. (1995). The cytochrome *bc* complex (menaquinone:cytochrome *c* reductase) in *Bacillus subtilis* has a nontraditional subunit organization. J Bacteriol 177, 6751-60.

[9] Bengtsson, J., Tjalsma, H., Rivolta, C. and Hederstedt, L. (1999). Subunit II of *Bacillus subtilis* cytochrome *c* oxidase is a lipoprotein. J Bacteriol 181, 685-8.

[10] De Vrij, W., Azzi, A. and Konings, W.N. (1983). Structural and functional properties of cytochrome *c* oxidase from *Bacillus subtilis* W23. Eur J Biochem 131, 97-103.

[11] Winstedt, L., Yoshida, K., Fujita, Y. and von Wachenfeldt, C. (1998). Cytochrome *bd* biosynthesis in *Bacillus subtilis*: characterization of the *cydABCD* operon. J Bacteriol 180, 6571-80.

[12] Azarkina, N., Siletsky, S., Borisov, V., von Wachenfeldt, C., Hederstedt, L. and Konstantinov, A.A. (1999). A cytochrome *bb*'-type quinol oxidase in *Bacillus subtilis* strain 168. J Biol Chem 274, 32810-7.

[13] Yu, J. and Le Brun, N.E. (1998). Studies of the cytochrome subunits of menaquinone:cytochrome *c* reductase (*bc* complex) of *Bacillus subtilis*. Evidence for the covalent attachment of heme to the cytochrome *b* subunit. J Biol Chem 273, 8860-6.

[14] Lenaz, G. and Genova, M.L. (2010). Structure and organization of mitochondrial respiratory complexes: a new understanding of an old subject. Antioxid Redox Signal 12, 961-1008.

[15] Diaz, F., Enríquez, J.A. and Moraes, C.T. (2012). Cells lacking Rieske iron-sulfur protein have a reactive oxygen species-associated decrease in respiratory complexes I and IV. Mol Cell Biol 32, 415-29.

[16] Acín-Pérez, R., Bayona-Bafaluy, M.P., Fernández-Silva, P., Moreno-Loshuertos, R., Pérez-Martos, A., Bruno, C., Moraes, C.T. and Enríquez, J.A. (2004). Respiratory complex III is required to maintain complex I in mammalian mitochondria. Mol Cell 13, 805-15.

[17] Davies, K.M., Strauss, M., Daum, B., Kief, J.H., Osiewacz, H.D., Rycovska, A., Zickermann, V. and Kühlbrandt, W. (2011). Macromolecular organization of ATP synthase and complex I in whole mitochondria. Proc Natl Acad Sci U S A 108, 14121-6.

[18] Boekema, E.J. and Braun, H.P. (2007). Supramolecular structure of the mitochondrial oxidative phosphorylation system. J Biol Chem 282, 1-4.

[19] Bultema, J.B., Braun, H.P., Boekema, E.J. and Kouril, R. (2009). Megacomplex organization of the oxidative phosphorylation system by structural analysis of respiratory supercomplexes from potato. Biochim Biophys Acta 1787, 60-7.

[20] Nübel, E., Wittig, I., Kerscher, S., Brandt, U. and Schägger, H. (2009). Two-dimensional native electrophoretic analysis of respiratory supercomplexes from *Yarrowia lipolytica*. Proteomics 9, 2408-18.

[21] Schäfer, E., Dencher, N.A., Vonck, J. and Parcej, D.N. (2007). Three-dimensional structure of the respiratory chain supercomplex $I_1III_2IV_1$ from bovine heart mitochondria. Biochemistry 46, 12579-85.

[22] Schägger, H. and Pfeiffer, K. (2000). Supercomplexes in the respiratory chains of yeast and mammalian mitochondria. EMBO J 19, 1777-83.

[23] Magalon, A., Arias-Cartin, R. and Walburger, A. (2012). Supramolecular organization in prokaryotic respiratory systems. Adv Microb Physiol 61, 217-66.

[24] Stroh, A., Anderka, O., Pfeiffer, K., Yagi, T., Finel, M., Ludwig, B. and Schägger, H. (2004). Assembly of respiratory complexes I, III, and IV into NADH oxidase supercomplex stabilizes complex I in *Paracoccus denitrificans*. J Biol Chem 279, 5000-7.

[25] Sousa, P.M.F. et al. (2011). Supramolecular organizations in the aerobic respiratory chain of *Escherichia coli*. Biochimie 93, 418-425.

[26] Sousa, P.M.F., Videira, M.A.M. and Melo, A.M.P. (2013). The formate:oxygen oxidoreductase supercomplex of *Escherichia coli* aerobic respiratory chain. FEBS letters 587, 2559-64.

[27] Sousa, P.M.F., Videira, M.A., Bohn, A., Hood, B.L., Conrads, T.P., Goulao, L.F. and Melo, A.M.P. (2012). The aerobic respiratory chain of *Escherichia coli*: from genes to supercomplexes. Microbiology 158, 2408-18.

[28] Prunetti, L., Infossi, P., Brugna, M., Ebel, C., Giudici-Orticoni, M.T. and Guiral, M. (2010). New functional sulfide oxidase-oxygen reductase supercomplex in the membrane of the hyperthermophilic bacterium *Aquifex aeolicus*. J Biol Chem 285, 41815-26.

[29] Sone, N., Sekimachi, M. and Kutoh, E. (1987). Identification and properties of a quinol oxidase super-complex composed of a bc_1 complex and cytochrome oxidase in the thermophilic bacterium PS3. J Biol Chem 262, 15386-91.

[30] Niebisch, A. and Bott, M. (2003). Purification of a cytochrome *bc*-aa_3 supercomplex with quinol oxidase activity from *Corynebacterium glutamicum*. Identification of a fourth subunity of cytochrome aa_3 oxidase and mutational analysis of diheme cytochrome c_1. J Biol Chem 278, 4339-46.

[31] Berry, E.A. and Trumpower, B.L. (1985). Isolation of ubiquinol oxidase from *Paracoccus denitrificans* and resolution into cytochrome bc_1 and cytochrome *c*-aa_3 complexes. J Biol Chem 260, 2458-67.

[32] Liu, X., Gong, X., Hicks, D.B., Krulwich, T.A., Yu, L. and Yu, C.A. (2007). Interaction between cytochrome caa_3 and F_1F_0-ATP synthase of alkaliphilic *Bacillus pseudofirmus* OF4 is demonstrated by saturation transfer electron paramagnetic resonance and differential scanning calorimetry assays. Biochemistry 46, 306-13.

[33] García Montes de Oca, L.Y., Chagolla-López, A., González de la Vara, L., Cabellos-Avelar, T., Gómez-Lojero, C. and Gutiérrez Cirlos, E.B. (2012). The composition of the *Bacillus subtilis* aerobic respiratory chain supercomplexes. J Bioenerg Biomembr 44, 473-86.

[34] Matsson, M., Tolstoy, D., Aasa, R. and Hederstedt, L. (2000). The distal heme center in *Bacillus subtilis* succinate:quinone reductase is crucial for electron transfer to menaquinone. Biochemistry 39, 8617-24.

[35] Van Sujidam, J., Kossen, N. and Joha, A. (1978). Model for oxygen transfer in a shake flask. Biotechnol Bioeng 20, 1695-1709.

[36] Henning, W., Vo, L., Albanese, J. and Hill, B.C. (1995). High-yield purification of cytochrome aa_3 and cytochrome caa_3 oxidases from *Bacillus subtilis* plasma membranes. Biochem J 309 (Pt 1), 279-83.

[37] Smith, P.K. et al. (1985). Measurement of protein using bicinchoninic acid. Anal Biochem 150, 76-85.

[38] Schägger, H. and von Jagow, G. (1991). Blue native electrophoresis for isolation of membrane protein complexes in enzymatically active form. Anal Biochem 199, 223-31.

[39] Wittig, I., Braun, H.P. and Schägger, H. (2006). Blue native PAGE. Nat Protoc 1, 418-28.

[40] Krause, F. and Seelert, H. (2008). Detection and analysis of protein-protein interactions of organellar and prokaryotic proteomes by blue native and colorless native gel electrophoresis. Curr Protoc Protein Sci Chapter 19, Unit 19.18.

[41] Wittig, I., Karas, M. and Schägger, H. (2007). High resolution clear native electrophoresis for in-gel functional assays and fluorescence studies of membrane protein complexes. Mol Cell Proteomics 6, 1215-25.

[42] Sabaty, M., Avazeri, C., Pignol, D. and Vermeglio, A. (2001). Characterization of the reduction of selenate and tellurite by nitrate reductases. Appl Environ Microbiol 67, 5122-6.

[43] Zerbetto, E., Vergani, L. and Dabbeni-Sala, F. (1997). Quantification of muscle mitochondrial oxidative phosphorylation enzymes via histochemical staining of blue native polyacrylamide gels. Electrophoresis 18, 2059-64.

[44] Thomas, P.E., Ryan, D. and Levin, W. (1976). An improved staining procedure for the detection of the peroxidase activity of cytochrome P-450 on sodium dodecyl sulfate polyacrylamide gels. Anal Biochem 75, 168-76.

[45] Lauraeus, M., Haltia, T., Saraste, M. and Wikström, M. (1991). *Bacillus subtilis* expresses two kinds of haem-*A*-containing terminal oxidases. Eur J Biochem 197, 699-705.

[46] Hederstedt, L., Holmgren, E. and Rutberg, L. (1979). Characterization of a succinate dehydrogenase complex solubilized from the cytoplasmic membrane of *Bacillus subtilis* with the nonionic detergent Triton X-100. J Bacteriol 138, 370-6.

[47] Lancaster, C.R. and Kröger, A. (2000). Succinate: quinone oxidoreductases: new insights from X-ray crystal structures. Biochim Biophys Acta 1459, 422-31.

[48] Hederstedt, L. (2002). Succinate:quinone oxidoreductase in the bacteria *Paracoccus denitrificans* and *Bacillus subtilis*. Biochim Biophys Acta 1553, 74-83.

[49] Schnorpfeil, M., Janausch, I.G., Biel, S., Kröger, A. and Unden, G. (2001). Generation of a proton potential by succinate dehydrogenase of *Bacillus subtilis* functioning as a fumarate reductase. Eur J Biochem 268, 3069-74.

[50] Xu, J., Xu, X. and Verstraete, W. (2000). Adaptation of *E. coli* cell method for micro-scale nitrate measurement with the Griess reaction in culture media. J Microbiol Methods 41, 23-33.

[51] Wittig, I., Carrozzo, R., Santorelli, F.M. and Schägger, H. (2006). Supercomplexes and subcomplexes of mitochondrial oxidative phosphorylation. Biochim Biophys Acta 1757, 1066-72.

[52] Andrews, D., Mattatall, N.R., Arnold, D. and Hill, B.C. (2005). Expression, purification, and characterization of the CuA-cytochrome *c* domain from subunit II of the *Bacillus subtilis* cytochrome *caa*$_3$ complex in *Escherichia coli*. Protein Expr Purif 42, 227-35.

[53] Sone, N., Kutoh, E. and Yanagita, Y. (1989). Cytochrome *c*-$_{551}$ from the thermophilic bacterium PS3 grown under air-limited conditions. Biochim Biophys Acta 977, 329-34.

[54] Wittig, I., Beckhaus, T., Wumaier, Z., Karas, M. and Schägger, H. (2010). Mass estimation of native proteins by blue native electrophoresis: principles and practical hints. Mol Cell Proteomics 9, 2149-61.

Part IV – General Discussion and Conclusion

Chapter 8

A considerable amount of evidence supporting the existence of different respiratory chain supercomplexes in a variety of organisms has been challenging the reductionist approach of dissecting biological systems into their minimal constituent parts [1], as envisioned by the random collision model [2]. Although sometimes underestimated [3], this supramolecular organization is now supported by functional evidences that allow us to understand their physiological role in eukaryotic or prokaryotic native membranes, emphasizing the importance of studying the mechanisms underlying this process [4]. It is now clear that kinetic advantages are attributed to some respiratory chain supercomplexes such as the mitochondrial respirasomes, which integrate ubiquinone and cytochrome *c*, thus facilitating efficient substrate channeling within the respiratory enzymes [5]. Other functional advantages demonstrated to be directly related with respiratory chain supercomplexes involve the minimization of ROS production by complex I as well as the stabilization and final assembly of this complex [6,7].

These higher-order organizations are further extended to other metabolic pathways. For instance, many enzymes participating in the TCA cycle (e.g. malate dehydrogenase, citrate synthase) or the fatty acid β-oxidation (e.g. acyl-CoA dehydrogenases) processes in mitochondria are organized as large supramolecular structures anchored to the mitochondrial inner membrane [8,9]. Of particular interest are studies indicating direct and specific interactions of these supercomplexes with mitochondrial respiratory chain supercomplexes or individual complexes to optimize the efficiency of energy metabolism [10-12].

Recent improvements in fluorescence live-cell imaging have shown that the prokaryotic metabolic pathways are also tightly organized and that most of their molecules including proteins, lipids and nucleic acids are present in specific cellular microcompartments where they perform their function [13,14]. Thus, there are ample evidences suggesting that the compartmentalization and supramolecular organization of metabolic pathways are ubiquitous in nature. In the case of prokaryotic cells, these supramolecular assemblies should be analyzed in accordance with the surrounding environmental state, considering the inherent

metabolic flexibility of these organisms. In this dissertation, a thorough characterization of the respiratory chain supramolecular assemblies of *Escherichia coli* and *Bacillus subtilis* grown in the presence of oxygen was presented, taking advantage of the solubilization properties conferred by digitonin in maintaining the functional and structural properties of high molecular mass respiratory chain supercomplexes.

8.1 Escherichia coli *aerobic respiratory chain supercomplexes*

In the *E. coli* aerobic respiratory chain several supercomplexes were identified: *i*) one composed of the NADH dehydrogenases NDH-1 and NDH-2, *ii*) another containing two quinol oxygen reductases, cytochromes bo_3 and *bd*I, together with the aerobic formate dehydrogenase (FDH-O) and *iii*) a third one comprising SQR and cytochrome *bd*II quinol oxygen reductase (Figure 1).

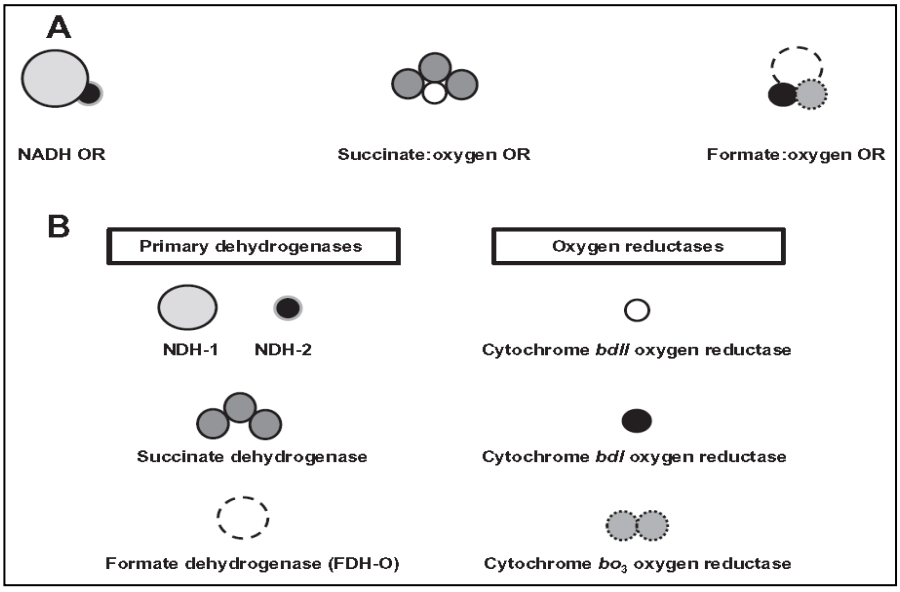

Fig. 1. Schematic representation of the *E. coli* aerobic respiratory chain supercomplexes (A) and individual complexes (B), as identified in this work. Adapted from [70].

In addition, two homo-oligomers were described in the aerobic respiratory chain of this organism, namely the trimeric assembly of SQR and the dimeric form of cytochrome bo_3 oxygen reductase.

8.1.1 The NADH:quinone oxidoreductase supercomplex

The *E. coli* NADH:quinone oxidoreductase supercomplex constitutes the first example of a respiratory chain supercomplex containing type I and II NADH:quinone oxidoreductases, that essentially promote the same reaction of catalyzing the electron transfer from NADH to ubiquinone which, in the case of NDH-1, is coupled with the translocation of protons to the periplasm, in contrast with NDH-2 enzymatic activity. As the binding-sites for the association of both enzymes in NADH:quinone oxidoreductase supercomplex remains unknown, several functional interpretations are hypothesized.

NDH-1 and NDH-2 are a potential source of ROS production in *E. coli* cells [15,16], thus being tempting to speculate that a supramolecular assembly comprising both proteins could limit the production of superoxide or H_2O_2 under stress conditions. For instance, it was recently suggested that conformational changes are induced to complex I in the mammalian mitochondrial respirasome, such that the FMN-containing subunit becomes potentially less prone to interact with oxygen species [17]. In agreement, the dissociation of $I+III_2$ supercomplexes was directly linked to an increase of ROS production [6]. While the source of ROS production by the *E. coli* NDH-1 and NDH-2 enzymes remains unclear, it may well be that the NADH:quinone oxidoreductase supercomplex regulates the level of ROS production.

An alternative role for the association of both enzymes may be related with the balance of the [NADH]/[NAD^+] ratio in the cytoplasm. NADH is produced by specific glycolytic and tricarboxylic acid cycle enzymes and represents a potential source of NAD^+, the main cellular oxidant [18]. The utilization of an alternative

NADH:ubiquinone oxidoreductase such as NDH-2 may be of use in balancing the [NADH]/[NAD^+] ratio necessary for specific cell pathways, as this enzyme is able to increase the flux of NADH oxidation through the respiratory chain while yielding smaller amounts of ATP, in comparison with the reaction promoted by NDH-1 [19]. In agreement, NDH-2 apparent K_M for NADH oxidation is higher than the one exhibited by NDH-1, suggesting that NDH-2 is particularly important in the presence of high NADH concentrations [20,21]. Thus, its association with NDH-1 is potentially convenient given the compartmentalized location of several metabolic pathways in prokaryotic cells [14].

Interestingly, since the free form of NDH-1 was not identified in digitonin solubilized membranes resolved by BN-PAGE of either the wild type *E. coli* or the strain devoid of NDH-2, it is suggested that the stability of NDH-1 complex could be dependent on the expression or the correct assembly of NDH-2. In agreement, the structural dependence of NDH-1 towards other respiratory chain enzymes was also observed in other organisms, as in the case of the mammalian mitochondria I_1+III_2+IV_n and I_1+III_2 supercomplexes [22,23].

8.1.2 The formate:oxygen oxidoreductase supercomplex

The *E. coli* formate:oxygen oxidoreductase supercomplex (FdOx) identified in this work constitutes the first example of a functional respiratory chain supercomplex that couples the electron transfer from the oxidation of formate by the aerobic formate dehydrogenase (FDH-O) to the reduction of oxygen, through cytochromes bo_3 or *bd*I oxygen reductases.

In light of the available knowledge, the reaction exhibited by this supercomplex represents a new metabolic pathway, never previously reported to occur in any prokaryotic cell. The physiological role of FdOx may thus be of important relevance, being reasonable to assume that the electrons generated by the oxidation of formate enter the quinone pool, are transferred to the terminal quinol

oxygen reductases and ultimately to oxygen with consequent energy conservation. Although being present in very low amounts in aerobically grown cells, FDH-O possesses an extremely high catalytic activity [24], presumably withdrawing the energy available in formate. Furthermore, it is well established that ubiquinone serves as the electron acceptor for FDH-O formate oxidation in aerobically grown cells [25].

The association of FDH-O with cytochromes *bd*I or bo_3 oxygen reductases in FdOx would contribute to the generation of two different H^+/e^- ratios. Considering the high amino acid sequence identity and similarity observed between FDH-O and FDH-N, the anaerobic counterpart, it is expected that both proteins share identical structures and catalytic function. In agreement, we have shown that FDH-O K_M value for formate oxidation is of the same order of magnitude to that exhibited by FDH-N. Thus, it is tempting to speculate that the catalytic function of FDH-O, through analogy with that reported for FDH-N [26], involves the oxidation of the formate compartmentalized in the periplasm, and requires the uptake of two protons from the cytoplasmic side of the membrane to the quinone pool, hence contributing for the production of a proton motive force with a H^+/e^- ratio of 1 [27]. Overall, the electron flow from formate oxidation by FDH-O to oxygen reduction *via* cytochrome bo_3 or *bd*I oxygen reductase would yield at least H^+/e^- ratios of 3 or 2, respectively [28].

The different affinity of both oxygen reductases towards oxygen [29,30] would potentially allow FdOx to perform its catalytic function regardless of the surrounding oxygen concentration. Thus, FdOx harbors two different electron flow pathways in a process that is potentially highly optimized by the confinement of the mobile electron carrier ubiquinone within its supramolecular assembly.

As in the case of NDH-1 complex, FDH-O seems to be structurally dependent on the terminal oxygen reductases, since the free form of the enzyme was not detected in the BN-PAGE analysis, either in wild type *E. coli* membranes or in any of the respiratory chain mutant strains analyzed. In agreement, the abolishment off

cytochromes *bo*$_3$ and *bd*I oxygen reductases expression significantly impaired FdOx *in gel* and polarographic activities.

8.1.3 The succinate:oxygen oxidoreductase supercomplex

Several indications suggesting the presence of a supramolecular association comprising SQR and cytochrome *bd*II oxygen reductase in the *E. coli* aerobic respiratory chain were presented in this dissertation.

The finding that this supercomplex could represent an alternative electron pathway, led us to investigate the efficiency of succinate oxidation by *E. coli* cells devoid of either terminal oxygen reductase. As mentioned in chapter 2, cytochrome *bd*II expression is able to supress the absence of the closely-related cytochrome *bd*I oxygen reductase in *E. coli* cells grown on succinate [31]. In this work, *E. coli* membranes devoid of cytochrome *bd*II oxygen reductase exhibited the lowest polarographic activity for succinate oxidation, indicating the importance of this terminal oxygen reductase in establishing this alternative pathway, in agreement with the proposed supercomplex composition.

In terms of energy conservation, since cytochrome *bd*II oxygen reductase was shown to contribute for the production of a proton motive force in *E. coli* cells [28], in contrast with SQR, a H^+/e^- ratio of at least 1 is expected. As we were not able to identify this supercomplex in the BN-PAGE analyses, information regarding the molecular mass and consequently the stoichiometry of such supramolecular assembly is still missing. Nevertheless, since the quinone in *E. coli* SQR was suggested to be involved in superoxide production [32], it is tempting to speculate that the association of both enzymes may provide a tight regulation of ROS production while concomitantly facilitating efficient substrate channeling within the respiratory enzymes.

8.1.4 Integrated perspective of the *E. coli* aerobic respiratory chain

In order to obtain a comprehensive view of the events involving the aerobic respiratory chain of *E. coli*, a quantitative analysis of the transcription and activity of this organism's respiratory chain components was performed throughout growth. The establishment of positive correlations between the transcription of specific respiratory chain genes corroborated the composition of the supramolecular assemblies identified.

The established correlations, as quantified by the Kendall's τ coefficient derived from the multi-level analysis, allowed the association of *nuoF*, *ndh* and *cydA* in one group and of *sdhA* and *appC* in another, representing preferential enzyme partners in the electron transfer chain of *E. coli*. Furthermore, multi-level correlations were also provided by a Principal Component Analysis, where the nearest variables connecting *fdoG* gene were *cydA*, formate:oxygen oxidoreductase activity and *cyoB*.

These integrative approaches were, to our knowledge, the first ever reported to combine gene transcription, enzyme activity and supramolecular organization. They suggest that the *E. coli* aerobic respiratory chain is tightly regulated, coordinating the transcription of specific respiratory chain components favoring the assembly of the identified respiratory chain supercomplexes, whose prevalence along growth was observed. In addition, these results allowed us to propose that cytochrome *bd*I oxygen reductase could be the preferential intermediate in oxygen reduction by the electrons that result from NADH oxidation by the NADH:quinone oxidoreductase supercomplex, possibly assembling a new NADH:oxygen oxidoreductase supercomplex. Although we were not able to identify such supramolecular structure in the BN-PAGE analyses, we have shown that digitonin solubilized wild type *E. coli* membranes produced KCN sensitive NADH:oxygen oxidoreductase activity in the sucrose gradient polarographic studies,

corroborating the proposed association of NDH-1, NDH-2 and cytochrome *bd*I oxygen reductase enzymes in a supercomplex.

8.2 Bacillus subtilis *aerobic respiratory chain supercomplexes*

The *B. subtilis* aerobic respiratory chain was recently analyzed in the context of its supramolecular organization [33]. In this work and taking advantage on the optimization of the electrophoretic techniques applied to digitonin solubilized membranes of wild type *B. subtilis* and respiratory chain mutant strains, we were able to perform an accurate determination of the respiratory chain components participating in supramolecular assemblies. Our results suggest that *B. subtilis* aerobic respiratory chain contains essentially four supercomplexes, three of which assembling the cytochrome *c* pathway and another comprising SQR and NAR (Figure 2). In addition, two homo-oligomers were identified in the aerobic respiratory chain of this organism, namely the dimeric assemblies of SQR and cytochrome *caa*$_3$ oxygen reductase.

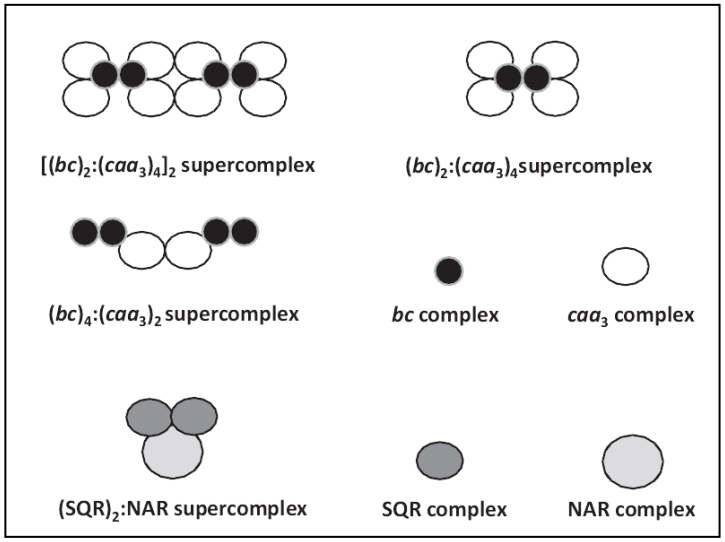

Fig. 2. Tentative representation of *B. subtilis* respiratory chain $(SQR)_2$:NAR and *bc*:*caa*$_3$ supercomplexes. *bc* dimers are represented as the central part of the $(bc)_2$:$(caa_3)_4$ supercomplex, whereas $[(bc)_2$:$(caa_3)_4]_2$ megacomplex represents the binding of two $(bc)_2$:$(caa_3)_4$ basic units, connected by cytochrome *c* oxygen reductases. Adapted from [71].

8.2.1 The *bc*:*caa*$_3$ megacomplex organization

The *B. subtilis* aerobic respiratory chain was shown to contain three supercomplexes with different molecular masses composed only of *bc* complex and *caa*$_3$ oxygen reductase, shown to correspond to different oligomers of the *bc*:*caa*$_3$ supercomplex. Different stoichiometries of the *bc*:*caa*$_3$ supercomplex were thus proposed, namely (*bc*)$_4$:(*caa*$_3$)$_2$, (*bc*)$_2$:(*caa*$_3$)$_4$ and [(*bc*)$_2$(*caa*$_3$)$_4$]$_2$ supercomplexes (Figure 2). The latter represents a megacomplex, possibly corresponding to the binding of two (*bc*)$_2$:(*caa*$_3$)$_4$ building blocks. This suggests that the *B. subtilis* respiratory chain cytochrome *c* pathway is organized in a string-like fashion, similarly to that proposed for plant, mammalian and fungi mitochondria [34-36], and never previously observed in prokaryotic respiratory chains. Thus, based on the suggested structural organization of the mammalian "respiratory string" [35], we propose that the building blocks assembly within the megacomplex structure may be mediated by their *caa*$_3$ oxygen reductase complex dimers.

Interestingly, as previously described in Chapter 6, *B. subtilis bc* complex and cytochrome *caa*$_3$ oxygen reductase are distinguished from the mithocondrial complexes III and IV, among other structural features, by assembling a covalently attached cytochrome *c* in QcrC [37] and CtaC [38] subunits, respectively. The suggested functional consequence for the association of both proteins in a supercomplex is that this respiratory pathway would not require a separate mobile cytochrome *c* for electron transfer between both enzymes. Thus, supramolecular organization is, in this context, beneficial as electron transfer requires intimate contact between both complexes.

Supercomplexes comprising complexes III (*bc*$_1$ complex) and IV (cytochrome *caa*$_3$ oxygen reductase), or analogues, are widespread among the bacterial supramolecular assemblies analyzed so far [39-41], revealing a tight regulation of

the respiratory chain cytochrome *c* pathway, regardless of the alternative pathways available.

8.2.2 The SQR:NAR oxidoreductase supercomplex

The *B. subtilis* SQR:NAR oxidoreductase supercomplex identified in this work represents the first example of a respiratory chain supercomplex that couples the electron transfer from the oxidation of succinate to the reduction of nitrate and was first proposed by Oca and colleagues [33]. In this study, we have confirmed the presence of this supercomplex by the detection of succinate:NBT and methyl viologen:nitrate oxidoreductase *in gel* activities. In agreement, the detected band was completely absent from *B. subtilis* membranes devoid of SQR. The deduced molecular mass of this band and its subsequent dissociation in the dimeric assembly of SQR upon analysis by 2D-BN-PAGE, allowed us to propose a stoichiometry for SQR:NAR supercomplex of 2:1.

B. subtilis aerobic respiratory chain relies solely on a menaquinone-dependent electron transfer to operate. In fact, this electron transfer was proposed to be kinetically controlled by membrane energization at the level of menaquinone reduction by the dehydrogenases [42]. Due to the negative redox potential of the *B. subtilis* menaquinone/menaquinol couple (-80 mV), free menaquinol is prone to rapid autoxidation [42]. Thus, the free diffusion of menaquinol in the membrane is potentially minimized by a supercomplex such as the one identified in this work, ensuring greater efficiency to the oxidative phosphorylation process.

The composition of $(SQR)_2$:NAR may also be explained by the unique succinate oxidation reaction proposed to occur in menaquinone-dependent SQRs. In contrast with the *E. coli* or mitochondrial enzyme catalytic reaction, the succinate oxidation performed by menaquinone-dependent SQRs involves the transfer of two electrons to menaquinone in an endergonic process, due to the higher midpoint redox potential of the succinate/fumarate couple (+ 30 mV) relatively to

the one exhibited by the menaquinone/menaquinol couple. This apparent thermodynamic problem was suggested to be circumvented by the concomitant uptake of two protons from the inner wall zone to the menaquinone binding site [43,44]. In contrast, through analogy with the *E. coli* enzyme, *B. subtilis* NAR likely promotes the reduction of nitrate to nitrite in the cytoplasm, with the concomitant uptake of two protons from the cytoplasm [45]. Besides being present in a supramolecular composition, SQR was also detected in its dimeric free form, as evaluated from the BN-PAGE *in gel* activities. This heterogeneous distribution of SQR potentially underlines a physiological mechanism to regulate different pathways of electron flow within the membrane. Thus, the supramolecular organization composed of SQR and NAR may be advantageous in balancing the electrochemical proton potential that is negatively affected by the endergonic reaction promoted by SQR (Figure 3).

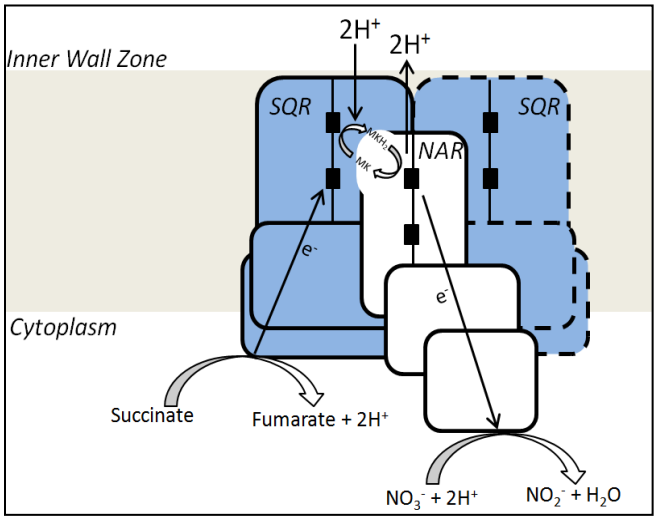

Fig. 3. Tentative representation of the alternative pathway occurring in $(SQR)_2$:NAR supercomplex. Black boxes represent hemes b_D and b_P. MKH_2, menaquinol; MK, menaquinone.

Moreover, besides oxygen, the preferred terminal electron acceptor of *B. subtilis* respiratory chain is nitrate, because of its high midpoint redox potential (+430 mV). Overall, $(SQR)_2$:NAR supercomplex may have an important role in maintaining a viable respiratory chain when oxygen concentration fluctuations occur in the environment.

8.3 Conclusion

In conclusion, this work has provided evidences suggesting the assembly of several supramolecular organizations favoring specific respiratory chain pathways in *E. coli* and *B. subtilis* cells grown in the presence of oxygen. These supercomplexes are proposed to contribute for a tight regulation of the proton motive force necessary to empower F_1F_O-ATP synthase in producing ATP or to promote secondary transport under aerobic conditions. In addition, some of these supercomplexes may be involved in minimizing reactive oxygen species production, which has harmful consequences for the cell.

It is now ascertained that *B. subtilis* and *E. coli* respiratory chain enzymes are distributed in highly dynamic mobile patches within the cytoplasmic membranes [46-49], probably being redistributed in response to the metabolic needs of the cell, ensuring an efficient regulation of specific electron flow pathways. This regulation is especially important in the context of the prokaryotic respiratory chains, considering the inherent metabolic flexibility of these organisms, allowing the assembly of supramolecular organizations (Table 1) different from those reported in the eukaryotic respiratory chains.

Nevertheless, many of the enzymes described in this work to be involved in such organizations represent the minimal functional units of the eukaryotic respiratory chain components, thus emphasizing the importance of further investigating their interactions, regulatory control and physiological impact on the cells. This common linkage between prokaryotic and eukaryotic supercomplexes is especially important in the context of the mammalian mitochondrial-related pathological implications in diseases and aging, which were shown to be directly correlated with changes in the respiratory chain supramolecular architecture [50-53]. In fact, supercomplex disorganization was suggested to be part of a *vicious circle* of oxidative stress and energy failure in the cells [54]. This disorganization, promoted by enhanced ROS generation, potentially yields a less efficient respiratory chain

electron channeling, which, together with the increased instability of complex I, results in a decreased NAD-linked respiration and ATP synthesis, hence leading to a respiratory deficiency in mitochondria.

Table 1
Prokaryotic respiratory chains (RC) supramolecular organization.

		Organism	RC Supercomplexes	References
Bacteria	Gram negative	*P. denitrificans*	NDH-1:(bc_1)$_4$:(caa_3)$_4$ (bc_1)$_4$:(caa_3)$_4$ (bc_1)$_4$:(caa_3)$_2$	[39,56]
		B. japonicum	bc_1:cbb_3	[57]
		R. marinus	ACIII:caa_3	[58]
		A. aeolicus	Sqr:bc_1:ba_3 HYD:SR	[59] [60]
		A. ferrooxidans	Cyc2:Rcy:Cyc1:caa_3	[61]
		E. coli	FDH-O:bo_3:*bd*I NDH-1:NDH-2 SQR:*bd*II	This work
	Gram positive	Bacterium PS3	bc_1:caa_3	[41]
		M. smegmatis	*bcc*:aa_3	[62]
		C. glutanicum		[63]
		B. pseudofirmus OF4	caa_3:F_1F_O-ATP synthase	[64]
		B. subtilis	(SQR)$_2$:NAR [(*bc*)$_2$:(caa_3)$_4$]$_2$ (*bc*)$_4$:(caa_3)$_2$ (*bc*)$_2$:(caa_3)$_4$	This work
			SQR:aa_3 *bc*:caa_3 aa_3:F_1-ATP synthase	[33]
Archaea		*S. acidocaldarius*	SoxABCD SoxM	[65,66]
		P. abyssi	HYD:SR	[67-69]
		T. neutrophilus		
		A. ambivalens		

Sqr - sulfide:quinone oxidoreductase
ACIII - alternative complex III
HYD - hydrogenase
SR - sulfur reductase

It should not be disregarded that, at any given point in time, prokaryotic respiratory complexes may exist as either supercomplexes or as individual complexes, depending on the metabolic needs of the cell or the amount of phospholipids in the membranes, allowing the respiratory chain the flexibility to accommodate the ATP demands of the cell. Flux control analysis represents, in this context, an additional approach in assessing the extent to which each respiratory enzyme is rate-controlling a specific metabolic pathway [55], bringing new insights on the structure of the prokaryotic respiratory chains and potentially corroborating the supramolecular assemblies identified in this work.

The challenge in the future will be to investigate protein complex location and supramolecular assembly in real time while providing evidences for the diffusion coefficients of the electron carriers involved in each pathway as well as for the requirement of specific phospholipids in maintaining functionally active supercomplexes in *B. subtilis* and *E. coli* membranes. In addition, electroelution of the identified supercomplexes from the BN-PAGE analyses and subsequent characterization by cryo-electron microscopy, either using amphipol-solubilized supercomplexes or performing tomographic analysis on digitonin-solubilized specimens, may provide invaluable information in terms of the supercomplexes' overall structure and mechanism, and on the specific domains essential for establishing protein-protein or protein-lipid interactions.

8.4 References

[1] Van Regenmortel, M.H. (2004). Reductionism and complexity in molecular biology. Scientists now have the tools to unravel biological and overcome the limitations of reductionism. EMBO Rep 5, 1016-20.

[2] Hackenbrock, C.R., Chazotte, B. and Gupte, S.S. (1986). The random collision model and a critical assessment of diffusion and collision in mitochondrial electron transport. J Bioenerg Biomembr 18, 331-68.

[3] Trouillard, M., Meunier, B. and Rappaport, F. (2011). Questioning the functional relevance of mitochondrial supercomplexes by time-resolved analysis of the respiratory chain. Proc Natl Acad Sci U S A 108, E1027-34.

[4] Barrientos, A. and Ugalde, C. (2013). I Function, Therefore I Am: Overcoming Skepticism about Mitochondrial Supercomplexes. Cell Metab 18, 147-9.
[5] Acín-Pérez, R., Fernández-Silva, P., Peleato, M.L., Pérez-Martos, A. and Enriquez, J.A. (2008). Respiratory active mitochondrial supercomplexes. Mol Cell 32, 529-39.
[6] Maranzana, E., Barbero, G., Falasca, A.I., Lenaz, G. and Genova, M.L. (2013). Mitochondrial Respiratory Supercomplex Association Limits Production of Reactive Oxygen Species from Complex I. Antioxid Redox Signal
[7] Moreno-Lastres, D., Fontanesi, F., García-Consuegra, I., Martín, M.A., Arenas, J., Barrientos, A. and Ugalde, C. (2012). Mitochondrial complex I plays an essential role in human respirasome assembly. Cell Metab 15, 324-35.
[8] Sumegi, B. and Srere, P.A. (1984). Binding of the enzymes of fatty acid beta-oxidation and some related enzymes to pig heart inner mitochondrial membrane. J Biol Chem 259, 8748-52.
[9] Srere, P.A. (2000). Macromolecular interactions: tracing the roots. Trends Biochem Sci 25, 150-3.
[10] Ovádi, J., Huang, Y. and Spivey, H.O. (1994). Binding of malate dehydrogenase and NADH channelling to complex I. J Mol Recognit 7, 265-72.
[11] Wang, Y., Mohsen, A.W., Mihalik, S.J., Goetzman, E.S. and Vockley, J. (2010). Evidence for physical association of mitochondrial fatty acid oxidation and oxidative phosphorylation complexes. J Biol Chem 285, 29834-41.
[12] Sumegi, B. and Srere, P.A. (1984). Complex I binds several mitochondrial NAD-coupled dehydrogenases. J Biol Chem 259, 15040-5.
[13] Nevo-Dinur, K., Govindarajan, S. and Amster-Choder, O. (2012). Subcellular localization of RNA and proteins in prokaryotes. Trends Genet 28, 314-22.
[14] Rudner, D.Z. and Losick, R. (2010). Protein subcellular localization in bacteria. Cold Spring Harb Perspect Biol 2, a000307.
[15] Esterházy, D., King, M.S., Yakovlev, G. and Hirst, J. (2008). Production of reactive oxygen species by complex I (NADH:ubiquinone oxidoreductase) from *Escherichia coli* and comparison to the enzyme from mitochondria. Biochemistry 47, 3964-71.
[16] Seaver, L.C. and Imlay, J.A. (2004). Are respiratory enzymes the primary sources of intracellular hydrogen peroxide? J Biol Chem 279, 48742-50.
[17] Schäfer, E., Dencher, N.A., Vonck, J. and Parcej, D.N. (2007). Three-dimensional structure of the respiratory chain supercomplex $I_1III_2IV_1$ from bovine heart mitochondria. Biochemistry 46, 12579-85.
[18] Berg, J., Tymoczko, J. and Stryer, L. (2002) Biochemistry, W H Freeman. New York.
[19] Melo, A.M., Bandeiras, T.M. and Teixeira, M. (2004). New insights into type II NAD(P)H:quinone oxidoreductases. Microbiol Mol Biol Rev 68, 603-16.
[20] Yagi, T. (1989). [Structure and function of NADH-quinone oxidoreductase in respiratory chain]. Tanpakushitsu Kakusan Koso 34, 351-63.
[21] Friedrich, T. et al. (1994). Two binding sites of inhibitors in NADH: ubiquinone oxidoreductase (complex I). Relationship of one site with the ubiquinone-binding site of bacterial glucose:ubiquinone oxidoreductase. Eur J Biochem 219, 691-8.
[22] Lenaz, G. and Genova, M.L. (2009). Structural and functional organization of the mitochondrial respiratory chain: a dynamic super-assembly. Int J Biochem Cell Biol 41, 1750-1772.

[23] Schägger, H., de Coo, R., Bauer, M.F., Hofmann, S., Godinot, C. and Brandt, U. (2004). Significance of respirasomes for the assembly/stability of human respiratory chain complex I. J Biol Chem 279, 36349-53.

[24] Sawers, G., Heider, J., Zehelein, E. and Böck, A. (1991). Expression and operon structure of the *sel* genes of *Escherichia coli* and identification of a third selenium-containing formate dehydrogenase isoenzyme. J Bacteriol 173, 4983-93.

[25] Pinsent, J. (1954). The need for selenite and molybdate in the formation of formic dehydrogenase by members of the *coli*-aerogenes group of bacteria. Biochem J 57, 10-6.

[26] Sawers, R.G. (2005). Formate and its role in hydrogen production in *Escherichia coli*. Biochem Soc Trans 33, 42-6.

[27] Jormakka, M., Törnroth, S., Byrne, B. and Iwata, S. (2002). Molecular basis of proton motive force generation: structure of formate dehydrogenase-N. Science 295, 1863-8.

[28] Borisov, V.B., Murali, R., Verkhovskaya, M.L., Bloch, D.A., Han, H., Gennis, R.B. and Verkhovsky, M.I. (2011). Aerobic respiratory chain of *Escherichia coli* is not allowed to work in fully uncoupled mode. Proc Natl Acad Sci U S A 108, 17320-4.

[29] Kita, K., Konishi, K. and Anraku, Y. (1984). Terminal oxidases of *Escherichia coli* aerobic respiratory chain. II. Purification and properties of cytochrome b_{558}-*d* complex from cells grown with limited oxygen and evidence of branched electron-carrying systems. J Biol Chem 259, 3375-81.

[30] Kita, K., Konishi, K. and Anraku, Y. (1984). Terminal oxidases of *Escherichia coli* aerobic respiratory chain. I. Purification and properties of cytochrome b_{562}-*o* complex from cells in the early exponential phase of aerobic growth. J Biol Chem 259, 3368-74.

[31] Sturr, M.G., Krulwich, T.A. and Hicks, D.B. (1996). Purification of a cytochrome *bd* terminal oxidase encoded by the *Escherichia coli app* locus from a delta *cyo* delta *cyd* strain complemented by genes from *Bacillus firmus* OF4. J Bacteriol 178, 1742-9.

[32] Zhao, Z., Rothery, R.A. and Weiner, J.H. (2006). Effects of site-directed mutations in *Escherichia coli* succinate dehydrogenase on the enzyme activity and production of superoxide radicals. Biochem Cell Biol 84, 1013-21.

[33] García Montes de Oca, L.Y., Chagolla-López, A., González de la Vara, L., Cabellos-Avelar, T., Gómez-Lojero, C. and Gutiérrez Cirlos, E.B. (2012). The composition of the *Bacillus subtilis* aerobic respiratory chain supercomplexes. J Bioenerg Biomembr 44, 473-86.

[34] Bultema, J.B., Braun, H.P., Boekema, E.J. and Kouril, R. (2009). Megacomplex organization of the oxidative phosphorylation system by structural analysis of respiratory supercomplexes from potato. Biochim Biophys Acta 1787, 60-7.

[35] Wittig, I., Carrozzo, R., Santorelli, F.M. and Schägger, H. (2006). Supercomplexes and subcomplexes of mitochondrial oxidative phosphorylation. Biochim Biophys Acta 1757, 1066-72.

[36] Heinemeyer, J., Braun, H.P., Boekema, E.J. and Kouril, R. (2007). A structural model of the cytochrome *c* reductase/oxidase supercomplex from yeast mitochondria. J Biol Chem 282, 12240-8.

[37] Yu, J., Hederstedt, L. and Piggot, P.J. (1995). The cytochrome *bc* complex (menaquinone:cytochrome *c* reductase) in *Bacillus subtilis* has a nontraditional subunit organization. J Bacteriol 177, 6751-60.

[38] Saraste, M., Metso, T., Nakari, T., Jalli, T., Lauraeus, M. and Van der Oost, J. (1991). The *Bacillus subtilis* cytochrome-*c* oxidase. Variations on a conserved protein theme. Eur J Biochem 195, 517-25.

[39] Berry, E.A. and Trumpower, B.L. (1985). Isolation of ubiquinol oxidase from *Paracoccus denitrificans* and resolution into cytochrome bc_1 and cytochrome c-aa_3 complexes. J Biol Chem 260, 2458-67.

[40] Niebisch, A. and Bott, M. (2001). Molecular analysis of the cytochrome bc_1-aa_3 branch of the *Corynebacterium glutamicum* respiratory chain containing an unusual diheme cytochrome c_1. Arch Microbiol 175, 282-94.

[41] Sone, N., Sekimachi, M. and Kutoh, E. (1987). Identification and properties of a quinol oxidase super-complex composed of a bc_1 complex and cytochrome oxidase in the thermophilic bacterium PS3. J Biol Chem 262, 15386-91.

[42] Azarkina, N. and Konstantinov, A.A. (2002). Stimulation of menaquinone-dependent electron transfer in the respiratory chain of *Bacillus subtilis* by membrane energization. J Bacteriol 184, 5339-47.

[43] Schirawski, J. and Unden, G. (1998). Menaquinone-dependent succinate dehydrogenase of bacteria catalyzes reversed electron transport driven by the proton potential. Eur J Biochem 257, 210-5.

[44] Lancaster, C.R. et al. (2005). Experimental support for the "E pathway hypothesis" of coupled transmembrane e^- and H^+ transfer in dihemic quinol:fumarate reductase. Proc Natl Acad Sci U S A 102, 18860-5.

[45] Bertero, M.G., Rothery, R.A., Palak, M., Hou, C., Lim, D., Blasco, F., Weiner, J.H. and Strynadka, N.C. (2003). Insights into the respiratory electron transfer pathway from the structure of nitrate reductase A. Nat Struct Biol 10, 681-7.

[46] Lenn, T., Leake, M.C. and Mullineaux, C.W. (2008). Are *Escherichia coli* OXPHOS complexes concentrated in specialized zones within the plasma membrane? Biochem Soc Trans 36, 1032-6.

[47] Lenn, T., Leake, M.C. and Mullineaux, C.W. (2008). Clustering and dynamics of cytochrome *bd*-I complexes in the *Escherichia coli* plasma membrane *in vivo*. Mol Microbiol 70, 1397-407.

[48] Johnson, A.S., van Horck, S. and Lewis, P.J. (2004). Dynamic localization of membrane proteins in *Bacillus subtilis*. Microbiology 150, 2815-24.

[49] Meredith, D.H., Plank, M. and Lewis, P.J. (2008). Different patterns of integral membrane protein localization during cell division in *Bacillus subtilis*. Microbiology 154, 64-71.

[50] Gómez, L.A., Monette, J.S., Chavez, J.D., Maier, C.S. and Hagen, T.M. (2009). Supercomplexes of the mitochondrial electron transport chain decline in the aging rat heart. Arch Biochem Biophys 490, 30-5.

[51] Rosca, M.G., Vazquez, E.J., Kerner, J., Parland, W., Chandler, M.P., Stanley, W., Sabbah, H.N. and Hoppel, C.L. (2008). Cardiac mitochondria in heart failure: decrease in respirasomes and oxidative phosphorylation. Cardiovasc Res 80, 30-9.

[52] Osenbroch, P., Auk-Emblem, P., Halsne, R., Strand, J., Forstrøm, R.J., van der Pluijm, I. and Eide, L. (2009). Accumulation of mitochondrial DNA damage and bioenergetic dysfunction in CSB defective cells. FEBS J 276, 2811-21.

[53] Lenaz, G. and Genova, M.L. (2010). Structure and organization of mitochondrial respiratory complexes: a new understanding of an old subject. Antioxid Redox Signal 12, 961-1008.

[54] Lenaz, G. and Genova, M.L. (2012). Supramolecular organisation of the mitochondrial respiratory chain: a new challenge for the mechanism and control of oxidative phosphorylation. Adv Exp Med Biol 748, 107-44.

[55] Kacser, H. and Burns, J.A. (1979). Molecular democracy: who shares the controls? Biochem Soc Trans 7, 1149-60.

[56] Stroh, A., Anderka, O., Pfeiffer, K., Yagi, T., Finel, M., Ludwig, B. and Schägger, H. (2004). Assembly of respiratory complexes I, III, and IV into NADH oxidase supercomplex stabilizes complex I in *Paracoccus denitrificans*. J Biol Chem 279, 5000-7.

[57] Keefe, R.G. and Maier, R.J. (1993). Purification and characterization of an O_2-utilizing cytochrome-*c* oxidase complex from *Bradyrhizobium japonicum* bacteroid membranes. Biochim Biophys Acta 1183, 91-104.

[58] Refojo, P.N., Teixeira, M. and Pereira, M.M. (2010). The alternative complex III of *Rhodothermus marinus* and its structural and functional association with *caa*$_3$ oxygen reductase. Biochim Biophys Acta 1797, 1477-82.

[59] Guiral, M., Tron, P., Aubert, C., Gloter, A., Iobbi-Nivol, C. and Giudici-Orticoni, M.T. (2005). A membrane-bound multienzyme, hydrogen-oxidizing, and sulfur-reducing complex from the hyperthermophilic bacterium *Aquifex aeolicus*. J Biol Chem 280, 42004-15.

[60] Prunetti, L., Infossi, P., Brugna, M., Ebel, C., Giudici-Orticoni, M.T. and Guiral, M. (2010). New functional sulfide oxidase-oxygen reductase supercomplex in the membrane of the hyperthermophilic bacterium *Aquifex aeolicus*. J Biol Chem 285, 41815-26.

[61] Castelle, C., Guiral, M., Malarte, G., Ledgham, F., Leroy, G., Brugna, M. and Giudici-Orticoni, M.T. (2008). A new iron-oxidizing/O_2-reducing supercomplex spanning both inner and outer membranes, isolated from the extreme acidophile *Acidithiobacillus ferrooxidans*. J Biol Chem 283, 25803-11.

[62] Megehee, J.A., Hosler, J.P. and Lundrigan, M.D. (2006). Evidence for a cytochrome *bcc*-*aa*$_3$ interaction in the respiratory chain of *Mycobacterium smegmatis*. Microbiology 152, 823-9.

[63] Niebisch, A. and Bott, M. (2003). Purification of a cytochrome *bc*-*aa*$_3$ supercomplex with quinol oxidase activity from *Corynebacterium glutamicum*. Identification of a fourth subunity of cytochrome *aa*$_3$ oxidase and mutational analysis of diheme cytochrome c_1. J Biol Chem 278, 4339-46.

[64] Liu, X., Gong, X., Hicks, D.B., Krulwich, T.A., Yu, L. and Yu, C.A. (2007). Interaction between cytochrome *caa*$_3$ and F_1F_0-ATP synthase of alkaliphilic *Bacillus pseudofirmus* OF4 is demonstrated by saturation transfer electron paramagnetic resonance and differential scanning calorimetry assays. Biochemistry 46, 306-13.

[65] Lübben, M., Arnaud, S., Castresana, J., Warne, A., Albracht, S.P. and Saraste, M. (1994). A second terminal oxidase in *Sulfolobus acidocaldarius*. Eur J Biochem 224, 151-9.

[66] Lübben, M., Kolmerer, B. and Saraste, M. (1992). An archaebacterial terminal oxidase combines core structures of two mitochondrial respiratory complexes. EMBO J 11, 805-12.

[67] Dirmeier, R., Keller, M., Frey, G., Huber, H. and Stetter, K.O. (1998). Purification and properties of an extremely thermostable membrane-bound sulfur-reducing

complex from the hyperthermophilic *Pyrodictium abyssi*. Eur J Biochem 252, 486-91.

[68] Laska, S. and Kletzin, A. (2000). Improved purification of the membrane-bound hydrogenase-sulfur-reductase complex from thermophilic archaea using epsilon-aminocaproic acid-containing chromatography buffers. J Chromatogr B Biomed Sci Appl 737, 151-60.

[69] Laska, S., Lottspeich, F. and Kletzin, A. (2003). Membrane-bound hydrogenase and sulfur reductase of the hyperthermophilic and acidophilic archaeon *Acidianus ambivalens*. Microbiology 149, 2357-71.

[70] Sousa, P.M.F., Videira, M.A.M. and Melo, A.M.P. (2013). The formate:oxygen oxidoreductase supercomplex of *Escherichia coli* aerobic respiratory chain. FEBS letters 587, 2559-64.

[71] Sousa, P.M.F., Videira, M.A., Santos, F.A., Hood, B.L., Conrads, T.P. and Melo, A.M.P. (2013). The *bc*:*caa*$_3$ supercomplexes from the Gram positive bacterium *Bacillus subtilis* respiratory chain: A megacomplex organization? Arch Biochem Biophys 537, 153-60.

ITQB-UNL | Av. da República, 2780-157 Oeiras, Portugal
Tel (+351) 214 469 100 | Fax (+351) 214 411 277

www.itqb.unl.pt

IICT | Rua da Junqueira Nº86, 1º, 1300-344 Lisboa, Portugal
Tel (+351) 213 616 340 | Fax (+351) 213 631 460

www.iict.pt